Cell Entry of Bluetongue Virus

Sarah Jane Gold
(B.Sc. Hons)

Thesis submitted in partial fulfilment of the
requirements for the degree of
Doctor of Philosophy

School of Pharmacy
UNIVERSITY OF LONDON

Pirbright Laboratory
INSTITUTE FOR ANIMAL HEALTH

March 2010

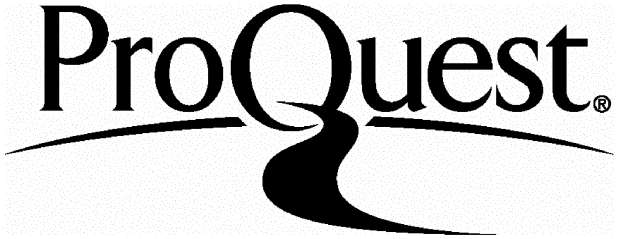

This thesis describes research conducted in the School of Pharmacy, University of London (and the Institute for Animal Health) between October 2005 and March 2010 under the supervision of Professor H.O. Alpar. I certify that the research described is original and that any parts of the work that have been conducted by collaboration are clearly indicated. I also certify that I have written all the text herein and have clearly indicated by suitable citation any part of this dissertation that has already appeared in publication.

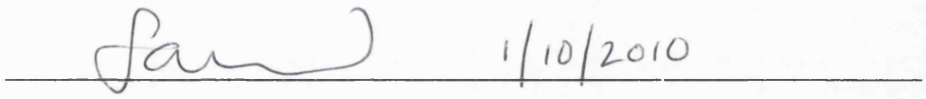

1/10/2010

Signature Date

Abstract

Pharmacological and dominant-negative (Dn) inhibitors of endocytosis were used to investigate the cell entry pathway used by BTV-1 in mammalian cells. Infection, but not cell entry was inhibited in BHK, Vero and BPAEC cells, by reagents that raise endosomal pH suggesting that virus must be delivered to acidic compartments for infection. Entry and infection of BHK cells was not inhibited by three different dominant-negative inhibitors (Dn Eps15, AP180C and Dn Dynamin-2) of clathrin-mediated endocytosis, and during entry, virus did not co-localise with transferrin-positive early-endosomes. The failure of Dn Dynamin-2 to inhibit BTV-1 infection also excludes a role for caveolae during entry. This conclusion was supported by showing that Dn Caveolin-1 and depletion of cellular cholesterol using methyl-β-cyclodextrin or nystatin did not inhibit infection. The observations that methyl-β-cyclodextrin and nystatin did not inhibit infection also rule out a role for other cholesterol/lipid raft-dependent pathways in entry. However, entry was inhibited by the dynamin inhibitor, dynasore, indicating that entry is dependent on a form of dynamin. During entry, BTV-1 was co-localised with dextran, a marker for macropinocytosis. EIPA, a known macropinocytosis inhibitor, blocked entry of both BTV-1 and dextran but not transferrin. Disruption of the actin cytoskeleton using cytochalasin D and latrunculin A inhibited infection further suggesting a role for macropinocytosis in entry. Dn Rab 34 which has been shown to inhibit macropinocytosis in some cell types also inhibited BTV-1 infection. During the first 2 hours of entry, BTV-1 was increasingly co-localised with LAMP-1 indicating that virus is delivered to late-endosomes and/or lysosomes by-passing early endosomes, a characteristic also shared by macropinocytosis.

In summary, BTV-1 entry and infection of BHK cells can occur independently of cholesterol, and clathrin- and caveolae-mediated endocytosis, but depends on a specific form of dynamin, and shares characteristics in common with macropinocytosis.

Acknowledgments

The biggest thanks of all must go to my principal supervisor Dr. Terry Jackson; thank you for your guidance, encouragement and continual good humour throughout the course of these studies.

Thanks also to my two co-supervisors, Dr. Paul Monaghan for teaching me how not to do microscopy and to Professor Peter Mertens for enabling me to present this data at the dsRNA Symposium. Thank you also Professor Oya Alpar, my supervisor at the School of Pharmacy.

I would also like to thank the many people for their kind gifts of reagents, without which this study would not have been possible including Professor Jean Gruenberg (University of Geneva) for providing the mouse monoclonal antibody Mab 4A1, Dr. Harvey McMahon (University of Cambridge) for providing dominant-negative AP180C, Dr. Mark McNiven (Mayo Clinic) for providing wild type and dominant-negative dynamin-2, Dr. Alexandre Benmerah (Université Paris Descartes) for providing control and dominant-negative Eps15, Dr. Mel Silverman (University of Toronto) for providing wild type and dominant-negative Rab 34 and Professor Ari Helenius (Institute of Biochemistry, Zürich) for providing wild type and dominant-negative Caveolin-1.

A very special big thank you all members of the Picornavirus Structure Group and Bio-Imaging for their kind help and support throughout my studies and for all the Bongo Hut tea breaks, some a little longer than they should have been! Special thanks must go to Stephen for answering every stupid question possible; to Beck for many a late night dinner and chat and to Pippa and Jenny in Bio-Imaging for making things better when they went wrong. Work in this thesis would also not have been completed without the help and guidance of the Arbovirology division, with special thanks to Karin for teaching me to purify BTV-1 and to Andrew for making the trips to SOP fun.

Lastly I must thank all of my family, both Hudson and Gold, for being patient and pretending to understand what I am doing – thank you to my Mum and Dad for always believing I would finish this! And finally to my two 'other-half's' a great big hug to you both - thank you Sophie for always being at the end of the telephone, and Ed thank you for always being by my side, you know how much you mean to me.

Table of Contents

List of Figures

List of Tables

Abbreviations

AP180C	Adaptor protein 180
AP2	Clathrin adaptor complex
BAR domain	Bin–Amphiphysin–Rvs domain
BHK	Baby hamster kidney
BPAEC	Bovine pulmonary aortic endothelial cells
BT	Bluetongue
BTV	Bluetongue virus
BTV-X	Bluetongue virus (X = serotype)
$CaCl_2$	Calcium chloride
CCP	Clathrin-coated pit
CCV	Clathrin-coated vesicle
CHC	Clathrin heavy chain
CHO	Chinese hamster ovary
CLASPs	Clathrin-associated sorting protein
CLC	Clathrin light chain
CLIC/GEEC	CLathrin Independent Carriers/GPI-AP Enriched Endocytic Compartments
CME	Clathrin-mediated endocytosis
CO_2	Carbon dioxide
CPE	Cytopathic effect
CtBP1/BARS	C-terminal-binding protein-1/Brefeldin A-ADP-ribosylated substrate
DAPI	4',6'-Diamidino-2-Phenylindole
DC	Dendritic cell
dH_2O	Distilled water
DIC	Differential interference contrast
DMEM	Dulbecco's modified eagles medium
Dn	Dominant-negative
dsRNA	Double-stranded ribonucleic acid
DTT	Dithiothreitol
EEA-1	Early-endosomal antigen-1
eGFP	Enhanced green fluorescent protein
EGFR	epidermal growth factor receptor
EIPA	5-(N-Ethyl-N-isopropyl)amiloride
ELIspot	Enzyme-Linked Immunospot
Eps15	Epidermal growth factor receptor substrate 15
FACS	Flow cytometry
FBS	Foetal bovine serum
g	Gravity
GAGs	Glycosaminoglycans
GAP	GTPase activating protein
GEECs	GPI-AP enriched early-endosomal compartments
GFP	Green fluorescent protein
GMEM	Glasgow minimum essential medium
GRAF1	GTPase Regulator Associated with Focal Adhesion Kinase-1
h	Hour/hours
hpi	Hours post infection
HRP	Horseradish peroxidase
ICTVdb	International Committee of Taxonomy of Viruses database
ISVP	Infectious sub-virus particle
Kb	Kilo base
KC	Culicoides sonorensis cell line
LAMP-1	Lysosomal-associated membrane protein 1
LAMP-2	Lysosomal-associated protein 2
°C	Degrees centigrade

m.o.i.	Multiplicity of infection
Mab	Monoclonal antibody
MEB	Mesenteron escape barrier
MEVP	Membrane enveloped virus particle
$MgCl_2$	Magnesium chloride
MIB	Mesenteron infection barrier
min	Minute/minutes
MβCD	Methyl-β-cyclodextrin
NH_4Cl	Ammonium chloride
NS2	Non-structural protein 2
NS3	Non-structural protein 3
OIE	Office International des Epizooties
PBS	Phosphate buffered saline
PDGFR	platelet derived growth factor receptor
PFM	Paraformaldehyde
pH	Potential of hydrogen
PKC	Protein kinase C
RGD	Arginine-Glycine-Aspartic Acid
RNA	Ribonucleic acid
rpm	Revolutions per minute
RT	Room temperature
SDS	Sodium dodecyl sulphate
SFM	Serum free media
SiRNA	Short interfering ribonucleic acid
SV40	Simian Virus 40
TBS	Tris buffered saline
$TCID_{50}$	Tissue culture infectious dose
TLP	Triple-layered particle
Tn	Transferrin
V	Volts
VIB	Viral inclusion body
VPX	Viral protein (X = protein number)
wt	Wild type
γδ T	Gamma-delta T cell

1 Introduction

1.1 General Introduction: Bluetongue Virus

Bluetongue virus (BTV) is the 'type' species of the genus *Orbivirus* within the family *Reoviridae,* which includes many important pathogens for animals and man (Mertens, 2005). Viruses of the family *Reoviridae* are characterised primarily by their genome of nine to twelve segments of linear double-stranded RNA (dsRNA).

The orbiviruses are able to infect a wide range of host species including mammals, birds, marsupials, rodents and in some cases humans (Mertens, 2005). They are responsible for several important diseases such as bluetongue (BT) which primarily affects sheep, deer, goats and cattle. Other important or emerging orbiviruses include *African horsesickness virus* (ASHV), *Peruvian horsesickness virus* (PHSV) and *Equine encephalosis virus* (EEV), which primarily infect equids, and *Epizootic haemorrhagic disease virus* (EHDV) which infects deer species in the USA (Allison et al., 2010; Mertens, 2005) and has recently started causing disease in cattle in the Mediterranean region including Turkey, Israel, and Morocco (Temizel et al., 2009). Arthropod vectors are responsible for the transmission of all orbiviruses, and BTV, AHSV, EHDV and EEV are all transmitted by adult female *Culicoides* midges (see below). Table 1.1 shows the 22 currently named species of the genus *Orbivirus*, and the number of serotypes within each species (ICTV, 2008).

Bluetongue virus (BTV) causes 'bluetongue', which was previously classified by the Office International des Epizooties (OIE) as a list 'A' disease of ruminants. Bluetongue is a 'transboundary' infectious but non-contagious disease that is transmitted by certain species of biting midge (*Culicoides spp.*). The virus is able to infect most ruminants, including cattle, deer and goats, but is an economically important disease primarily in sheep (Mellor, 2003; Mertens and Diprose, 2004; Purse et al., 2005). In 2007 there were 24 known serotypes of BTV, until Toggenburg Orbivirus was discovered in BTV-positive goats in north-eastern Switzerland and was designated as a 25th serotype (Hofmann et al., 2008). Bluetongue is an

Virus Serogroup (Species)	Serotypes	Host Species	Principal vector
African horse sickness virus species (AHSV)	AHSV 1 to 9	Equids, dogs, camels cattle, sheep, goats, elephants, predatory carnivores and in some circumstances humans	*Culicoides*
Bluetongue virus species (BTV)	BTV 1 to 25	Cattle, sheep, goats, camels, elephants, predatory carnivores.	*Culicoides*
Changuinola virus species (CGLV)	Twelve "named" serotypes	Humans, rodents, sloths.	Phlebotomine flies, mosquitoes
Chenuda virus species (CNUV)	Seven "named" serotypes	Seabirds	Ticks: *Argas, Ornithodoros*
Chobar Gorge virus species (CGV)	Two "named" serotypes	Bats	Ticks: *Ornithodoros*
Corriparta virus species (CORV)	Three "named" serotypes	Humans, rodents.	Culicine mosquitoes
Epizootic hemorrhagic disease virus species (EHDV)	EHDV 1 to 8	Cattle, sheep, deer, camels, llamas, wild ruminants, marsupials.	*Culicoides*
Equine encephalosis virus species (EEV)	EEV 1 to 7	Equids	*Culicoides*
Eubenangee virus species (EUBV)	Four "named" serotypes	Unknown (isolated from insect vectors)	*Culicoides* and Anopheline, Culicine mosquitoes.
Ieri virus species (IERIV)	Three "named" serotypes	Birds	*Culex* mosquitoes
Great Island virus species (GIV)	Thirty six "named" serotypes.	Seabirds, rodents, humans.	Ticks: *Argas, Ornithodoros, Ixodes.*
Lebombo virus species (LEBV)	Single serotype (LEBV-1)	Humans, rodents.	Culicine mosquitoes.
Orungo virus species (ORUV)	ORUV-1 to 4	Humans, camels, cattle, goats, sheep, monkeys	Culicine mosquitoes.
Palyam virus species (PALV)	Eleven "named" serotypes	Cattle, sheep	*Culicoides* and Culicine mosquitoes
Umatilla virus species (UMAV)	Four "named" serotypes	Birds	Culicine mosquitoes
Wad Medani virus species (WMV)	Two "named" serotypes	Domestic animals	Ticks: *Boophilus, Rhipicephalus, Hyalomma, Argas.*
Wallal virus species (WALV)	Two "named" serotypes	Marsupials	*Culicoides.*
Warrego virus species (WARV)	Two "named" serotypes	Marsupials	*Culicoides* and Anopheline, Culicine mosquitoes
Wongorr virus species (WGRV)	Eight "named" or "numbered" serotypes	Cattle, macropods	Culicoides and mosquitoes
St Croix river virus	One isolate identified	Possibly from Deer	Ticks
Peruvian horse sickness virus	An uncertain number of numbered types	Cattle	mosquitoes
Yunnan Orbivirus (YUOV)	One isolate identified	Unknown	Isolated: Culex tritaeniorhynchus mosquitoes

Table 1.1: The *Orbivirus* genus
The table shows all 22 named species of the *Orbivirus* genus, and the number of serotypes within each species. For each species the host species and principal vector is listed. Reproduced, with permission from http://www.reoviridae.org/dsRNA_virus_proteins/ReoID/orbiviruses.htm

economically important disease. Losses, both direct, through disease symptoms and fatalities, and indirect through trade disruptions were estimated worldwide in 1996 to be in excess of US$3 billion per year (Tabachnick et al., 1996) and in the USA alone the disruption of trade is reported to cost US$125 million a year (Purse et al., 2005). Direct losses through mortality and morbidity can be very high and in some outbreaks mortality rates of up to 70% in naïve and susceptible breeds of sheep have been seen. It has been estimated that since the viruses emergence in Europe in 1998, the disease has caused the death of over 2 million sheep (Purse et al., 2005). The northward emergence of BTV is estimated to have cost the European livestock industries in excess of €150 million during 2007 alone (Szmaragd et al., 2007).

Bluetongue was first described by Spruel in 1905 although it had been recognised earlier in South Africa during 1876. The disease was originally named 'malarial catarrhal fever' although it was later renamed as 'bluetongue' because sheep with severe clinical signs of the disease sometimes develop a swollen and cyanotic tongue. Bluetongue is endemic in most tropical and subtropical regions of the world between the latitudes 45 to 53°N and 35°S. This includes much of Mediterranean Europe, North and South America, Africa, India, Australia and China, (Purse et al., 2005). Although endemic in many regions not all BTV serotypes are present in all locations as shown in Table 1.2. In endemic areas disease in indigenous sheep breeds is often mild or in apparent. Severe clinical disease is more frequently seen on introduction of the virus, or new strains of virus to serologically naïve animals in new or non-endemic areas. Disease is particularly severe in improved breeds of sheep, such as the European fine wool and mutton breeds, and in exceptional cases mortality levels in infected flocks can reach up to 70%, as occurred in Sicily during 2002.

Although the global distribution of BTV has historically had a northern limit of latitude 50°N; during the recent northern European epidemic, the virus has spread far beyond this.

Geographical area	Bluetongue virus serotype I = virus serotype isolated S = serological evidence for the presence of each serotype (detection of neutralising antibodies) R = Detection of relevant serotype specific RNA (by RT-PCR and sequence analysis)																							
-	**1**	**2**	**3**	**4**	**5**	**6**	**7**	**8**	**9**	**10**	**11**	**12**	**13**	**14**	**15**	**16**	**17**	**18**	**19**	**20**	**21**	**22**	**23**	**24**	**25**
Africa	I	I	I	I	I	I	I	I	I	I	I	I	I	I	I	I	I	-	I	I	-	I	-	I	-
Middle East	-	I	-	I	-	I	-	-	S	I	-	S	S	S	I	I	S	-	S	S	-	-	-	I	-
Pakistan + India	I	I	I	I	S	I	S	S	I	S	S	S	S	S	S	I	I	I	-	S	S	-	I	-	-
Australia	I	I	I	-	-	-	I	-	I	-	-	S	-	-	I	I	-	-	-	I	I	-	I	-	-
South East Asia and Indonesia	I	I	I	I	-	-	I	-	I	I	S	I	S	-	-	S	I	S	S	S	I	-	I	-	-
China	I	I	I	I	-	-	-	-	-	-	-	I	-	-	I	I	-	-	-	-	-	-	-	-	-
USA	I	I	I	-	I	I	-	-	-	I	I	-	I	I	-	-	I	-	I	-	-	I	-	I	-
Central and South America	I	-	I	I	-	I	-	I	-	-	I	I	I	I	-	S	I	-	-	-	-	-	-	-	-
Europe	I*	I*	I	I*	-	I*	-	I*	I*	I	R		-	-	-	I*	-	-	-	-	-	-	-	-	R*

Table 1.2: The Geographical Distribution of BTV Serotypes

The geographical distribution of the 25 known BTV serotypes throughout the regions of the world. KEY: I = virus serotype isolated; S = serological evidence for the presence of each serotype (detection of neutralising antibodies); R = Detection of relevant serotype specific RNA (by RT-PCR and sequence analysis); *denotes BTV serotypes currently circulating in Europe. Reproduced, with permission from: www.iah.bbsrc.ac.uk/dsRNA_virus_proteins/btv-serotype-distribution.htm and Dr S Maan (IAH).

The disease has become highlighted in recent years due to the emergence of the virus into southern, central and northern Europe, which prior to 1998 had been largely free of BT, apart from limited epizootics in the Mediterranean region. Before 1998 these outbreaks were associated with a single serotype on each occasion including: BTV-10 in the Iberian peninsula and Morocco in 1956 to 1960; BTV-4 in Cyprus sporadically from 1964 onwards, BTV-3 in Lesbos and Rhodes in 1979, and BTV-4 in Turkey during the 1980's (Mellor, 2003). However, since 1998, there have been outbreaks across the whole of the Mediterranean region, involving at least five different BTV serotypes (BTV-1, 2, 4, 9 and 16). In August 2006, BTV-8 from a sub-Saharan origin was detected for the first time in northern Europe (Diseases, 2006; Maan et al., 2008). This occurrence of disease was 900 km further north than any previous BTV incursion into Europe and animal holdings in Germany, Belgium, the Netherlands, France, Luxembourg and Switzerland were infected. Other serotypes were also circulating in southern Europe in 2006 with BTV-1 and BTV-4 present in Italy and Portugal respectively. The following year BTV-8 re-emerged and the infected range of Europe was expanded to include Austria, Denmark, the UK, Sweden, Switzerland, Spain, Greece, Italy and the Czech Republic; whilst BTV-1 was confirmed in France, Italy, Portugal and Spain. BTV-8 again overwintered and re-emerged in 2008 further expanding its range infecting animal holdings in Sweden, Hungary and Austria.

In 2008 BTV-6 (vaccine strain) was introduced by an unknown route into the Netherlands and spread to Belgium and Germany. Also in Belgium the BTV-11 vaccine strain was detected (De Clercq et al., 2009). BTV-1 continued to circulate in France and Italy; BTV-4 in Portugal and BTV-25 was identified and described for the first time in Switzerland. The large number of serotypes now circulating in Europe and the use of live vaccine strains of BTV-2, 4, 9 and 16 in southern Europe provides great potential for reassortment between different strains, topotypes and serotypes.

Midges blown on winds across the channel pose a threat of further new incursions to the UK. There are also risks of new incursions, into uninfected countries, due to importation of livestock infected with different serotypes; indeed in 2008 BTV-1 and 8 have been detected in the UK and the Netherlands in imported cattle, whilst BTV-6 was detected in imported animals in Belgium (Menzies et al., 2008).

1.2 Tropism and Pathogenesis

1.2.1 The Animal Host

Pathogenesis of BT is similar in sheep and cattle, although disease in sheep is often more severe (Darpel et al., 2007). In cattle, infection can be asymptomatic, although cattle are considered important reservoir hosts and a major source of virus transmission. However, in the recent outbreaks in northern Europe disease in cattle was unusually severe (although with case fatality rates <1%) (Darpel et al., 2007). In sheep and cattle the disease is characterised by a fever lasting for several days. Severely affected animals (mainly sheep) often show increased respiration and hyperaemia of the lips, mucous linings of the mouth, nose and eyelids. The hyperaemia can be accompanied by excess salivation, frothing at the mouth and nose, nasal discharge and oedema of the head and neck. Infected animals lose condition rapidly, especially muscle tone, which affects meat, milk and wool yield. Bluetongue can also cause male sterility and pregnant ewes to abort their foetuses, or lambs to be born with congenital abnormalities. The frequency and severity of clinical signs in animals varies greatly with breed, individual and the serotype and strain of virus.

BTV has a wide tropism in the animal host and infects a number of different cell types including endothelial cells (Maclachlan et al., 2009; Schwartz-Cornil et al., 2008), mononuclear phagocytes (Barratt-Boyes et al., 1992), γδ T cells (Takamatsu et al., 2003), dendritic cells (DC) (Hemati et al., 2009), and a variety of leukocytes (Maclachlan et al., 2009; Schwartz-Cornil et al., 2008), which are postulated to play a major role in virus dissemination. After cutaneous inoculation, virus travels to regional

lymph nodes, followed by dissemination to secondary sites of replication (principally the lungs and spleen) (Maclachlan et al., 2009; Schwartz-Cornil et al., 2008).

1.2.2 In the Insect Vector

When a virus particle is ingested by a haematophagus arthropod during blood feeding on a viraemic ruminant host, the virus passes through the insect in a clearly defined and well studied sequence but barriers to infection must also be overcome.

The virus firstly passes into the lumen of the insect mid gut with the blood meal where it must infect or bypass the monolayer of cells lining the gut wall before it is inactivated or excreted. The most important barrier to BTV transmission in *Culicoides* vector species appears to be the mesenteron infection barrier (MIB) which controls the initial establishment of a persistent infection in cells of the gut wall (Fu et al., 1999; Mellor, 2000). If this barrier is overcome the virus infects and multiplies in the monolayer of mesenteronal cells, and progeny virions (~80 nM in diameter) are released through their abluminal surface, passing through the basal lamina of the mesenteron into the haemocoel. The pore size of the mesenteron has been measured to be 10 nM and so an active transport mechanism is thought to exist for this process to occur (Mellor, 2000). In some susceptible individuals the virus is only able to multiply to low levels and is confined to the gut cell wall cells, unable to escape. In these midges a mesenteron escape barrier (MEB) to virus infection is said to be present and although infected these midges are unable to transmit virus (Jennings and Mellor, 1987). One study of *C.sonorensis* females found that 43.6% had a MEB (Jennings and Mellor, 1987).

BTV has a wide tropism in the insect host and has been shown to replicate in mid-gut cells, neural tissues, fat body cells and salivary glands of infected midges but not in hindgut cells, muscle cells, Malpighian tubule cells or oocyte/nurse cells (Fu et al., 1999). The progeny viruses disseminate through the haemocoel, and must reach the salivary glands. Another barrier to infection occurs here, the dissemination barrier

(DB), which can prevent virus from infecting secondary target organs from the haemocoel, mediated by fat body cells that can absorb virus, possibly acting as part of an insect immune system. Viral infection of the salivary gland cells occurs with a second round of replication. Viruses replicate rather than simply accumulating in the salivary glands, as virus inclusion bodies (VIB's) have been seen in EM studies (Fu et al., 1999). The virus is released with the saliva into the salivary ducts where it is available to infect a second vertebrate host during a subsequent blood meal. Studies with *C.sonorensis* have shown that in the saliva 0.32 to 7.79 $TCID_{50}$ can be excreted (Fu et al., 1999), and this quantity has been shown to be enough to reliably infect a susceptible sheep (Mellor, 2000).

There is no conclusive evidence for transovarial transmission of any *Culicoides*-borne viruses in these insect vectors. A study by Fu *et al.* found that oocytes and nurse cells of *C.sonorensis* did not become infected in infected midges (Fu et al., 1999). This was proposed as evidence that a transovarial transmission barrier exists in these midges which prevents the virus accessing the ovarial tissues (Fu et al., 1999). However, studies by White *et al.* have detected BTV nucleic acid sequences by RT-PCR in larvae reared from surveillance sites in the field, indicating that although no infectious virus was recovered, at least some genetic components of the virus had been transmitted vertically. These authors also suggest that such vertical transmission could represent an important overwintering mechanism for the virus (White et al., 2005).

1.2.3 Virus Transmission

Bluetongue virus is transmitted by insect vectors and therefore disease is normally restricted to areas where these vector species occur. Cattle can act as a 'virus reservoir' for BTV as they can be sub-clinically infected and viraemic for up to 100 days (Hourrigan 1975) and are therefore able to transmit the virus to vectors during a blood meal. Indeed, transmission of BTV is often thought to occur silently in endemic areas through disease resistant host animals such as cattle (Purse et al., 2005).

The geographical distribution, abundance and seasonal activity of insect vectors are thought to determine the occurrence of BT and hence climate change is thought to be having an effect on vector distribution and the spread of BTV. The major insect vector responsible for transmission in southern Europe and Africa is *C.imicola*, whilst in North America the vector is *C.sonorensis* (Mellor, 1990, 2000; Purse et al., 2005). Recently BTV has been found further north in Europe than before and in part, this is thought to reflect a change in the distribution of *C.imicola* (Purse et al., 2005). However, there have also been outbreaks of BT in areas of northern Europe, which have been shown to be free of *C.imicola* by entomological survey (Meiswinkel et al., 2008). This is thought to indicate the involvement of other *Culicoides* species, such as *C.obsoletus* and *C.pulicaris* during the recent spread of BTV in the region.

In 1998, BTV-9 appeared in Greece, signalling the start of a decade of costly outbreaks of bluetongue disease across the whole of Europe. In 2006 a sub-Saharan strain of BTV-8 appeared for the first time in the Netherlands (OIE, 2006). This virus re-emerged in 2007 and infected tens of thousands of holdings across northern Europe causing devastating animal losses. Other BTV serotypes are now also present in Europe including BTV-1, 2, 4, 6, 9, 11, 16 and 25. Recent evidence has identified northern Palaearctic *Culicoides* (particularly members of the *C.obsoletus* and *C.pulicaris* complexes) as competent vectors for BTV transmission, despite initial thoughts that these species would not support BTV replication and transmission. However, it is now clear they can be infected with BTV and, although the rate of infection in some cases is low compared to other competent vector species, they can reach massive population densities, increasing the chance of virus transmission to susceptible ruminant hosts (Carpenter, In press).

1.2.4 Overwintering Mechanisms

Adult *Culicoides* cannot survive freezing temperatures and disappear during the cold winters that are experienced in northern Europe, but are abundant in early and late summer. *Culicoides* midges usually survive the winter months as larvae, which are

able to tolerate the low temperatures. The survival of the virus from one 'vector season' to the next is called 'overwintering', several different mechanisms have been proposed for this, both in the midge and the ruminant host, although the mechanisms involved are not fully understood.

Viraemia in the mammalian host is essential for transmission of BTV. The maximum reported duration of viraemia is approximately 100 days in cattle (Hourrigan and Klingsporn, 1975) and approximately 50 days in sheep (Takamatsu et al., 2003) although up 54 days have been reported in some goat species (Koumbati et al., 1999). The new midges emerging in the early summer should not therefore be re-infected by feeding on cattle or sheep following a BT outbreak in the previous year. However, several clear instances of overwintering have been identified.

An overwintering mechanism for the re-infection of midges from ruminants has been postulated by Takamatsu *et al.* (Takamatsu et al., 2003). The authors provide evidence that the virus could overwinter in the animal host by establishing a persistent infection of γδ T cells (Takamatsu et al., 2003). Feeding of *Culicoides* midges induces skin inflammation, which is accompanied by recruitment of large numbers of activated γδ T cells. The interaction of persistently infected γδ T cells with skin fibroblasts would result in increased virus production at 'biting sites', favouring transmission to the insect vector. However, a more recent study (Lunt et al., 2006) presented data inconsistent with that of Takamatsu *et al.* (Takamatsu et al., 2003). Lunt *et al.* were unable to isolate virus from skin fibroblast cultures created from skin biospies from experimentally infected sheep or naturally infected cattle. The authors also investigated the possible persistence of virus infection in γδ T lymphocytes by analysing cultures of blood leukocytes. However, they failed to detect virus in cultures collected from beyond 7 days post infection indicating that the persistently infected blood leukocytes are an unlikely source of BTV recrudescence (Lunt et al., 2006).

Another mechanism postulated for BTV overwintering is transplacental (vertical) transmission in the mammalian host (Gibbs et al., 1979; Wilson et al., 2009; Wilson and Mellor, 2009). Studies investigating this overwintering mechanism have given conflicting results; some studies have reported experimental transplacental infection by BTV (Parsonson et al., 1994b) whereas others have shown that wild type strains of the virus fail to cross the placental barrier (Parsonson et al., 1994a). Recently evidence for transplacental transmission has been obtained from several countries including Holland and Northern Ireland (Darpel et al., 2009; Menzies et al., 2008; Santman-Berends et al., 2009). Darpel *et al.* showed that ~33% of calves born to dams naturally infected with the strain of BTV-8 circulating in Europe during pregnancy in 2007-2008 were RT-PCR positive and therefore had been infected transplacentally (Darpel et al., 2009).

In temperate regions of the world that do not endure harsh winters, midges are thought to be able to survive throughout the winter months and could possibly transmit virus almost continuously. In colder more northern regions midges usually die-off as a consequence of the adverse weather conditions in winter. However, recent studies have shown that small overwintering populations of midges may be able to survive and remain active in indoor livestock housing (Baldet et al., 2008; Losson et al., 2007), although the authors acknowledge that they could not be certain that the trapped midges were not newly emerged from local breeding sites (Losson et al., 2007). Studies have also suggested that BTV can overwinter in populations of vertically infected immature life stages of the vector (e.g. *Culicoides* larvae) as BTV RNA was detected in field-collected pools of larvae (White et al., 2005). However, no infectious virus was recovered and this study could not conclude whether the BTV-RNA positive larvae would have developed into adult midges with the potential to transmit virus (White et al., 2005).

The above studies have suggested many different potential mechanisms for BTV overwintering; however, the exact mechanism(s) involved in this phenomenon remain to be elucidated.

1.3 Bluetongue Virus Structure

Orbiviruses have a segmented genome consisting of ten segments of dsRNA which are packaged within an icosahedral protein capsid (Mertens and Diprose, 2004). BTV was the first orbivirus whose genome was fully sequenced; firstly with each segment being indvidually sequenced but more recently techniques for rapid full genome sequencing of individual isolates have been developed (Ghiasi et al., 1985; Maan et al., 2007a; Maan et al., 2007b). The structure and biochemistry of the BTV virion has also been widely studied.

Each of the ten dsRNA segments encodes for one of the ten viral proteins (as seen in Figure 1.1). Seven proteins are structural components of the virus particle (VP1 to VP7), which can be resolved by polyacrylamide gel electrophoresis analysis of purified virus particles (Mertens et al., 1987); whilst the other three segments encode non-structural proteins produced during infection (NS1 to NS3/3a) (Mertens et al., 1984). The known functions associated with each of the ten proteins are further discussed below and described in Table 1.3. Past studies, using cryo-electron microscopy and X-ray crystallography, have resolved the atomic structure of the BTV core and the organisation of the genome segments packaged within it (Gouet et al., 1999; Grimes et al., 1998; Grimes et al., 1997; Mertens and Diprose, 2004; Stuart et al., 1998).

1.3.1 Bluetongue virus particle

BTV is a non-enveloped virus. The seven structural proteins assemble to produce a three-layered icosahedral capsid (outer capsid, core and subcore layers), which surrounds the genome of ten linear segments of dsRNA. However, five different structural states in which the BTV virion exists have been described (Peter Mertens, personal communication), but only three of these are well defined and characterised particles that can be purified and are known to be infectious; the intact virus particle, the infectious sub-virus particle or ISVP and the core-particle (Mertens et al., 1987;

Mertens and Diprose, 2004). The remaining two particle types are the subcore and the membrane enveloped virus particles (MEVP) that are released from infected cells by budding.

1.3.1.1 The BTV Intact Virus Particle

The intact BTV particle has a diameter of ~80 nM and has the full complement of seven structural proteins, with an outer capsid composed of 180 copies of VP2 and 360 copies of VP5 arranged with icosahedral symmetry as 60 and 120 trimers respectively (Mertens et al., 1987). These outer capsid components are the most variable proteins of the virus particle and jointly determine virus serotype (Mertens et al., 1989). VP2 is encoded by segment two and is the second largest protein (Mertens et al., 1984), as well as being the most variable protein and controlling serotype, VP2 has been shown to interact with host-cell surface receptors serving as a 'virus-attachment' protein (see Sections 1.4 and 1.6.2) (Hassan and Roy, 1999; Mertens et al., 1989; Roy, 2005). Segment six encodes VP5, the smaller outer capsid protein. VP5 has also been shown to act as a membrane permeabilisation protein after a change in conformation caused by pH, resulting in the protein mediating release of viral particles from endosomal compartments, thus aiding initiation of infection (see Sections 1.4 and 1.6.3) (Hassan et al., 2001; Mertens et al., 1984).

1.3.1.2 Infectious Sub-Virus Particles of BTV

Infectious sub-viral particles (ISVP's) can be generated by treating intact virus with chymotrypsin which cleaves VP2 (Mertens et al., 1987; Mertens et al., 1996). The cleavage sites have not been identified, but it is thought that the protein cleaves into three or four products, depending on virus strain, and these remain associated with the particle (Mertens et al., 1987). ISVP's are thought to be important for infection of the insect vector (see Section 1.3.1.6).

1.3.1.3 The Core and Subcore of BTV

The internal capsid or core-particle consists of a 'core-surface' layer composed of VP7, which surrounds a subcore shell composed of VP3. The atomic structure of the BTV core has been determined, as has that of many of its constituent proteins (Grimes et al., 1998; Mertens et al., 1984; Mertens and Diprose, 2004). The arrangement of the proteins that make up the core-particle can be seen in Figure 1.1.

The outer surface of the core is formed by 780 copies of VP7 (which is encoded by segment seven) arranged as 260 trimers, with T=13 *l* icosahedral symmetry. VP7 has been shown to be involved in cell entry of *Culicoides* cells (see Section 1.6.4) (Tan et al., 2001; Xu et al., 1997). It also has a higher specific infectivity for *Culicoides* cell lines than mammalian cell lines and so is thought to be important for infection of the midge host (see Sections 1.3.1.6 and 1.6.4) (Mertens et al., 1996; Tan et al., 2001).

The underlying subcore structure is composed of 120 molecules of VP3 and is encoded by segment three. This protein layer initially self-assembles determining the overall structure and organisation of the capsid. The VP3 protein interacts with the internal minor proteins and with the dsRNA segments of the virus genome (Diprose et al., 2001; Gouet et al., 1999).

The subcore-particle also contains three other minor viral proteins VP1, VP4 and VP6 encoded by segments one, four and nine respectively. These proteins are the components of the viral transcriptase complex which is activated by removal of the outer capsid proteins; and are involved in the synthesis and capping of viral mRNAs and in the replication of viral progeny (see Figure 1.1). Within the core-particle there are 12 copies of VP1, each of which is associated with a dimer of VP4 (24 copies per particle) and a hexamer of VP6 (72 copies per particle), together these form the replication complexes, ten to twelve of which are present in each particle

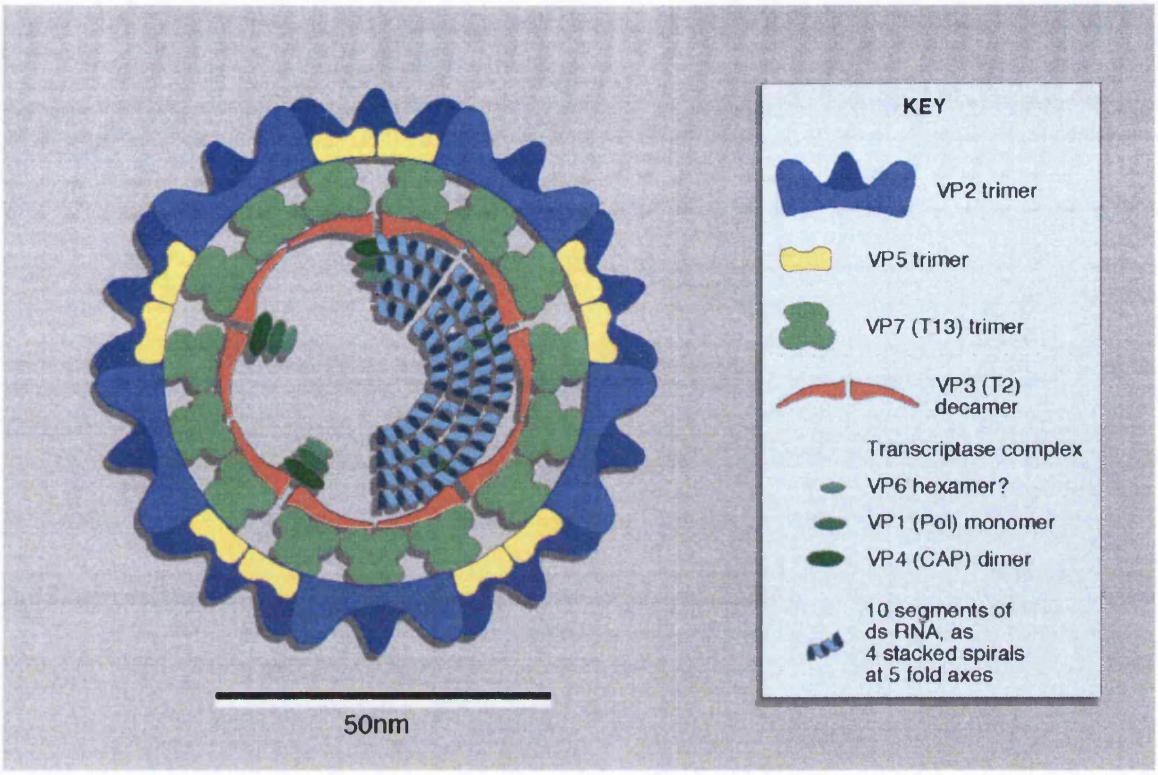

Figure 1.1: The Structural Proteins of BTV
The structure of the virus particle has been described. The figure above shows the position of each structural protein within the intact virion.
Reproduced, with permission from "The bluetongue virus core: a nano-scale transcription machine" by Mertens and Diprose, 2004.

RNA segment	Length, bp	Protein encoded	Protein role
1	3954	VP1	RNA dependent RNA polymerase.
2	2926	VP2	Outer capsid structural protein. Most variable protein which controls serotype. Cell attachment protein.
3	2770	VP3	Structural protein. Part of the sub-core capsid layer. Interacts with the internal minor proteins.
4	1981	VP4	Capping enzyme found within the sub-core.
5	1769	NS1	Non-structural protein. Responsible for forming tubules, which are characteristic of orbivirus replication in the cell cytoplasm.
6	1638	VP5	Outer capsid structural protein. Role in controlling serotype. Causes membrane fusion; has a role in membrane penetration during initiation of infection.
7	1156	VP7	Outer core structural protein. Involved in cell entry.
8	1124	NS2	Non structural protein. Viral inclusion body matrix protein.
9	1046	VP6	Non structural protein. Acts as a helicase.
10	822	NS3 NS3a	Non structural protein. Cytotoxic, can disrupt cell membranes, so possibly involved in cell exit.

Table 1.3: The RNA Segments of BTV
The table shows the ten RNA segments of BTV and describes the proteins encoded by each segment and the role of each protein.
Reproduced, with permission from: www.iah.bbsrc.ac.uk/dsRNA_virus_proteins/BTV.htm

(Stuart et al., 1998). Each protein has a distinct function with VP1 being an RNA-dependent RNA polymerase (Roy et al., 1988; Urakawa et al., 1989); VP4 a capping and transmethylase enzyme (Le Blois et al., 1992; Ramadevi et al., 1998) and VP6 a helicase (Stauber et al., 1997).

1.3.1.4 The Non-Structural Proteins of BTV

Three non-structural proteins (NS1, NS2 and NS3) are also produced in infected cells where they are involved in virus replication and release of progeny virus particles. NS1 (which is encoded by segment five) is found pre-dominantly in the cytoplasm, with only small amounts in the VIB (Eaton et al., 1988). NS1 is the most abundant BTV protein and elicits a strong antibody response in infected animals; thus making it a good marker for detecting infection and for diagnostic tests (Anderson et al., 1993). NS1 also forms tubules in infected cells, which are characteristic of orbivirus replication in the cell cytoplasm (Murphy et al., 1971).

NS2 is encoded by segment eight and is a highly expressed protein that is a primary constituent of the intracellular VIB that are characteristic of BTV and other orbivirus infections.

Segment ten encodes both NS3 and NS3A which are translated by initiation at two different, in frame initiation codons near to the 5' end of Seg-10 mRNA (Wu et al., 1992). The protein is found associated with the golgi apparatus, smooth surfaced vesicles and the plasma membrane at points of virus egress (Hyatt et al., 1991; Wu et al., 1992). These proteins have been shown to be cytotoxic, with the ability to disrupt cell membranes and are expressed at higher levels in insect cells than in mammalian cells. This has prompted speculation that they are of importance in viral egress in insect systems (Guirakhoo et al., 1995; Hyatt et al., 1993; Van Dijk and Huismans, 1988).

1.3.1.5 Other Particle Types

The two other BTV particles are the membrane enveloped virus particle (MEVP) and the subcore. MEVP are produced by virions budding from the cell surface and gaining a membranous envelope in the process. MEVP are infectious but the membrane is thought to be unstable and they have unknown significance in the progression of the disease in the infected animal (Peter Mertens, personal communication) (Mertens and Diprose, 2004). Subcores have a single complete protein layer composed of VP3 (see Section 1.3.1.3). Subcores are unstable and are therefore considered unlikely to be infectious. They can be purified from whole virus in some orbiviruses such as *Equine encephalosis virus*. Subcores have been purified for BTV but they are relatively unstable and readily degrade, and also are thought to be a transition state in assembly or breakdown of the intact virion (Huismans et al., 1987).

1.3.1.6 Particle Infectivity

The three BTV particle types that have been characterised have differing specific infectivity's for different cell types. ISVP's have a similar infectivity to disaggregated virus in the mammalian cell lines that have been tested, but they have been shown to have enhanced infectivity (of ~1000 times) for insect cell lines such as the *C.sonorensis* cell line, KC cells, and for adult vector insects (Mertens et al., 1996). Bluetongue virus cores have a specific infectivity that is similar to that of intact virus for KC cells, but show a reduced infectivity for mammalian cell lines such as BHK cells. Cores have been shown to be non-infectious for the mammalian CHO cell line but can initiate virus replication by lipofection. This strongly suggests that different virus particles enter cells by different mechanisms, and that the primary route of infection in the insect vector is via ISVP's, (Mertens et al., 1996). ISVP's and intact virus particles are both highly infectious for insect and mammalian cell lines. The outer capsid proteins are removed during cell entry and transcriptionally active core-particles are released into the cytosol where virus replication occurs. However, the core-particle is also infectious in its own right demonstrating that VP7 (the core surface protein) can

also mediate cell-attachment and membrane-penetration possibly by a distinct mechanism. Indeed monoclonal antibodies to VP7 or polyclonal antibodies to purified BTV cores can neutralise core-particle infectivity, but not that of either ISVP or intact virus (Mertens personal communication) (I.R.Hutchinson, 1999), supporting the hypothesis that VP7 mediates cell-attachment/penetration by core-particles, but significantly is much less important in these roles than with either of the other two particle types.

1.4 BTV entry, replication and egress

Studies of BTV entry, assembly and egress from cells have led to the proposal of a replication cycle which is shown in Figure 1.2. Parts of this replication cycle are described in more detail in the following sections.

1.4.1 BTV endocytosis

After the BTV virion has bound to the host-cell membrane through cellular interactions with VP2 and VP5 in the outer capsid, it is most likely internalised (Hassan et al., 2001; Hassan and Roy, 1999; Mertens and Diprose, 2004). Early studies using purified virus particles suggested that the BTV outer capsid proteins were removed in a low pH environment (Verwoerd et al., 1972) and shortly after initiation of infection (1 hour) virions are converted to core-particles (Huismans et al., 1987). Evidence from electron microscopy studies in the 1980's suggested that BTV entered mammalian cells via endocytosis and that addition of the virus concurrent with raising endosomal pH with ammonium chloride, methylamine or nigericin inhibited BTV replication (Hyatt et al., 1989). However, the infectivity of the BTV core, which has already lost its outer capsid components is unaffected by ammonium chloride (I.R.Hutchinson, 1999). These studies demonstrate the requirement for a low pH dependent step associated with the early stages of infection and initiation of virus replication and confirm that uptake of intact BTV-1 virus particles by the endocytic route is required to initiate productive infection (Hyatt et al., 1989). Further to this, analysis of thin sections of BTV infected

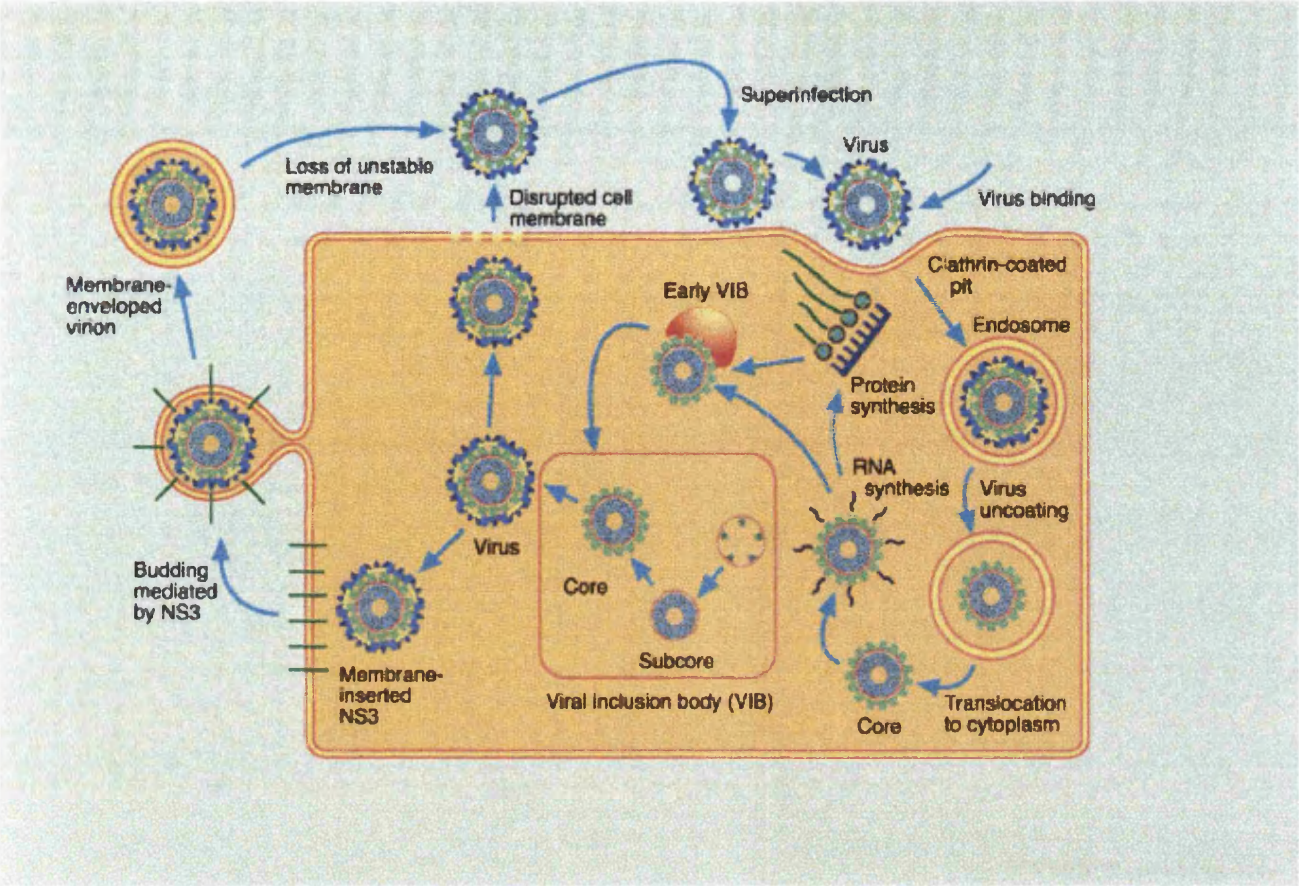

Figure 1.2: The BTV Replication Cycle
The proposed BTV replication cycle was drawn together from the many studies of virus entry, translation, replication and egress.
Virus particles bind at the host-cell surface and are proposed to enter via clathrin-mediated endocytosis whereby they are taken up into a clathrin-coated pit and are transported onto acidic endosomes. Here with the prevailing low pH, the virus particle is uncoated and the core-particle translocated into the cytoplasm. The core-particle is transcriptionally active and the site of mRNA synthesis. Progeny virus particles are assembled with the virus inclusion body (VIB), a characteristic of BTV replication. The newly formed virions exit the cell via budding through interactions with NS3 or by disruption of the cell membrane. The progeny virions can go on to re-infect the same host-cell via superinfection or can infect nearby host-cells.
Reproduced, with permission from, "The bluetongue virus core: a nano-scale transcription machine" by Mertens and Diprose, 2004.

cells at 18 hours post infection revealed virus particles in coated vesicles and in smooth surfaced vesicles which appeared to be endosomes (Hyatt et al., 1989).

For a virus to be visualised by electron microscopy a large amount of input virus particles are required. This could potentially saturate the usual entry pathway and consequently although BTV has been seen in endosomes it is possible that this does not represent a specific or perhaps the only entry mechanism. However, a more recent study has confirmed uptake of BTV-10 into early-endosomes by co-localisation of the outer capsid protein VP5 with transferrin and has demonstrated that separation of the outer capsid and inner capsid occurs within the acidic endosome (Forzan et al., 2007). This study also concluded that entry and infection of Vero or Hela cells by BTV-10 occurs via clathrin-mediated endocytosis, as shown by RNA interference using the μ2 subunit of the AP2 adaptor complex (Forzan et al., 2007). Uncoating of the virus particle is essential for virus replication as transcription of BTV mRNA can only occur when the outer coat proteins VP2 and VP5 have been removed (Hyatt et al., 1989; Van Dijk and Huismans, 1988). The inner core-particle is released into the host-cell cytoplasm thereby initiating the viral replication processes (Mertens and Diprose, 2004).

1.4.2 BTV Transcription and Translation

The replication phase of the BTV infection cycle, as seen in Figure 1.2, is initiated when the transcriptionally active virus core is delivered into the cytoplasm of a susceptible host cell (Van Dijk and Huismans, 1980).

Viruses which replicate within the cytoplasm of a host cell must do so in a way which prevents the induction of host cell anti-viral responses. The role of the core-particle is therefore at least partially to compartmentalise the dsRNA from the cytoplasm. Throughout the replication cycle the ten segments of the BTV genome remain packaged within the core, helping to prevent the activation of host defence

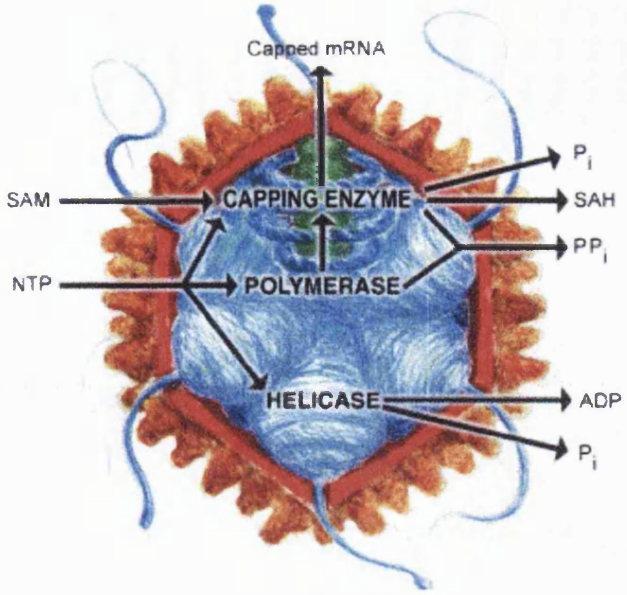

Figure 1.3: The BTV Core Particle during Transcription
This cartoon illustrates the enzymes present within the BTV core particle. Transcription complexes are located at the 5 fold axes and transcribe the mRNAs from each individual segment. For efficient transcription and in order for the enzymes to function; substrates must enter the core particle and waste products must be allowed out. Newly synthesized capped mRNAs are extruded through pores at the 5 fold axes of the core particle.
Reproduced with permission, from "The bluetongue virus core: a nano-scale transcription machine" by Mertens and Diprose, 2004.

mechanisms that would be caused by contact between the dsRNA and the host cell cytoplasm.

The core-particle contains all of the necessary enzymes for transcription and translation, including a helicase (VP6), RNA-dependent RNA polymerase (VP1) and capping enzyme (VP4), as shown in Figure 1.3, all of which make up the transcription complex which is located at the 5 fold axis of the core-particle.

Prior to transcription the two strands of the parental dsRNA segment must be unwound by the helicase, VP6, in order to allow the negative sense template strands to enter the polymerase active site (Stauber et al., 1997). The RNA-dependent RNA polymerase (VP1), requires Mg2+, and transcribes positive sense ssRNA copies from the negative RNA strand of the dsRNA genome, which acts as a template. This process requires nucleotide triphosphates (NTPs) as substrates which enter the core-particle through pores and produces pyrophosphate (PPi) as a by-product (Diprose et al., 2001). The resulting daughter strand is capped with a 5' type 1 cap-structure by VP4. These transcription complexes within the core-particle transcribe the ten genome segments, producing full length mRNA copies, which are extruded through pores at the 5 fold axis of the particle as shown in Figure 1.3(Diprose et al., 2001; Gouet et al., 1999; Grimes et al., 1998; Mertens and Diprose, 2004).

The mRNA copies are subsequently translated into viral proteins in the host cell cytoplasm through interactions of the cap structure with eIF4E. As the 3' ends of viral mRNAs do not possess a poly (A) tail, circularisation of the viral mRNAs during translation is not possible, as is the usual process for host cell mRNAs. It is currently not proven how BTV circularises its mRNA in order for translation to occur, although it has been hypothesised that inverted repeats in the viral UTR may be involved (Roy, 1989).

1.4.3 BTV Assembly and Egress

Progeny virions are formed within a granular matrix known as a VIB which is located next to the nucleus and can be visualised by electron or confocal microscopy, as seen in Figure 1.2 (Hyatt et al., 1989; Mertens and Diprose, 2004). This site of replication is characteristic of BTV infections. The progeny core-particles form and package the viral genome segments within the matrix of the VIB, while outer capsid proteins are added as cores leave the VIB and enter the host-cell cytoplasm. One copy of each of the viral mRNAs is also assembled with the newly synthesised proteins to form nascent virus particles, which mature by a process that involves negative RNA strand synthesis from the positive stand template, thereby reforming dsRNA genome segments within the progeny core-particles.

Mature BTV virions are released from the cell by several distinct processes. Immunogold labelling of VP2 by immunoelectron microscopy in BTV-1 infected SVP cells has revealed that virions are released both as MEVP which 'bud' through the plasma membrane and also as non-enveloped particles, which are extruded directly through the cellular membrane (Eaton and Hyatt, 1989; Hyatt et al., 1989). These studies indicate that released particles and those at the cell surface both remained in association with the cortical layer of the cytoskeleton (Eaton and Hyatt, 1989; Hyatt et al., 1989). More recent studies have shown that the association of mature BTV particles with intermediate filaments are driven by the interaction of VP2 with vimentin, as disruption of vimentin either directly (with acrlyamide) or indirectly (with colchinies) inhibits the trafficking and egress of mature virus particles from infected cells (Bhattacharya et al., 2007). In mammalian cell cultures infected with BTV, the majority of cells show cytopathic effect (CPE), which in many cases involves cell lysis within 24-48 hours post infection. This process inevitably also results in the release of virus particles from the cell cytoplasm into the surrounding culture medium. The relative importance of this release mechanism in the insect vector and mammalian host are poorly understood and all three mechanisms may play a role in the BTV life cycle.

However, productive and persistent BTV infection of *Culicoides* cell cultures does not cause obvious CPE and there are no apparent signs of infection (e.g. increased mortality) in adult midges, thus suggesting that cell damage and lysis do not play a major part of BTV release from cells of the vector insect. Some mammalian cells can also be persistently infected such as γδ T cells (Takamatsu et al., 2003) again suggesting that they also have some mechanism to avoid CPE and cell lysis caused by BTV infection.

The newly-formed progeny virions can infect nearby cells, or are able to re-infect the same cell via a process called 'superinfection' (Mertens and Diprose, 2004). Superinfection of the same cell by progeny viruses, or even other distinct virus strains has been shown to increase the multiplicity of infection (m.o.i.) and enhances the kinetics of BTV replication (Hyatt et al., 1989). This process of superinfection appears likely to be essential for exchange of genome segments by reassortment between distinct virus strains, when they infect the same cell.

1.5 Introduction: Virus Cell Entry Pathways

In order to replicate, viruses must transfer their genome into a susceptible cell and deliver it to a site of replication, such as the cytoplasm or nucleus. Virus internalisation is initiated by binding to specific receptors at the cell surface and culminates in host-cell membrane-penetration. Enveloped viruses are able to enter the cell by direct penetration through the plasma membrane, where the viral envelope fuses with the plasma membrane enabling the genome and viral proteins to be released into the cytoplasm. Viruses which can directly penetrate the plasma membrane by these methods include sindbis virus (Wang et al., 2007) and vaccinia virus (Izmailyan et al., 2006). Enveloped viruses, such as influenza, enter cells following uptake by endocytosis (Lakadamyali et al., 2004; Wang and Jiang, 2009). In contrast non-enveloped viruses appear to exclusively depend on the mechanism of endocytosis for cell entry (Pelkmans and Helenius, 2003).

For non-enveloped viruses, membrane-penetration follows virus endocytosis. Several different endocytosis pathways operate in mammalian cells which deliver cargos to distinct intracellular locations (Doherty and McMahon, 2009b; Mayor and Pagano, 2007). Broadly these can be divided into clathrin-dependent and clathrin-independent mechanisms.

Figure 1.4 shows the different cellular endocytosis pathways, discussed below, which have the potential to be used by viruses for infection of host-cells.

Virus entry by endocytosis is thought to be advantageous for viruses for several reasons. Firstly, virus particles are able to bind anywhere on the cell surface, as cellular receptors destined for endosomes coat the entire plasma membrane. Secondly, following uptake into endocytic vesicles viruses can be actively transported through the cell by 'borrowing' pre-existing endocytic and intracellular transport pathways. Many cellular transport pathways move incoming particles from the periphery of the cell to the interior and viruses using them will therefore be transported to a region near the nucleus, a site of replication for many viruses. Active transport through the cell by endocytosis is also advantageous as the virus does not have to diffuse passively through the cytoplasm, and so is transported more quickly.

Furthermore, to avoid triggering an immune response a virus can shield its exterior proteins by using an endocytosis pathway for transport as the incoming virions are not exposed to the cytoplasm. Endosomes characteristically have a low internal pH which many viruses have evolved to use as part of their entry mechanism, to trigger uncoating of the capsid and release of the genome (Pelkmans and Helenius, 2003). Some viruses are able to uncoat in early-endosomes such as foot-and-mouth disease virus (Berryman et al., 2005; Martin-Acebes et al., 2007), adenovirus type 2 (Gastaldelli et al., 2008) and influenza (Lakadamyali et al., 2004), whereas other viruses such as lymphocytic choriomeninigitis virus (LMCV) (Quirin et al., 2008) require a lower pH to trigger infection and are trafficked to late-endosomes where virus uncoating occurs..

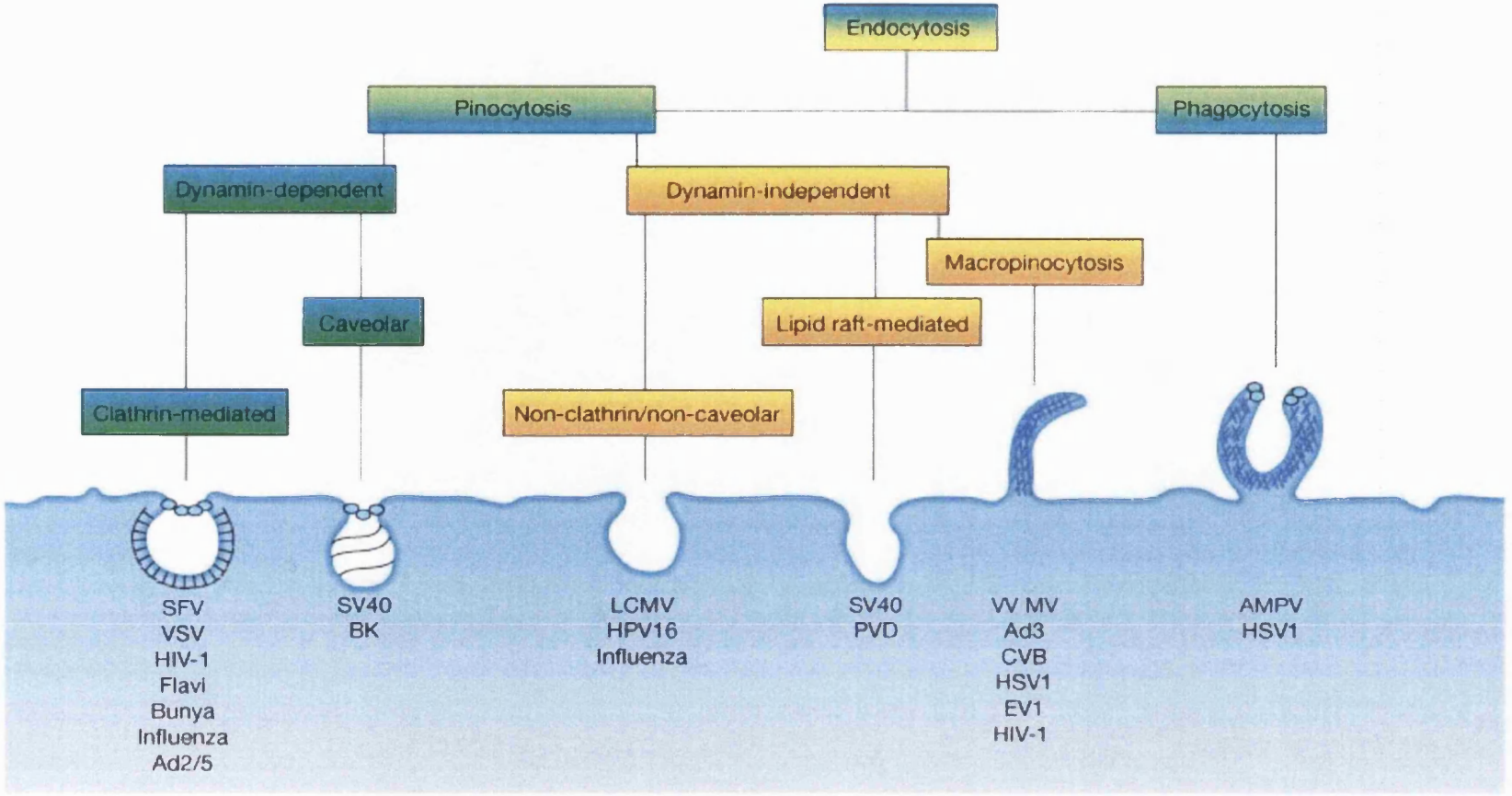

Figure 1.4: The Described Endocytosis Pathways and the viruses that use them for entry and infection
The different endocytosis pathways potentially used by viruses for infection as defined by use of cellular proteins such as dynamin, clathrin and caveolin. Dynamin is shown as small blue circles at the neck of forming endocytic vesicles. The blue lines represent actin.
The viruses shown are: semliki forest virus (SFV); vesicular stomatis virus (VSV); human immunodeficiency virus 1(HIV-1); flaviviruses (Flavi); bunyaviruses (Bunya); influenzavirus (Influenza); adenovirus 2/5 (Ad2/5); simian virus 40 (SV40); BK virus (BK); human papilloma virus 16 (HPV16); lymphocytic choriomeningitis virus (LCMV); polyomavirus (PVD); vaccina virus mature virion (VV MV); adenovirus 3 (Ad3); coxsackievirus B (CVB); herpes simplex virus 1 (HSV1); echovirus 1(EV1) and mimivirus (AMPV). Reproduced from, Virus entry by macropinocytosis, Mercer and Helenius, *Nature Cell Biology,* (2009), 11, 510 – 520.

1.5.1 Clathrin-Mediated Endocytosis

Clathrin-mediated endocytosis is the most well characterised endocytosis pathway and is used for cell entry by a wide range of enveloped and non-enveloped viruses. In part, this could reflect the role of clathrin-mediated endocytosis as the major pathway for receptor dependent endocytosis in many different cell types.

Clathrin-mediated endocytosis involves the formation of clathrin coated vesicles (CCV) that deliver surface receptors and their cargoes to intracellular vesicles (normally early- or sorting- endosomes). This process is initiated by cargo binding to a cellular receptor at the plasma membrane which forms a complex. Clathrin is then recruited locally from the cytosol to the site of pit formation by a process that involves proteins known as adaptors (Doherty and McMahon, 2009b). As the plasma membrane invaginates to form a pit it is coated with clathrin on the cytoplasmic face (CCP) (Ehrlich et al., 2004; Heuser, 1980). Clathrin is a "three legged" structure (or triskelion) composed of three copies each of the 190 kDa clathrin heavy chain (CHC) and the smaller 15 kDa clathrin light chain (CLC) (Kirchhausen and Harrison, 1981; Ungewickell and Branton, 1981). The pit invaginates further as a result of clathrin polymerisation. Other proteins that are involved in this process include BAR proteins which promote dynamin recruitment (see Section 1.5.1.1) and bring the membrane surrounding the neck of the pit into close apposition (Doherty and McMahon, 2009b). The membrane protein dynamin forms a helical polymer around the pit neck and, upon GTP hydrolysis, mediates the scission of the vesicle from the plasma membrane thereby releasing the clathrin-coated vesicle (CCV) containing ligand-receptor complexes into the interior of the cell (Praefcke and McMahon, 2004). This process is rapid and it has been demonstrated that CCP assembly and release from the membrane can take as little as 50 to 150 seconds (Bellve et al., 2006; Merrifield et al., 2005). The CCV is then rapidly depleted of clathrin by auxilin and hsc70 generating a naked vesicle which undergoes further trafficking within the cell before delivering its

cargo through fusion with an intracellular compartment (Doherty and McMahon, 2009b).

Clathrin-mediated endocytosis delivers cargo to early-endosomes. These are often called sorting- endosomes as ligands and receptors are transported away to different destinations. Fusion of the uncoated clathrin-vesicle with early-endosomes is dependent on Rab 5 GTPase and the contents of the vesicle are released into the endosome lumen. Early-endosomes are tubulo-vesicular structures bounded by a single membrane and have a moderately acidic lumen of pH~6.3-6.8 which allows for the dissociation of some ligands from their receptors (Jovic et al., 2010). Early-endosomes are characterised by components of their membrane such as the peripheral membrane protein early-endosomal antigen-1 (EEA-1) which is recognised as a specific marker for early-endosomes (Mu et al., 1995). In early-endosomes sorting occurs for transport onwards to late-endosomes and lysosomes or to recycling-endosomes *en route* back to the cell surface. A pH gradient exists between early- and late-endosomes, with the latter compartment having a more acidic pH of ~5.5. The cation independent mannose-6-phosphate receptor is concentrated within late-endosomes and is a characteristic marker for these compartments (Nicoziani et al., 2000) whilst lysosomal antigen proteins-1 and -2 (LAMP-1 and LAMP-2) are markers of late-endosomes and also lysosomes, in which they are the major protein components of the membrane (Eskelinen, 2006; Pelchen-Matthews et al., 2003). Several acid-activated viruses such as influenza virus (Yoshimura and Ohnishi, 1984) and foot-and-mouth disease virus (Berryman et al., 2005) are known to exploit the low pH within vesicles derived from the clathrin pathway to trigger capsid uncoating and/or membrane-penetration (see Section 1.5). Viruses can be transported from the early-endosomes to recycling- or late-endosomes and lysosomes where infection may also be initiated (Gastaldelli et al., 2008; Quirin et al., 2008). Receptors are also recycled back to the plasma membrane for re-use, either directly from the early-endosome or via

recycling-endosomes in processes that are regulated by Rab 4 and Rab 11 (Sonnichsen et al., 2000; Urbe et al., 1993; van der Sluijs et al., 1992).

At least twenty adaptor proteins have been identified which aid in the processes of cargo selection and CCP formation, membrane invagination and fission. They are central to endocytosis as they connect transmembrane receptors to clathrin and components of the plasma membrane such as phospholipids (Doherty and McMahon, 2009b; Edeling et al., 2006; Owen et al., 2004). Some adaptor proteins (known as clathrin-associated sorting proteins [CLASPs]), such as Autosomal recessive hypercholesterolaemia protein (ARH), Disabled-2 (Dab2), AP2 and arrestins are involved in sorting and recruitment of cargo to the CCV. The adaptor proteins epsin, amphiphysin, and BAR domain containing proteins are also involved with membrane deformation and assembly of the CCP as well as recruitment of dynamin to the neck of the budding vesicle (Doherty and McMahon, 2009b; Edeling et al., 2006; Ford et al., 2002; Miele et al., 2004; Peter et al., 2004). Of the adaptor proteins the AP2 complex, clathrin assembly protein 180 (AP180) and epidermal growth factor receptor substrate 15 (Eps15) are important as they are often targeted to study endocytosis (see Section 1.5.1.2). The AP2 complex is composed of α (100 KDa), β2 (100 kDa), μ2 (50 kDa) and σ2 (19 kDa) subunits called adaptins. AP2 links clathrin to receptors and thereby aids cargo selection (Nankoe and Sever, 2006). AP180 is a neuronal clathrin adaptor and binds directly to the AP2 α subunit forming a complex which is able to recruit clathrin (Hao et al., 1999; Mishra et al., 2001). Eps15 acts as a scaffolding protein by binding to the AP2 adaptor complex and is required for pit formation. It is involved in clathrin-mediated endocytosis of a number of ligands such as transferrin and EGF (Benmerah et al., 1999).

1.5.1.1 The Dynamins

One essential cellular protein required for clathrin-mediated endocytosis is dynamin, a large 100 kDa GTPase which has been strongly implicated in scission of CCV from the plasma membrane. Dynamin is important for endocytosis as it is not only

required for clathrin-mediated endocytosis but also for other endocytosis pathways (e.g. the caveolae-mediated pathway; see Section 1.5.2.1). Dynamin has been described as a 'mechanoenzyme' or 'pinchase' with the ability to constrict and sever the forming vesicle from the donor membrane. Dynamin has been shown to self-assemble forming helical ring structures around the 'neck' of the forming CCP, thus suggesting an important role for this protein in the constriction and scission of the budding vesicle (Cao et al., 2000; Hinshaw and Schmid, 1995; McNiven et al., 2000). As well as an involvement in scission of budding events in endocytic pathways, dynamin has also been shown to be involved in budding events at the golgi in the secretory pathway (Cao et al., 1998; McNiven et al., 2000; Urrutia et al., 1997).

Dynamin is expressed in mammalian tissues as three distinct isoforms, dynamin-1, dynamin-2 and dynamin-3, with each isoform existing as a number of alternative splice variants (Cao et al., 1998; McNiven et al., 2000). Originally each isoform was believed to have four splice variants; however, recent studies have shown that dynamin-1 has 8 and dynamin-3 has 13 different splice forms (Cao et al., 1998). Each of the dynamin isoforms have different tissue distributions in mammalian tissues; dynamin-2 is ubiquitously expressed, whilst dynamin-1 is specifically expressed on neurons and dynamin-3 is pre-dominantly expressed in the brain, lungs and testes (Cao et al., 1998; Ferguson et al., 2007; Liu et al., 2008; Urrutia et al., 1997). The splice variants of dynamin-2 appear to differentially regulate endocytic processes and have been implicated in clathrin-mediated endocytosis, caveolae-mediated endocytosis, macropinocytosis and phagocytosis (Cao et al., 2007; Gold et al., 1999; Mercer and Helenius, 2009; Schlunck et al., 2004). Dominant-negative mutants of each of the splice variants of dynamin-2 (known as '*aa*', '*ab*', '*ba*', and '*bb*') all inhibit clathrin-mediated endocytosis, as shown by a block to entry of transferrin in cells expressing the dominant-negative proteins. The dominant-negative mutant of dynamin-2 '*aa*' is most commonly used in studies to demonstrate a requirement for dynamin in virus entry (Cao et al., 1998; Cao et al., 2000).

Recently a novel rapid-acting and reversible inhibitor of dynamins, dynasore, has been described (Macia et al., 2006). Dynasore inhibits most forms of dynamin including dynamin-1 and dynamin-2, and addition of the reagent prevents uptake of endocytosis maker ligands such as transferrin, low-density lipoprotein and cholera toxin. Dynasore has proven a powerful tool to study endocytosis as it appears to inhibit most forms of dynamin and is fast acting (Macia et al., 2006). Dynasore has now been widely used to demonstrate a requirement for dynamin in endocytosis and infection of viruses such as human papillomavirus type 16 (Abban et al., 2008), bovine papillomavirus type 1 (Abban et al., 2008), vaccinia virus (Mercer and Helenius, 2009) and murine norovirus 1 (Gerondopoulos et al., 2010).

1.5.1.2 Tools to Study Clathrin-Mediated Endocytosis

Clathrin-mediated endocytosis can be studied by following entry of marker ligands that predominantly follow one uptake pathway, or by co-localisation of cargo with markers of endosomal compartments (see above). Transferrin enters cells by clathrin-mediated endocytosis as is used as a marker for early- and/or recycling-endosomes. Cholera toxin B has been shown to use caveolae as its preferred uptake pathway but may also be internalised by clathrin-mediated endocytosis on some cell types whereas dextran (and Lucifer Yellow) are commonly used as marker ligands for macropinocytosis/fluid-phase entry. A number of inhibitors such as chlorpromazine which induces the mis-assembly of clathrin coated pits through interactions with AP2 at the plasma membrane, (Wang et al., 1993) and methyl-β-cyclodextrin can also be used to study endocytosis and these will be discussed further in the results chapters.

Virus uncoating in the endosomal system can be inhibited by pharmacological reagents which raise endosomal pH, such as concanamycin-A and ammonium chloride (Huss and Wieczorek, 2009; Martin-Acebes et al., 2007; Martinez et al., 1996). These reagents raise endosomal pH by different mechanisms. Concanamycin-A is a potent and specific inhibitor of the vacuolar ATPase which inhibits endosomal acidification thereby increasing endosome pH (Huss and Wieczorek, 2009). Ammonium chloride

(NH_4Cl) diffuses across membranes and when in the acidic interior of endosomes becomes protonated thus increasing the pH within the endosomal lumen (Fletcher et al., 1965; Sandvig and Olsnes, 1980).

Other methods to inhibit clathrin-mediated endocytosis are dominant-negative inhibitors of adaptor proteins and accessory molecules, such as AP180, Eps15 and dynamin-2. The C-terminal domain of AP180 (AP180C) contains the putative clathrin-binding site and when expressed in mammalian cells functions as a dominant-negative inhibitor of clathrin-mediated endocytosis (Ford et al., 2001). Over expression of a deletion mutant of Eps15 (Eps15 EΔ95-295) results in the mis-localisation of AP2 which interferes with its recruitment to the plasma membrane and clathrin mediated-endocytosis (Benmerah et al., 1999). As well as dominant-negative inhibitors, the AP2 complex can be targeted using small interfering RNA (SiRNA). A SiRNA to μ2 adaptin of the AP2 complex inhibited clathrin-mediated endocytosis of the transferrin receptor and also inhibited BTV-10 infection of Hela cells by 60% (Forzan et al., 2007; Fraile-Ramos et al., 2003).

1.5.1.3 Clathrin-Mediated Endocytosis and Viral Infection

A number of viruses such as human immunodeficiency virus (HIV) (Miyauchi et al., 2009), semliki forest virus (Helenius et al., 1980), african swine fever virus (Hernaez and Alonso, 2010), borna disease virus (Clemente and de la Torre, 2009), vesicular stomatitis virus (Sun et al., 2005), influenza (Lakadamyali et al., 2004), foot-and-mouth disease virus (Berryman et al., 2005; O'Donnell et al., 2005) and the human rhinovirus minor receptor group (DeTulleo and Kirchhausen, 1998) have been shown to use clathrin-mediated endocytosis as their major entry pathway into mammalian cells. Many viruses are acid activated and require the low pH within endosomal compartments for uncoating and release of their genetic material; viruses such as foot-and-mouth disease virus and human rhinovirus serotype 14 (Bayer et al., 1999; Berryman et al., 2005) have been shown to require early-endosomes whilst infection of

others such as human rhinovirus serotype 2 and influenza (Prchla et al., 1994; Sieczkarski et al., 2003) require exposure to the lower pH of late-endosomes.

1.5.2 Clathrin-Independent Endocytosis

1.5.2.1 Caveolae-Mediated Endocytosis

The most widely studied clathrin-independent endocytosis pathway is the caveolae-mediated pathway. This pathway is dependent on caveolin, dynamin, actin, lipid rafts and cholesterol.

In the caveolar pathway cargoes are internalised into flask-shaped invaginations of the plasma membrane termed caveolae or 'little caves'. Caveolae are 50-80 nM in diameter and are morphogenically distinct from clathrin-coated pits (Lajoie and Nabi, 2007; Stan, 2005). Caveolae exist on the surface of many mammalian cell types and can constitute approx one third of the plasma membrane of some cell types and are especially abundant in smooth muscle, fibroblasts, adipocytes and endothelial cells (Parton and Simons, 2007). As well as single caveolae, multi-caveolar assemblies where many caveolae are connected together at the plasma membrane have also been observed (Doherty and McMahon, 2009b; Parton and Simons, 2007).

Caveolae are formed at lipid rafts. Internalisation of caveolae is not a constitutive event but instead is triggered by binding of ligands, and is dependent on GM1 ganglioside, the actin cytoskeleton, and the recruitment of dynamin for vesicle scission (Henley et al., 1998; Kirkham et al., 2005; Pelkmans, 2005; Pelkmans et al., 2002). Once internalised, caveolae deliver their contents to caveosomes. These are membrane bound cytoplasmic organelles that were first described by Pelkmans *et al.* as distinct endosomal compartments which fused with simian virus 40 (SV40) containing caveolae (Pelkmans et al., 2001). Caveosomes are devoid of markers of classical endocytosis pathways, have a neutral pH and possess multiple flask-shaped caveolar domains enriched in caveolin-1(Parton and Simons, 2007). Recently caveolae have also been shown to be capable of fusing with early-endosomes, thus delivering

their cargo to an acidic environment (see Section 1.5.3) (Pelkmans et al., 2001). The caveosome is believed to be a sorting compartment thus playing a major role in trafficking of ligands and cargo. Ligands such as cholera toxin are trafficked onto the golgi complex, caveolin-1 is recycled back to the plasma membrane, whereas SV40 exits from the caveosome and travels along microtubule-dependent carriers to the endoplasmic reticulum (Norkin and Kuksin, 2005).

1.5.2.1.1 Tools to Study Caveolae-Mediated Endocytosis

A dominant-negative inhibitor of caveolin-1, with GFP tagged to its N-terminus, is commonly used to study this pathway (Pelkmans et al., 2001). As caveolae-mediated entry also requires dynamin for scission of the caveolae from the plasma membrane, the caveolae pathway can also be inhibited by expression of the dominant-negative mutant of dynamin-2 '*aa*' (Damm et al., 2005; Henley et al., 1998; Pelkmans et al., 2001; Pelkmans et al., 2002).

Caveolae-mediated endocytosis is dependent on cholesterol, and caveolae have been shown to disappear in cells treated with pharmacological inhibitors which extract or sequester plasma membrane cholesterol such as methyl-β-cyclodextrin or nystatin and filipin respectively (Ilangumaran and Hoessli, 1998; Norman et al., 1972; Rothberg et al., 1992; Weissmann and Sessa, 1967).

To confirm inhibition of the caveolae-mediated pathway, ligands such as cholera toxin B or control viruses (such as SV40) which are both internalised by this pathway can be used (Henley et al., 1998; Pelkmans et al., 2001). Alternatively cholesterol can be visualised using fluorescent cholesterol binding markers such as filipin III (Bittman and Fischkoff, 1972).

1.5.2.1.2 Caveolae-Mediated Endocytosis and Viral Infection

Much of our knowledge of caveolae and the caveolae-mediated pathway comes from studies with SV40, a non-enveloped DNA virus, (Pelkmans, 2005; Pelkmans and Helenius, 2002; Pelkmans et al., 2001; Pelkmans et al., 2002). A number of other

viruses have also been shown to use caveolae to gain entry for infection including echovirus 1 (Pietiainen et al., 2004; Pietiainen et al., 2005), amphotrophic murine lukeamia virus (Beer et al., 2005), BK virus (Moriyama et al., 2007), human papillomavirus type 31 (Smith et al., 2008) and cell-cultured adapted variants of foot-and-mouth disease virus (O'Donnell et al., 2008).

1.5.2.2 Lipid raft Mediated pathways

A number of non-caveolae entry pathways also originate from lipid rafts. These pathways can be investigated using reagents which extract or sequester cholesterol from the plasma membrane such as methyl-β-cylodextrin or nystatin (see Section 1.5.2.1.1). The differential requirement for dynamin by these pathways can be investigated using dominant-negative mutants of dynamin and the pharmacological inhibitor dynasore (see Section 1.5.1.1). Recently a flotillin-1-dependent pathway has been identified that can mediate uptake of heparan sulphate proteoglycans (Payne et al., 2007) and this pathway may also be raft associated.

Caveolae-independent, lipid raft mediated pathways can also be exploited by viruses for entry and infection. Viruses shown to use these pathways include rotavirus (Sanchez-San Martin et al., 2004), SV40 (Damm et al., 2005), HIV (Vidricaire and Tremblay, 2007), human papillomavirus type 16 (Spoden et al., 2008), feline infectious peritonitis virus (Van Hamme et al., 2008), SARS coronavirus (Wang et al., 2008) and porcine circovirus 2 for infection (Misinzo et al., 2009).

1.5.2.2.1 Clathrin Independent Carrier/GPI-AP Enriched Endocytic Compartments Pathway

Other novel clathrin-, caveolin- and lipid raft-independent processes have recently been identified however presently very little is known of these processes of endocytosis (Lajoie and Nabi, 2007). These pathways have different requirements for cellular proteins such as dynamin, flotillin, small GTPases and for cholesterol and other specific lipids (Damm et al., 2005; Doherty and McMahon, 2009a; Glebov et al., 2006;

Kumari and Mayor, 2008; Lajoie and Nabi, 2007; Lamaze et al., 2001; Mayor and Pagano, 2007; Naslavsky et al., 2003; Nishi and Saigo, 2007; Sandvig et al., 2008).

One such pathway is the CLIC/GEEC (CLathrin Independent Carriers/GPI-AP Enriched Endocytic Compartments) pathway which delivers cargo from CLICs (which are a distinct clathrin-independent vesicle) to tubular-vesicular acidic-endosomes termed GPI-AP enriched early-endosomal compartments or GEECs (Chadda et al., 2007; Kalia et al., 2006; Lundmark et al., 2008; Sabharanjak et al., 2002). The vesicles derived from this pathway can also fuse with early- and recycling-endosomes thereby further exposing their contents to low pH (Chadda et al., 2007; Chatterjee and Mayor, 2001; Kalia et al., 2006; Sabharanjak et al., 2002). The intracellular destination for material internalised by this pathway appears to differ between cell types and CLIC/GEECs can also fuse with late-endosomes in BHK cells (Fivaz et al., 2002; Sabharanjak et al., 2002). It is unknown if these differences reflect the presence of specific CLIC/GEEC subtypes or are due to other cell type-dependent factors.

The CLIC/GEEC pathway is regulated by the protein GTPase Regulator Associated with Focal Adhesion Kinase-1 (GRAF1), which exhibits GAP activity for the small G proteins RhoA and Cdc42 (Chadda et al., 2007; Lundmark et al., 2008). This entry mechanism is sensitive to actin disruption and mild cholesterol depletion and is not inhibited by the expression of dominant-negative dynamin proteins that inhibit clathrin-mediated endocytosis (Chadda et al., 2007; Kalia et al., 2006; Sabharanjak et al., 2002). Flotillin has also been found to be concentrated in the membranes of early CLIC/GEEC intermediates and so may play a role in endocytosis by this pathway (Lundmark et al., 2008).

Disruption of the CLIC/GEEC pathway can cause compensatory endocytosis of GPI-linked proteins via clathrin-mediated endocytosis (Sabharanjak et al., 2002), but whether these internalised proteins are trafficked to their intended destinations remains unclear.

1.5.2.3 Macropinocytosis

Studies of macropinocytosis have been hampered by a lack of specific markers for macropinosomes or other components of the pathway. Historically macropinocytosis was considered to be simple non-specific uptake mechanism, however, it is now clear from the large and rapidly expanding number of studies on this process that it is far more complex than originally perceived and it remains to be seen if there are in fact multiple macropinocytosis pathways, which may be regulated by cell type specific factors. However, recent studies have made attempts to describe and characterise this pathway more fully. Nevertheless, markers such as fluorescent dextran and lucifer yellow have proven to be useful tools for microscopy studies (Jones, 2007; Kerr and Teasdale, 2009).

Macropinocytosis is responsible for the majority of fluid-phase entry in a number of cell types and is particularly active in specialised antigen presenting cells such as dendritic cells (Kerr and Teasdale, 2009; Mercer and Helenius, 2009; Swanson and Watts, 1995). Macropinocytosis is constitutive in some cell types such as macrophages but in others requires activation by growth factors such as receptor tyrosine kinases or pharmacological activators of protein kinase C (Grimmer et al., 2002; Kerr and Teasdale, 2009; Mercer and Helenius, 2009; Swanson and Watts, 1995).

A defining characteristic of macropinocytosis is a requirement for actin-dependent reorganisations of the plasma membrane to form macropinosomes, morphologically heterogenic vesicles lacking coat structures and ranging in size from 0.5 to 5 μM (Mercer and Helenius, 2009; Swanson and Watts, 1995). The shape of the macropinosomes can take many forms, either blebbing of the plasma membrane, lamellipodial formation or the generation of circular ruffles. These structures subsequently close-up to form macropinosomes (Doherty and McMahon, 2009b; Jones, 2007; Mercer and Helenius, 2009). Transmission electron microscopy experiments on cells undertaking virus uptake have been extremely useful to aid

visualisation of the size, shape and coat structures on the virus containing vesicles thus characterising the process further.

It is thought unlikely that macropinosomes mature via a common pathway and are delivered to a single pre-defined location (Swanson and Watts, 1995). In macrophages, macropinosomes have been shown to move inwards from the plasma membrane, towards the centre of the cell and in doing so lose water and shrink which appears to decrease their internal pH. Macropinosomes have been shown to fuse with either early- or recycling- endosomes, or with late-endosomes and lysosomes, or with the plasma membrane thus recycling their contents back to the extracellular space (Hamasaki et al., 2004; Hewlett et al., 1994; Jones, 2007; Racoosin and Swanson, 1993). During trafficking macropinosomes acquire markers of late-endosomes such as Rab 7 before eventually merging with lysosomes (Kerr and Teasdale, 2009; Racoosin and Swanson, 1993; Swanson and Watts, 1995). However, trafficking of macropinosomes through the cell and fusions with endosomal compartments remains unclear and thus requires further study, although these events appear to be different for different cargoes and cell types.

1.5.2.3.1 Tools to Study Macropinocytosis

As macropinosome formation is dependent on actin re-arrangements, inhibitors of actin microfilaments are commonly used to inhibit macropinocytosis. Pharmacological inhibitors called cytochalasins act immediately and cause disruption of the actin microfilaments, thus inhibiting membrane ruffling. Cytochalasin B causes the actin microfilaments to be shortened by blocking monomer addition to the growing end (Krishan, 1972; Miranda et al., 1974a; Miranda et al., 1974b) whilst cytochalasin D binds to the positive end of F-actin and prevents further addition of G-actin thus preventing growth of the microfilament (Sampath and Pollard, 1991). Other pharmacological actin microfilament inhibitors also exist such as latrunculin A which causes polymerization of the actin microfilaments (Coue et al., 1987) and jasplakinolide which stabilises actin microfilaments (Holzinger, 2009; Holzinger and Meindl, 1997).

Another cytoskeletal element, microtubules, has also been shown to be important for macropinosome fusion, and thus this process can be inhibited by microtubule disrupting drugs such as nocodazole (Jones, 2007; Vasquez et al., 1997). A type of macropinocytosis that involves Rac1-dependent membrane ruffling is also cholesterol sensitive (Grimmer et al., 2002; Lajoie and Nabi, 2007).

The role of dynamin in macropinocytosis is currently unclear. Dynamin is expressed in mammalian cells as three distinct isoforms: dynamin-1 to -3; each existing as a number of splice variants (Cao et al., 2007). The different spliced variants of dynamin-2 appear to regulate different endocytic processes and dominant-negative mutants of the '*ba*' and '*bb*' splice variants of dynamin-2 inhibit uptake of dextran, suggesting a role for these dynamin variants in macropinocytosis and fluid-phase entry (see Section 1.5.1.1) (Amyere et al., 2002; Cao et al., 2007). Dynamin-1 has also been suggested to play a role in PDGF-stimulated macropinocytosis (Liu et al., 2008). Studies to further elucidate the role of dynamin in fluid-phase endocytosis and macropinocytosis have given conflicting results (Cao et al., 2007; Huang et al., 2008; Meier et al., 2002; Mercer and Helenius, 2008; Schlunck et al., 2004). It has been suggested that these discrepancies could partly result from the use of different methods to trigger macropinocytosis and by the use of different approaches to inhibit dynamin, either by expression of dominant-negative proteins or the pharmacological inhibitor dynasore (Cao et al., 2007; Ferguson et al., 2007; Liu et al., 2008; McNiven et al., 2000). Similarly, viruses that use macropinocytosis for infection such as vaccinia virus appear to display different sensitivities to dynamin inhibition and this virus has been reported to be both dynamin-dependent (Huang et al., 2008) and dynamin-independent (Mercer and Helenius, 2008).

Activation of receptor tyrosine kinases, like epidermal growth factor receptor (EGFR) and platelet derived growth factor receptor (PDGFR), lead to an increase in actin polymerization at the cell surface resulting in an elevation in actin-mediated ruffling and ultimately an increase in macropinosome formation. The dynamics of the

actin cytoskeleton is co-ordinated by the three Rho-GTPases; Rho, Rac and Cdc42 (Nobes and Marsh, 2000; West et al., 2000). Macropinocytosis has been shown to be inhibited when membrane ruffling is inhibited in leukocytes and macrophages by the expression of dominant-negative Rac 1 (N17 Rac 1) (Allen et al., 1997; Cox et al., 1997; West et al., 2000). The GTPase Arf 6 activates Rac and has also been implicated in the regulation of macropinosome formation (Santy and Casanova, 2001; Song et al., 1998).

Intracellular trafficking, targeting and fusion of endosomes is controlled by Rab GTPases which act as molecular switches and play important roles in the formation and movement of endocytic vesicles (Zerial and McBride, 2001). Rab 34 has been implicated in macropinocytosis/fluid-phase entry and has been observed associated with macropinosomes at the sites of membrane ruffling (Sun et al., 2003). However, it is currently unknown if the involvement of Rab 34 is cell type specific as other studies found that Rab 34 was localised to the golgi and plays a role in the secretory pathway and was not involved in macropinocytosis (Goldenberg et al., 2007).

Rab 5 has also been implicated in membrane ruffling and macropinocytosis (Lanzetti et al., 2004; Schnatwinkel et al., 2004) and expression of dominant-negative or constitutively active Rab 5 was found to block infection of coxsackievirus B via macropinocytosis in caco-2 cells (Coyne et al., 2007). Similarly, overexpression of the dominant-negative GDP bound mutant Rab 5 S34N inhibited circular ruffle formation (Lanzetti et al., 2004).

Amiloride and its more potent analogue, 5-(N-Ethyl-N-isopropyl) amiloride [EIPA], inhibit N^+/H^+ exchangers in the plasma membrane and thus inhibit macropinocytosis (Dowrick et al., 1993; Gerondopoulos et al., 2010; Kee et al., 2004) but do not appear to inhibit other endocytic pathways such as clathrin-mediated endocytosis (Kerr and Teasdale, 2009; West et al., 1989). Amilorides and their analogues are thought to act by lowering cytoplasmic pH (Pannocchia et al., 1996).

However a recent study has suggested that amiloride (and its related compounds) do not directly inhibit macropinocytosis, instead the inhibitory effects are due to submembranous acidification which appears to prevent signalling through Rac 1 and Cdc42 (Koivusalo et al., 2010).

Cellular kinases are also required for macropinocytosis, such as the p21-activated kinase (PAK1) and phophatidylinositol 3-kinase (PI3K). PAK1 binds and activates Rac; it has been observed in membrane ruffles and is required for actin remodelling and macropinosome formation (Dharmawardhane et al., 2000; Knaus et al., 1998). PAK1 phosphorylates serine 147 of the C-terminal-binding protein-1/Brefeldin A-ADP-ribosylated substrate (CtBP1/BARS) and has been demonstrated to be essential for the final fission of macropinosomes from the plasma membrane (Dharmawardhane et al., 2000; Doherty and McMahon, 2009b; Mercer and Helenius, 2009). The role of PAK1 in macropinocytosis has been investigated using the PAK1 auto-inhibitory domain (AID), which functions as a dominant-negative inhibitor, and a dominant-negative mutant (D355A) of CtBP-1. In macrophages, macropinocytosis is dependent on PI3K which is required for membrane closure to create macropinosomes (Araki et al., 2003). This process can be inhibited by PI3K inhibitors such as wortmannin and LY290042. However, these reagents can also affect other types of endocytosis (Amyere et al., 2002; Amyere et al., 2000; Araki et al., 2003; Falcone et al., 2006).

1.5.2.3.2 Macropinocytosis and Viral Infection

A number of viruses have been shown to exploit macropinocytosis, or macropinocytosis-like endocytic pathways, for cell entry and infection including vaccinia virus (Huang et al., 2008; Locker et al., 2000; Mercer and Helenius, 2008), coxsackievirus B3 (Coyne et al., 2007), HIV (Marechal et al., 2001), kaposi's sarcoma-associated herpesvirus (KSHV) (Raghu et al., 2009), echovirus 11 (Karjalainen et al., 2008; Liberali et al., 2008) and adenovirus type 3 (Amstutz et al., 2008). Adenoviruses type 2 also requires macropinocytosis for entry; however macropinocytosis is not used

directly for virus entry but appears to enhance virus escape from early-endosomes (Meier et al., 2002). Some of these viruses have the ability to utilise multiple entry pathways, such as HIV which enters via macropinocytosis in macrophages and endothelial cells but in other cell types uses clathrin-mediated endocytosis (Marechal et al., 2001; Miyauchi et al., 2009).

1.5.2.4 Phagocytosis

Phagocytosis is a specific form of endocytosis that is used for engulfing solid particles such as bacteria. Cargoes are internalised in a plasma membrane coated compartment, a phagosome. Phagocytosis is also involved in the acquisition of nutrients in some cells types and has an important role in the immune system as it is a major mechanism used for removal of pathogens and cell debris (Marsh, 2001; Mayor and Pagano, 2007).

Phagocytosis is distinct from macropinocytosis despite both processes being formed from actin-dependent extensions of the plasma membrane (Mayor and Pagano, 2007). The membrane re-arrangements of phagocytosis are distinctive and result in the formation of a cup shaped protrusion that is formed from two opposing membrane extensions which envelope around the cargo destined to be internalised (Doherty and McMahon, 2009b; Kerr and Teasdale, 2009; Marsh, 2001; Mayor and Pagano, 2007).

Some phagocytosis cargoes are first coated with opsonins, host proteins which aid recognition by cellular receptors (Marsh, 2001). Then the particle is enclosed within a membrane bound phagosome by an actin-dependent clathrin-independent process which is mediated through the direct interaction of the Fc receptor with the opsonised particle thereby creating a tight-fitting vesicle around the particle as it is internalised (Marsh, 2001).

The molecular mechanisms of phagocytosis have still to be clearly defined although some cellular proteins required for the other endocytic mechanisms have been shown to be required. Phagocytosis, like macropinocytosis requires cortical actin

for the complex plasma membrane re-arrangements which occur (Amyere et al., 2002). Dynamin-2 has been shown to be required for phagosome scission in macrophages and may also be required in other cell types (Abban et al., 2008; Gold et al., 1999; Marth and Kelsall, 1997).

1.5.3 Pathway Merging

As described above, endocytosis comprises of several different routes for receptor and cargo internalisation. Historically, these pathways were considered as being distinct mechanisms. However, it is now clear that fusion between vesicles derived from seemingly different pathways can occur post uptake.

Two pathways shown to be capable of merging are the caveolae-mediated pathway and the endo-lysosomal pathway. Live-cell imaging has shown that caveolin-1 positive vesicles are able to associate with early-endosomes in a so called 'kiss-and-run' mechanism (Pelkmans and Helenius, 2003). These studies have shown that caveolin-1 and two caveolae cargo (SV40 and cholera toxin) are trafficked in a Rab 5-dependent manner to early-endosomes. However, for SV40 it is unclear if this leads to productive infection as the virus appeared to be trapped within the endosomes from where a productive infection could not occur (Pelkmans and Helenius, 2003).

Other studies have shown that vesicles derived from a number of clathrin-independent pathways can fuse with early- or late-endosomes (Delaney et al., 2002; Naslavsky et al., 2003; Sharma et al., 2003). Similarly, a number of viruses have been shown to use such mechanisms for infectious entry including foot-and-mouth disease virus (O'Donnell et al., 2008), human papillomavirus type 31 (Smith et al., 2008), LMCV (Quirin et al., 2008; Rojek et al., 2008a), KSHV (Raghu et al., 2009) and mouse polyomavirus (Liebl et al., 2006; Mannova and Forstova, 2003). These studies demonstrate that viruses can transfer between different entry pathways within cells. This may be an advantage as viruses that require exposure to low pH for infection can

enter cells via clathrin-independent pathways but still be exposed to acidic endosomes for uncoating and membrane-penetration (Pelkmans and Helenius, 2003).

1.5.4 The Ability of Viruses to use Multiple Entry Pathways

As discussed above viruses can use many different endocytosis pathways to gain entry into cells. However, evidence is accumulating which shows that some viruses are able to use more than one endocytosis pathway for infection. For example, Simian Virus 40 (SV40) has been shown to enter cells by caveolae and is then transport via caveosomes to the endoplasmic reticulum (Pelkmans et al., 2001). However, studies with caveolin deficient cells and embryonic fibroblasts derived from caveolin-1 knockout mice have shown that SV40 can also infect cells via a caveolae independent pathway (Damm et al., 2005). This pathway is cholesterol and tyrosine kinase dependent but independent of clathrin, dynamin, and Arf 6.

Human immunodeficiency virus (HIV) has also been shown to exploit multiple entry mechanisms. Productive entry of HIV can occur by direct fusion at the plasma membrane (Marsh and Helenius, 2006). However, recent studies have shown that HIV can also infect cells via a dynamin-dependent endocytosis mechanism (Miyauchi et al., 2009). In addition, Daecke *et al.*, have shown that HIV infection is inhibited in cells where clathrin-mediated endocytosis has been inhibited by expression of dominant-negative mutants of Eps15 and dynamin (Daecke et al., 2005). Studies of HIV-1 infection in polarised trophoblastic cells have identified a clathrin-, caveolae-, and dynamin-independent entry pathway that requires cholesterol (Vidricaire and Tremblay, 2007). In these cells HIV-1 did not initially co-localise with transferrin, but at later time points some virions were seen to migrate to transferrin-enriched endosomes, which suggests trafficking occurs from the non-classical pathway to early-endosomes (Vidricaire and Tremblay, 2007).

Influenza virus is an example of another virus that can use both clathrin-dependent and clathrin-independent endocytosis for infectious entry. On entry, virions

traffic through early-endosomes to late endosomes where exposure to low pH triggers fusion between the viral and endosomal membranes and release of the vRNPs into the cell (Lakadamyali et al., 2004). However, influenza virions have been observed by EM micrographs in smooth vesicles suggesting that non-clathrin uptake mechanisms may also be used (Matlin et al., 1981). Further studies have shown that different serotypes of influenza can enter cells via different mechanisms; entry of influenza A virus H5N1 into the human lung carcinoma cell line A549 occurs via clathrin-mediated endocytosis (Wang and Jiang, 2009), whereas entry of influenza H1N1 into Hela cells is via a clathrin- and caveolin-independent pathway as dominant-negative mutants of Eps15 and caveolin-1 did not block infection (Lakadamyali et al., 2004; Sieczkarski and Whittaker, 2002). However, although these findings were originally interpreted to indicate that clathrin-mediated endocytosis was blocked it is now know that epsin 1 serves as a cargo-specific adaptor for influenza virus entry and it is possible that influenza virus enters cells through an Eps15-independent clathrin-mediated pathway (Chen and Zhuang, 2008). Other studies by Rust *et al.*, (Rust et al., 2004) have used real-time fluorescence microscopy to follow entry of individual influenza viruses in living cells. This study concluded that influenza viruses enter cells via multiple endocytic pathways, including both clathrin-mediated and a clathrin- and caveolin-independent endocytosis pathway. Both of these entry mechanisms were shown to result in viral fusion with intracellular membrane compartments and thus infection.

In Vero cells, dengue virus serotype 1 was shown to enter by clathrin-mediated endocytosis whereas serotype 2 entered the same cells via a non-classical endocytosis pathway that was shown to be clathrin-, caveolae-, and lipid raft-independent but dynamin-dependent (Acosta et al., 2009). Other studies on the entry mechanisms of several dengue serotypes into HepG2 cells showed that although the majority of virus used clathrin-mediated endocytosis for entry, around ~20% was able to use macropinocytosis, showing that multiple entry mechanisms can be utilised simultaneously (Suksanpaisan et al., 2009).

Some viruses, such as foot-and-mouth disease virus (FMDV) can use multiple uptake mechanisms as the results of virus adaption for growth in cultured cells. Field strains of FMDV use clathrin-mediated endocytosis for entry (Berryman et al., 2005; O'Donnell et al., 2005) whereas cell culture adapted variants of the virus have been shown to enter cells via caveolae (O'Donnell et al., 2008).

It is clear from the studies described above that many more viruses that can use multiple entry mechanisms for infection will be discovered in the future and that these viruses will provide fundamental insights into endocytosis.

1.6 The Role of Structural Proteins in Bluetongue Virus Uptake

1.6.1 The BTV Receptor

The replication cycle is initiated by virus binding to a specific cellular receptor on the target cell membrane. This can lead to internalisation of the virus particle using one of the many known endocytic pathways as described above (see Section 1.5 and Figure 1.4).

For BTV, the identity of the cellular attachment receptor is currently unknown although several molecules have been implicated and could be involved. One proposed class of proteins hypothesised to be the BTV cellular receptor is the glycoproteins, with a second protein molecule serving as a co-receptor (Hassan and Roy, 1999). In mouse fibroblast L929 cells which are BTV permissive, glycophorin A was able to block BTV-10 entry completely, suggesting that it is the BTV receptor molecule. Also VP2, one of the surface proteins of the intact virion, has been shown to be the only BTV protein that binds to glycoporin A; further suggesting glycophorin A is the host-cell receptor, at least for this virus strain, and that VP2 is the entry protein (Hassan and Roy, 1999).

1.6.2 The Role of VP2 in BTV Entry

VP2 is thought to be the primary cell-attachment protein, partly because it is the outermost protein on the virion surface, but also because it is the primary target for

neutralising antibodies. Early studies demonstrated that BTV particles lacking VP2 but with exposed VP5 and VP7 were incapable of binding to BHK cells, indicating that VP2 may be responsible for cell binding (Huismans and Erasmus, 1981). More recently, studies using purified proteins have demonstrated that VP2 is likely to play a major role in virus entry into mammalian cells (Hassan et al., 2001; Hassan and Roy, 1999). These studies also demonstrated that VP2 binds strongly to glycophorin A, a component of erythrocytes. This, the authors suggest, indicates that VP2 may be responsible for the transmission of the virus from the vector to the host via the bloodstream (Hassan and Roy, 1999). VP2 appears to be proteolytically degraded once the virions reach endosomal compartments (Hassan and Roy, 1999), which is important for degradation of the intact particle to release the virus-core. However, although VP2 does not interact with host-cell membranes, VP5 exhibits membrane-interacting properties after it has undergone a low pH activation step that may alter its conformation, enabling it to become fusion-competent (Forzan et al., 2004).

1.6.3 The Role of VP5 in BTV Entry

VP5 has been shown to share structural features with class 1 fusion proteins of several enveloped viruses. Purified VP5 can bind to mammalian cells but was not able to be internalised suggesting it is not involved in cell-attachment or receptor-mediated endocytosis. In the BTV replication cycle VP5 is thought to act as a membrane-permeabilisation protein that mediates release of viral particles from endosomal compartments into the cytoplasm after undergoing a pH-dependent conformational change that renders it capable of interacting with cellular membranes (Forzan et al., 2004). This ability to destabilise and penetrate cellular membranes may result in translocation of the core-particle from acidic endosomes into the cellular cytoplasm for replication (Forzan et al., 2004; Hassan et al., 2001).

1.6.4 The Role of VP7 in BTV Entry

The outer protein on the BTV core-particle is VP7. Bluetongue virus core-particles are highly infectious for *Culicoides* vectors and *Culicoides*-derived cell

cultures (KC cells) (Mellor, 2000; Mertens et al., 1987; Mertens et al., 1996). The specific infectivity of in vitro-generated cores for KC cells was directly comparable to that of the intact virus particles and core-particles were similarly infectious when oral infectivity studies were carried out using *Culicoides* species (Mertens et al., 1996). The high level of core-associated infectivity for KC cells suggests the initial stages of core-cell interaction and entry use an alternative entry mechanism to that used by complete particles (Tan et al., 2001).

VP7 has an arginine-glycine-aspartate (RGD) tripeptide motif present at amino acid residues 168 to 170, one of the ligand sites recognised by members of the integrin family such as fibronectin, vitronectin and fibrinogen. This motif has been shown to be accessible on the exterior of the core-particle and could therefore play a role in cell entry (Grimes et al., 1998). RGD motifs are important for the binding of many ligands and other viruses to cells. *Foot-and-mouth disease virus* binds to integrins on the host-cell membrane surface via an 'RGD loop' on the exposed surface of VP1 (Jackson et al., 2004; Jackson et al., 1997). Invertebrates such as *Drosophila melanogaster* and *Caenorhabditis elegans*, possess cell surface integrin subunits similar to those of vertebrates (Brower, 2003). *Drosophila* has a αPS2 integrin subunit which is an RGD-binding α family (Brower, 2003). Further studies on *Drosophila* have shown that binding of the αPS2βPS integrin to ligands can be decreased by the presence of RGD peptides (Bunch et al., 2005), indicating that these peptides bind to the integrin and block binding to its ligand. Due to the RGD motif present on VP7, this protein has been proposed as the attachment protein of BTV for cellular receptors in *C.sonorensis* (Xu et al., 1997). However, this does not explain the much higher specific infectivity of ISVP for *Culicoides* cells and insects. It also fails to explain why antibodies to VP7 which neutralise core-particles, do not neutralise the infectivity of virus or ISVP for insect cells (Hutchinson et al 1999). However, another study using invertebrate cell lines has indicated that the RGD of BTV VP7 is responsible for the *Culicoides* cell binding activity of this protein (Tan et al., 2001). This study also demonstrated that RGD site specific

monoclonal antibodies blocked core-like particles binding to KC cells (Tan et al., 2001). It is therefore plausible that RGD-integrin binding is an initial step of BTV core attachment to insect cells (Tan et al., 2001). However, studies by Hutchinson (I.R.Hutchinson, 1999) showed that BTV cores did not bind the integrin αVβ3; which has a relaxed specificity and therefore the ability to bind a wide range of ligands and is demonstrated to be the best RGD-binding integrin (Arnaout et al., 2002). Further studies by Hutchinson showed that binding of the BTV core-particle to fixed KC cells was inhibited by glycosaminoglycans (GAGs) (I.R.Hutchinson, 1999). GAGs are expressed on virtually all cell types (Jackson et al., 1991). The potency of inhibition of binding was correlated with the degree of sulphation of the GAG and therefore negative charge, suggesting that electrostatic interactions may be a basis of initial binding of BTV cores to fixed KC cells (I.R.Hutchinson, 1999).

1.7 Members of the family *Reoviridae* and their entry mechanisms

Viruses belonging to other genera of the family *Reoviridae* have been investigated to determine their cell-attachment and entry mechanisms. Entry mechanisms for two genera are described below.

1.7.1 Orthoreoviruses

Similar to BTV, *Orthoreovirues* have a genome comprising of 10 dsRNA segments. The intact virion is comprised of eight different structural proteins formed into two concentric capsids. The outer capsid proteins, σ1 and σ3 are involved in cell-attachment and membrane-penetration respectively (Chandran and Nibert, 2003). Mammalian orthoreoviruses have two recognised subviral particles; intermediate subvirion particles (ISVP's) and core-particles. The ISVP has lost σ3, (following degradation by endocytic proteases), σ1 is conformationally altered and μ1 is the major surface protein (Borsa et al., 1981; Chandran and Nibert, 2003; Guglielmi et al., 2006). The ISVP's remain highly infectious indicating that σ3 is not directly required for cell entry. Orthoreovirus ISVP have also been shown to be capable of directly penetrating the plasma membrane, possibly due to cell-attachment protein σ1 being in a fully

extended conformation (Jiang and Coombs, 2005). Unlike BTV, mammalian orthoreovirus core-particles are non-infectious and lack μ1 and σ1, which also shows that these proteins are important for infection (Chandran and Nibert, 2003) although like core-particles of BTV in CHO cells, orthoreovirus core-particles are able to initiate infection and replication if transfected directly into cells (Jiang and Coombs, 2005).

Junctional adhesion molecule-A (JAM-A) functions as a receptor for reoviruses and binds the σ1 head (Barton et al., 2001; Campbell et al., 2005; Forrest and Dermody, 2003; Kirchner et al., 2008; Tyler et al., 2001). Co-receptors such the β1 integrin (Maginnis et al., 2006) and sialic acid (for serotype 3 strains) (Guglielmi et al., 2006) have been shown to further mediate reovirus internalisation.

Post-attachment, it is proposed that orthoreovirus virions are removed from the cell surface membrane by receptor-mediated endocytosis, (Chandran and Nibert, 2003; Jiang and Coombs, 2005). Internalisation of the virus is followed by a stepwise uncoating of the outer capsid in an acidic endosomal compartment, such as endosomes or lysosomes, to produce ISVP's (Borsa et al., 1981; Martinez et al., 1996). ISVP particle release from acidic cellular compartments is not fully understood, although these particles have been shown to be able to form small pores in model membranes (Agosto et al., 2006). These pores are not large enough to allow release of an ISVP or core-particle and the authors propose that pore formation in a vacuole such as an endosome or lysosome might lead to osmotic swelling of the compartment enabling release (Agosto et al., 2006) into the cytosol where replication occurs (Chandran and Nibert, 2003; Jiang and Coombs, 2005).

1.7.2 Rotaviruses

The entry mechanisms used by members of the genus *Rotavirus* could also offer some insights into generalised entry and infection mechanism used by other reoviruses.

Similar to BTV, rotaviruses have a multilayered capsid organisation consisting of a subcore, core and outer capsid. The innermost capsid (equivalent to the BTV subcore) consists of VP2 which encases the viral genome of 11 dsRNA segments. The core surface layer is formed from VP6, whilst the outer capsid of the intact virus or triple-layered particle (TLP), is composed of VP4 and VP7 (Li et al., 2009; Pesavento et al., 2006; Ruiz et al., 2009). Each of these proteins has multiple functions. VP7 interacts with a number of cellular receptors (including integrins αVβ3 and αxβ2) that appear to be involved in entry after the initial attachment of the virus to the cell surface (Zarate et al., 2004). VP4 functions in both cell-attachment and membrane-penetration (Lopez and Arias, 2004; Pesavento et al., 2006). Treatment of rotavirus with trypsin enhances infection and may facilitate entry by direct penetration through the plasma membrane (Kaljot et al., 1988; Keljo et al., 1988). Cleavage of VP4 generates two proteins, VP8* and VP5* both of which remain associated with the virus (Clark et al., 1981; Estes et al., 1981; Lopez and Arias, 2004). This cleavage may be important for infection *in vivo* as rotavirus causes viral gasteroenteritis and as such will be exposed to proteases in the gut.

Entry of rotavirus into cells is very complex and involves two types of receptors, an attachment receptor and a number of post-attachment or co-receptors. For some strains the initial interaction is with sialic acid, although sialic acid-independent strains have been identified (Ciarlet et al., 2001; Zarate et al., 2000). Subsequent post-attachment steps appear to involve multiple receptors including hsp70 or one of several integrins; αVβ3, α4β1, α4β7, αxβ2 and α2β1 (Coulson et al., 1997; Graham et al., 2005; Graham et al., 2006; Lopez and Arias, 2004; Ruiz et al., 2009).

Whether rotavirus infection requires endocytosis or occurs by direct membrane-penetration is the topic of much debate. Rotavirus entry has been studied by electron microscopy in MA104 cells (Quan and Doane, 1983). At early time points the virus was visualised at the plasma membrane, associated with coated pits and within coated vesicles, indicating entry via clathrin-mediated endocytosis. After 1 hour multiple virus

particles were seen in lysosome-like structures (Quan and Doane, 1983). Rotavirus infection has been shown to be inhibited by bafilomycin A1, an endosomal proton pump inhibitor which raises endosomal pH, suggesting rotavirus penetration from the endosomes to the cytoplasm is blocked (Chemello et al., 2002). In contrast other more recent studies have concluded that rotavirus entry into MA104 cells is clathrin- and caveolae-independent (Sanchez-San Martin et al., 2004). Lipid rafts have been implicated to play a role in the infectivity of rotaviruses as entry and infection can be reduced or blocked by the depletion of cholesterol using methyl-β-cyclodextrin from the cell membrane (Arias et al., 2002; Lopez and Arias, 2004; Sanchez-San Martin et al., 2004). However, depletion of cholesterol could potentially alter the fluidity of the plasma membrane and inhibit infection by direct membrane-penetration. Dominant-negative dynamin '*aa*' has also been shown to reduce infection suggesting that entry requires dynamin (Sanchez-San Martin et al., 2004). However, it has been suggested that this observation could also be explained by a role for dynamin in post-entry virus replication (Sanchez-San Martin et al., 2004).

1.8 Summary

BTV has rapidly expanded northwards in recent years, posing a much larger threat to northern European economies, including the U.K. The current large number of circulating serotypes in continental Europe potentially increases the risk to the U.K. and also increases the chance of virus re-assortment, producing novel strains and new threats. Whilst the structure of the virus has now been solved, many of its molecular processes remain under investigated, including at the time of starting this Thesis, the molecular mechanisms of BTV cell entry.

The field of endocytosis research was once limited to only a few pathways. It is now clear that a much larger number of endocytic routes exist and many more may await discovery. Also it is now clear that endocytosis pathways that were once thought of as being distinct can in fact merge during post-uptake vesicle trafficking.

Furthermore it is likely that viruses have the potential to exploit all endocytic entry routes and that some viruses or different serotypes of the same virus can use different or even more than one entry pathway to initiate infection.

Endocytic pathways can be blocked at various steps by the addition of pathway specific inhibitors, or by dominant-negative versions of proteins that regulate endocytosis. The ability of these reagents to inhibit BTV infection of mammalian cells will be assessed in this Thesis.

Aims

At the start of my studies, there was an incomplete understanding of the cell entry mechanisms used by Bluetongue virus (BTV). This PhD thesis aims to gain a better understanding of the mechanism of endocytosis used by BTV to enter mammalian cells and to map the intracellular virus trafficking pathway that leads to infection.

2 Materials & Methods

2.1 Cell Culture

Baby Hamster Kidney cells, strain 13 (BHK) and Bovine Pulmonary Aortic Endothelial cells (BPAEC) were purchased from the European Cell Culture Collection. Vero cells were provided by the central services unit (CSU) at the Institute for Animal Health (IAH).

BHK cells were maintained in Glasgow Minimum Essential Medium (GMEM) (Sigma) containing 10% foetal bovine serum (FBS) (Autogen Bioclear), 2 mM glutamine (IAH), 100 U/ml penicillin (IAH), 100 µg/ml streptomycin (IAH) and 5% tryptose phosphate broth solution (Sigma).

BPAEC cells were maintained in Dulbecco's Modified Eagle's Medium (DMEM) (Sigma) with 25 mM HEPES buffer containing 15% FBS (Autogen Bioclear), 2 mM glutamine (IAH), 100 U/ml penicillin (IAH) and 100 µg/ml streptomycin (IAH).

Vero cells were maintained in DMEM containing 10% FBS (Autogen Bioclear), 2 mM glutamine (IAH), 100 U/ml penicillin (IAH), 100 µg/ml streptomycin (IAH) and 2.5 µg/ml amphotericin B (IAH).

All cells were grown at 37°C, 5% CO_2 and routinely passaged three times a week.

2.2 Virus Purification

BTV-1 reference strain (RSArrrr/01, ICTVdb isolate accession number 41010B4F) was purified according to previously published methods (Burroughs et al., 1994; Mertens et al., 1987).

Infectious virus stocks were prepared as follows. A confluent 175 cm^2 flask of BHK cells was washed once with serum-free medium and 50 ml fresh serum-free medium with 50 µl virus stock added. The flask was incubated at 37°C, 5% CO_2 until complete cytopathic effect (CPE) was observed. The supernatant from this flask was

used to infect 40 confluent roller bottles (850 cm^2 roller bottles) of BHK cells, 50 ml per roller bottle. The roller bottles were incubated at 37°C until CPE was observed.

Media from the 40 roller bottles was pooled on ice, and centrifuged at 3,000 g, for 0.5 hours at 4°C (Centrifugation 1). The resulting supernatant was incubated for 1 hour at 4°C with an equal volume of saturated ammonium sulphate solution in 0.04 M sodium phosphate buffer, pH 7.6. A cytoplasmic extract was made from the cell pellet generated by centrifugation 1 using 0.5% Triton-TNE (0.2 M NaCl, 5 mM EDTA and 50 mM Tris pH 8.0), and a 40 ml glass homogeniser (Wheaton). The extract was transferred to plastic universals (Ramboldi) and centrifuged at 800 g for 10 minutes at 4°C. Supernatants were retained on ice and the triton extraction repeated on the pellets twice more, until a total volume of 80 ml was obtained. Remaining pellets were discarded and the supernatants combined.

The ammonium sulphate treated supernatant was centrifuged at 3,000 g for 30 minutes at 4°C. The supernatant was discarded and the pellets resuspended in 40 ml 0.5% Triton-TNE and combined with the cytoplasmic extracted cell supernatants. Six discontinuous sucrose gradients (5 ml 66% w/w sucrose: 10 ml 40% w/v sucrose both in 0.2 Tris-HCL pH 8.0) were made in SW28 tubes (Beckman), and the combined supernatants layered onto them, balanced with 0.5% Triton-TNE and centrifuged at 8,000 g for 3 hours at 4°C. The discs at the 40%/60% interface were collected and resuspended in 0.2 M Tris-HCl, pH 8.0, by passing through a syringe and needle (20 ml syringe and needle, Becton Dickinson); in a total volume of 36 ml. Virus was stored at 4°C overnight.

Sodium Deoxycholate (final concentration of 3%) was added to the virus suspension. Two discontinuous sucrose gradients were made and the material re-centrifuged as before. Discs were collected and resuspended in 30 ml 0.2 M Tris buffer, 3 ml 200 nM Dithiothreitol (DTT) (Sigma) and 3 ml 10% Sodium Lauroyl

Sarcosine (NLS) (Sigma); and the solution was incubated at 37°C in a water bath until it clarified (~15 minutes).

Clarified virus was run on 2 discontinuous gradients in SW40 tubes (Beckman), as before, with 40% sucrose made up to 0.1% NLS. A blue band formed at the sucrose interface and was removed with a glass pasteur pipette and dialysed twice overnight in Slide-A-Lyzer dialysis cassettes (Pierce) twice against 3 L 0.1% NLS in 0.1 M Tris (pH 8.0) buffer at 4°C. Purified virus was stored at 4°C.

2.3 Analysis of the Purified Virus

The purified viruses were analysed by SDS-PAGE to ensure they were intact and had not degraded during purification.

2.3.1 Protein Analysis – Sodium Dodecyl Suiphate Polyacrylamide Gel Electrophoresis (SDS-PAGE)

Samples were prepared by mixing purified virus with an appropriate volume of 3 times sodium dodecyl sulphate (SDS) sample buffer (New England BioLabs, [NEB]) and 1 µl 1.25 M dithiotheritol reducing agent (DTT) (NEB); and heated at 100°C for 3 minutes. A 10% acrylamide gel was cast, and samples run alongside a broad range pre-stained protein marker (NEB). Gels were run at 240 V/40 mA for 2.5 hours. Gels were stained gently shaking overnight in coomassie blue stain, destained the following day until bands appeared and then dried with heat onto filter paper.

2.3.2 Tissue Culture Infectious Dose ($TCID_{50}$) Assay

BHK-21 cells were prepared in 96 well plates (NUNC) and incubated overnight at 37°C, 5% CO_2, to be approximately 50% confluent the next day.

A dilution series of the purified virus was made from 10^{-1} to 10^{-16} by sequentially adding 100 µl of virus to 900 µl serum-free medium. Media was removed from the cells and 100 µl serum-free medium added to every well. An additional 100 µl of serum-free medium was added to the control wells. Starting with the lowest virus dilution, 10^{-16};

100 µl of the dilution was added to 8 wells in a row across the plate, this was repeated up the dilution series.

Plates were sealed with film (Greiner) and incubated at 37°C, 5%CO_2 for 1 week. Plates were monitored routinely and progress scored on a record sheet, with '++' for complete CPE, '+' for partial CPE and '–' for no CPE. At day seven the plates were re-scored and the titre calculated using the method of Spearman-Karber and expressed as $\log_{10}$ $TCID_{50}$/ml. To verify CPE, plates were stained with methylene blue cell stain overnight, and rinsed with water the following day.

This assay was repeated twice and the results averaged to give the final titre. The purified BTV-1 (RSArrrr/01) used in all of these studies was calculated to be $10^{8.75}$ $TCID_{50}$/ml on BHK cells, and to be at a concentration of 130 ug/ml.

2.3.3 Titration of Purified BTV on Coversiips

The purified BTV-1 was titred on BHK and Vero cells by confocal microscopy.

Cells were prepared on coverslips as in method 2.6.1.The next day cells were washed twice with serum-free medium, virus dilutions made in serum-free medium and 200 µl of virus added per coverslip. Virus (at each dilution) was bound to the cells and internalised for 1 hour at 37°C, 5% CO_2. Coverslips were then washed three times with serum-free medium to remove virus and 1 ml 2% FBS maintenance media added. Infection was allowed to continue for a further 7 hours. Coverslips were then fixed and processed and labelled with Orab 1 (anti-NS2) as per method 2.6.5.

Coverslips were assessed visually by confocal microscopy, see method 2.8, for the level of infection. A dilution of 1/2000 (0.065 ug/ml of purified BTV-1) was selected for all future infection studies on BHK cells, as it gave a frequency of infection of 50% (i.e. 50% of the cells were infected) which equates to an m.o.i. of 0.5.

2.4 Antibodies and Reagents

2.4.1 Primary Antibodies

Rabbit anti-BTV/NS2 (Orab 1) and the Guinea-pig anti-BTV/VP5 antibodies were produced at IAH using recombinant NS2 and BTV-1 as the immunogens respectively. Mab 9E10 (anti-c-myc) was from the Developmental Studies Hybridoma Bank (University of Iowa). The mouse monoclonal antibody (Mab 4A1) to Lysosomal Antigen -1 (LAMP-1) was a kind gift from Professor Jean Gruenberg (University of Geneva). Monoclonal anti-actin antibody, clone AC-40 was used for western blot (Sigma).

2.4.2 Secondary Antibodies

Species specific Alexa-fluor conjugated secondary antibodies used for confocal microscopy were from Invitrogen (Molecular Probes). The Goat anti-Rabbit biotinylated secondary antibody used in the enzyme-linked immunospot assay was from Southern Biotech. An anti-mouse HRP secondary antibody was used for western blot (Promega).

2.4.3 Reagents

Pharmacological reagents were made up into stock concentrations and stored according to manufacturers guidelines. Methyl-β-cyclodextrin (stock 100 mM in DMEM), Nystatin (stock 25 mg/ml in DMSO), Progesterone (stock 1 mg/ml in Ethanol), Cytochalasin D (stock 20 mM in DMSO), Dynasore monohydrate (stock 20 mM in DMSO) and 5-(N-Ethyl-N-isopropyl) amiloride (EIPA) (stock 50 mM in DMSO) were from Sigma. Concanamycin-A (stock 10 mM in DMSO) and Ammonium Chloride (5 M in water) were from Fluka. Latrunculin A (stock 1 mM in DMSO) was from Invitrogen.

Alexa-fluor labelled Transferrin (stock 5 mg/ml in PBS) and Dextran were from Molecular probes (now Invitrogen). Filipin III (in PBS) was from Sigma and Phalloidin (in Methanol) from Invitrogen.

The plasmid for expression of c-myc tagged AP180C was from Harvey McMahon (MRC, Cambridge, UK). Plasmids for expression of green fluorescent protein (GFP)-tagged wild type and dominant-negative dynamin-2 (K44A) were from Mark

McNiven (Mayo Clinic, Rochester, USA). Plasmids for expression of green fluorescent protein (GFP)-tagged control Eps15 (D3Δ2) and dominant-negative Eps15 (EΔ95-295) were from Alexandre Benmerah (Université Paris Descartes, Paris, France). Plasmids for expression of green fluorescent protein (GFP)-tagged wild type Rab 34 and dominant-negative Rab 34 were from Mel Silverman (Institute of Medical Science and Department of Medicine, University of Toronto, Toronto, Canada). Plasmids for expression of green fluorescent protein (GFP)-tagged wild type and dominant-negative Caveolin-1 were from Ari Helenius (Institute of Biochemistry, Zürich, Switzerland).

2.5 Enzyme-Linked Immunospot Assay

An enzyme-linked immunospot assay was used to investigate the effect of specific inhibitors of endocytic pathways on BTV entry.

2.5.1 Quantification of Infected Cells using the Enzyme-Linked Immunospot Assay

Target cells (BHK, BPAEC or Vero) were seeded onto 96 well tissue culture plates (Nunc), and incubated overnight at 37°C, 5% CO_2, to be between 70 and 80% confluent the following day.

All steps use 200 µl solution per well unless stated. Cells were washed once with serum-free medium and infected with purified virus diluted in serum-free medium, 100 µl per well for 1 hour at 37°C, 5% CO_2. Cells were washed twice with serum-free medium to remove virus, and incubated with 2% FBS maintenance medium for between 6 and 12 hours. Cells were fixed with 4% Paraformaldehyde (PFM) (Sigma) in phosphate buffered saline (PBS) (Sigma) for 1 hour at room temperature, washed with PBS three times, and stored overnight at 4°C.

All subsequent steps were carried out at room temperature. Cells were washed twice with PBS; permeablised with 0.1% Triton X-100 (Sigma) in PBS (Sigma) for 15 minutes; washed five times with PBS, and non-specific binding blocked using 200 µl of block buffer (100 ml TBS [10 ml of 1M Tris pH 7.5 in 500 ml 0.85% saline]

supplemented with 1mM $CaCl_2$, 0.5mM $MgCl_2$, 10% Normal Goat Serum [Harlan Lab Sera] and 1% Teleostean Gelatin [Sigma]) for 45 minutes. Cells were incubated in turn with an anti BTV primary antibody diluted in block buffer (Orab 1), 100 µl per well for 1 hour; a Rabbit biotinylated secondary antibody (Southern Biotechnology Associates) diluted in block buffer at 1/500, 100-150 µl per well for 1 hour and streptavidin alkaline phosphatase (Caltag Laboratories), diluted 1/1000 in block buffer, 150 µl a well for 45 minutes. Between each step cells were washed five times with PBS.

Next 150 µl of alkaline phosphatase substrate solution (made up as directed by the manufacturer) (BIO-RAD) was added to each well and cells monitored under a light microscope until colour developed, with infected cells turning blue-black. Cells were washed four times with distilled water and the plate left to air dry for 10 minutes before counting.

Plates were read and data recorded using software available on the KS ELISPOT Compact from Zeiss. Data was analysed by subtracting any counted infection spots on background wells from all other well counts.

2.5.2 Inhibition of Endocytosis using the Enzyme-Linked Immunospot Assay

All pharmacological inhibitors were diluted in serum-free medium. To quantify the effects on infection by specific inhibitors of endocytosis, drugs were added to the cells under four different treatment conditions either; (1) mock-treated (i.e. treated with the solvent for the drug only) and then infected with BTV-1; (2) pre-treated with the drug for 30 minutes or 1 hour before infection and the drug maintained on the cells during the 1 hour incubation with virus; (3) the drug was added to the cells for 1.5 or 2 hours immediately after the virus inoculum was removed from the cells or (4) the drug was added for 1.5 or 2 hours, 1.5 or 2 hours after the virus inoculums were removed. The plate was then washed as described in method 2.5.1, and the assay continued as described.

2.6 Immunofluoresence

2.6.1 Setting up of Coverslips

Cells were plated onto borosilicate 13 mm coverslips (BDH) in a 24 well tissue culture plate (Falcon, Becton Dickinson Labware), and incubated for a minimum of 16 hours at 37°C, 5% CO_2 to be between 40-60% confluent the next day.

2.6.2 Endocytosis of Alexa-fluor labelled ligands

Cells were prepared on coverslips as in method 2.6.1. The next day cells were washed twice with serum-free medium and depleted of cellular iron by incubation for 30 minutes in serum-free medium. Medium was removed and 568-Alexa labelled transferrin (25 µg/ml) added. For dextran entry, cells were serum-starved for 1 hour before addition of 568-Alexa labelled dextran (5mg/ml) in serum-free medium at 37°C for the times indicated on the figures. Entry was stopped by the addition of 4% paraformaldehyde, including 0.25% glutaraldehyde for transferrin. Coverslips were processed for confocal microscopy as in method 2.6.4.

2.6.3 Labelling of Cellular Cholesterol and Actin Filaments

Cells were prepared on coverslips as in method 2.6.1. The next day cells were washed twice with serum-free medium and mock-treated or pre-treated with 7.5 mM methyl-β-cyclodextrin for 30 minutes at 37°C. Cells were fixed by the addition of 4% paraformaldehyde and cellular cholesterol visualised at 430 nm immediately after labelling with 125 µg/ml filipin III diluted in PBS for 15 minutes at room temperature. Coverslips were mounted in fluoromount G (Southern Biotech) instead of vectorshield.

Cells on coverslips (prepared as above) were washed twice with serum-free medium and mock-treated or pre-treated with cytochalasin D or latrunculin A for 30 minutes at 37°C. Cells were fixed by the addition of 4% paraformaldehyde, permeabilised with 0.1% Triton X-100, and actin filaments visualised by incubation with 488-Alexa labelled phalloidin diluted in block buffer for 10 minutes at room temperature.

2.6.4 Detection of Intracellular Antigen with Cell Permeabilisation

After completion of the assay, coverslips were washed twice with PBS, fixed with 4% PFM at room temperature for 40 minutes, and washed three times with PBS. Coverslips were either labelled immediately or stored at 4°C under PBS.

All subsequent steps were carried out at room temperature. Cells were permeablised with 0.1% Triton X-100 in block buffer for 20 minutes. When using Mab 4A1 to identify LAMP-1 positive compartments, the cells were permeablised with 0.5% Saponin (in place of Triton X-100) for 15 minutes and 0.1% Saponin was included in all subsequent steps. Cells were then washed twice with PBS and non-specific binding blocked with block buffer (100 ml TBS [10 ml of 1M Tris pH 7.5 in 500 ml 0.85% saline] supplemented with 1mM $CaCl_2$, 0.5mM $MgCl_2$,10% Normal Goat Serum [Harlan Lab Sera] and 1% Teleostean Gelatin [Sigma]) for 30 minutes. Cells were incubated with primary antibody to detect the antigen of interest, 200 µl per coverslip, diluted in block buffer for 1 hour, washed three times with PBS, and incubated with a species specific Alexa-fluor labelled secondary conjugate antibody (Molecular Probes), 200 µl per coverslip at 1/200 diluted in block buffer, for 1 hour. Coverslips were washed three times with PBS, stained with 4', 6'-Diamidino-2-Phenylindole (DAPI) (Sigma) at 1/10,000 made fresh in H_2O for 10 minutes at room temperature and then washed three times with PBS. The coverslips were then dipped in deionised H_2O, excess water blotted off and mounted in vectashield mounting medium for fluorescence (Vector Laboratories), on a glass slide (Agar Scientific), sealed with clear nail varnish and stored at 4°C.

2.6.5 Infection of Cells on Coverslips

Infection of cells prepared on coverslips was carried out as per the enzyme-linked immunospot assay.

Cells were prepared on coverslips as in method 2.6.1. The next day cells were washed twice with serum-free medium, virus dilutions made in serum-free medium and

200 µl of virus added per coverslip. Virus (m.o.i. = 0.5) (see Methods 2.3.2 and 2.3.3) was bound to the cells and internalised for 1 hour at 37°C, 5% CO_2. Coverslips were then washed three times with serum-free medium to remove virus and 1 ml 2% FBS maintenance media added. Infection was allowed to continue (see individual figure legends for infection times). Coverslips were then fixed and processed as per method 2.6.4.

2.6.6 Treatment of Coverslips with Pharmacological Inhibitors prior to Infection

Cells were prepared on coverslips as in method 2.6.1. The following day cells were washed twice with serum-free medium, and pre-treated with 200 µl drug at pre-determined concentrations or mock-treated (including the solvent for the drug) for 30 minutes at 37°C, 5% CO_2. Cells were then washed with serum-free medium and virus (m.o.i. = 0.5) added diluted in drug or solvent (for mock-treatment) for 1 hour at 37°C, 5% CO_2. Infection was continued as in method 2.6.5.

2.6.7 Raising Endosomai pH using Ammonium Chloride post initiation of Infection

Cells were prepared on coverslips as in method 2.6.1. The following day cells were washed twice with serum-free medium, and pre-treated with 200 µl drug at pre-determined concentrations or mock-treated (including the solvent for the drug) for 30 minutes at 37°C, 5% CO_2. Cells were then washed with serum-free medium and virus (m.o.i. = 0.5) added diluted in drug or solvent (for mock-treatment) for 1 hour at 37°C, 5% CO_2. Cells were then washed with serum-free medium to remove drug and excess virus. After washing, infection was continued in fresh medium containing 25 mM ammonium chloride for 11 hours. Addition of ammonium chloride immediately after the virus inoculua were removed rapidly increases endosomal pH, and prevented any further acid-induced infection. Cells were fixed and processed for confocal microscopy as in method 2.6.4.

2.6.8 BTV-1 Binding and Internalisation

Cells were prepared on coverslips as in method 2.6.1, but aimed to be around 60-70% confluent the following day.

The cells were placed on ice and washed twice with cold serum-free medium and 200 µl BTV-1 (13 µg/ml) diluted in serum-free medium added. Cells were incubated on ice for 40 minutes to allow BTV-1 to bind. Cells were then removed from ice, washed twice with cold serum-free medium to remove unbound virus, washed twice with warmed serum-free medium and 200 µl of warmed serum-free medium added. The cells were then incubated for various time points at 37°C, 5% CO_2 to allow bound virus to enter the cell.

Cells were put on ice, washed twice with cold serum-free medium, fixed and processed for confocal microscopy as per method 2.6.4.

2.6.9 Treatment of Coverslips with Pharmacological Inhibitors prior to BTV-1 Binding and Internalisation

Cells were prepared on coverslips as in method 2.6.1, but aimed to be around 60-70% confluent the following day.

The following day cells were washed twice with serum-free medium, and pre-treated with 200 µl drug at pre-determined concentrations used in the enzyme-linked immunospot assay, for 30 minutes to 1 hour at 37°C, 5% CO_2.

The cells were placed on ice and washed twice with cold serum-free medium and 200 µl BTV-1 (13 µg/ml) diluted in drug added. Cells were incubated on ice for 40 minutes to allow BTV-1 to bind. Cells were then removed from ice, washed twice with cold serum-free medium to remove unbound virus, washed twice with warmed serum-free medium and 200 µl of warmed drug added. The cells were then incubated for 30 minutes at 37°C, 5% CO_2 to allow bound virus to enter the cell.

Cells were put on ice, washed twice with cold serum-free medium, and fixed by the addition of 4% paraformaldehyde. Cells were processed for confocal microscopy as per method 2.6.4.

2.7 Transient Transfection

2.7.1 Preparation of Plasmid DNA

Plasmid DNA was transformed into 50 µl DH5α competent cells by incubation on ice for 30 minutes, followed by heat-shock at 42°C for 45 seconds and a further 2 minutes on ice. LB broth (1 ml) was added to the cells and they were incubated shaking at 37°C for 45 minutes. Transformed cells were spread onto LB-agar plates and selected using the appropriate antibiotic, with incubation at 37°C overnight. The following day cultures were grown with the appropriate antibiotic selection and minipreps carried out using the Qiagen Miniprep kit (Qiagen) according the manufacturer's instructions. Selected minipreps were re-cultured and plasmid DNA for transfections purified using the Qiagen Endotoxin Free Maxiprep kit (Qiagen) according the manufacturer's instructions.

2.7.2 Transient Transfection of Cell Lines

Cells were seeded on baked sterile coverslips in transfection medium (cell culture medium without 100 U/ml penicillin and 100 µg/ml streptomycin), aiming to be around 40% confluent the next day.

Two master mixes were made; the first of 1 µg plasmid DNA with 50 µl opti-MEM (Invitrogen) per coverslip, and the second 1 µl Lipofectamine 2000 (Invitrogen) with 50 µl opti-MEM per coverslip. Each master mix was incubated for 5 minutes at room temperature, and then the two combined, mixed and incubated at room temperature for 20 minutes.

Cells were washed once with 1 ml opti-MEM, and 500 µl fresh opti-MEM added to each coverslip. One hundred microlitres of the transfection complex was added directly to the 500 µl opti-MEM, and the plate swirled to mix. Coverslips were incubated

at 37°C, 5% CO_2 for 4 hours and then the opti-MEM removed and 1 ml transfection medium added. Each transfection was allowed to run for an optimised length of time.

2.8 Image Capture

All coverslips were viewed on a Leica SP2 Confocal Scanning Laser Microscope and all images were taken using the 63 x lens. All data was collected sequentially to eliminate cross-talk between fluorescent antibodies. Images were processed using Adobe Photoshop software.

2.9 Data Analysis

Student's *t* test was used to determine statistical significance (*P* values: * <0.05, ** <0.01, *** <0.001).

2.10 Flow Cytometry

2.10.1 Flow Cytometry: Detection of Virus Binding

Cells were removed from flasks with trypsin, collected by centrifugation at 200 g for 3 minutes (Sorvall Legend *RT*, 1,000 rpm) at room temperature, resuspended in cell culture medium and allowed to recover at 37°C with continuous rotation for 30 minutes to 1 hour. Cells were then collected by centrifugation (as above), resuspended in ice-cold FACS buffer, (20 mM Tris pH 7.6, 1 mM $CaCl_2$, 0.5 mM $MgCl_2$, 2% v/v Normal Goat Serum [Harlan Lab Sera], 2% w/v Bovine Serum Albumin [MP Biomedicals] in 0.85% Saline). 1 x 10^6 cells were plated out in a 96 well round bottomed plate (Western). The plate was centrifuged at 850 g (Sorvall Legend *RT*, 2,000 rpm) for 1 minute at 4°C and buffer removed. Cell pellets were disrupted by gently vortexing the plate for 5 seconds. Next 30 µl of purified virus (100 µg/ml) diluted in cold FACs buffer was added to each well, and the plate incubated on ice for 45 minutes. The plate was centrifuged; buffer removed and cell pellets broken up as before.

Virus binding was detected with an anti-BTV antibody, PM10, diluted in FACS buffer, 30 µl per well for 30 minutes on ice. The plate was washed as described above and a goat, anti-Guinea pig Alexa-fluor 488-conjugated secondary antibody (Molecular

Probes) added at 1/200 dilution in FACS buffer, 30µl per well for 30 minutes on ice. The plate was then washed twice, and the cells resuspended in 200 µl 1% paraformaldehyde (Sigma) in PBS, transferred to FACS tubes (Becton Dickinson) and 6,000 cells per sample read on the FACS Calibur machine (Becton Dickinson).

2.10.2 Flow Cytometry: Concanamycin-A Treatment of BHK and BPAEC cells

Cells were removed from flasks with trypsin, collected by centrifugation at 200 g for 3 minutes (Sorvall Legend RT, 1,000 rpm) at room temperature, resuspended in cell culture medium and allowed to recover at 37°C with continuous rotation for 30 minutes to 1 hour. Cells were then collected by centrifugation (as above), and re-suspended in 1ml of serum-free medium or 12 nM concancmycin-A and pre-treated at 37°C rotating for 30 minutes. Cells were then collected by centrifugation (as above) and re-suspended in ice-cold FACS buffer. The assay was completed as in method 2.10.1.

2.11 Western Blot

Samples were run on an 8% acrylamide resolving gel (including 1.5 M Tris pH 8.8) and a 4% acrylamide stacking gel (including 1 M Tris pH 6.8) (see Appendix). Samples were made as described in method 2.3.1, loaded onto the gel using a Hamilton syringe, and run at 100-200 V, until the proteins reached the bottom of the gel. The proteins were transferred onto Hybond-C extra membrane (Amersham) by running at 100 V for 1.5 hour.

The membrane was blocked in block buffer (see Appendix), gently shaking overnight at 4°C. The membrane was then incubated with primary antibody in block buffer for 1 hour at room temperature and then washed in 1 x PBS-Tween for 1 hour at room temperature, with the wash solution changed every 15 minutes. The membrane was then incubated with secondary HRP antibody in block buffer for 1 hour at room temperature and then washed as before. The membrane was then incubated in ECL reagents (Pierce), made up as per manufacturers instructions, for 5 minutes at room

temperature. The bands were visualised and the film (Kodak) developed manually using developer (Polycon Manual X-ray Developer, Champion Photochemistry) and fixer (B&W Amfix, Film and Paper Fixer, Champion Photochemistry).

3 Methods to Investigate BTV Endocytosis

3.1 Introduction

The objective of this thesis is to gain a better understanding of the cell entry mechanisms used by BTV-1 to enter and infect mammalian cells. To achieve this objective I have investigated the effects of pharmacological and dominant-negative (Dn) inhibitors of specific endocytic pathways on BTV entry and infection.

Immunofluoresence confocal microscopy is an established method to study virus entry as it allows the cellular location of the virus to be clearly defined. The first part of this chapter describes the development of confocal microscopy to follow BTV during cell entry using an antibody (PM10) that binds to the outer viral-capsid protein VP5 (see Method 2.4.1 and Appendix II). Virus entry experiments necessitate using a high input virus concentration in order to detect virus during the entry process. This raises the possibility that virus may be forced into entering cells via endocytic pathways that are either not normally used, or are non-productive for infection. It is generally accepted that infection at a low multiplicity of infection (m.o.i.) of <1.0 encourages virus entry by the most efficient and physiologically relevant route (DeTulleo and Kirchhausen, 1998). Therefore, to confirm the results of the entry experiments, I also investigated the effects of the inhibitors on infection of target cells using BTV-1 at an m.o.i. of 0.5 to encourage virus entry by the most efficient route. The second part of this chapter describes the development of assays to quantify BTV-1 infection at low m.o.i.

At the outset of my studies the objectives were novel as very little was known of BTV cell entry mechanisms. My plan was to use primary endothelial cells as they are a major target of BTV in the animal host. However, to quantify the effects of expression of dominant-negative proteins on infection requires high transfection efficiency, which is difficult to achieve with primary cells. Therefore it was decided to undertake initial experiments using established cell lines (e.g. BHK, Vero and BPAEC cells) with a view

to using the knowledge gained to investigate entry in endothelial cells (see Chapter 10).

The BTV-1 reference strain (IAH reference number RSArrrr/01, ICTVdb isolate accession number 41010B4F) was used for these studies. This isolate was chosen as BTV-1 has recently caused outbreaks of BT in Europe, and has been present in France since 2007; recent outbreaks have also occurred in Portugal, Spain, Italy, Morocco and Tunisia. Virus stocks were grown using BHK cells. Intact virus particles were gradient purified according to published methods (see Method 2.2) (Mertens et al., 1987) and used for all experiments. The m.o.i. was determined by virus titration on BHK cells using confocal microscopy to identify infected cells (see Method 2.3.3). For infection experiments, virus was used at a dilution that resulted in ~50% of the cells being infected (m.o.i. = 0.5), unless otherwise stated.

3.2 Detecting BTV at the Cell Surface

Confocal microscopy was developed to follow BTV-1 entry by BHK cells. BTV-1 (13 µg/ml) was bound to the cells on ice for 40 minutes to limit cell entry. Unbound virus was removed by washing and the cells fixed using cold 4% paraformaldehyde (PFM). Virus was then labelled with PM10 (anti-VP5), and a goat, anti-Guinea pig Alexa-fluor 488-conjugated antibody. Images were collected on the Leica SP2 confocal microscope (see Methods 2.6.8 and 2.8). Figure 3.1, panels (A), (C) and (E) shows typical images of BTV-1 (shown as green) at the cell surface. Differential interference contrast (DIC) was used to show the plasma membrane. Panels (B), (D) and (F) show the same cells as in (A), (C) and (E) overlaid with DIC image. Virus particles (shown as green) can be seen at the cell surface.

3.2.1 Detecting BTV Inside the Cell

BTV-1 was bound to BHK cells as above (see Section 3.2 and Figure 3.1), unbound virus removed by washing and entry initiated by the addition of pre-warmed medium (37°C) (see Method 2.6.8). After 5, 10, 15, 30, 60 and 90 minutes entry was

stopped by the addition of cold 4% paraformaldehyde on ice. The cells were then permeabilised with 0.1% Triton X-100 and virus particles visualised by labelling with PM10 (anti-VP5) and a goat, anti-Guinea pig Alexa-fluor 488-conjugated secondary antibody (as in Figure 3.1). Images were collected on the confocal scanning laser microscope with sections taken through the centre of the cell.

Figure 3.2 shows representative cells. After 5 minutes, very little virus (shown as green) had entered the cells as shown by a clear cytosol and the majority of the virus is associated with the plasma membrane (Figure 3.2, Panel A). By 10 and 15 minutes post-internalisation, virus could be seen inside the cell cytosol, although some virus remained at the cell surface (Figure 3.2, Panels B and C). By 30 minutes virtually all the virus had entered the cell but most remained at the cell periphery. At 60 and 90 minutes virus could still be seen and had a vesicular appearance consistent with prolonged presence in endocytic vesicles. These results suggest that BTV-1 enters BHK cells with a slower kinetics than expected for entry by clathrin-mediated endocytosis. As virtually all of the virus was taken up by 30 minutes, this time point was chosen for all subsequent entry experiments with pharmacological and dominant-negative inhibitors.

3.3 Quantification of Infection

The traditional method to quantify BTV infection is by tissue culture infectious dose ($TCID_{50}$) as defined by Spearman-Karber (Darpel, 2007). This is an end point dilution assay in which virus titre is determined by assessing CPE of BHK cells seven days after infection. However, this method is inappropriate to quantify the effects of pharmacological inhibitors on BTV infection as it relies on multiple rounds of virus replication after the inhibitor has been removed from the cells.

It was therefore necessary to develop other methods to quantify BTV-1 infection. Two methods to quantify infection at a low m.o.i. were developed.

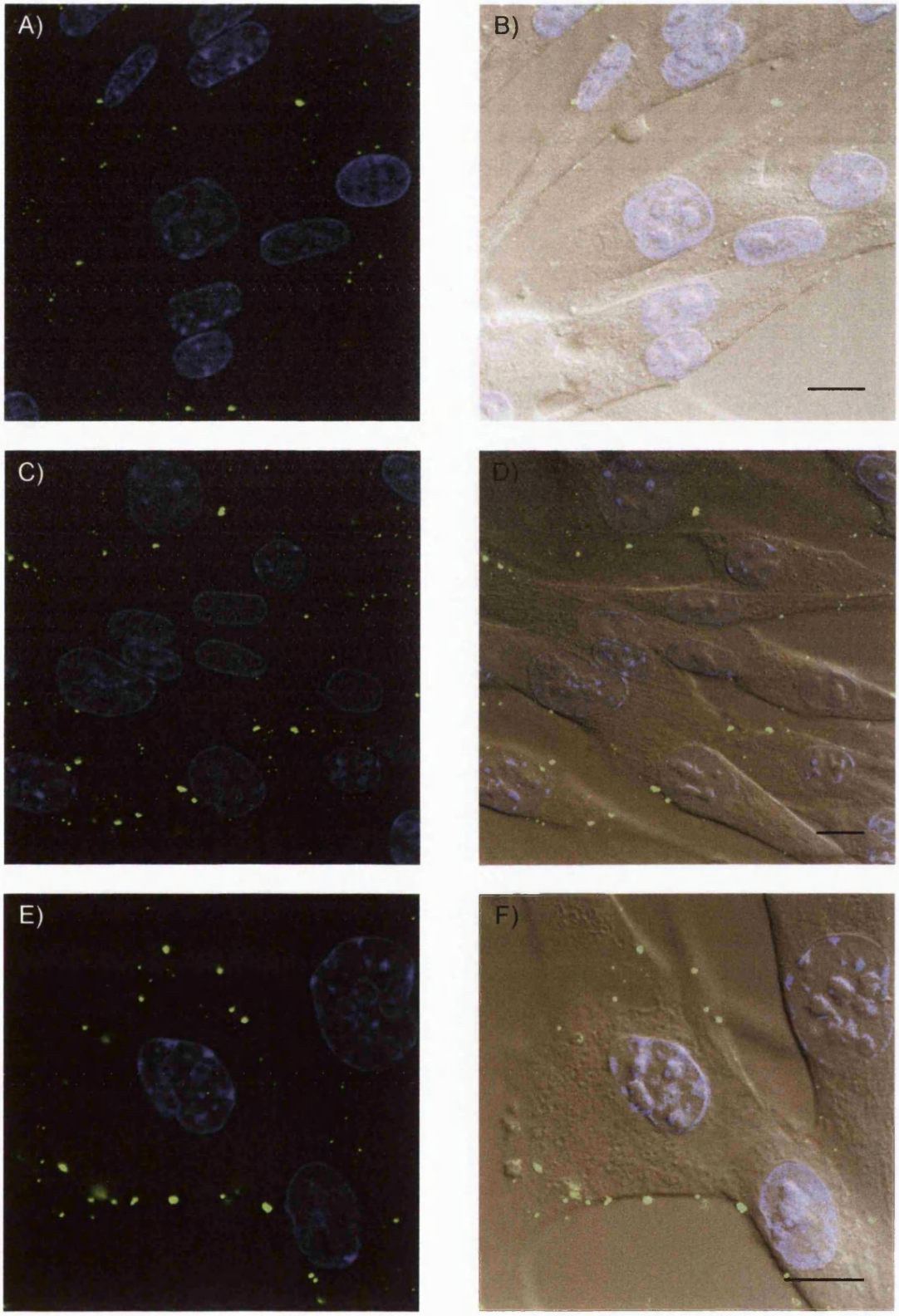

Figure 3.1 : BTV binding to BHK Cells
BTV-1 (13 μg/ml) was bound on ice to BHK cells for 40 min. Excess unbound virus was removed by washing and the cells fixed on ice with 4% PFM. Virus was labelled using PM10 (anti-VP5) and is shown as green. The cell nuclei are shown as blue. Scale bars = 10 μm. Panels (A), (C) and (E) show representative cells. Panels (B), (D) and (F) show an overlay with DIC to show the cell membrane.

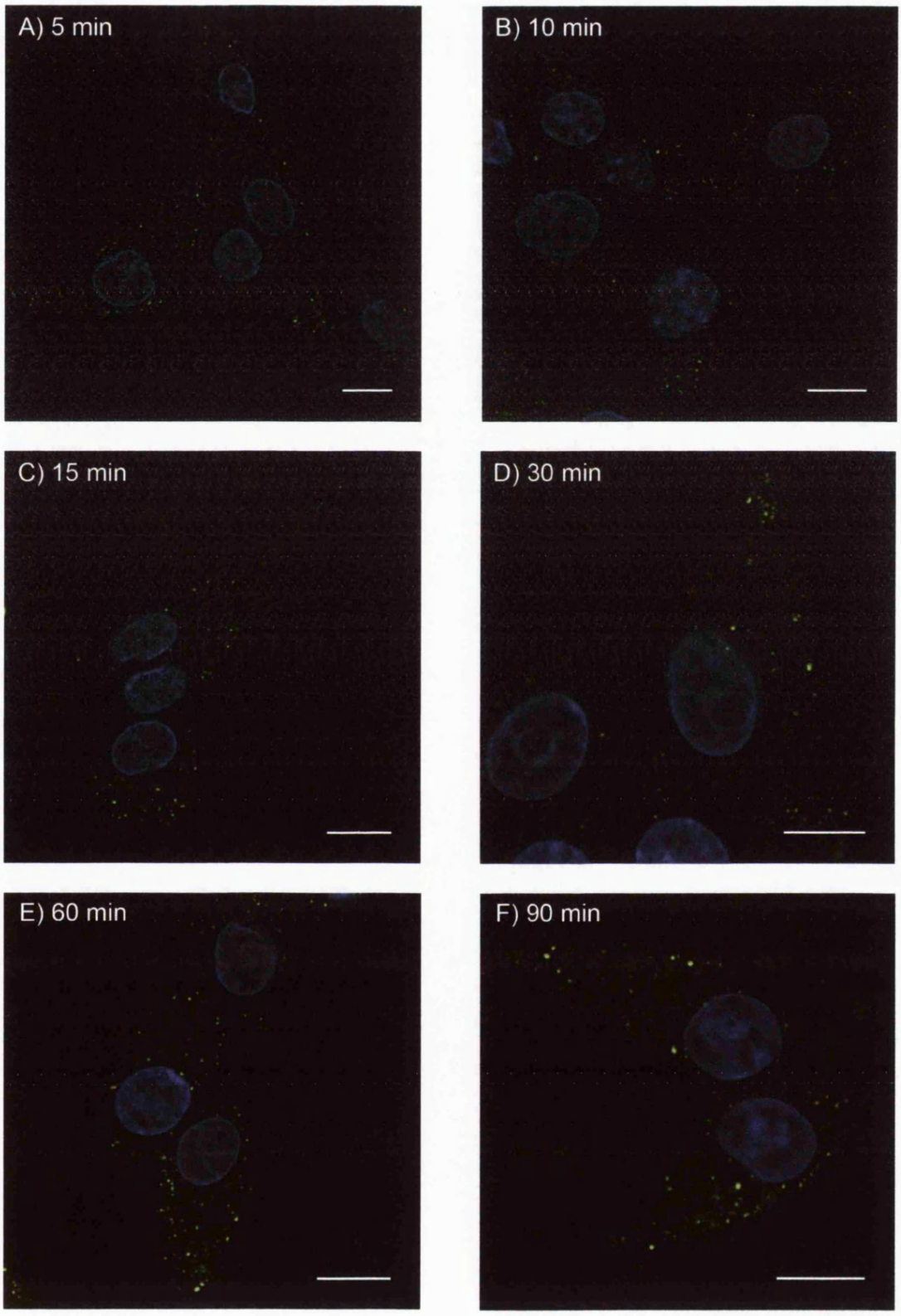

Figure 3.2: BTV-1 entry by BHK cells
BTV-1 (13 μg/ml) was bound to BHK cells on ice for 40 min. Unbound virus was removed by washing and entry initiated by the addition of pre-warmed medium (37°C). Virus entry was continued for the time indicated on the figure. Entry was stopped by the addition of cold 4% PFM. Virus was labelled using PM10 (anti-VP5), and is shown as green. The cell nuclei are shown as blue. Scale bars = 10 μm.

3.3.1 Quantification of BTV Infection by Confocal Microscopy

BHK cells were incubated with dilutions of BTV-1 for 1 hour at 37°C. Excess virus was then removed by washing and infection allowed to proceed for a further 7 hours. Infection was stopped and the cells fixed with the addition of 4% paraformaldehyde. Cells were then permeabilised with 0.1% Triton X-100 and infected cells visualised by labelling with Orab 1 (rabbit, anti-NS2 polyclonal sera) followed by a goat, anti-Rabbit Alexa-fluor 568-conjugated secondary antibody. NS2 is a non-structural protein which locates to VIB's in the cytoplasm of infected cells, therefore its detection can be used as a marker for virus replication and to count the number of infected cells.

Figure 3.3, panel (A) shows labelling for mock-infected cells and demonstrates that Orab 1 shows no cross-reactivity for BHK cells. At 1/100 virus dilution (Figure 3.3, Panel B), virtually all of the cells were infected, as seen by the presence of VIB's (shown as red). At 1/1000 virus dilution (Figure 3.3, Panel C), approximately 70% of the cells were infected. At 1/10,000 (Figure 3.3, Panel D), the level of infection is reduced further to approximately 5% of the cells.

This method clearly allows for individual infected cells to be identified. A dilution of 1/2000 was used for all subsequent experiments where infection was quantified by confocal microscopy.

3.3.2 Quantification of BTV Infection by Enzyme-Linked Immunospot Assay

An Enzyme-Linked Immunospot assay was also used to quantify BTV-1 infection. This assay can identify individual infected cells, at a low m.o.i. and was developed to quantify foot-and-mouth disease virus infection (Berryman et al., 2005; Burman et al., 2006; Dicara et al., 2008; Nunez et al., 2007).

A series of experiments were undertaken to optimise the assay for different cell lines, virus m.o.i., time of infection and the anti-viral antibody used for detection. A number of different primary antibodies to different viral proteins were tested and

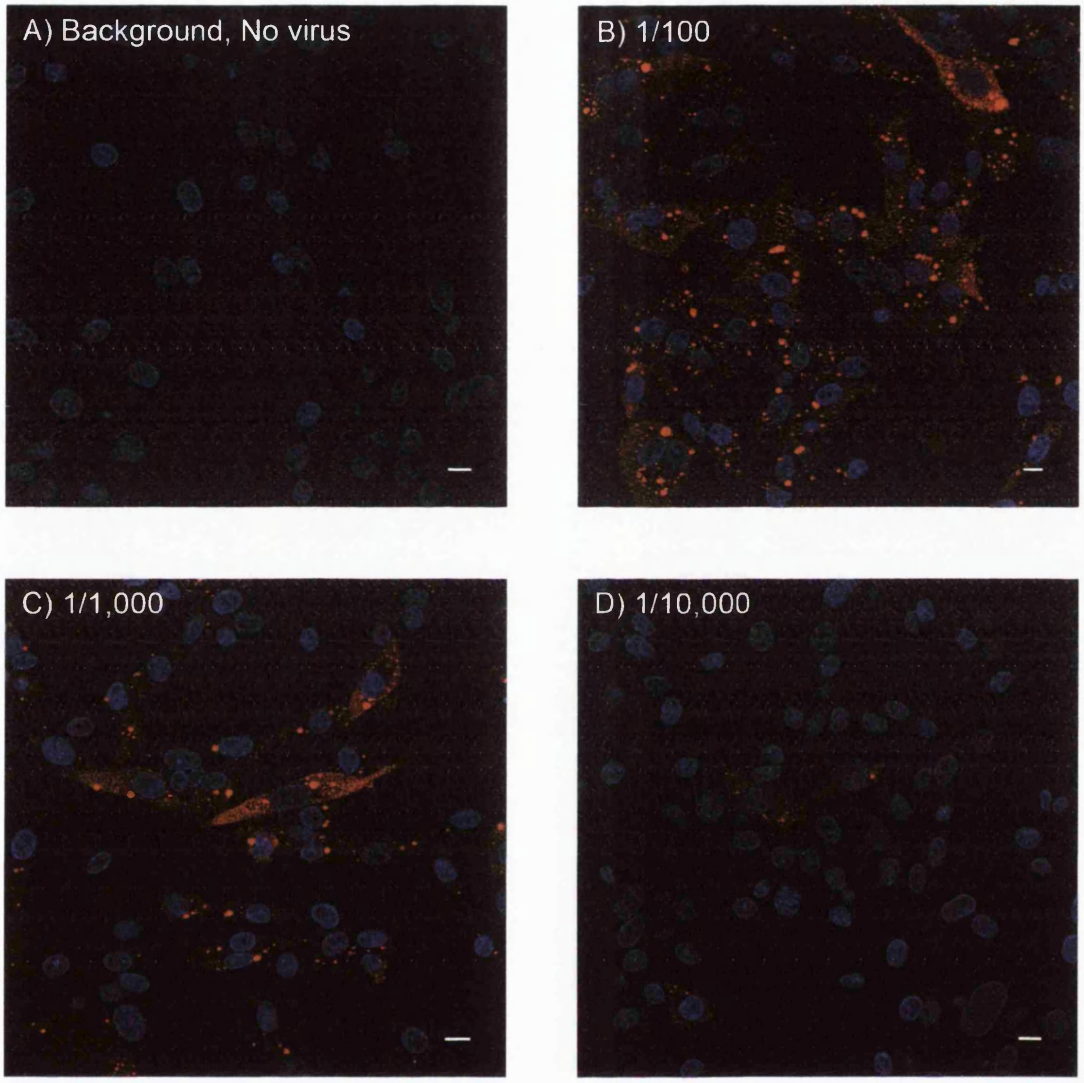

Figure 3.3: Quantification of BTV-1 infection using Immunofluoresence Confocal Microscopy

BHK cells were incubated with purified BTV-1 at various dilutions for 1 h at 37°C. The cells were washed and infection allowed to proceed for 7 h. Infection was stopped and the cells fixed with the addition of 4% PFM. Cells were permeablised and infected cells detected by labelling with Orab 1 (anti-NS2) which primarily labels VIB's which are shown as red. The cell nuceli are shown as blue. Scale bars = 10 μm. Panel (A) shows mock-infected cells and no cross-reactivity of Orab 1 for BHK cells. Panels (B), (C) and (D) show infection at virus dilutions of 1/100,1/10,00 and 1/10,000 respectively.

several were found to work well for the assay. The antibody which gave the best results was Orab 1 (rabbit, anti-NS2 polyclonal sera), and all subsequent assays were carried out using this antibody. Figure 3.4 shows an example of an enzyme-linked immunospot assay to quantify BTV-1 infection of BHK cells. Virus was applied to the cells as a dilution series as in figure 3.3. Briefly, cell monolayers in 96 well plates were incubated with BTV-1 for 1 hour, washed and infection continued for 9 hours. Infection was stopped and the cells fixed with the addition of 4% paraformaldehyde. Cells were permeablised with 0.1% Triton X-100 and non-specific binding sites blocked with block buffer. Infected cells were identified by sequential incubation with Orab 1; a goat, anti-Rabbit biotinylated secondary antibody and a streptavidin alkaline phosphatase conjugate, with washing between steps (see Method 2.5.1). On addition of streptavidin alkaline phosphatase substrate, infected cells appear blue-black. The cells (n ≥250-300) in one field of view in the centre of the well were scored for infection using a KS ELISPOT Compact reader (Carl Zeiss).

The data shown in figure 3.4 are representative wells of one experiment carried out in triplicate for each virus dilution. Panels (A) and (B) show two different control backgrounds. Panel (A) shows uninfected cells processed through the assay, whereas panel (B) shows infected cells where Orab1 was omitted. Panels (C)-(F), show images of infected cells at the indicated virus dilution.

Figure 3.5 shows the data from the above experiment in graph format. The data is shown as the mean and standard deviation of the number of infected cells for triplicate wells. At 1/10 virus dilution approximately 250 cells were infected. At 1/100 virus dilution the number of infected cells was similar to the 1/10 dilution suggesting saturation of the cells by BTV-1 and that virtually all of the cells were infected at these virus dilutions. At 1/1000 virus dilution approximately 170 cells were scored as infected, equating to approximately 70% infection as compared to the lower virus dilutions. This would appear to agree with the results seen by confocal microscopy (Figure 3.3, Panel

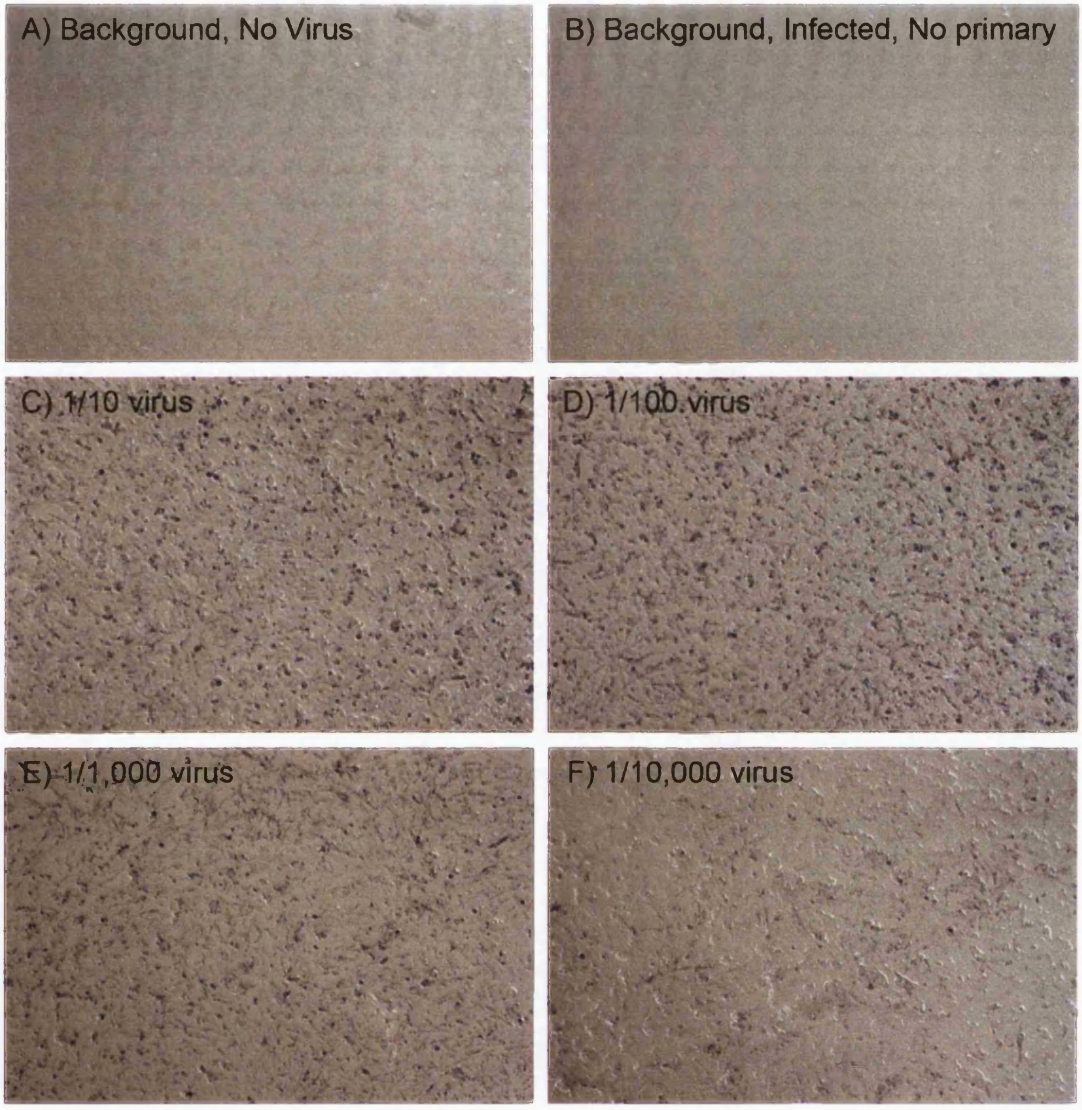

Figure 3.4: Quantification of BTV-1 infection by Enzyme-Linked Immunospot Assay (I) Cell monolayers, in 96 well plates were incubated with BTV-1 for 1 h at 37°C, washed and infection continued for 9 h. Infection was stopped and the cells fixed by the addition of 4% PFM. Cells were permeablised and non-specific binding sites blocked with block buffer. The cells were then incubated with Orab 1, followed by a goat, anti-Rabbit biotinylated secondary antibody and a streptavidin alkaline phosphatase conjugate. Incubation with a streptavidin alkaline phosphatase substrate caused the infected cells to turn blue-black and these were counted using a KS ELIspot Compact reader. Images are representative of triplicate wells. Panel (A) shows uninfected cells; panel (B) shows infected cells where Orab 1 was omitted from the assay. Panels (C)-(F) show infected cells at different virus dilutions. The data shows a decrease in infection with increasing virus dilution.

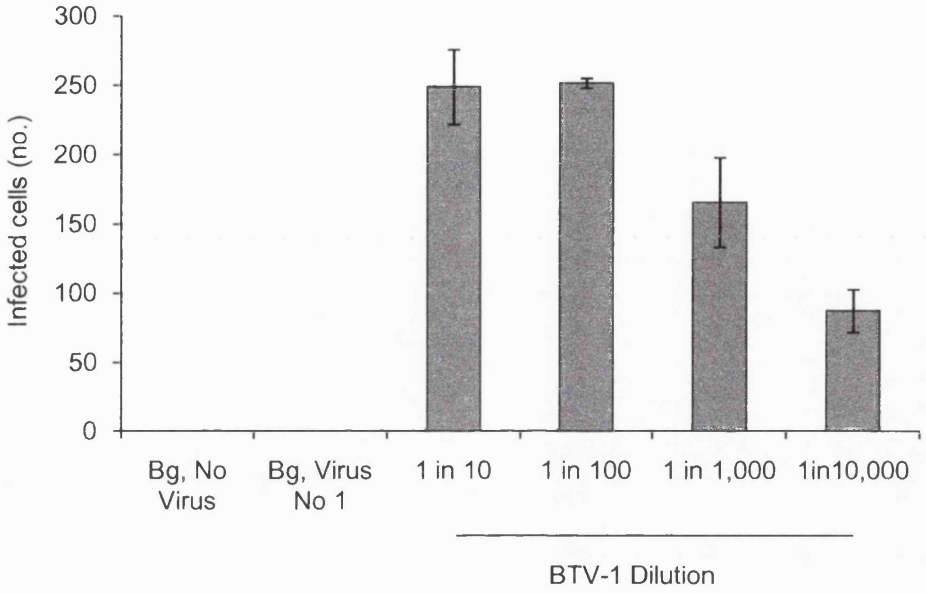

Figure 3.5: Quantification of BTV-1 infection by Enzyme-Linked Immunospot Assay (II)
The data from figure 3.4 is shown in graph format. Each bar shows the number of infected cells as the mean and standard deviation for triplicate samples. Bars show uninfected cells (Bg, No virus); infected cells where Orab 1 was omitted from the assay (Bg, Virus No 1) or infected cells at different virus dilutions.

C). At 1/10,000 virus dilution (Figure 3.5) approximately 80 cells were scored as infected equating to approximately 30% infection.

3.4 Conclusion

The aims of the work presented in this Chapter were to develop confocal microscopy to study BTV cell entry and assays to quantify infection at low m.o.i.. The images in figures 3.1 and 3.2 show that VP5 of the input virus can be readily detected at the cell surfaces and in the cytosol up to 1 hour after the initiation of virus entry. However, as VP5 is removed from the viral core during entry, as a prerequisite for core-particle transfer to the cytosol, it is not yet clear if the VP5 inside the cells is showing the location of intact virus or VP5 after virus uncoating. Nevertheless, this work shows that labelling for VP5 using PM10 can be used to indicate virus endocytosis.

The data shown in figure 3.3 show that NS2 labelling using Orab 1 can be readily used to indentify infected cells by confocal microscopy. The enzyme-linked immunospot assay was also used to quantify infected cells. Broadly, the two assays gave similar data. However, the confocal microscopy experiments show that more than one VIB, hence intense areas of NS2 labelling, can be detected in a single infected cell. This could explain the slightly higher level of infection for the 1/100 virus dilution scored by the enzyme-linked immunospot assay (70% infection) compared to the level scored by confocal microscopy (30% infection) as the enzyme-linked immunospot may count VIB's rather than individual infected cells. For this reason in subsequent experiments where the enzyme-linked immunospot assay was used for quantification of infection, the results were confirmed by confocal microscopy.

4 The Role of Endosomal pH and Clathrin-Mediated Endocytosis in BTV-1 Infection

4.1 Introduction

For a number of bluetongue virus serotypes infection has been shown to require exposure to the low pH within endosomes (Forzan et al., 2007; Hyatt et al., 1989; I.R.Hutchinson, 1999; Verwoerd et al., 1972). The first experiments described in this Chapter investigated the sensitivity of BTV-1 infection to raising endosomal pH using concanamycin-A or ammonium chloride. Concanamycin-A is a potent and specific inhibitor of the vacuolar ATPase which inhibits endosomal acidification thereby increasing endosome pH. Ammonium chloride is a lysosomotropic weak base that buffers the pH of acidic endosomes and also inhibits endosome acidification. Ammonium chloride is fast acting and has been shown to raise the pH in intracellular endosomes within 1 minute of addition (Ohkuma and Poole, 1978). A requirement for low endosomal pH usually indicates clathrin-mediated endocytosis as the entry mechanism as it is the major pathway for cargo delivery to acidic endosomes (see Section 1.5.1). The second series of experiments in this chapter investigated the role of clathrin-mediated endocytosis in BTV-1 entry and infection.

The involvement of clathrin-mediated endocytosis was investigated using dominant-negative mutants of the clathrin assembly protein AP180, and epidermal growth factor receptor substrate 15 (Eps15). AP180 binds clathrin and is required for clathrin cage assembly. The C-terminal domain (AP180C) contains the putative clathrin-binding site and when expressed in mammalian cells functions as a dominant-negative inhibitor of clathrin-mediated endocytosis (Ford et al., 2001). Eps15 binds to the AP2 adaptor present at clathrin-coated pits and is involved in clathrin-mediated endocytosis of a number of ligands (Benmerah et al., 1999). Over expression of a deletion mutant of Eps15 (Eps15-EΔ95-295; from here on known as Dn Esp15) results in the mis-localisation of AP2 which interferes with its recruitment to the plasma

membrane and clathrin mediated-endocytosis (Benmerah et al., 1999; Sieczkarski and Whittaker, 2002).

4.2 The Role of Endosomal pH on BTV Infection

4.2.1 The Effect of Raising Endosomal pH on BTV Infection of BHK cells

BHK cells were pre-treated with concanamycin-A for 30 minutes at 37°C. The cells were then incubated with BTV-1 (m.o.i. = 0.5) for 1 hour in the presence of the drug. At this point, the cells were washed to remove excess virus and drug, and incubation at 37°C continued for a further 5 hours in the absence of the drug. Mock-treated control cells were infected with BTV-1 using an equivalent dilution of DMSO (the solvent for concanamycin-A) in place of concanamycin-A. Infection was stopped and the cells fixed by the addition of 4% paraformaldehyde. Infection was then quantified using the enzyme-linked immunospot assay as described in Chapter 3 (see Section 3.3.2 and Method 2.5.2), using Orab 1 (anti-NS2) to detect infected cells.

Figure 4.1 shows representative well images of an experiment carried out using triplicate samples for each concanamycin-A dilution. Uninfected cells showed no cross-reactivity with the detecting antibodies (Panel A). Panel (B) shows BTV-1 infection in the absence of concanamycin-A (infected cells are shown as blue-black [see Chapter 3, Section 3.3.2]). Panels (C)-(F) show infected cells pre-treated with different concentrations of concanamycin-A (12 nM to 1 nM). A reduction in the number of infected cells was observed following concanamycin-A treatment.

Figure 4.2 shows quantification of the data from the above experiment in graph format. The number of infected cells (as shown by the presence of NS2 labelling) in the concanamycin-A treated wells was normalised to the level of infection in the absence of concanamycin-A (0 nM concanamycin-A; Shown as 100% on the figure). Each bar represents the mean and standard deviation for triplicate wells. The data show an > 80% decrease in the number of BTV-1 infected cells when concanamycin-A was added at 3 nM or above. At 1 nM the number of infected cells was ~60% of mock-treated cells

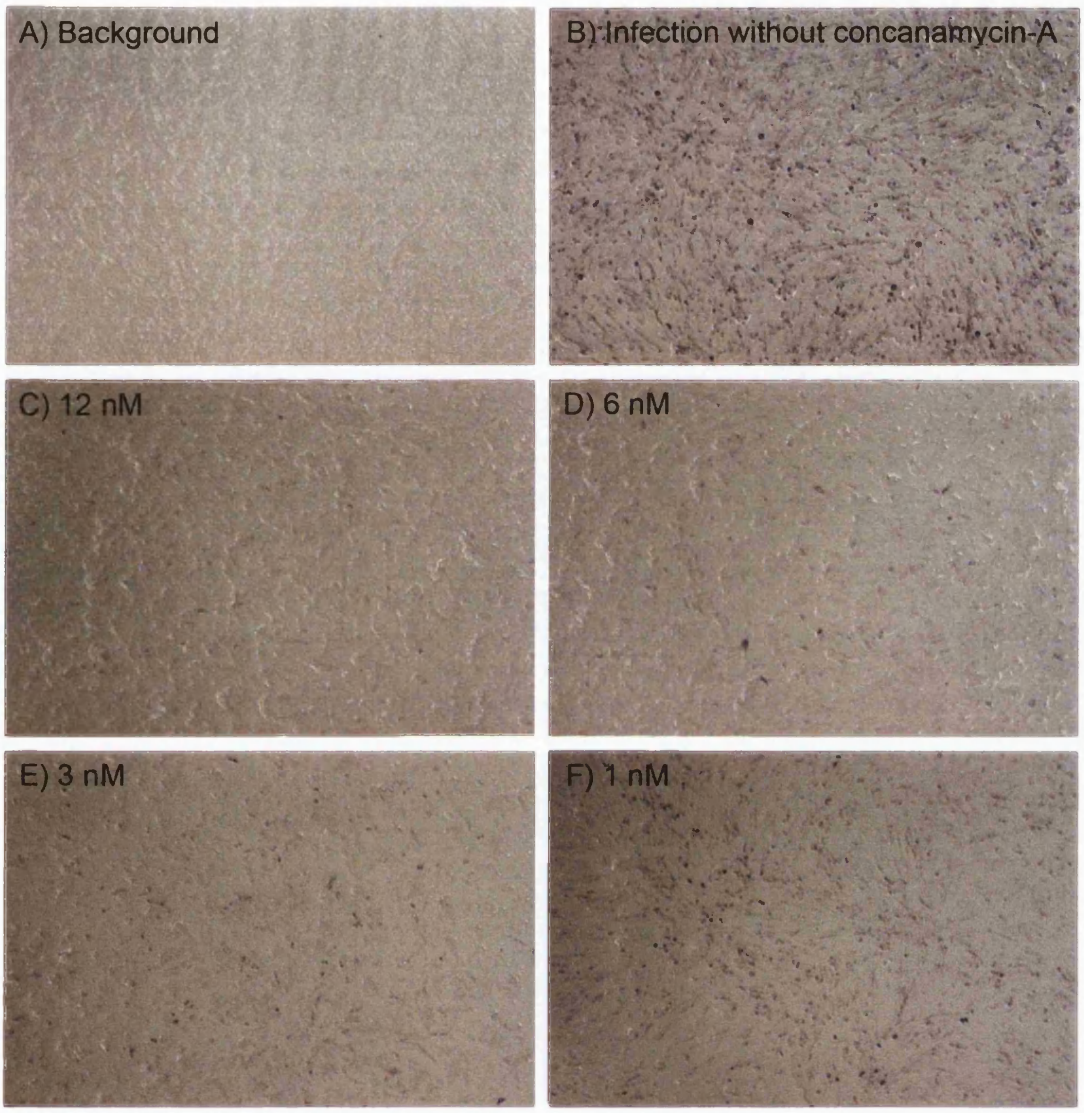

Figure 4.1: Concanamycin-A inhibits infection of BHK cells by BTV-1 (I)
Infection was quantified using the enzyme-linked immunospot assay as described in Chapter 3. Cells were mock or pre-treated with concanamycin-A and infected with BTV-1 for 1 h. The cells were washed and fixed at 6 hpi. Panel (A) shows uninfected cells. Panel (B) shows mock-treated cells, showing the level of BTV-1 infection in the absence of concanamycin-A. Panels (C)-(F) show infection of cells pre-treated with the indicated concetration of concanamycin-A. Infected cells are stained blue-black. Images shown are representative of triplicate wells.

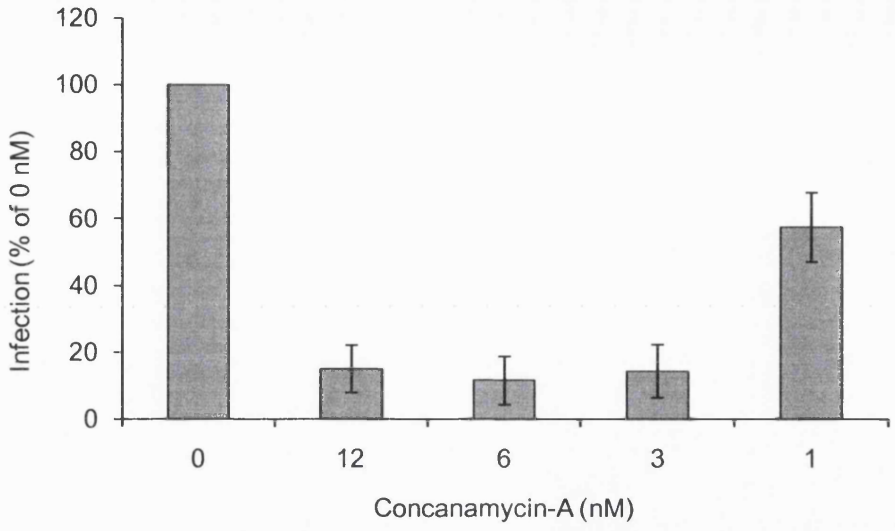

Figure 4.2: Concanamycin-A inhibits infection of BHK cells by BTV-1 (II)
The results from the experiment shown in figure 4.1 are shown in graph format. The data is shown as the mean level of infection normalised to the levels of infection seen in the absence of concanamycin-A (0 nM set as 100%); standard deviation is shown for triplicate wells. When added at ≥3 nM concanamycin-A treatment resulted in ~80% reduction in the number of infected cells.

These data confirm that BTV-1 infection of BHK cells requires a low endosomal pH.

To determine at which point in the virus replication cycle concanamycin-A was having an effect on infection, further experiments were carried out where the drug was added at different times during infection (see Method 2.5.2). Cells were pre-treated with 12 nM concanamycin-A (Treatment 2 on Figure 4.3) or mock-treated (Treatment 1 on Figure 4.3) and infected with BTV-1 (m.o.i. = 0.5) and infection quantified using the enzyme-linked immunospot assay as described for figure 3.4. The drug was also added to additional cell cultures after the 1 hour incubation with virus. On figure 4.3, treatment 3 indicates that the drug was added to the cells for 1.5 hours immediately after the virus was removed from the cells, whereas treatment 4 indicates that the drug was added for 1.5 hours, 1.5 hours after the virus inoculums were removed.

Figure 4.3, panels (A) and (B) show data for two independent experiments. The number of infected cells was normalised to the level of infection of the mock-treated cells (Treatment 1). Each bar represents the mean and standard deviation for triplicate wells. The data confirm that pre-treatment of BHK cells with concanamycin-A inhibits infection by BTV-1 (Treatment 2). Addition of the drug immediately after the virus was removed (Treatment 3) had a small inhibitory effect on infection which suggests that cell entry may not have been completed during the 1 hour incubation with virus. When the drug was added later during infection (Treatment 4), no inhibitory effect on infection was seen. These data show that raising endosomal pH only has an inhibitory effect during the early phase of infection and does not appear to interfere with subsequent intracellular virus replication. The effect of concanamycin-A treatment on BTV-1 infection was also investigated for Vero cells using the enzyme-linked immunospot assay; however, infection took longer to develop (as judged by NS2 labelling) than for BHK cells, therefore infection was stopped and the cells fixed at 10 hpi.

The experiment shown in figure 4.3 was repeated using Vero cells (Figure 4.4). The results were similar to those obtained with BHK cells as concanamycin-A inhibited

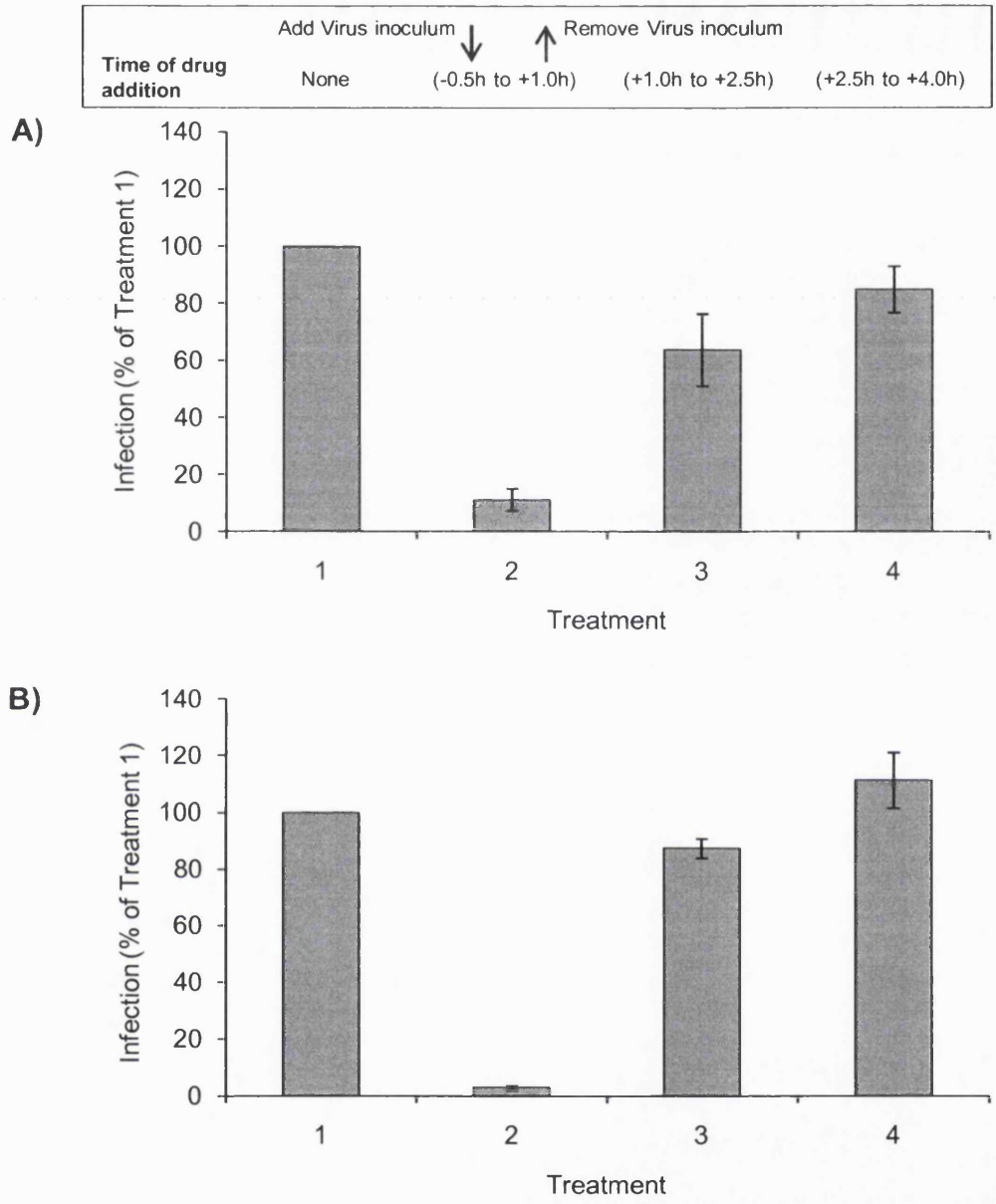

Figure 4.3: Raising endosomal pH inhibits BTV-1 infection of BHK cells
To examine at which point concanamycin-A was having an effect on infection, the drug was added at different times after the start of infection. Graphs (A) and (B) show independent experiments. All cells were infected with BTV-1 and cells fixed at 6 hpi. Infection was quantified using the enzyme-linked immunospot assay as described in Chapter 3. Each bar shows the mean and standard deviation for triplicate wells. The number of infected cells was normalised to the level of infection of the mock-treated cells (Treatment 1). Concanamycin-A treatments: (1) mock-treated cells infected with BTV-1 (i.e. in the absence of concanamycin-A); (2) for 30 min before infection was initiated and during the 1 h incubation with virus; (3) for 90 min immediately after virus inoculum was removed or (4) for 90 min, 90
min after virus inoculum was removed.

BTV-1 infection of Vero cells by ~90% when added as a pre-treatment (Treatment 2). Similar to BHK cells, when added immediately after the virus inoculum was removed (Treatment 3) concanamycin-A had a small inhibitory effect, but had no inhibitory effect when added at later times after infection had started (Treatment 4).

The experiment was also carried out using a bovine endothelial cell line (BPAEC). Figure 4.5, panels (A) and (B) show two independent experiments. Similar to BHK and Vero cells, concanamycin-A (12 nM) had a strong inhibitory effect on infection when added as a pre-treatment (Treatment 2) but did not appear to inhibit infection when added 1.5 hours after the virus was removed (Treatment 4). However, when added immediately after the virus was removed (Treatment 3) infection was inhibited by ~75%. This suggests that for BPAEC cells, virus enters with slower kinetics or that a significant proportion of internalised virus had not reached a low pH environment during the first hour of infection.

4.2.2 Active Endosomal Acidification is required for BTV Infection of BHK cells - Confirmation by Confocal Microscopy

The above experiments used the enzyme-linked immunospot assay to quantify infection and showed that BTV-1 infection requires a low endosomal pH for an early step in infection of BHK, Vero and BPAEC cells. In subsequent experiments, these data was verified for BHK cells using confocal microscopy to quantify infection (see 3.3.1).

To better synchronise the start of infection with addition of the drug, BTV-1 (m.o.i. = 0.5) was pre-bound to BHK cells for 40 minutes on ice in the presence or absence (mock-treated) of 12 nM concanamycin-A. Unbound virus and drug was removed by washing and infection initiated by the addition of pre-warmed medium (37°C). Infection was allowed to proceed for a further 12 hours. Infection was stopped and the cells fixed by the addition of 4% paraformaldehyde. Cells were then permeabilised with 0.1% Triton X-100 and infected cells detected by confocal

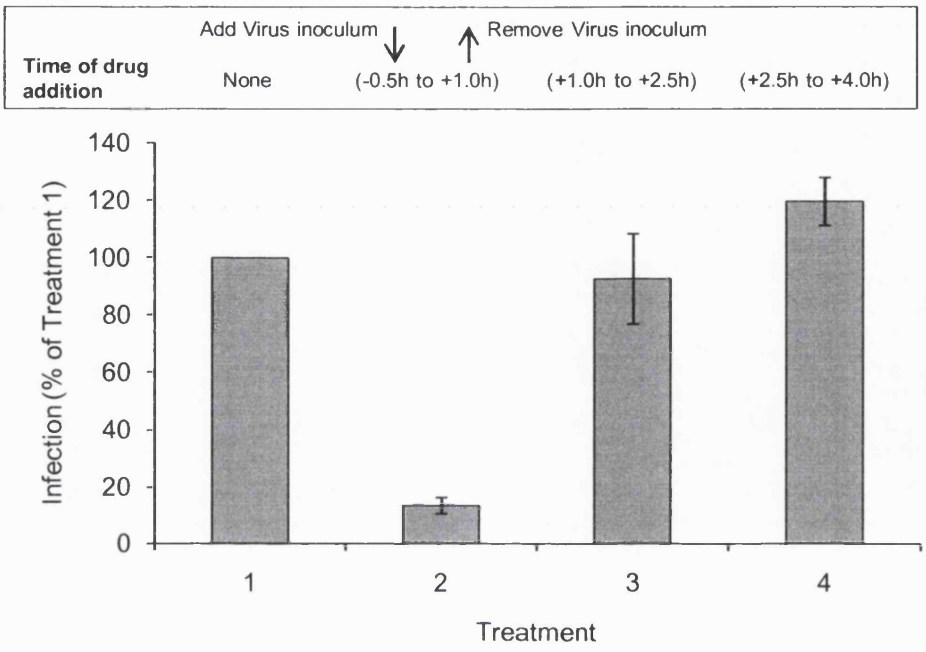

Figure 4.4: Raising endosomal pH inhibits BTV-1 infection of Vero cells
To examine at which point concanamycin-A was having an effect on infection, the drug was added at different times after the start of infection. All cells were infected with BTV-1 and cells fixed at 10 hpi. Infection was quantified using the enzyme-linked immunospot assay as described in Chapter 3. Each bar shows the mean and standard deviation for triplicate wells. The number of infected cells was normalised to the level of infection of the mock-treated cells (Treatment 1). Concanamycin-A treatments: (1) mock-treated cells infected with BTV-1 (i.e. in the absence of concanamycin-A); (2) for 30 min before infection was initiated and during the 1 h incubation with virus; (3) for 90 min immediately after virus inoculum was removed or (4) for 90 min, 90 min after virus inoculum was removed.

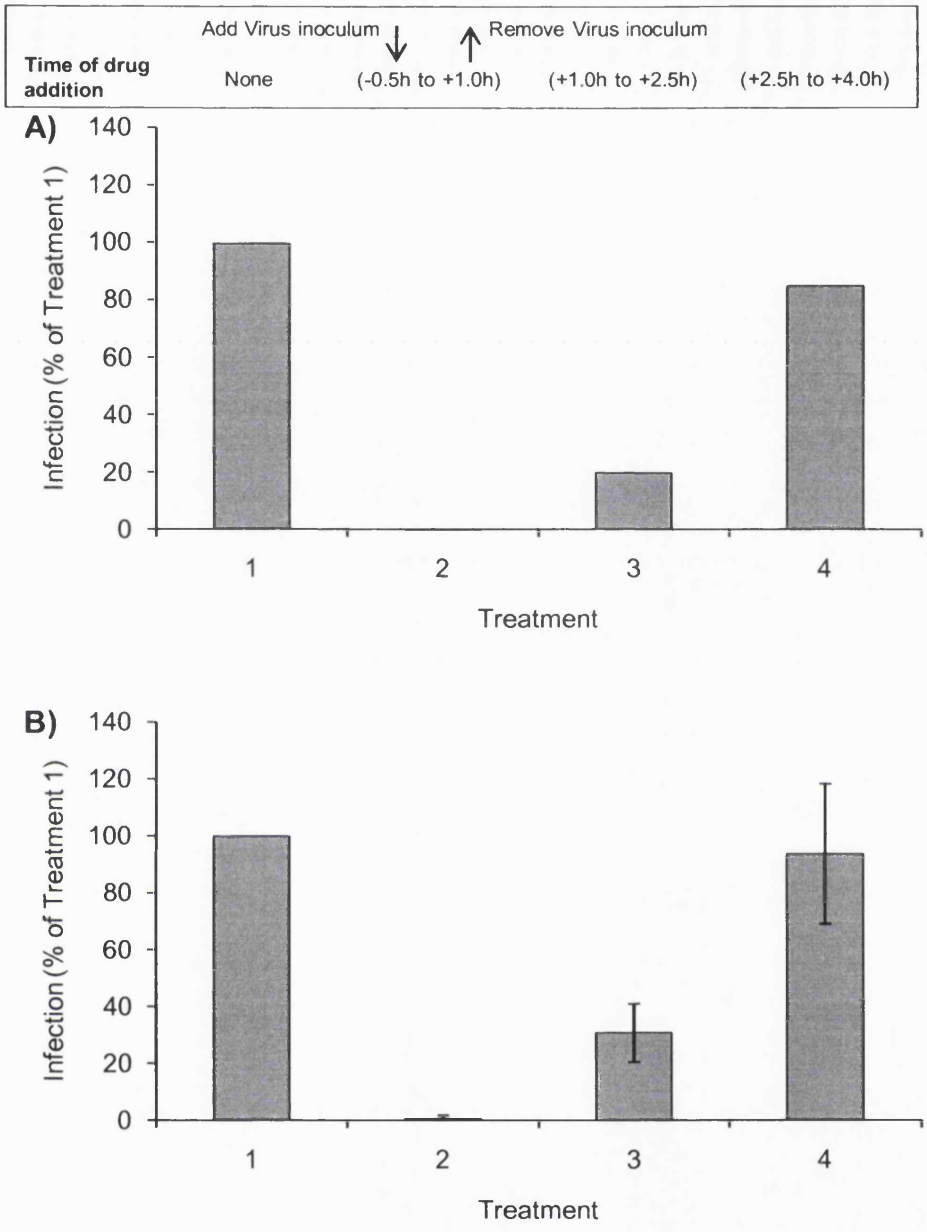

Figure 4.5: Raising endosomal pH inhibits BTV-1 infection of BPAEC cells To examine at which point concanamycin A was having an effect on infection, the drug was added at different times after the start of infection. Graphs (A) and (B) show independent experiments. All cells were infected with BTV-1 and cells fixed at 6 hpi. Infection was quantified using the enzyme-linked immunospot assay as described in Chapter 3. Graph (A) shows the mean of duplicate samples, whilst Graph (B) shows the mean and standard deviation for triplicate samples. The number of infected cells was normalised to the level of infection of the mock-treated cells (Treatment 1). Concanamycin-A treatments: (1) mock-treated cells infected with BTV-1 (i.e. in the absence of concanamycin-A); (2) for 30 min before infection was initiated and during the 1 h incubation with virus; (3) for 90 min immediately after virus inoculum was removed or (4) for 90 min, 90 min after virus inoculum was removed.

microscopy after labelling with Orab 1 (anti-NS2), followed by a goat, anti-Rabbit Alexa-fluor 568-conjugated secondary antibody as described in Chapter 3.

Cells were scored for infection by confocal microscopy (n ≥700 cells). Figure 4.6 (Panels A and B) shows that approximately 85% of the cells were infected in the absence of concanamycin-A, as judged by the presence of NS2 labelling in the cytoplasm, while < 5% of the cells were infected after treatment with concanamycin-A (Figure 4.6, Panels C and D). This data is consistent with the levels of inhibition of infection seen for BHK cells using the enzyme-linked immunospot assay to quantify infection (Figure 4.3).

4.2.3 BTV-1 shows a Slow Delivery Kinetics to Acidic Endosomes

The data shown in figures 4.3, 4.4 and 4.5 shows that addition of concanamycin-A immediately after the 1 hour incubation with virus had a noticeable but relatively small inhibitory effect on infection of BHK and Vero cells and a much greater effect on BPAEC cells. This suggests that BTV-1 may enter cells with relatively slow kinetics. Alternatively, after the virus is taken up it may traffic relatively slowly to acidic endosomes.

To determine the time taken for input virus to reach acidic compartments, BHK cells were treated with 12 nM concanamycin-A at various times after the start of infection and the level of infection quantified using confocal microscopy. BTV-1 was bound to BHK cells on ice in the absence (mock-treated; Mock on Figure 4.7) or presence (Pre-treatment [PT] on Figure 4.7) of 12 nM concanamycin-A and infection (m.o.i. = 0.5) initiated by the addition of pre-warmed medium as described above. Additional cultures were treated with the drug coincident with the start of infection (i.e. upon the addition of pre-warmed medium; Time 0 on Figure 4.7). The drug was also added to other cells at different times (30 to 480 minutes) after the start of infection (i.e.

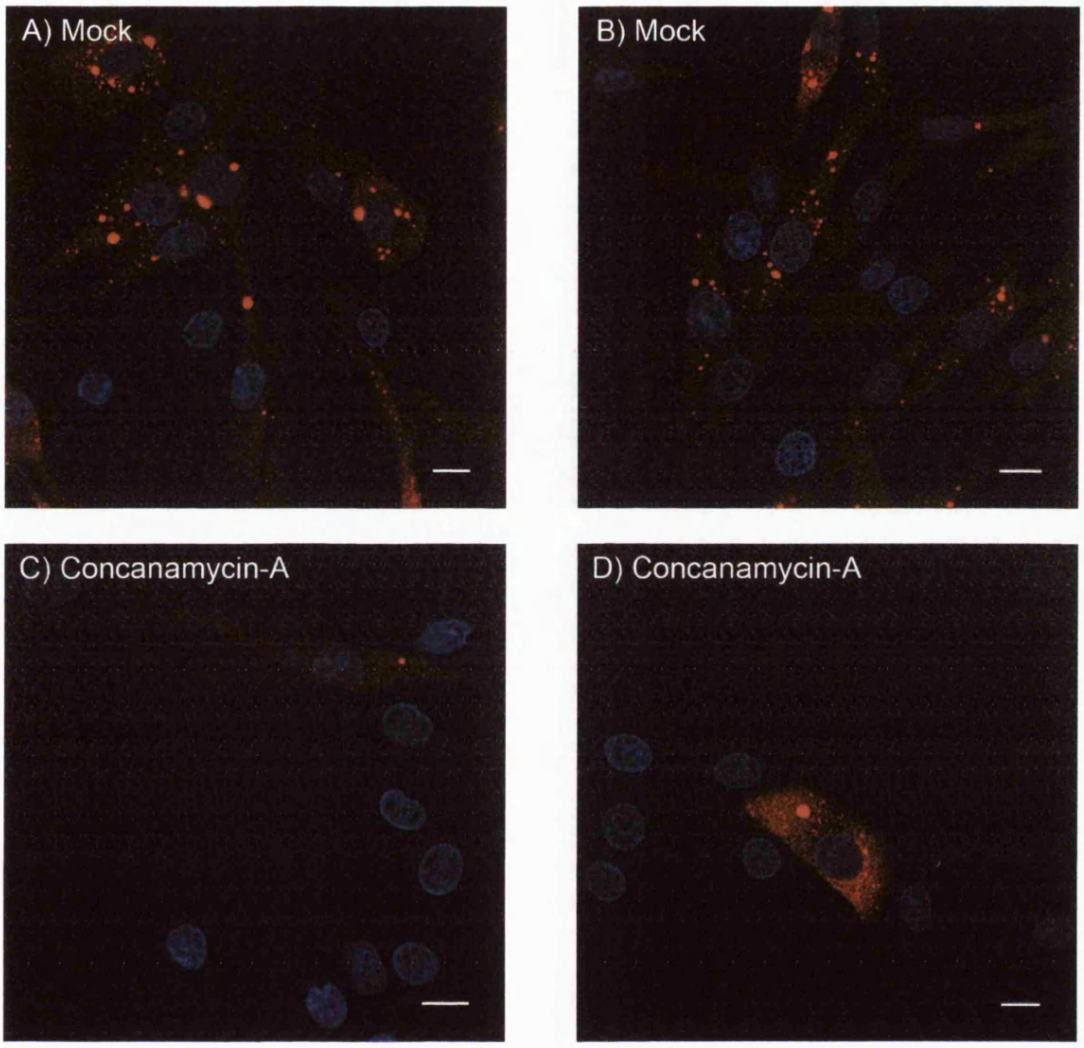

Figure 4.6: Active endosomal acidification is required for BTV-1 infection of BHK cells
BTV-1 (m.o.i. = 0.5) was bound on ice to cells in the presence or absence (mock-treated) of 12 nM concanamycin-A. Unbound virus was removed by washing and infection initiated by incubation at 37°C. Infection was allowed to proceed for 12 h. The cells were fixed and infection detected by labelling with Orab 1 (anti-NS2) followed by a goat, anti-Rabbit Alexa-fluor 568-conjugated secondary antibody. Infected cells were identified by confocal microscopy. Panels (A) and (B) show mock-treated cells infected with BTV-1. Panels (C) and (D) show infection in the presence of 12 nM concanamycin-A. In all panels infection is shown as red. The cell nuclei are shown as blue. Scale bar = 10 μm.

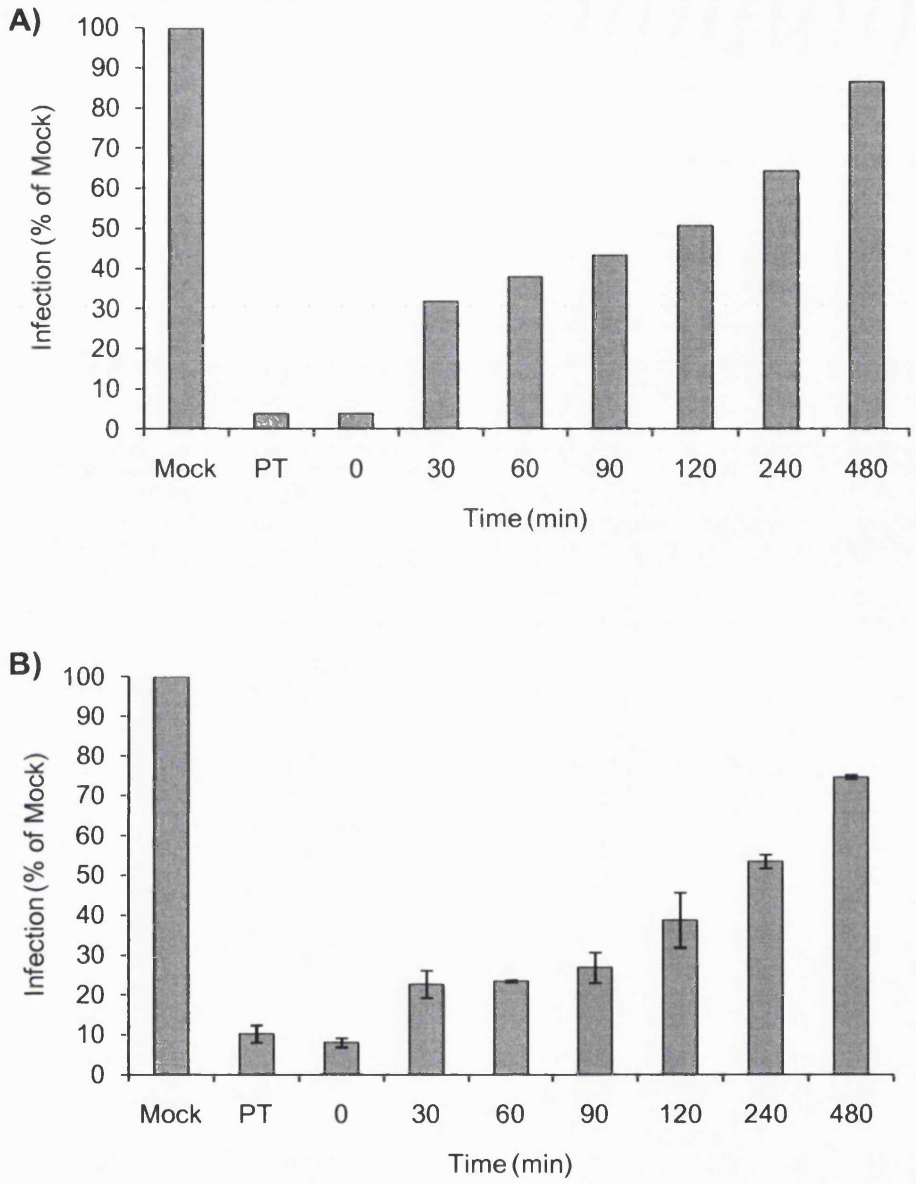

Figure 4.7: BTV-1 shows relatively slow delivery kinetics to acidic endosomes (I)

BTV-1 (m.o.i. = 0.5) was bound on ice to BHK cells in the presence or absence (mock-treated) of 12 nM concanamycin-A. Unbound virus and drug were removed by washing and infection initiated by incubation at 37°C. Additional cells were treated with the drug coincident with the start of infection (Time 0) or at the indicated times after the start of infection. Infection was allowed to proceed for 12 h. The cells were fixed and infection detected by labelling with Orab 1 (anti-NS2) followed by a goat, anti-Rabbit Alexa-fluor 568-conjugated secondary antibody. Infection was quantified by confocal microscopy as in figure 4.6 (n ≥360 cells). The percentage of drug treated cells that were positive for infection was normalised to the level of infection of the mock treated cells. Graph (A) shows the mean of duplicate samples, whilst Graph (B) shows the mean and standard deviation for triplicate samples. Raising endosomal pH 2 h after the start of infection reduced the number of infected cells to ~50% of the mock.

after the addition of pre-warmed medium). Infection was allowed to proceed for 12 hours, when it was stopped by the addition of 4% paraformaldehyde. Cells were permeabilised with 0.1% Triton X-100 and infected cells detected by labelling with Orab 1 (anti-NS2) and a goat anti-Rabbit Alexa-fluor 568-conjugated antibody as in Chapter 3.

Cells were scored for infection by confocal microscopy (n ≥360 cells). The percentage of drug-treated cells that were positive for infection was normalised to the level of infection of the mock-treated cells. Figure 4.7 panels (A) and (B) show two independent experiments; figure 4.7 panel (A) shows the mean of duplicate samples whilst figure 4.7 panel (B) shows the mean and standard deviation for triplicate samples. Consistent with the results above, pre-treatment (PT) of BHK cells with concanamycin-A inhibited infection by > 90% compared to the mock-treated cells (Figure 4.7). Adding the drug co-incident with infection (Time 0) also had a large inhibitory effect on infection (i.e. > 90% inhibition). When concanamycin-A was added 120 minutes after the initiation of infection it also had an inhibitory effect, reducing the frequency of infection by ~50%. When added at later times infection recovered reaching ~85% of the mock-treated cells when added at 480 minutes after the start of infection.

The above experiment was repeated using 25 mM ammonium chloride in place of concanamycin-A. Cells were mock-treated (Mock) or pre-treated (PT) with 25 mM ammonium chloride and infected with BTV-1 (m.o.i. = 0.5). The experiment was carried out as for concanamycin-A, with the drug being added at 0, 30 and 120 minutes after initiation of infection. Infection was detected by labelling with Orab 1 (anti-NS2) as above. Cells were scored for infection by confocal microscopy (n ≥600 cells). The percentage of drug-treated cells that were positive for infection was normalised to the level of infection of the mock-treated cells. Figure 4.8 shows the mean of duplicate samples. Adding ammonium chloride as a pre-treatment, or coincident with the start of infection reduced the frequency of infection to < 1% of the levels of the mock treated

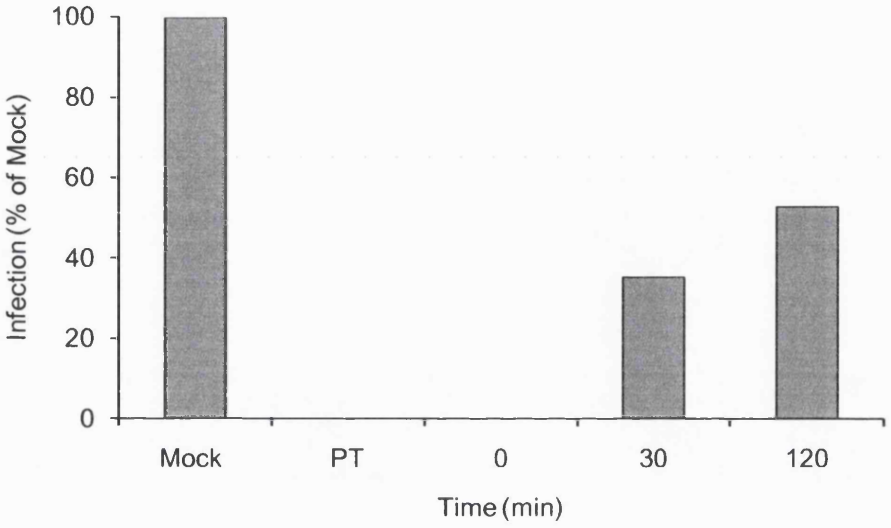

Figure 4.8: BTV-1 shows relatively slow delivery kinetics to acidic endosomes (II)
The experiment shown in figure 4.7 was repeated using 25 mM ammonium chloride in place of concanamycin-A. Ammonium chloride was added as a pre-treatment (PT), coincident with the start of infection (Time 0) or 30 and 120 min after the start of infection. Infection was quantified by confocal microscopy as in figure 4.6 (n ≥600 cells). The mean of duplicate samples is shown. Raising endosomal pH 2 h after the start of infection reduced the number of infected cells to ~50% of the mock.

cells. Adding the drug at 30 minutes post initiation of infection reduced the frequency of infection to ~35% of mock-treated cells whereas raising endosomal pH 120 minutes after the start of infection reduced the level of infection to ~50% of the mock. These results confirmed that ammonium chloride addition had the same inhibitory effect on BTV-1 infection of BHK cells as concanamycin-A (Figure 4.7).

4.2.4 Concanamycin-A Treatment of BHK Cells does not Inhibit Entry of Transferrin

The above experiments show that raising endosomal pH with concanamycin-A inhibits an early step of BTV-1 infection of BHK, Vero and BPAEC cells. Most likely, raising endosomal pH prevents acid-induced virus uncoating, and hence translocation of the viral core-particle to the cytosol. However, raising endosomal pH could also have other non-specific effects. For example, raising endosomal pH could inhibit receptor recycling, thereby reducing the level of virus binding to the cells and subsequent entry and infection.

To ensure that clathrin-mediated endocytosis was not inhibited, the effect of concanamycin-A on entry of transferrin (a commonly used marker of clathrin-mediated endocytosis) was examined. BHK cells were depleted of cellular iron by incubating in serum-free medium (GMEM) for 30 minutes at 37°C (see Method 2.6.2). The cells were then mock-treated (Figure 4.9, Panels A and B) or treated with 12 nM concanamycin-A (Figure 4.9, Panels C and D), for 30 minutes at 37°C (also in serum-free medium). The cells were then washed and allowed to internalise 568-Alexa labelled transferrin (25 µg/ml) for 15 minutes at 37°C. Entry of transferrin was stopped and the cells fixed by the addition of 4% paraformaldehyde including 0.25% glutaraldehyde and processed for confocal microscopy. Figure 4.9 shows that entry of transferrin (shown as red) appeared normal in concanamycin-A treated cells (Figure 4.9, Panels C and D) compared to mock-treated cells (Figure 4.9, Panels A and B), demonstrating that the clathrin pathway was not inhibited by concanamycin-A treatment.

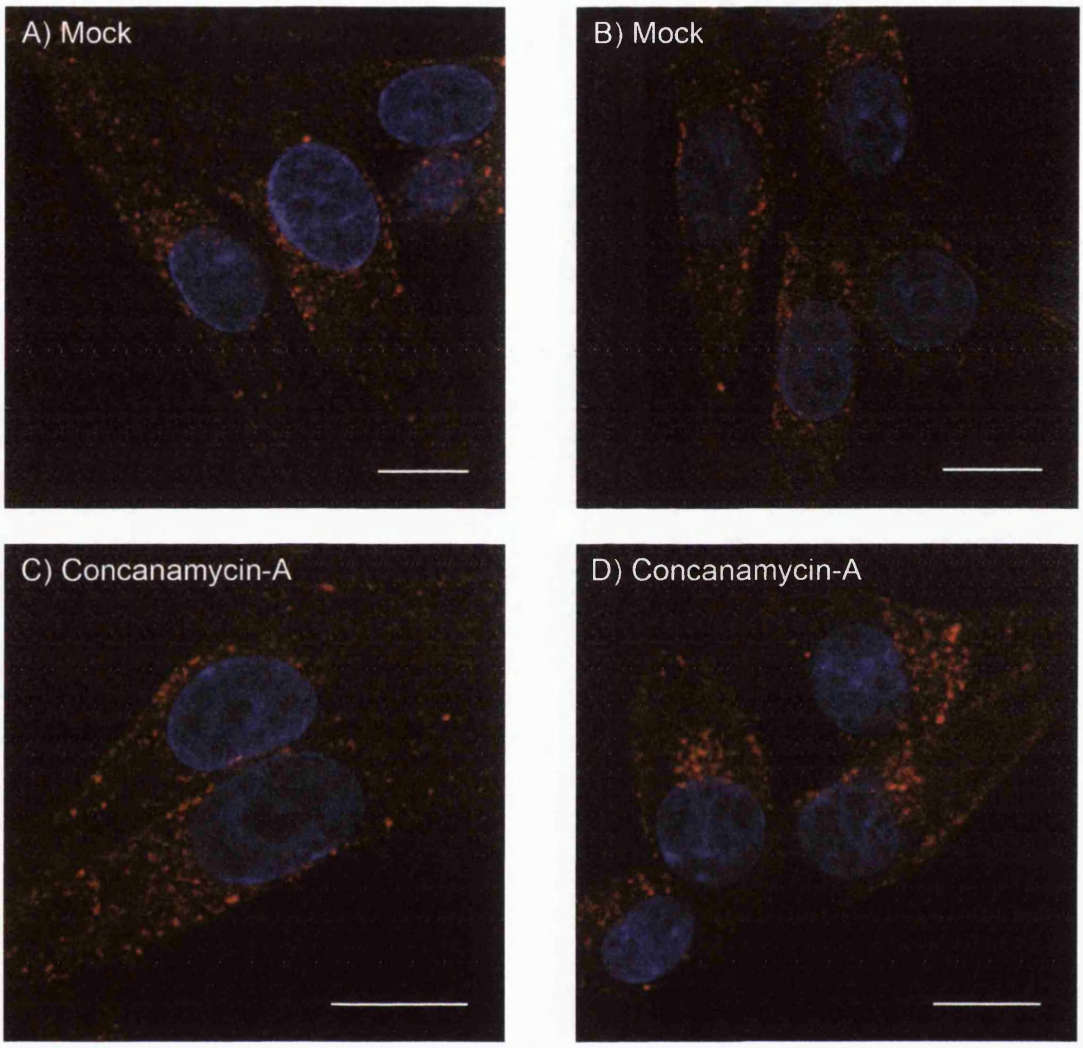

Figure 4.9: Concanamycin-A treatment does not block transferrin entry in BHK cells
Cells were depleted of cellular iron by incubation in serum-free medium for 30 min at 37°C and then mock-treated (A) and (B) or treated with 12 nM concanamycin-A (C) and (D) for 30 min at 37°C. The cells were then incubated with 25 μg/ml 568-Alexa labelled transferrin added for 15 min at 37°C. Entry of transferrin was stopped and the cells fixed by the addition of 4% PFM + 0.25% glutaraldehyde. Cells were visualised by confocal microscopy. Transferrin is shown as red. The cell nuceli are shown as blue. No inhibition of entry of transferrin was seen in the presence of concanamycin-A showing that the clathrin-mediated pathway was not inhibited by concanamycin-A. Scale bar = 10 μm.

4.2.5 Concanamycin-A Treatment does not Inhibit Virus Binding to BHK or BPAEC Cells

The above experiment shows that clathrin-mediated endocytosis of transferrin is not inhibited by concanamycin-A. However, it remains possible that concanamycin-A reduces cell-surface expression of BTV attachment receptors. The receptor for BTV attachment to mammalian cells is unknown. Therefore to verify that concanamycin-A does not reduce the level of BTV attachment receptors at the plasma membrane, virus binding to cells was measured as an indicator of receptor levels.

Cells were harvested using trypsin, collected by centrifugation, and allowed to recover in cell culture medium for 30 minutes at 37°C. Cells were then mock-treated or incubated with 12 nM concanamycin-A for 30 minutes at 37°C (see Method 2.10.2). The cells were transferred to a 96-well plate and incubated with BTV-1 (100 µg/ml) for 45 minutes on ice. The cells were processed for flow cytometry using PM10 (anti-VP5) and a goat, anti-Guinea pig Alexa-fluor 488-conjugated secondary antibody to detect cell-bound virus as described in the methods section (see Method 2.10.1).

Figure 4.10, panel (A) shows a typical histogram for the mean fluorescent intensity for virus binding to BHK cells (shown as the clear histogram) and for the background antibody binding levels in the absence of virus (shown as grey). The shift to the right indicates virus binding to the cells.

Figure 4.10, panel (B) shows the data in graph format for virus binding to BHK and BPAEC cells in the presence or absence of concanamycin-A. Each bar shows the mean and standard deviation for the level of virus binding to cells treated with 12 nM concanamycin-A normalised to the level of virus binding in mock-treated cells for triplicate samples from two independent experiments (E1 & E2) for each cell line (BHK and BPAEC cells). This analysis shows that treatment of either cell line with 12 nM concanamycin-A does not inhibit virus binding to the cells.

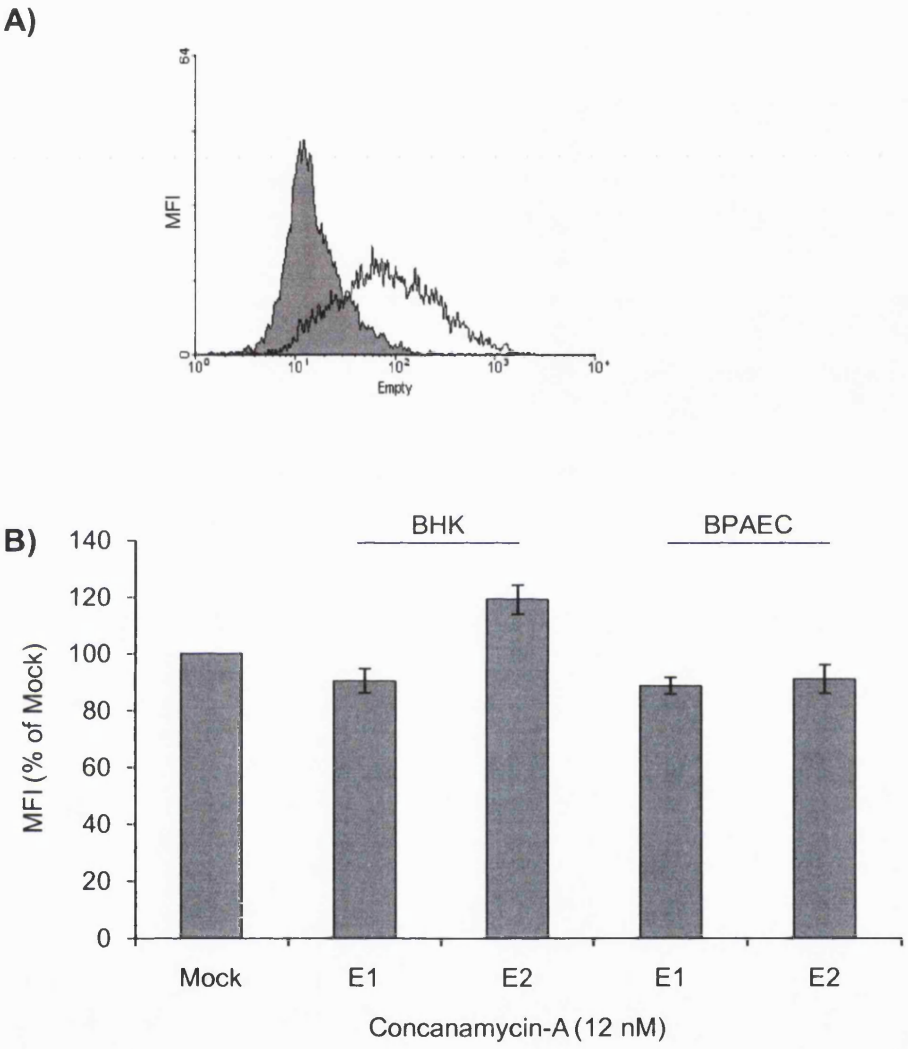

Figure 4.10: Concanamycin-A treatment does not inhibit BTV-1 binding to BHK and BPAEC cells

BTV-1 was bound for 30 min to mock-treated cells or cells incubated with 12 nM concanamycin-A. Virus binding was detected by flow cytometry using PM10 (anti-VP5) followed by a goat, anti-Guinea Pig Alexa-fluor 488-conjugated secondary antibody. Cells were fixed in 1% paraformaldehyde and 6,000 cells per sample read.

Panel (A) shows a typical histogram of virus binding (clear) to BHK cells. Background levels (i.e. no virus) is shown as the grey histogram.

Panel (B) shows the mean and standard deviation for BTV-1 binding to the cells treated with concanamycin-A normalised to the level of virus binding in mock-treated cells. Triplicate samples from two independent experiments are shown (E1, E2) for either BHK cells or BPAEC cells. No inhibition of virus binding to either cell line was seen after concanamycin-A treatment.

4.2.6 Concanamycin-A Treatment of BHK Cells does not Inhibit BTV Entry

Figure 4.10, panel (B) shows that virus binding to BHK cells was not inhibited by concanamycin-A treatment. Next the effect of concanamycin-A on virus entry was investigated. Cells were pre-treated with 12 nM concanamycin-A (Figure 4.11, Panels B and C) or mock-treated (Figure 4.11, Panel A) for 30 minutes at 37°C. BTV was bound to the cells in the presence or absence (mock) of the drug for 40 minutes on ice (see Method 2.6.8 and 2.6.9). Unbound virus was removed by washing and entry initiated by the addition of pre-warmed medium (37°C). After 30 minutes entry was stopped and the cells fixed by the addition of 4% paraformaldehyde. The cells were then permeabilised with 0.1% Triton X-100 and labelled for BTV-1 with PM10 (anti-VP5) as described in Chapter 3. Figure 4.11 panels (B) and (C) shows that virus appears to enter cells normally following concanamycin-A treatment, as compared to mock-treated cells (Figure 4.10, Panel A). Figure 4.11, panels (D)-(F) show merged images for fluorescence with differential interference contrast (DIC) to clearly show the plasma membrane.

In summary, the above experiments show that raising endosomal pH inhibits BTV-1 infection of BHK, Vero and BPAEC cells. The block to infection occurs during an early phase of the virus replication cycle but does not appear to interfere with subsequent intracellular virus replication. The flow cytometry (Figure 4.10) and virus entry experiments (Figure 4.11) show that the block to infection was not due to a reduction of virus attachment receptors or virus internalisation. Together, these observations are consistent with a requirement for low endosomal pH in virus uncoating and endosomal membrane-penetration by the core-particle. Raising endosomal pH after the start of infection (Figures 4.3 to 4.8) suggests that BTV-1 may enter BHK cells with relatively slow kinetics, or that post-entry virus-delivery to acidic endosomes is relatively slow. This could indicate that BTV-1 is not using clathrin-mediated endocytosis for infection (see Section 4.4).

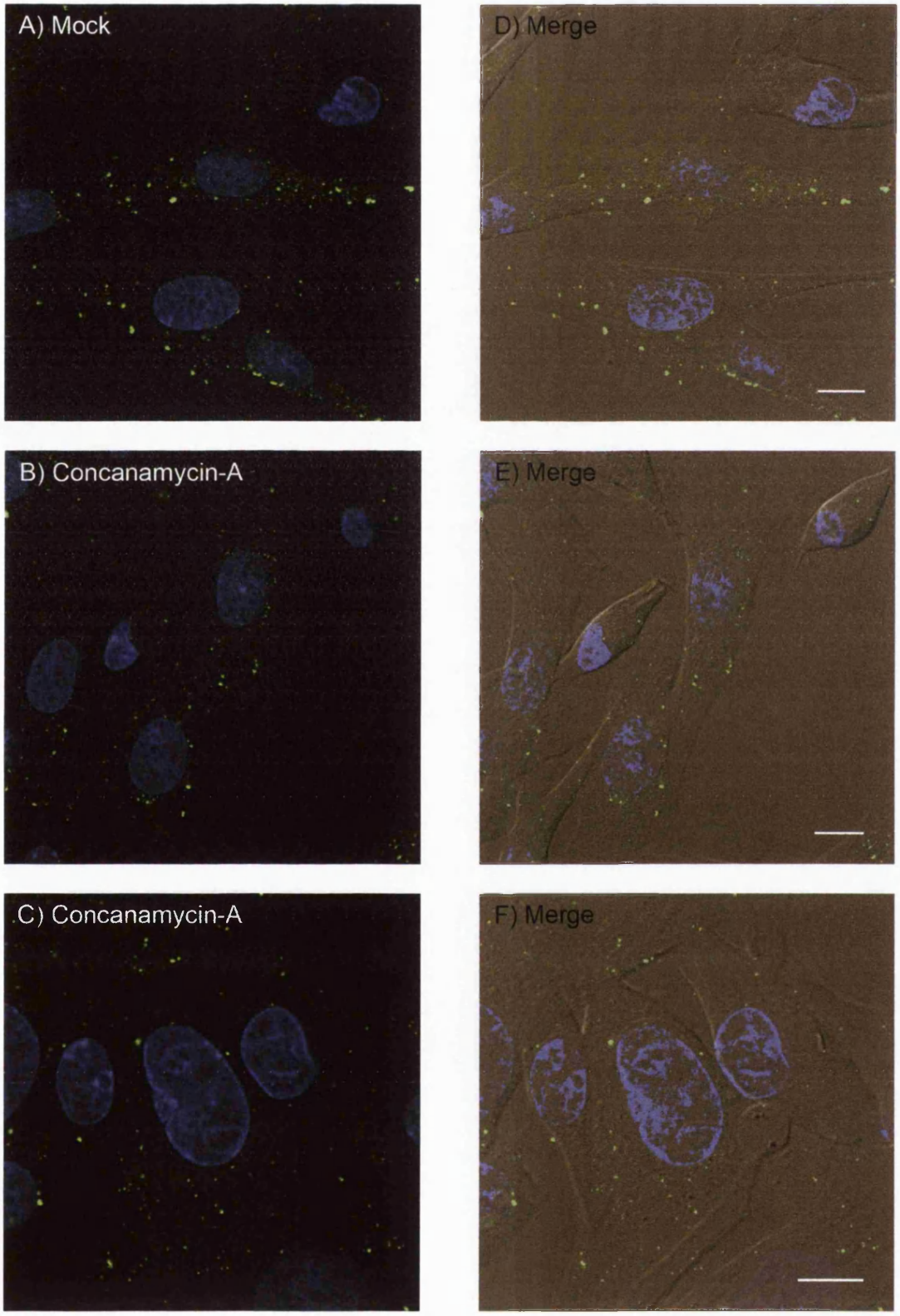

Figure 4.11: Concanamycin-A treatment does not block BTV-1 entry in BHK cells
Cells were pre-treated with 12 nM concanamycin-A (B) and (C) or mock-treated (A) for 30 min. BTV was then bound to the cells in the presence of the drug. Unbound virus was removed by washing and entry initiated by warming to 37°C. Entry was stopped and the cells fixed with the addition of 4% PFM. Cells were processed for confocal microscopy. BTV was labelled with PM10 (anti-VP5) and a goat, anti-Guinea Pig Alexa-fluor 488-conjugated secondary antibody. BTV is shown as green. The cell nuclei are shown as blue. Scale bar = 10 μm. Panels (D-F) show merged images with DIC for the same cells as in panels (A-C). No inhibition of BTV uptake was seen in the presence of concanamycin-A.

4.3 The Role of Clathrin-Mediated Endocytosis in BTV Infection

The experiments described above have shown that raising endosomal pH inhibits BTV-1 infection of BHK, Vero and BPAEC cells. An inhibitory effect of raising endosomal pH on virus infection usually indicates virus entry by clathrin-mediated endocytosis as this is the major pathway for cargo/receptor uptake to acidic endosomes (see Section 1.5.1). In the following experiments, the role of clathrin-mediated endocytosis was investigated using dominant-negative mutants of AP180 or Eps15 (see Section 1.5.1.2 and 4.1), proteins that are normally required for the formation of clathrin-coated vesicles.

BHK cells were transfected to express Dn Eps15 or a control Eps15 (D3Δ2); which does not inhibit clathrin-mediated endocytosis (Benmerah et al., 1999) as fusions with eGFP; or c-myc tagged AP180C (see Section 1.5.1.2 and Method 2.7.2). Transfected cells expressing Dn Eps15 or control Eps15 proteins were identified by confocal microscopy using the eGFP fusion tag. Cells transfected with AP180C were permeabilised, and expressing cells were identified by labelling with 9E10 (anti-c-myc) and a goat, anti-mouse IgG1 Alexa-fluor 488-conjugated secondary antibody. Transfected cells expressing either AP180C or Eps15 are shown as green on the figures below.

At 12 hour post-transfection, the cells were assessed for inhibition of clathrin-mediated endocytosis by scoring entry of transferrin (see Method 2.6.2). Cellular iron was depleted from the cells by incubating with serum-free medium for 30 minutes prior to internalisation of 568-Alexa labelled transferrin for 15 minutes at 37°C. Excess transferrin was removed by washing with cold GMEM, internalisation stopped and the cells fixed by the addition of 4% paraformaldehyde including 0.25% glutaraldehyde for 40 minutes on ice. The ability of Dn Eps15 or AP180C expressing cells to undergo clathrin-mediated endocytosis was determined by scoring entry of transferrin by confocal microscopy. Cells were scored as transferrin positive if the ligand had

accumulated in the perinuclear region giving a clear indication of successful entry and transport through the cell.

The ability of the transfected cells to internalise BTV-1 was also assessed (see Method 2.6.8). At 12 hours post-transfection, BTV (13 µg/ml) was bound to the cells for 40 minutes on ice. Excess unbound virus was removed by washing and entry initiated by the addition of pre-warmed medium (37°C). After 30 minutes, virus entry was stopped and the cells fixed by the addition of 4% paraformaldehyde. The cells were then permeabilised with 0.1% Triton X-100 and processed for confocal microscopy using PM10 (anti-VP5) to label the virus as described in Chapter 3. BTV is shown as red in all images. The percentage of control Eps15, Dn Eps15 or AP180C expressing cells that internalised virus was determined by scoring the cells for virus entry.

4.3.1 Expression of Dn Eps15 does not Inhibit BTV-1 Entry or infection

Figure 4.12 shows cells expressing control Eps15 or Dn Eps15 (shown as green) after a 15 minute incubation with transferrin (shown as red). Panels (A), (C) and (E) show entry of transferrin. Panels (B), (D) and (F) show merged images for red and green fluorescence for the same cells. Cells expressing the control protein (Figure 4.12, Panel A) showed a normal pattern of transferrin uptake as compared to non-expressing cells, while cells expressing the Dn Eps15 protein showed a reduction in transferrin uptake (Figure 4.12, Panels C and E).

Cells expressing control Eps15 or Dn Eps15 (n ≥100 cells) were scored for transferrin entry by confocal microscopy. Cells were scored as transferrin negative if the ligand had not accumulated in the perinuclear region and transferrin positive if the ligand had accumulated thus giving a clear indication of successful entry and transport through the cell. The percentage of cells expressing Dn Eps15 that was positive for transferrin uptake (with perinuclear accumulations of the ligand) was normalised to the level of transferrin uptake for cells expressing the Eps15 control. Figure 4.14 panel (A) shows the mean for two independent experiments and shows

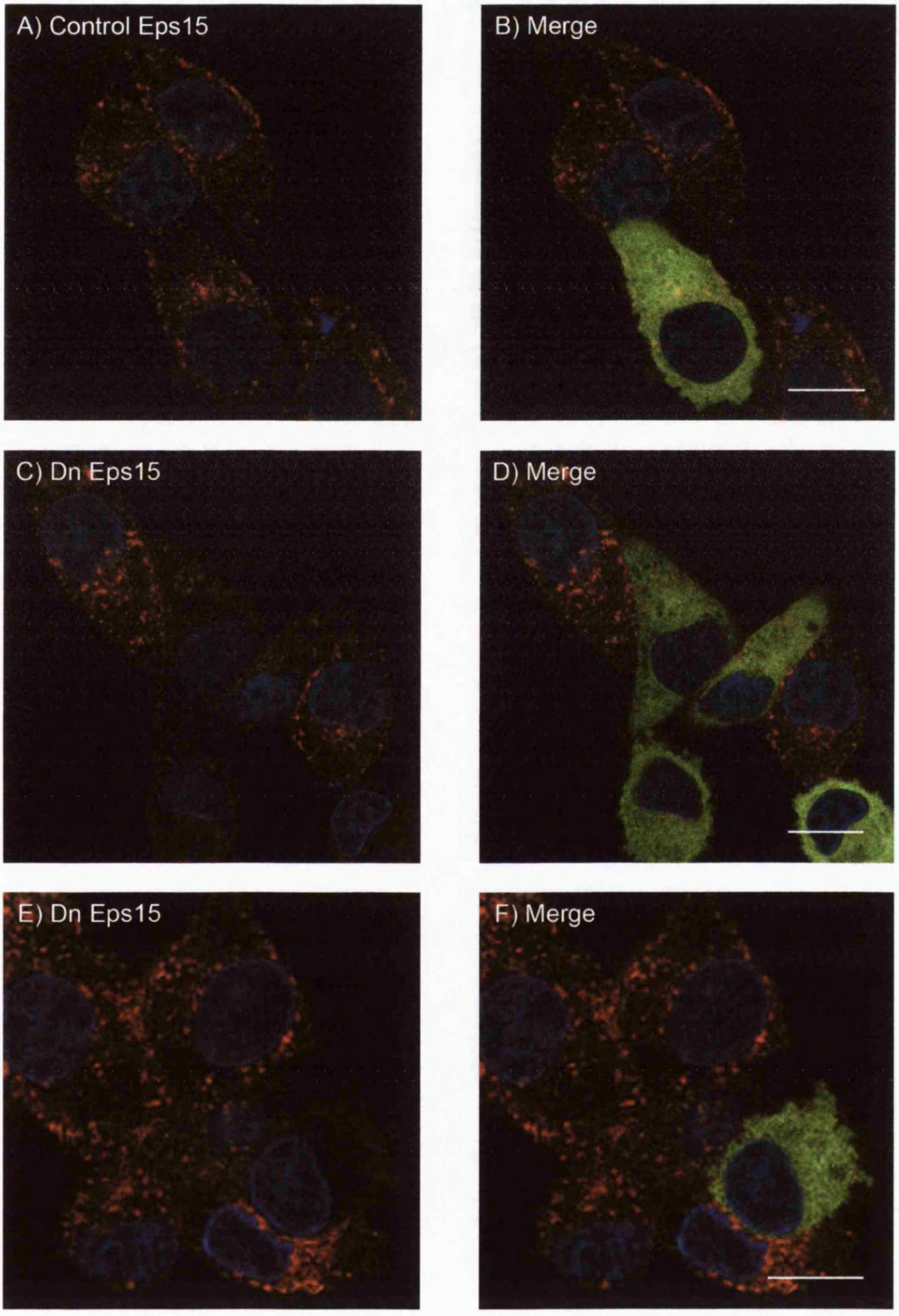

Figure 4.12: Expression of Dn Eps15 inhibits clathrin-mediated endocytosis of transferrin
BHK cells were transfected to express Eps15 control (A) and (B) or Dn Eps15 (C-F) for 12 h and then 568-Alexa labelled transferrin was taken up continuously for 15 min at 37°C. Cells were fixed and visualised by confocal microscopy. Transferrin is shown as red. Cells expressing a transgene are shown as green. Panels (C), (D) and (F) show merged images for red and green fluorescence. Cells expressing Dn Eps15 proteins show reduced entry of transferrin. The cell nuclei are shown as blue. Scale bar = 10 μm.

that expression of Dn Eps15 inhibited clathrin-mediated endocytosis of transferrin by ~44-50%, indicating a block to clathrin-mediated endocytosis.

The effect of Dn Eps15 on BTV-1 entry was also investigated. Figure 4.13 shows cells expressing the control Eps15 or Dn Eps15 (shown as green) after a 30 minute incubation with BTV-1 (shown as red). Panels (A), (C) and (E) show virus entry. Panels (B), (D) and (F) show merged images for red and green fluorescence for the same cells. Cells expressing the control protein showed a normal pattern of BTV-1 entry when compared to cells that were not expressing a transgene (Figure 4.13, Panel A). In contrast to entry of transferrin, cells expressing the Dn Eps15 protein showed normal virus entry (Figure 4.13, Panels C and E).

Cells expressing control Eps15 or Dn Eps15 (n ≥100 cells) were scored for virus entry by confocal microscopy. The percentage of cells expressing Dn Eps15 that was positive for virus entry was normalised to the level of virus entry for cells expressing control Eps15. Figure 4.14 panel (B) shows the mean for two independent experiments and shows that expression of Dn Eps15 did not appear to inhibit BTV-1 internalisation into BHK cells.

4.3.2 Expression of AP180C does not Inhibit BTV-1 Entry

As the block to entry of transferrin caused by expression of Dn Eps15 was only 50%, a second more potent inhibitor of clathrin-mediated endocytosis (AP180C) was also investigated. Again the inhibitory effect of the dominant-negative protein on clathrin-mediated endocytosis was assessed by quantifying internalisation of transferrin by AP180C expressing cells. Cells were scored as transferrin negative if the ligand had not accumulated in the perinuclear region and transferrin positive if the ligand had accumulated thus giving a clear indication of successful entry and transport through the cell.

Figure 4.15 shows cells expressing AP180C (shown as green) after a 15 minute incubation with transferrin (shown as red). Panel (A) shows transferrin uptake whilst

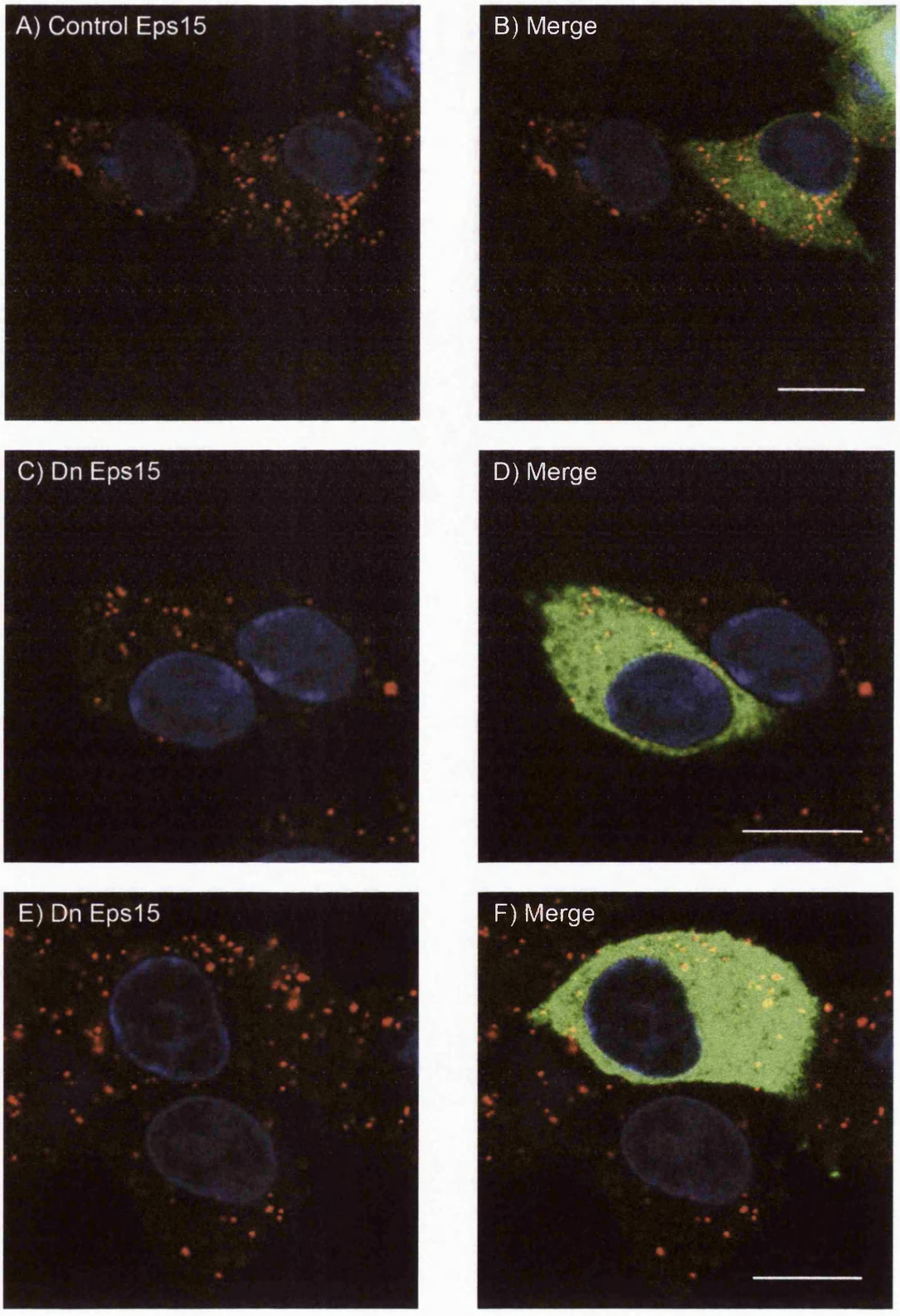

Figure 4.13: Expression of Dn Eps15 does not block BTV-1 entry
BHK cells were transfected to express Eps15 control (A) and (B) or Dn Eps15 (C-F) for 12 h and then BTV-1 was taken up for 30 min at 37°C. Cells were fixed and virus labelled for BTV with PM10 (shown as red). Cells expressing a transgene are shown as green. Panels (C), (D) and (F) show merged images for red and green fluorescence. Cells expressing Dn Eps15 proteins show normal BTV-1 uptake. The cell nuclei are shown as blue. Scale bar = 10 μm.

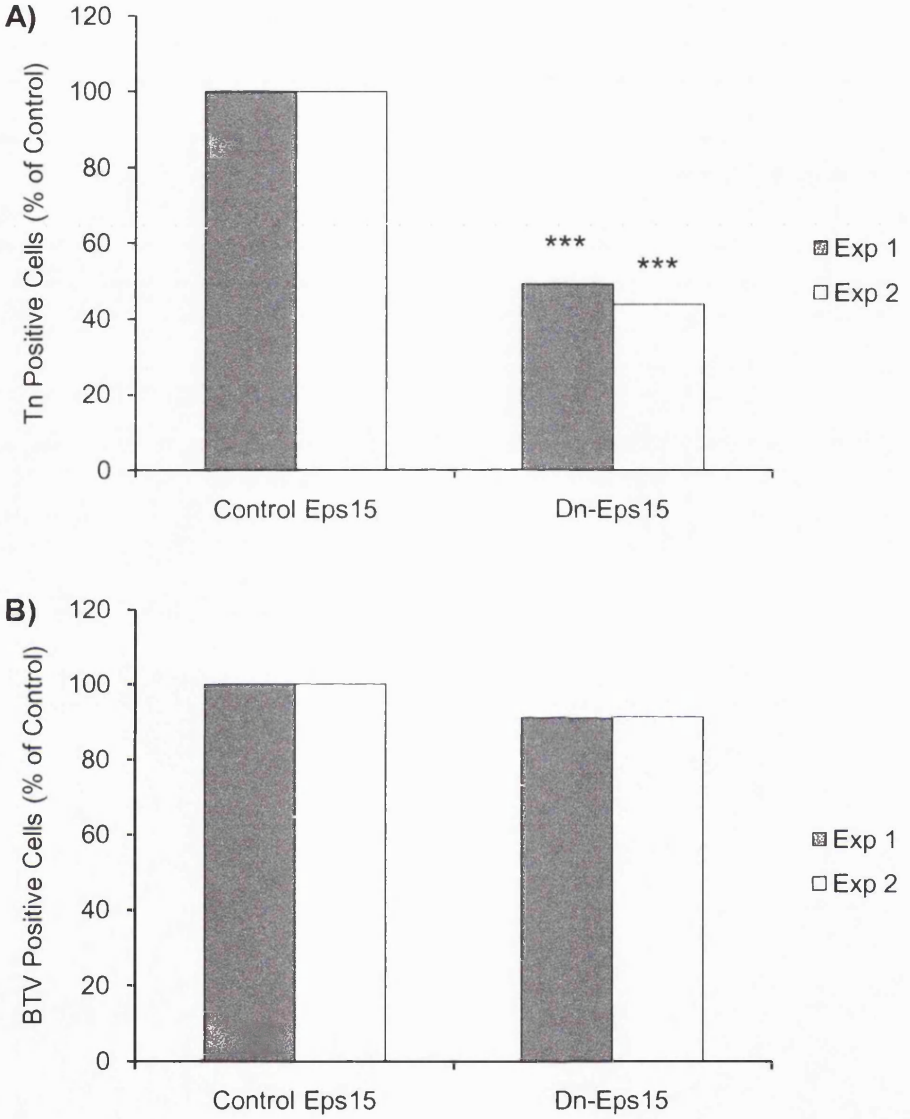

Figure 4.14: Entry of transferrin and BTV-1 by BHK cells expressing Dn Eps15

Panel (A): BHK cells expressing control Eps15 or Dn Eps15 were scored for the presence of transferrin (n ≥ 100 cells). The percentage of cells expressing Dn Eps15 that was positive for entry of transferrin as shown by accumulation of the ligand in the perinuclear region of the cell, was normalised to the level of entry of transferrin for cells expressing the control Eps15. The mean of duplicate samples for two independent experiments is shown (Exp 1, Exp 2) (*P* values: *** <0.001).

Panel (B): BHK cells expressing control Eps15 or Dn Eps15 proteins were scored for virus entry (n ≥ 100 cells). The percentage of cells expressing Dn Eps15 that was positive for BTV-1 was normalised to the level of virus entry for cells expressing the control Eps15. The mean of duplicate samples for two independent experiments is shown (Exp 1, Exp 2).

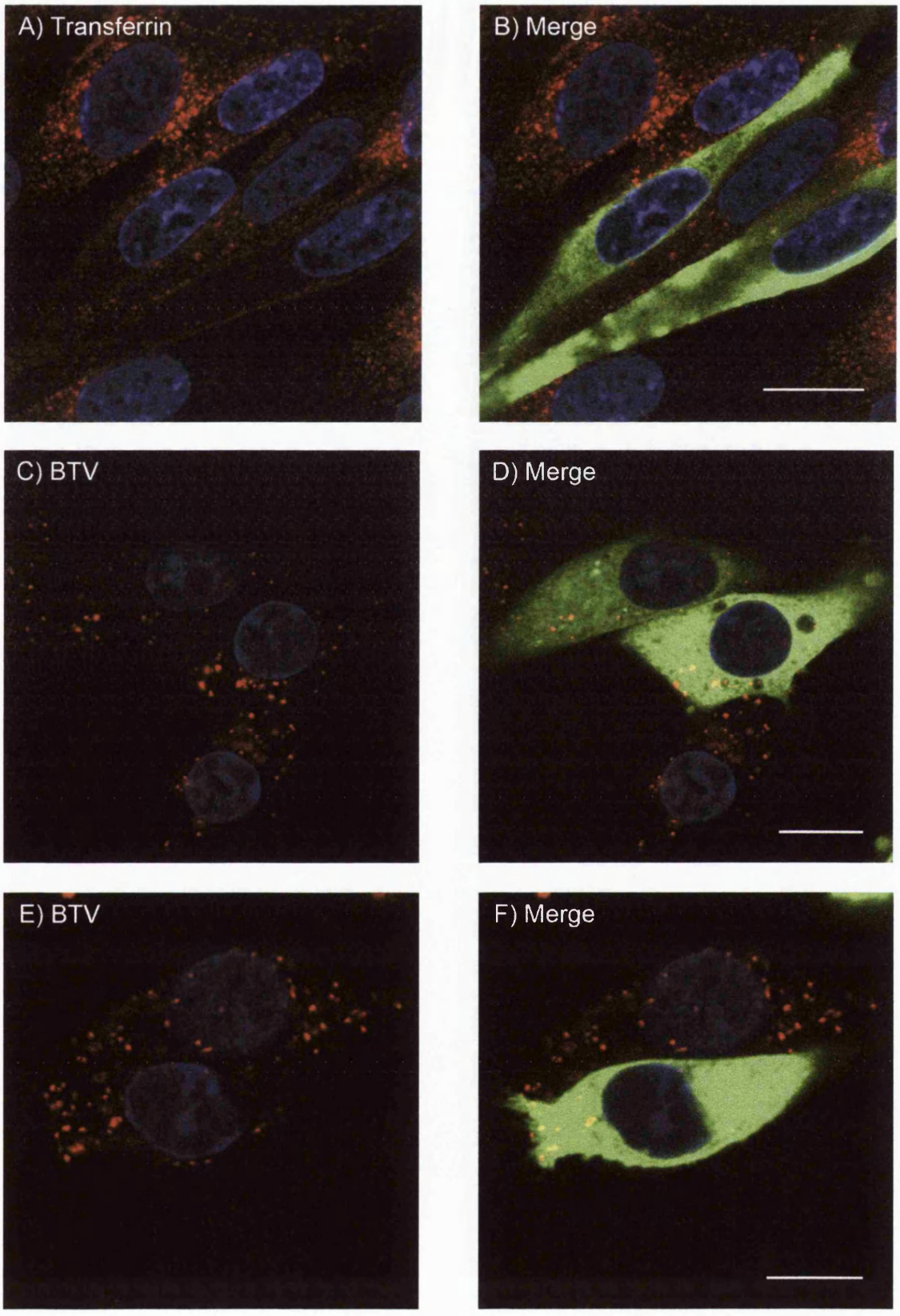

Figure 4.15: Expression of AP180C does not block BTV-1 entry
BHK cells were transfected to express AP180C. AP180C expressing cells were identified by labelling with 9E10 (anti-c-myc) and are shown as green. The cells were allowed to take up 568-Alexa labelled transferrin (A) and (B) (shown as red); or BTV (C-F). BTV-1 was labelled using PM10 (shown as red). Panels (B), (D) and (F) show merged images for red and green fluorescence. Cells expressing AP180C inhibited entry of transferrin (A) and (B) but not virus (C-F). The cell nuclei are shown as blue. Scale bar = 10 μm.

panel (B) shows a merged image for red and green fluorescence for the same cells. Cells expressing AP180C showed a strong inhibition to transferrin uptake whilst non-expressing cells showed a normal pattern of transferrin uptake with perinuclear accumulations of the ligand (Figure 4.15, Panels A and B). Cells expressing AP180C (n ≥120 cells) were scored for entry of transferrin by confocal microscopy. Over-expression of wt AP180 inhibits clathrin-mediated endocytosis and cannot be used as a control for AP180C. Therefore, for experiments with AP180C the percentage of cells expressing the dominant-negative protein (Expressing cells [EC]) that were positive for transferrin uptake was normalised to the results obtained for cells of the non-expressing population (NEC) (i.e. the non-green cells). Figure 4.16, panel (A) shows the mean and standard deviation for two independent experiments for triplicate coverslips. The data shows a 78-82% decrease in entry of transferrin in AP180C expressing cells as compared to the non-expressing cells, confirming AP180C as a potent inhibitor of the clathrin pathway.

The ability of the AP180C transfected cells to internalise BTV-1 was also investigated. Figure 4.15 shows cells expressing AP180C (shown as green) after a 30 minute incubation with BTV-1 (shown as red). Panels (C) and (E) show virus entry whilst panels (D) and (F) show merged images for red and green fluorescence for the same cells. Cells of the non-expressing population showed a normal pattern of BTV-1 entry when compared to mock-transfected cells (data not shown). In contrast to entry of transferrin, cells expressing AP180C also internalised virus and the pattern of virus labelling was indistinguishable from cells of the non-expressing population (see Figure 4.15, Panels C and E).

Cells expressing AP180C (n ≥100 cells) were scored for virus entry by confocal microscopy. The percentage of cells expressing the dominant-negative protein that were positive for virus entry was normalised to the results obtained for cells of the non-expressing population (i.e. the non-green cells). Figure 4.16 panel (B) shows the mean

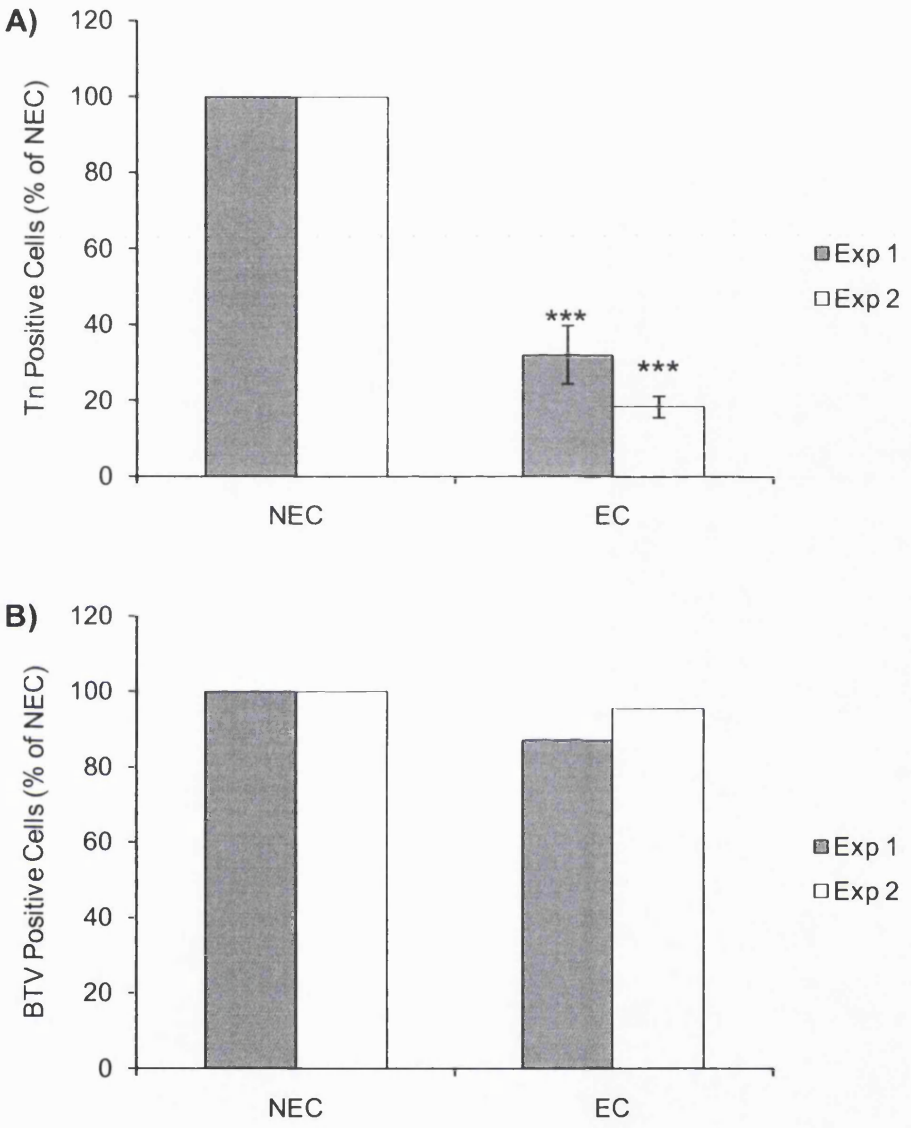

Figure 4.16: Entry of transferrin and BTV-1 by BHK cells expressing AP180C

Panel (A): BHK cells expressing AP180C (EC) (n ≥120 cells) and the non-expressing cells (NEC) were scored for the presence of transferrin. The percentage of cells expressing AP180C that was positive for entry of transferrin as shown by accumulation of the ligand in the perinuclear region of the cell, was normalised to the level of entry of transferrin for the NEC. The mean of triplicate samples for two independent experiments is shown (Exp 1, Exp 2) (*P* values: *** <0.001).

Panel (B): BHK cells expressing AP180C (EC) (n ≥100 cells) and the non-expressing cells (NEC) were scored for virus entry. The percentage of cells expressing AP180C that was positive for BTV-1 entry was normalised to the level of virus entry for the NEC. The mean of duplicate samples for two independent experiments is shown (Exp 1, Exp 2).

and standard deviation for two independent experiments, showing that expression of AP180C did not appear to inhibit virus entry.

The above results show that expression of AP180C strongly blocks entry of transferrin thus indicating a block to the clathrin pathway, but does not inhibit BTV-1 entry. These results together with the Eps15 data above show that BTV-1 entry into BHK cells can occur by an entry mechanism that is clathrin-independent.

4.3.3 The Effect of AP180C on BTV-1 Infection

Virus entry experiments require a high input virus concentration to allow detection by confocal microscopy during entry. This raises the possibility that virus may be forced to enter cells via non-specific endocytic pathways (as previously discussed; see Section 3.1) that are non-productive for infection. Therefore, the effect of AP180C on BTV-1 infection was investigated using a low multiplicity of infection (m.o.i. = 0.5), to encourage virus entry by the most efficient or normal route.

BHK cells were transfected to express AP180C as described above (see Method 2.7.2). At 12 hours post-transfection, cells were allowed to take up virus (m.o.i. = 0.5) for 1 hour at 37°C (see Method 2.6.5). Excess virus was removed by washing and infection continued for a further 11 hours. At this point, infection was stopped by the addition of 4% paraformaldehyde and the cells processed for confocal microscopy. AP180C expressing cells were identified by labelling with 9E10 (shown as green) whilst infected cells were identified by labelling with Orab 1 (anti-NS2) as described in Chapter 3 (NS2 labelling is shown as red). Figure 4.17, panels (A) and (C) show infected cells whilst panels (B) and (D) show merged images for red and green fluorescence for the same cells. Expression of AP180C did not appear to inhibit BTV-1 infection of BHK cells (as judged by the presence of NS2).

Three independent transfections were carried out with duplicate coverslips for each experiment (Figure 4.18). Cells expressing AP180C (n $\geq$150 cells) were scored for BTV-1 infection by confocal microscopy. The percentage of cells expressing the

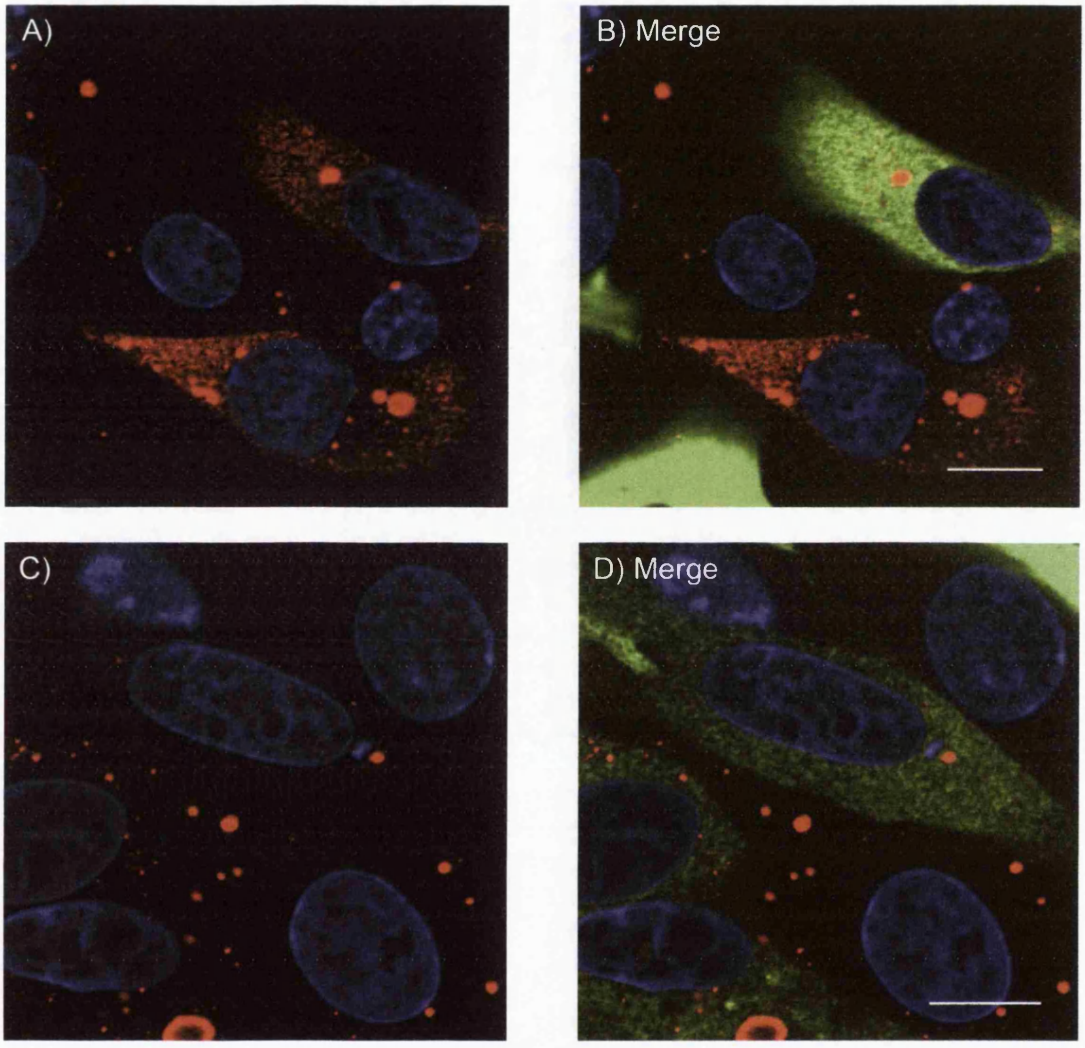

Figure 4.17: Expression of AP180C does not inhibit BTV-1 infection of BHK cells
BHK cells were transfected to express AP180C. At 12 h post-transfection the cells were infected with BTV-1 (m.o.i. = 0.5). AP180C expressing cells were identified by labelling with 9E10 (anti-c-myc) and are shown as green. Infected cells were identified by labelling with Orab 1 (anti-NS2) and are shown as red. Panels (A) and (C) show NS2 labelling whilst panels (B) and (D) show merged images for red and green fluorescence.The cell nuclei are shown as blue. Scale bar = 10 μm. Data shows that expression of AP180C does not inhibit BTV-1 infection of BHK cells. Quantification of the data is shown in figure 4.18

A)

Experiment	Non-Expressing cells	Expressing cells
1	100	96
1	100	75
2	100	100
2	100	96
3	100	70
3	100	68

B)

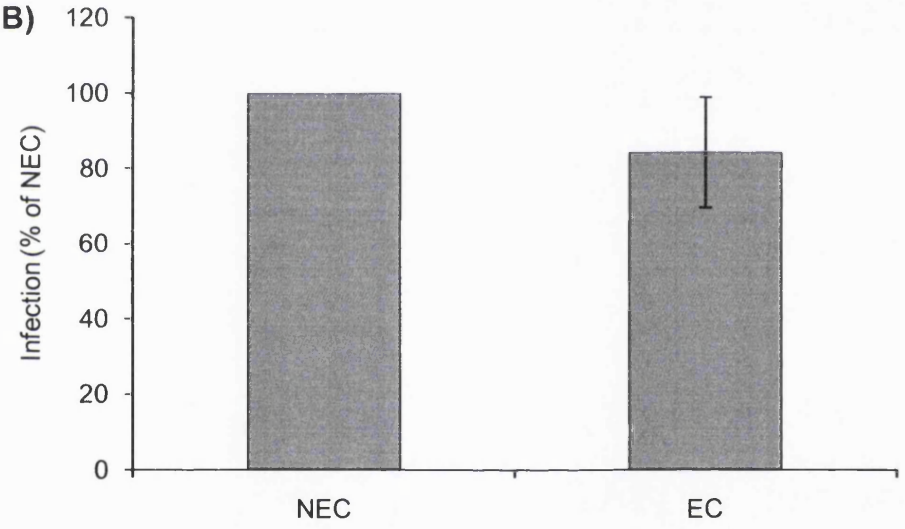

Figure 4.18: Expression of AP180C does not inhibit BTV-1 infection of BHK cells (II)
BHK cells were transfected to express AP180C. At 12 h post-transfection the cells were infected with BTV-1 (m.o.i. = 0.5). AP180C expressing cells were identified by labelling with 9E10 (anti-c-myc). Infected cells were identified by labelling with Orab 1 (anti-NS2). The cells were scored for infection by confocal microscopy (n ≥150 expressing cells). The frequency of infection of the AP180C expressing cells (EC) was normalised to the level of infection of the non-expressing cells (NEC). Panel (A) shows the normalised data for six individual transfections for three independent experiments. Panel (B) shows the mean and standard deviation for the combined data.

dominant-negative protein (Expressing cells [EC]) that were positive for infection was normalised to the results obtained for cells of the non-expressing population (NEC) (i.e. the non-green cells). Figure 4.18, panel (A) shows the data obtained for each transfection. Figure 4.18, panel (B) shows this data combined in graph format, with the mean and standard deviation shown for the three independent experiments. This data shows that expression of AP180C does not significantly inhibit BTV-1 infection and confirms that BTV-1 infection of BHK cells can occur via a clathrin-independent mechanism.

4.4 Conclusion

The results of the above experiments have confirmed that active endosomal acidification is required for BTV-1 infection of BHK, Vero and BPAEC cells. Similar results were obtained for the three cell lines using the enzyme-linked immunospot assay to quantify infection. The inhibitory effect of concanamycin-A on BTV-1 infection of BHK cells was confirmed using confocal microscopy to quantify infection. When concanamycin-A was added as a pre-treatment, a strong inhibitory effect on infection was observed whereas little effect was seen when the drug was added 1.5 hours after the start of infection. However, different results were seen for the cell lines when concanamycin-A was added immediately after removal of the virus inoculum. A small but noticeable inhibition of infection was seen with BHK and Vero cells (10-30%) which was much greater for BPAEC cells (~75% inhibition). Addition of concanamycin-A at different times after the start of infection showed that although a low endosomal pH was essential for infection, BTV-1 was delivered to acidic compartments with relatively slow kinetics ($t_{1/2}$ of ~2 hours). This suggests that virus may enter the cell slowly or that a significant proportion of internalised virus does not reached a low pH environment during the first hour of infection.

The inhibition of infection due to concanamycin-A treatment was shown not to be the result of blocking clathrin-mediated endocytosis, or a reduction of virus binding

(as shown by flow cytometry) to the cells, or an inability of the virus to be efficiently internalised.

The role of clathrin-mediated endocytosis in BTV-1 infection of BHK cells was also investigated. Entry via the clathrin-mediated pathway has been reported for BTV-10 infection of HeLa and Vero cells (Forzan et al., 2007). In my studies, expression of Dn Eps15 did not inhibit BTV-1 entry by BHK cells despite showing a block to clathrin-mediated endocytosis of transferrin. However, for some viruses such as mouse hepatitis virus type 2 (Pu and Zhang, 2008), entry via the clathrin pathway has been shown to be Eps15-independent, indicating that my results could be explained if BTV-1 similarly used an Eps15-independent clathrin-mediated endocytosis mechanism for entry. However, I confirmed that clathrin-mediated endocytosis was not the major pathway for BTV-1 infection of BHK cells by expression of dominant-negative AP180 (AP180C). Expression of this dominant-negative protein did not inhibit BTV-1 entry or infection of BHK cells despite having a strong inhibitory effect on transferrin uptake. Collectively, these data show that under conditions where transferrin internalisation is inhibited by up to 80%, virus entry and infection appear relatively unaffected showing that BTV-1 can infect BHK cells using a mechanism that is clathrin-independent.

The antibody used to detect infection (Orab 1) detects NS2. In infected cells NS2 appears diffuse throughout the cells and also as coalesced, distinct punctuate spots i.e. in VIB's. Infected cells (as shown by confocal microscopy) can have multiple VIB's. Therefore, it is possible that the enzyme-linked immunospot assay could count VIB's rather than infected cells. For this reason, although the enzyme-linked immunospot assay was very useful for experiments to rapidly screen the effect of pharmacological reagents on BTV-1 infection, the confocal microscope was used as the method of choice to score infection in subsequent experiments.

5 The Role of Dynamin in BTV-1 Infection

5.1 Introduction

The results obtained in Chapter 4 show that the low pH within endosomes is essential for an early step in BTV-1 infection of BHK cells. The requirement for low pH during entry usually indicates uptake via clathrin-mediated endocytosis. However, the results presented in Chapter 4 concluded that infection of BHK cells can occur via an entry mechanism that is clathrin-independent. Recently, vesicles derived from clathrin-independent pathways have been shown to fuse with, and deliver receptors or cargos to low pH compartments (see Section 1.5.3). For example, caveolae can deliver SV40 to early-endosomes through transient interactions (Pelkmans et al., 2001). The caveolae-mediated endocytosis pathway is dependent on caveolin-1; intact lipid rafts, cholesterol and dynamin (see Section 1.5.2.1). Dynamin is a large GTPase which mediates caveolae scission from the plasma membrane (McNiven et al., 2000; Praefcke and McMahon, 2004) (see Section 1.5.1.1). A number of other endocytic pathways including clathrin-mediated endocytosis also require dynamin-2 for vesicle scission (Cao et al., 2007; McNiven et al., 2000; Praefcke and McMahon, 2004). In this Chapter the role of dynamin in BTV-1 infection was investigated using expression of Dn Dynamin-2 '*aa*', which has a K44A mutation in the first GTP-binding element and hence, is unable to bind GTP (Cao et al., 2000).

5.2 Expression of Dn Dynamin-2 blocks transferrin uptake in BHK cells

BHK cells were transfected to express wt or Dn Dynamin-2 as fusions with eGFP (see Method 2.7.2). At 12 hours post-transfection, the cells were incubated in serum-free medium for 30 minutes to deplete cellular iron. The cells were then allowed to internalise 568-Alexa labelled transferrin for 15 minutes at 37°C. Entry of transferrin was halted; the cells fixed by the addition of cold 4% paraformaldehyde including 0.25% glutaraldehyde and the cells processed for confocal microscopy. Transferrin uptake is shown as red on figure 5.1, panels (A), (C) and (E). Transfected cells expressing wt or Dn Dynamin-2 were identified by the eGFP tag (shown as green).

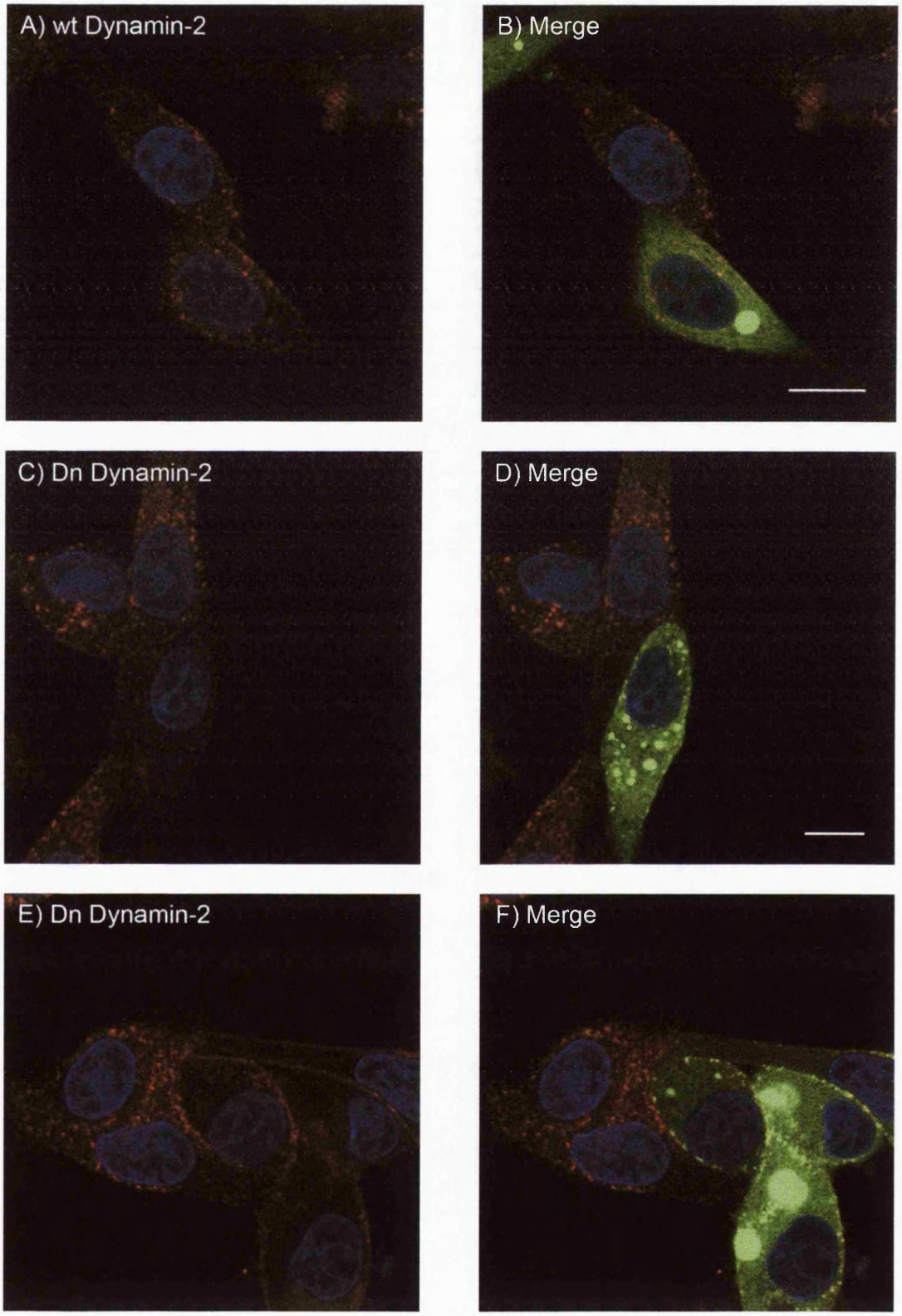

Figure 5.1: Expression of Dn Dynamin-2 blocks transferrin entry in BHK Cells
BHK cells were transfected to express wt (A) and (B) or Dn Dynamin-2 (C-F) for 12 h and then 568-Alexa labelled transferrin was taken up continuously for 15 min at 37°C. Cells were fixed and visualised by confocal microscopy. Transferrin is shown as red. Cells expressing dynamin are shown as green; wt (B) or Dn Dynamin-2 (D) and (F). Panels (C), (D) and (F) show merged images for red and green fluorescence. Cells expressing Dn Dynamin-2 show reduced uptake of transferrin. The cell nuclei are shown as blue. Scale bar = 10 μm.

Figure 5.1, panels (B), (D) and (F) show merged images for red and green fluorescence for the same cells. Cells expressing wt Dynamin-2 (Figure 5.1, Panels A and B) showed normal entry of transferrin (with perinuclear accumulations of the ligand) that was indistinguishable from that seen in cells of the non-expressing population. In contrast, cells expressing Dn Dynamin-2 showed a block to entry of transferrin (an absence of perinuclear acculations of the ligand) (Figure 5.1, Panels C-F) confirming a block to clathrin-mediated endocytosis and that endogenous dynamin had been inhibited.

The ability of cells expressing wt or Dn Dynamin-2 to internalise 568-Alexa labelled transferrin was quantified. Cells were scored (n ≥100 cells) for transferrin uptake by confocal microscopy. The percentage of cells expressing Dn Dynamin-2 that was positive for transferrin uptake (with perinuclear accumulations of the ligand) was normalised to the level of transferrin uptake by the cells expressing the wild type protein. Figure 5.3, panel (A) shows the mean for duplicate transfections from two independent experiments (Exp 1, Exp 2). These data show that expression of Dn Dynamin-2 inhibited entry of transferrin by 64 to 74% when compared to the level of entry of transferrin by cells expressing the wild type protein.

The above results show that expression of Dn Dynamin-2 inhibited clathrin-mediated endocytosis of transferrin. The ability of Dn Dynamin-2 to inhibit entry of BTV-1 was also assessed.

BHK cells were transfected to express wt or Dn Dynamin-2 as fusions with eGFP (as above and see Method 2.7.2). At 12 hours post-transfection, BTV-1 (13 µg/ml) was bound to the cells (see Method 2.6.8) for 40 minutes at 4°C. Excess unbound virus was removed by washing and virus entry initiated by the addition of warm medium (37°C). After 30 minutes, virus internalisation was stopped and the cells fixed by the addition of 4% paraformaldehyde. The cells were permeabilised with 0.1% Triton X-100 and processed for confocal microscopy using PM10 and a goat, anti-

Guinea pig Alexa-fluor 568-conjugated secondary antibody to label virus (see Chapter 3 and Method 2.6.4). Figure 5.2, panel (A) shows BTV-1 entry (shown as red), and figure 5.2, panel (B) shows an overlay with green fluorescence due to expression of wt Dynamin-2. Figure 5.2, panels (C) and (E) shows BTV-1 entry (shown as red), with panels (D) and (F) showing an overlay with green fluorescence due to expression of Dn Dynamin-2. The cells expressing wt Dynamin-2 showed a normal pattern of BTV-1 entry when compared to cells that were not expressing dynamin (i.e. the non-green cells on Figure 5.2, Panels C and E). In contrast to the results with transferrin, cells expressing the dominant-negative protein also internalised virus (Figure 5.2, Panels D and E). Furthermore the pattern of virus labelling was indistinguishable from cells of the non-expressing population.

Cells expressing wt or Dn Dynamin-2 were scored for BTV-1 entry (n $\geq$100 cells) by confocal microscopy. The percentage of cells expressing Dn Dynamin-2 that was positive for virus entry was normalised to the level of virus entry by the cells expressing the wild type protein. Figure 5.3, panel (B) shows the mean of duplicate coverslips from two independent experiments (Exp 1, Exp 2). These data show that expression of Dn Dynamin-2 did not inhibit virus entry when compared to the level of virus entry by cells expressing the wild type protein.

The above experiments show that expression of Dn Dynamin-2 strongly blocks clathrin-mediated endocytosis of transferrin but did not inhibit entry of BTV-1.

5.3 Expression of Dn Dynamin-2 does not block BTV Infection

As discussed previously (see Section 3.1), virus entry experiments require a high input virus concentration to allow for virus detection during entry. This raises the possibility that virus may be forced to enter cells via endocytic pathways that are not normally used, or are non-productive for infection. Therefore the effect of Dn Dynamin-2 on BTV-1 infection was also investigated at a low m.o.i. of 0.5 to encourage virus entry by the most efficient route.

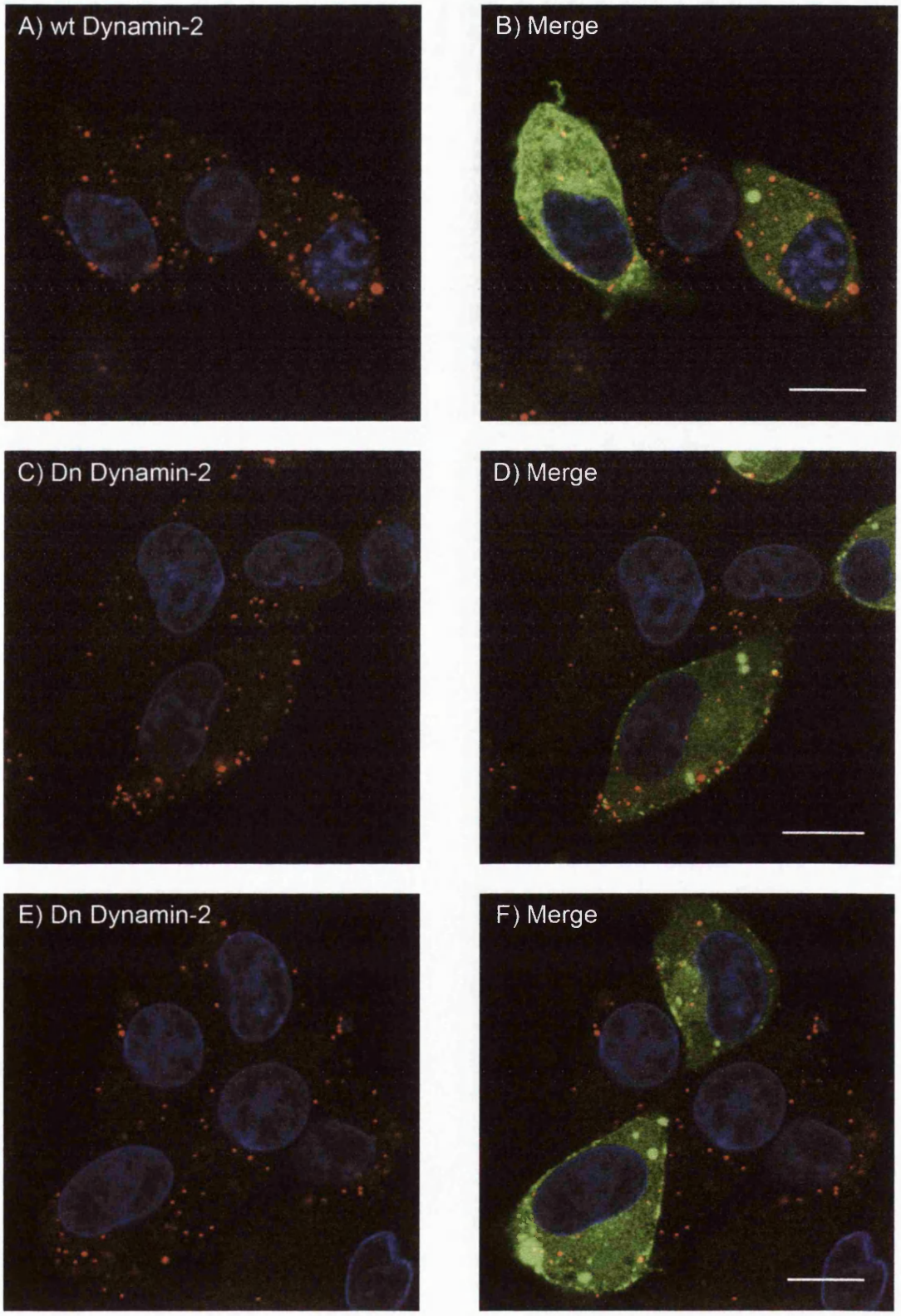

Figure 5.2: Expression of Dn Dynamin-2 does not block BTV-1 entry in BHK cells
BHK cells were transfected to express wt (A) and (B) or Dn Dynamin-2 (C-F) for 12 h. BTV-1 was bound to the cells at 4°C for 40min. Unbound virus was removed by washing and entry initiated by a shift to 37°C. Cells expressing dynamin are shown as green; wt (B) or Dn Dynamin-2 (D) and (F). Virus was detected by labelling with PM10 (anti-VP5) and is shown as red. Panels (B), (D) and (F) show merged images for red and green fluorescence. Cells expressing Dn Dynamin-2 show normal virus uptake. The cell nuclei are shown as blue. Scale bar = 10 μm.

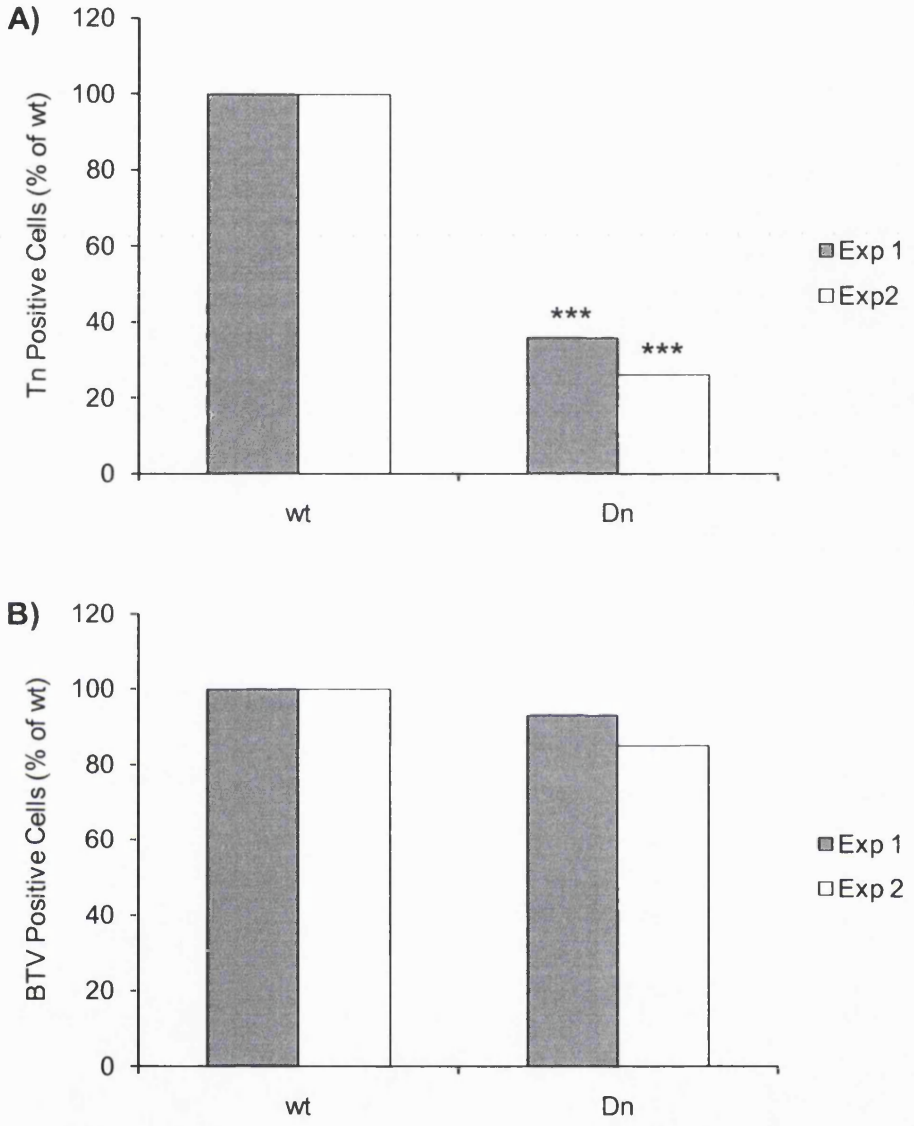

Figure 5.3: Entry of transferrin and BTV-1 by BHK cells expressing Dn Dynamin-2

BHK cells were transfected to express wt or Dn Dynamin-2 for 12 h and allowed to take up 568-Alexa labelled transferrin (see Figure 5.1) or BTV-1 (see Figure 5.2). The cells expressing wt or Dn Dynamin-2 were scored (n ≥100 cells) for the presence of transferrin as shown by accumulation of the ligand in the perinuclear region of the cell, (Panel A) or BTV-1 (Panel B). The frequency of transferrin or BTV-1 uptake by cells expressing Dn Dynamin-2 was normalised to uptake by the cells expressing the wt protein. The mean of duplicate transfections for two independent experiments is shown (Exp 1, Exp2) (*P* values: *** <0.001).

At 12 hours post-transfection (with wt or Dn Dynamin-2), the cells were infected with BTV-1 for 1 hour at 37°C. Excess virus was removed by washing with medium and infection continued for a further 11 hours. Infection was stopped and the cells fixed by the addition of 4% paraformaldehyde. The cells were permeabilised with 0.1% triton X 100 and processed for confocal microscopy using Orab 1 and a goat, anti-Rabbit Alexa-fluor 568-conjugated secondary antibody to identify infected cells (as described in Chapter 3). Cells expressing wt or Dn Dynamin-2 were identified by the eGFP tag and are shown as green on Figure 5.4.

Figure 5.4, panel (A) shows BTV-1 infection (shown as red), and panel (B) shows an overlay of cells expressing wt Dynamin-2 (shown as green) and that the cells expressing wt Dynamin-2 are able to be infected with BTV. Figure 5.4, panels (C) and (E) shows BTV-1 infection (shown as red). Figure 5.4, panels (D) and (F) show an overlay of cells expressing Dn Dynamin-2 (shown as green) and that BHK cells expressing Dn Dynamin-2 are also infected with BTV-1.

Cells expressing wt or Dn Dynamin-2 were scored (n $\geq$150 cells) for infection (i.e. the presence of NS2 labelling) by confocal microscopy. The percentage of cells expressing Dn Dynamin-2 that was positive for infection was normalised to the level of infection by the cells expressing the wild type protein. The results are shown in figure 5.5. These data show that expression of Dn Dynamin-2 did not inhibit BTV-1 infection when compared to the level of infection in cells expressing the wild type protein.

5.4 Conclusion

Using transferrin as a control ligand, expression of Dn Dynamin-2 was shown to inhibit clathrin-mediated endocytosis but not BTV-1 cell entry or infection of BHK cells. These observations are consistent with the results showing that BTV-1 entry and infection are not inhibited by expression of other dominant-negative inhibitors (AP180C and Dn Eps15) of the clathrin pathway, and support the conclusion that BTV-1 can infect BHK cells using a clathrin-independent mechanism (see Chapter 4). The failure

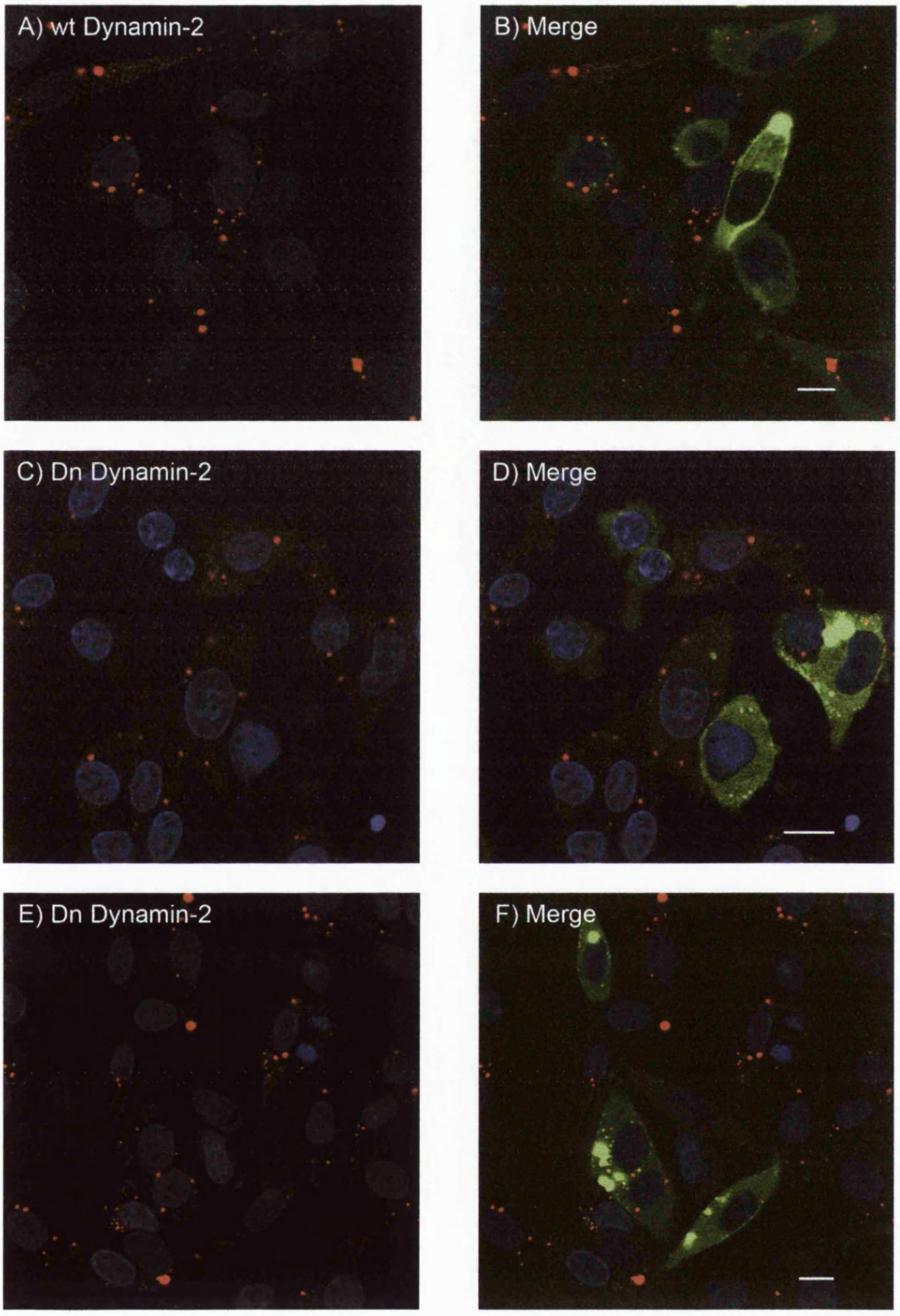

Figure 5.4: Expression of Dn Dynamin-2 does not inhibit BTV-1 infection of BHK cells (I) BHK cells were transfected to express wt (A) and (B) or Dn Dynamin-2 (C-F) for 12 h and then infected with BTV-1 (m.o.i. = 0.5). Wt or Dn Dynamin-2 expressing cells are shown as green. Infected cells were identified by labelling with Orab 1 (anti-NS2) and are shown as red. Panels (B), (D) and (F) show merged images for red and green fluorescence.The cell nuclei are shown as blue. Scale bar = 10 μm.

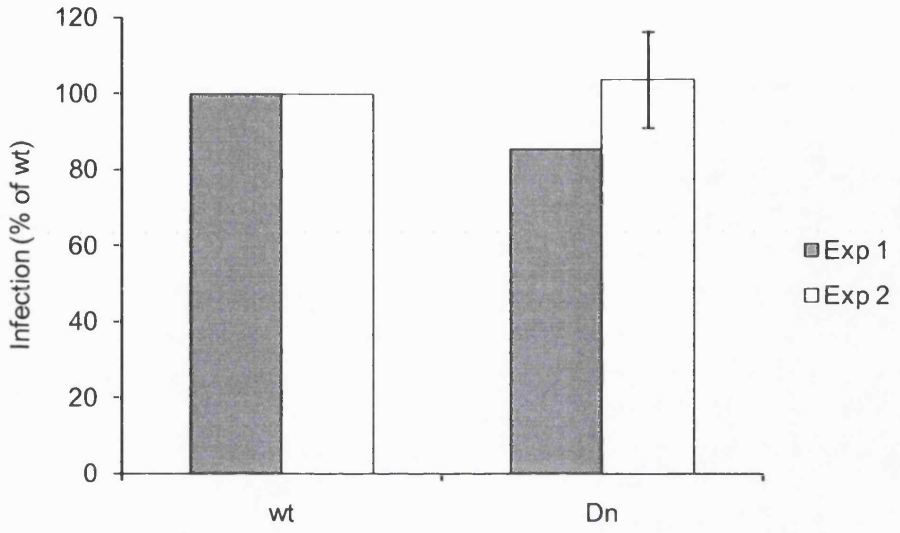

Figure 5.5: Expression of Dn Dynamin-2 does not inhibit BTV-1 infection of BHK cells (II)
BHK cells were transfected to express wt or Dn Dynamin-2 for 12 h and infected with BTV-1 (see Figure 5.4). The cells expressing wt and Dn Dynamin-2 ($n \geq 150$ cells) were scored for the presence of NS2 by confocal microscopy. The frequency of NS2 labelling for cells expressing Dn Dynamin-2 was normalised to NS2 labelling for the cells expressing the wt protein. The data is shown for two independent experiments. The grey bars (Exp 1) show the mean for duplicate samples. The white bars show (Exp 2) the mean and standard deviation for triplicate samples.

of Dn Dynamin-2 to inhibit BTV-1 entry and infection can also be interpreted to indicate that caveolae are not required for BTV-1 infection of BHK cells as like clathrin-mediated endocytosis, scission of caveolae from the plasma membrane also requires dynamin and is inhibited by a Dn Dynamin-2.

It is now clear that different forms of dynamin (see Section 1.5.1.1) and the different splice variants of dynamin-2 are required for distinct endocytic pathways. The above experiments were carried out using the *'aa'* splice variant of dynamin-2 which is known to inhibit both clathrin- and caveolae-mediated endocytosis. However, although the experiments presented in this chapter strongly suggest that the clathrin and caveolae pathways are not required for BTV entry they do not completely exclude a role for dynamin.

The role of dynamin in BTV infection is further investigated in Chapter 7.

6 The Role of Cholesterol and Caveolae in BTV-1 Infection

6.1 Introduction

In Chapter 5 it was shown that BTV-1 infection of BHK cells was not inhibited by Dn Dynamin-2 implying that cell entry is not mediated by caveolae, as dynamin is required for caveolae-mediated endocytosis. The caveolae pathway is also dependent on caveolin-1; lipid rafts and cholesterol (see Section 1.5.2.1). A number of non-caveolae entry pathways also originate from lipid rafts. These pathways have different requirements for cellular proteins such as dynamin, flotillin, small GTPases, and for cholesterol and other specific lipids and can be exploited by viruses for infection (see Section 1.5.2 and 1.5.2.2). The integrity of lipid rafts, hence raft-mediated endocytic processes, is dependent on cholesterol and can be inhibited by cholesterol depletion or sequestration.

In this chapter the role of cholesterol in BTV-1 infection will be investigated using methyl-β-cyclodextrin (MβCD) and nystatin, and the role of caveolae investigated using dominant-negative Caveolin-1.

6.2 Selective Depletion of Cholesterol from BHK Cells

MβCD binds and extracts cholesterol from the plasma membrane. Normally cholera toxin B is used as a control ligand to assess the effects of cholesterol depletion on lipid raft mediated endocytosis (Henley et al., 1998). However cholera toxin B was found not to bind to BHK cells (data not shown) and could not be used as an indicator ligand for raft disruption. Therefore, to verify that cholesterol extraction from the plasma membrane was successful, filipin III labelling was used (Keller and Simons, 1998). Filipin III binds cholesterol and can be detected by confocal microscopy immediately after cell labelling.

BHK cells were either mock-treated (Mock) or pre-treated with 7.5 mM MβCD for 30 minutes at 37°C. MβCD was removed by washing with medium and the cells fixed by the addition of 4% paraformaldehyde for 30 minutes on ice. Cells were then

incubated with 125 µg/ml filipin III for 15 minutes at room temperature, mounted in fluoromount G and immediately viewed by confocal microscopy at 430 nm (see Method 2.6.3).

Filipin III fluorescence was detected at the plasma membrane and within the cytosol of mock-treated cells (Figure 6.1, Panels A and B). Although the fluorescence due to filipin binding was relatively unaffected in the cytosol of cells treated with MβCD the intense plasma membrane fluorescence was greatly reduced (Figure 6.1, Panels C and D), indicating extensive and selective cholesterol depletion from the plasma membrane.

6.3 Depletion of Cholesterol does not Inhibit BTV Infection of BHK Cells

Next the effect of cholesterol depletion on BTV-1 infection was investigated. BHK cells were mock-treated or pre-treated with 7.5 mM MβCD as described above. The cells were then infected with BTV-1 (m.o.i. = 0.5) for 1 hour in the presence or absence (Mock) of the drug. The cells were washed to remove excess virus and drug and infection continued for a further 5 hours when the cells were fixed with 4% paraformaldehyde and infection quantified using the enzyme-linked immunospot assay as described in Chapter 3. Additional cultures were treated with the drug after the 1 hour incubation with virus to control for any effects of the drug on post-entry intracellular virus replication (see Method 2.5.2).

Figure 6.2, panels (A) and (B) show data for two independent experiments. Each bar represents the number of infected cells normalised to the level of infection of the mock-treated cells. The mean and standard deviation for triplicate wells is shown. The numbers beneath the bars represent the conditions of drug addition: (1) cells were infected in the absence of MβCD (i.e. the mock-treated cells); (2) the drug was added for 30 minutes before infection was initiated and remained present only during the 1 hour incubation with virus; (3) the drug was added for 1.5 hours immediately after the virus inoculum was removed and (4) the drug was added for 1.5 hours, 1.5 hours after

the virus inoculum had been removed. The data shows that MβCD does not appear to inhibit infection of BHK cells by BTV-1 when added as a pre-treatment (Treatment 2).

Similarly, no inhibition of infection was observed when the drug was added after the start of infection (Treatment 3 and Treatment 4). These results indicate that under conditions that severely deplete cholesterol from the plasma membrane infection by BTV-1 is not inhibited.

The above results were confirmed using confocal microscopy to quantify infection. The experimental procedure was similar to that used in figure 6.2 with MβCD added to the cells before or after the 1 hour incubation with virus. BHK cells were mock-treated (Mock) or pre-treated (Pre) with 7.5 or 5.0 mM MβCD for 30 minutes at 37°C and then infected with BTV-1 (m.o.i. = 0.5) for 1 hour at 37°C in the presence or absence (Mock) of the drug (see Method 2.6.6). Excess virus and drug were removed by washing with medium, and infection continued for 11 hours. When added as a post-treatment (Post), MβCD was present for 1.5 hours immediately after the 1 hour incubation with virus. However, in this experiment 25 mM ammonium chloride was added to all of the cells immediately after the 1 hour incubation with virus (see Method 2.6.7). Addition of ammonium chloride would be expected to rapidly increase endosomal pH and prevent further acid-induced infection events (see Figure 4.8). This allowed the entry phase of infection (i.e. before the addition of ammonium chloride) to be separated from post-entry virus replication (i.e. after the addition of ammonium chloride). This allowed the effects of MβCD on entry and post-entry replication to be clearly separated as when MβCD was added after the addition of ammonium chloride, any inhibitory effects could only result from a block to post-entry virus replication.

Infection was stopped and the cells fixed by the addition of 4% paraformaldehyde. Infected cells were detected by labelling with Orab 1 (anti-NS2), followed by a goat, anti-Rabbit Alexa-fluor 568-conjugated secondary antibody. Cells were scored for infection by confocal microscopy (n ≥500 cells). The percentage of

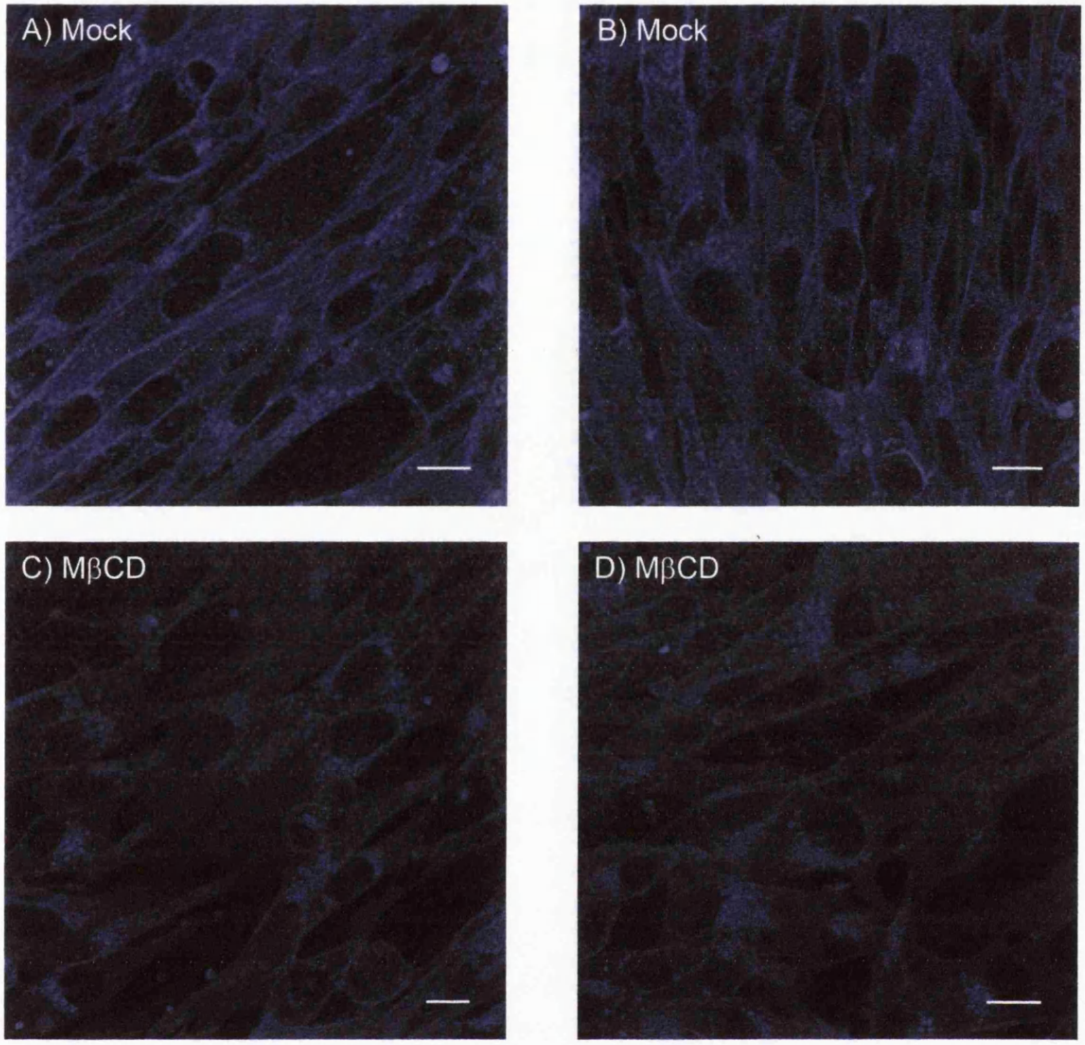

Figure 6.1: Methyl-β-Cyclodextrin selectively depletes cholesterol from the plasma membrane of BHK cells
BHK cells were mock-treated (A) and (B) or pre-treated with 7.5 mM methyl-β-cyclodextrin (C) and (D) for 30 min at 37°C. Methyl-β-cyclodextrin was removed by washing and the cells fixed for 30 min on ice. Cells were stained with 125 μg/ml filipin III for 15 min at RT and viewed by confocal microscopy. Blue shows fluorescence due to filipin III binding to cholesterol. For mock cells, fluorescence was seen at the cell surfaces and within the cytosol (A) and (B).
After methyl-β-cyclodextrin treatment (C) and (D), fluorescence at the cell surfaces was no longer seen indicating selective cholesterol depletion. Scale bar = 10 μm.

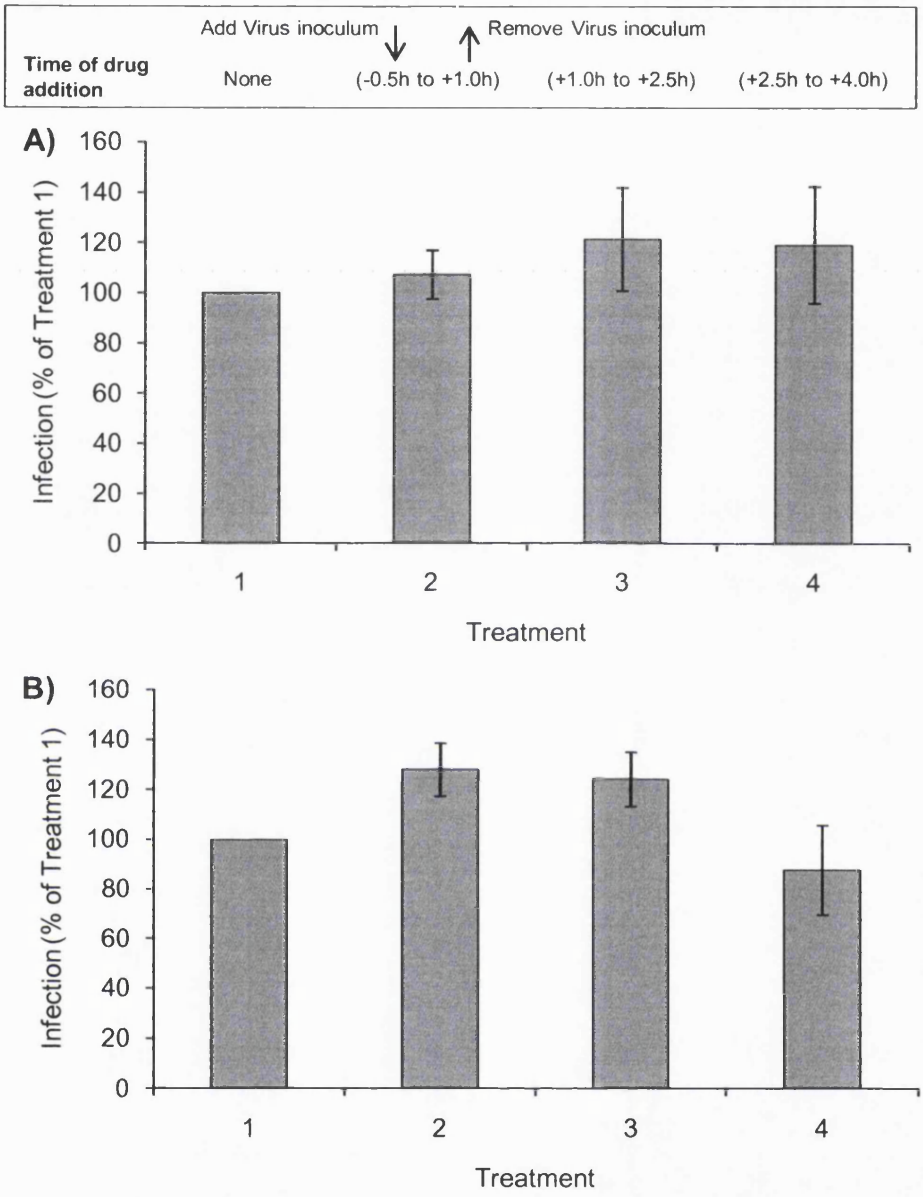

Figure 6.2: Methyl-β-Cyclodextrin does not inhibit BTV-1 infection of BHK cells (I)

BHK cells were mock-treated (Treatment 1) or treated with 7.5 mM methyl-β-cyclodextrin and infected with BTV-1 (m.o.i. = 0.5). The drug was added as three different treatments: for 30 min before infection was initiated and remained present only during the 1 h incubation with virus (shown as Treatment 2); the drug was added for 90 min immediately after virus inoculum was removed (Treatment 3); the drug was added for 90 min, 90 min after virus inoculum was removed (Treatment 4). Infection was quantified using the enzyme-linked immunospot assay (see Chapter 3). Graphs (A) and (B) show two independent experiments. Each bar represents the number of infected cells expressed as the percentage infection of the mock-treated cells (Treatment 1). The mean and standard deviation for triplicate samples.

drug-treated cells that were positive for infection was normalised to the level of infection of the mock-treated cells. Figure 6.3 shows the mean and standard deviation of triplicate samples for two independent experiments and shows that MβCD treatment did not inhibit infection compared to mock-treated cells. However in some experiments, a small but reproducible increase in the number of infected cells following MβCD treatment was observed (see Chapter 9). This was also observed for some of the experiments using the enzyme-linked immunospot assay to quantify infection (see Figures 6.2 and 6.4).

Together the above results strongly suggest that the cell entry mechanism used by BTV-1 to infect BHK cells does not require cholesterol and is unlikely to be mediated by caveolae, or other lipid raft-mediated endocytic pathways.

6.4 MβCD does not Inhibit BTV Infection of Vero Cells

The experiment shown in figure 6.2 was repeated using Vero cells (Figure 6.4). In figure 6.4 each bar represents the number of infected cells normalised to the level of infection of the mock-treated cells (Treatment 1). The mean and standard deviation for triplicate wells is shown. The numbers beneath the bars represent the treatment conditions and when the drug was added (see Section 6.3). The data shows that MβCD does not appear to inhibit BTV-1 infection of Vero cells.

6.5 Nystatin does not Inhibit BTV Infection of BHK Cells

To confirm the MβCD results, the experiments shown in figures 6.2 and 6.4 were repeated using BHK cells treated with a combination of nystatin (25 µg/ml) and progesterone (10 µg/ml). Nystatin sequesters cholesterol in the plasma membrane disrupting raft structure and integrity, thereby inhibiting endocytosis mediated by lipid rafts, whereas progesterone inhibits cholesterol bio-synthesis. As nystatin sequesters cholesterol within the plasma membrane, fillipin III labelling could not be carried out to show the effects of the drugs.

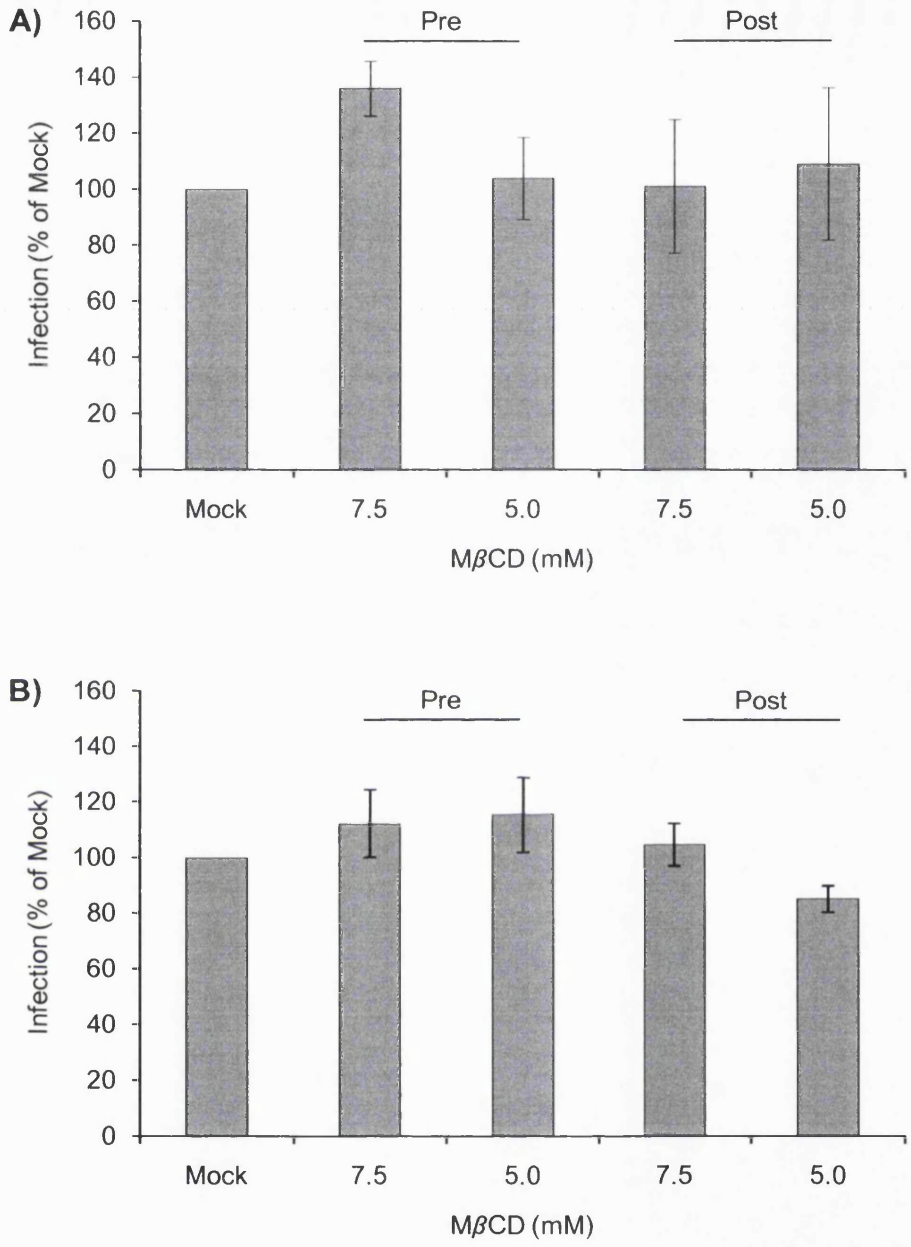

Figure 6.3: Methyl-β-Cyclodextrin does not inhibit BTV-1 infection of BHK cells (II)

BHK cells were mock-treated or pre-treated with 7.5 mM or 5 mM methyl-β-cyclodextrin for 30 min at 37°C and then infected with BTV-1 (m.o.i. = 0.5) for 1 h at 37°C in the presence (Pre) or absence (Mock) of the drug. Cells were then washed and infection allowed to proceed for 11 h in the presence of 25 mM ammonium chloride. When added after the start of infection (i.e. as a post-treatment [Post]) the drug was added for 90 min, after the virus innoculum was removed. Cells were fixed with 4% PFM and processed for confocal microscopy using Orab 1 (anti-NS2) to detect infected cells. Cells were then scored for infection (n ≥500 cells). Each bar represents the number of infected cells expressed as the percentage infection of the mock-treated cells. The mean and standard deviation of triplicate samples is shown for two independent experiments (A) and (B).

The experiment was carried out as for MβCD (see Figures 6.2 and 6.4). Figure 6.5, panels (A) and (B) show two independent experiments. The percentage of drug-treated cells that were positive for infection was normalised to the level of infection of the mock-treated cells. The mean and standard deviation for triplicate wells is shown. The numbers beneath the bars represent the treatment conditions and when the drug was added (see Section 6.3). The data in Figure 6.5, panels (A) and (B) show that no inhibitory effect BTV-1 infection was seen when the cells were treated with nystatin and progesterone. These results are consistent with those obtained using MβCD (Figures 6.2, 6.3 and 6.4). However, in the absence of a suitable positive control to show the effect of nystatin and progesterone on raft-mediated endocytosis the results must be considered preliminary. However, this data supports the conclusion that the cell entry mechanism used by BTV-1 to infect BHK cells does not require cholesterol and is therefore unlikely to be mediated by caveolae, or other lipid raft-mediated endocytic pathways.

6.6 Expression of Dn Caveolin-1 does not Inhibit BTV-1 Infection of BHK Cells

The results obtained using MβCD, and nystatin with progesterone strongly suggest that the entry pathway used by BTV-1 to infect BHK cells is not dependent on caveolae. The role of caveolae in BTV-1 infection was further investigated using a dominant-negative mutant of caveolin-1 (see Section 1.5.2.1.1).

BHK cells were transiently transfected to express wt or Dn Caveolin-1 as fusions with eGFP as described above for other dominant-negative proteins (see Method 2.7.2). At 12 hours post-transfection, the cells were allowed to take up virus (m.o.i. = 0.5) for 1 hour at 37°C. Excess virus was removed by washing with medium and infection continued for a further 11 hours. Infection was stopped and the cells fixed by the addition of 4% paraformaldehyde and the cells processed for confocal microscopy. Cells expressing wt or Dn Caveolin-1 were identified by the eGFP tag and are shown as green. Infected cells were identified using Orab 1 (anti-NS2) and a goat,

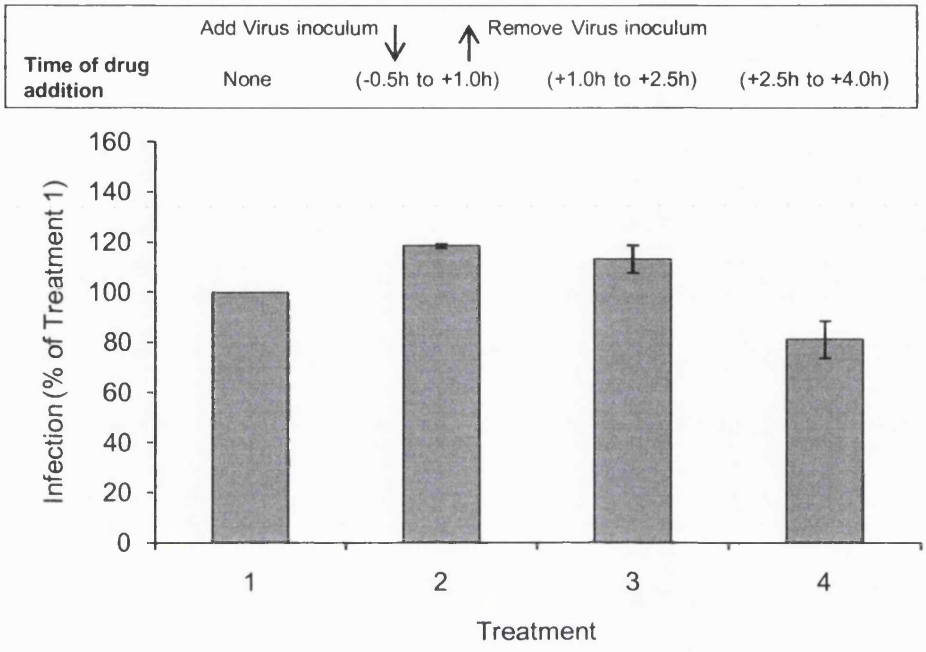

Figure 6.4: Methyl-β-Cyclodextrin does not inhibit BTV-1 infection of Vero cells

Vero cells were mock-treated (Treatment 1) or treated with 7.5 mM methyl-β-cyclodextrin and infected with BTV-1 (m.o.i. = 0.5). The drug was added as three different treatments: for 30 min before infection was initiated and remained present only during the 1 h incubation with virus (shown as Treatment 2); the drug was added for 90 min immediately after the virus inoculum was removed (Treatment 3); the drug was added for 90 min, 90 min after the virus inoculum was removed (Treatment 4). Infection was quantified using the enzyme-linked immunospot assay (see Chapter 3). Each bar represents the number of infected cells expressed as the percentage infection of the mock-treated cells. The mean and standard deviation is shown for triplicate samples.

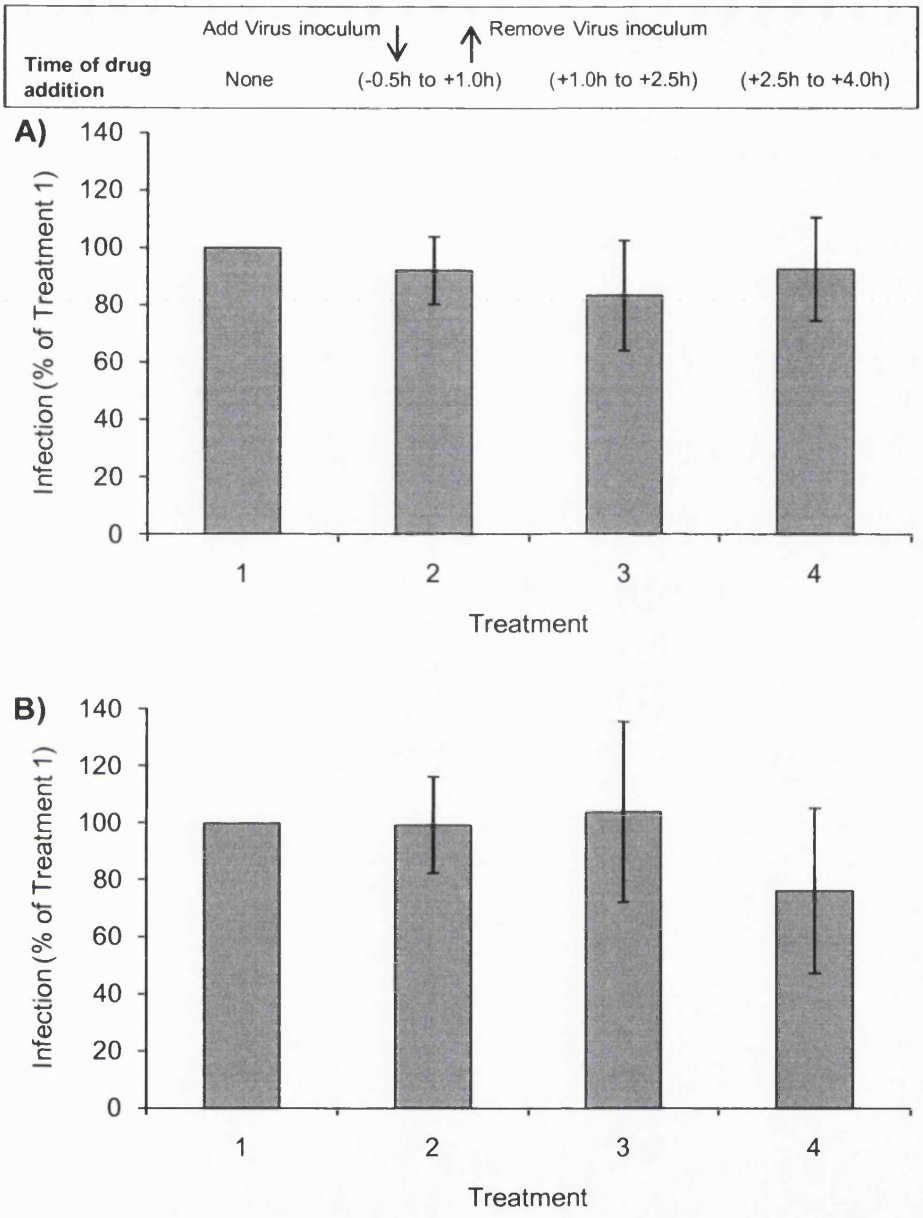

Figure 6.5: Nystatin and progesterone treatment does not inhibit BTV-1 infection of BHK cells

BHK cells were mock-treated (Treatment 1) or treated with 25 µg/ml nystatin and 10 µg/ml progesterone and infected with BTV-1 (m.o.i. = 0.5). The drug was added as three different treatments: for 30 min before infection was initiated and remained present only during the 1 h incubation with virus (shown as Treatment 2); the drug was added for 90 min immediately after virus inoculum was removed (Treatment 3); the drug was added for 90 min, 90 min after virus inoculum was removed (Treatment 4). Infection was quantified using the enzyme-linked immunospot assay (see Chapter 3). Graphs (A) and (B) show two independent experiments. Each bar represents the number of infected cells expressed as the percentage infection of the mock-treated cells. The mean and standard deviation is shown for triplicate samples.

anti-Rabbit Alexa-fluor 568-conjugated secondary antibody and are shown as red.

Figure 6.6, panel (A) shows BTV-1 infected cells (red) and panel (B) shows an overlay of cells expressing wt Caveolin-1 (green) and that cells expressing wt Caveolin-1 are able to be infected with BTV. Figure 6.6, panels (C) and (E) shows BTV-1 infected cells (red), and panels (D) and (F) shows overlay of cells expressing Dn Caveolin-1 (green) and shows that expression of Dn Caveolin-1 does not appear to inhibit BTV-1 infection of BHK cells.

Cells expressing wt or Dn Caveolin-1 were scored (n $\geq$150 cells) for infection (presence of NS2 labelling) by confocal microscopy. The percentage of cells expressing Dn Caveolin-1 that was positive for infection was normalised to the level of infection by the cells expressing the wt protein. The results are shown in figure 6.7, panels (A) and (B) show the mean and standard deviation for triplicate coverslips for two independent transfection experiments. These data show that expression of Dn Caveolin-1 does not inhibit BTV-1 infection when compared to the level of infection of cells expressing the wild type protein. These results support the conclusion made with MβCD, and nystatin with progesterone that caveolae are not required for BTV-1 infection. However, as I was unable to find a suitable control ligand to show that caveolae-mediated endocytosis had been inhibited the results obtained using Dn Caveolin-1 must also be regarded as preliminary.

6.7 Conclusion

Cholesterol is essential for the integrity of lipid rafts, hence raft-dependent endocytosis. BHK cells treated with MβCD and labelled with filipin III were shown to have greatly reduced plasma membrane fluorescence indicating that cholesterol had been efficiently and selectively extracted from the plasma membrane. Under the same conditions MβCD treatment did not block BTV-1 infection of BHK or Vero cells. Similarly, treatment of cells with nystatin and progesterone, which is known to inhibit

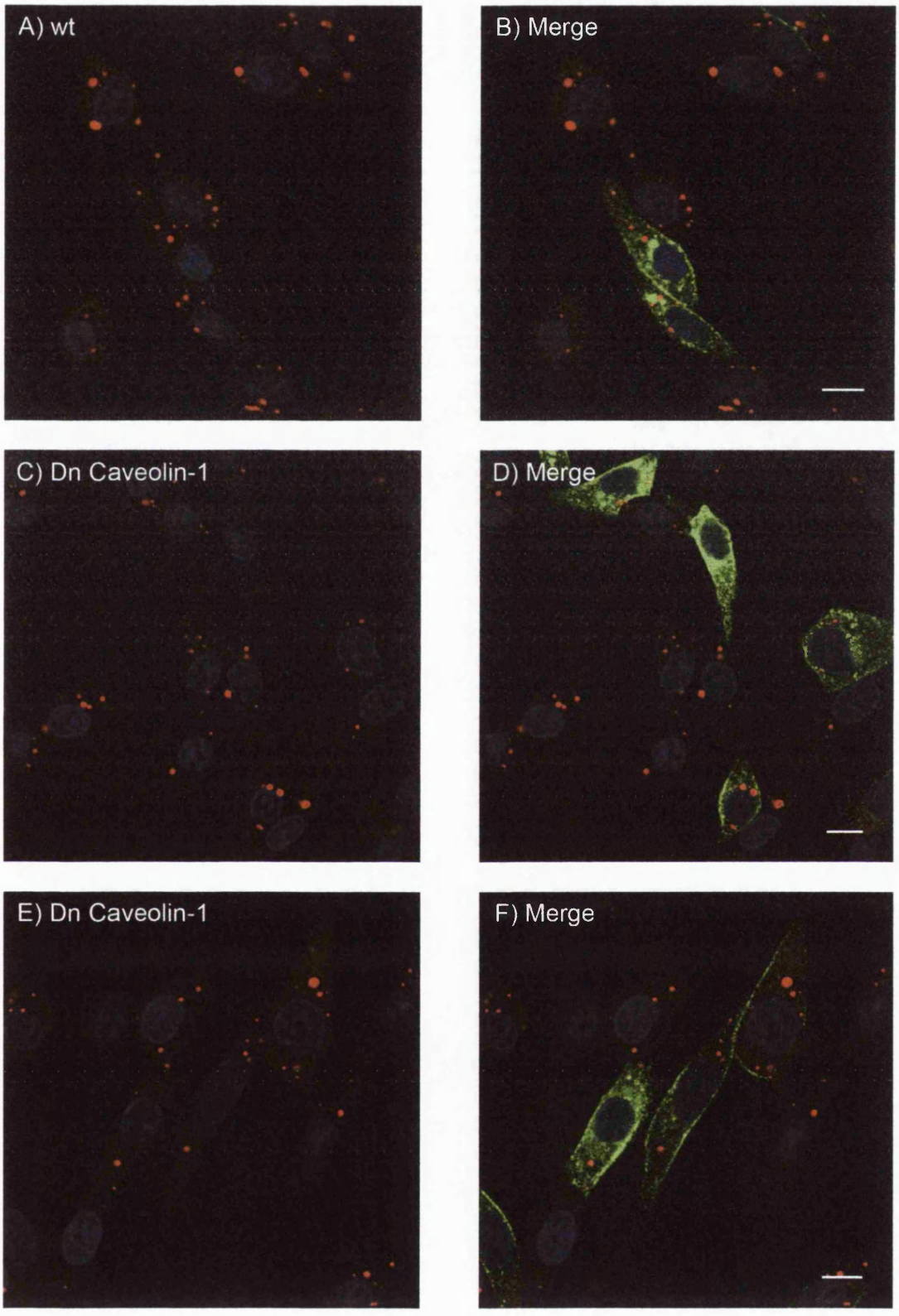

Figure 6.6: Expression of Dn Caveolin-1 does not inhibit BTV-1 infection of BHK cells (I) BHK cells were transfected to express wt (A) and (B) or Dn Caveolin-1 (C-F). At 12 h post transfection the cells were infected with BTV-1 (m.o.i. = 0.5). Wt and Dn Caveolin-1 expressing cells are shown as green. Infected cells were identified by labelling with Orab 1 (anti-NS2) and are shown as red. Panels (B), (D) and (F) show merged images for red and green fluorescence. The cell nuclei are shown in blue. Scale bar = 10 um.

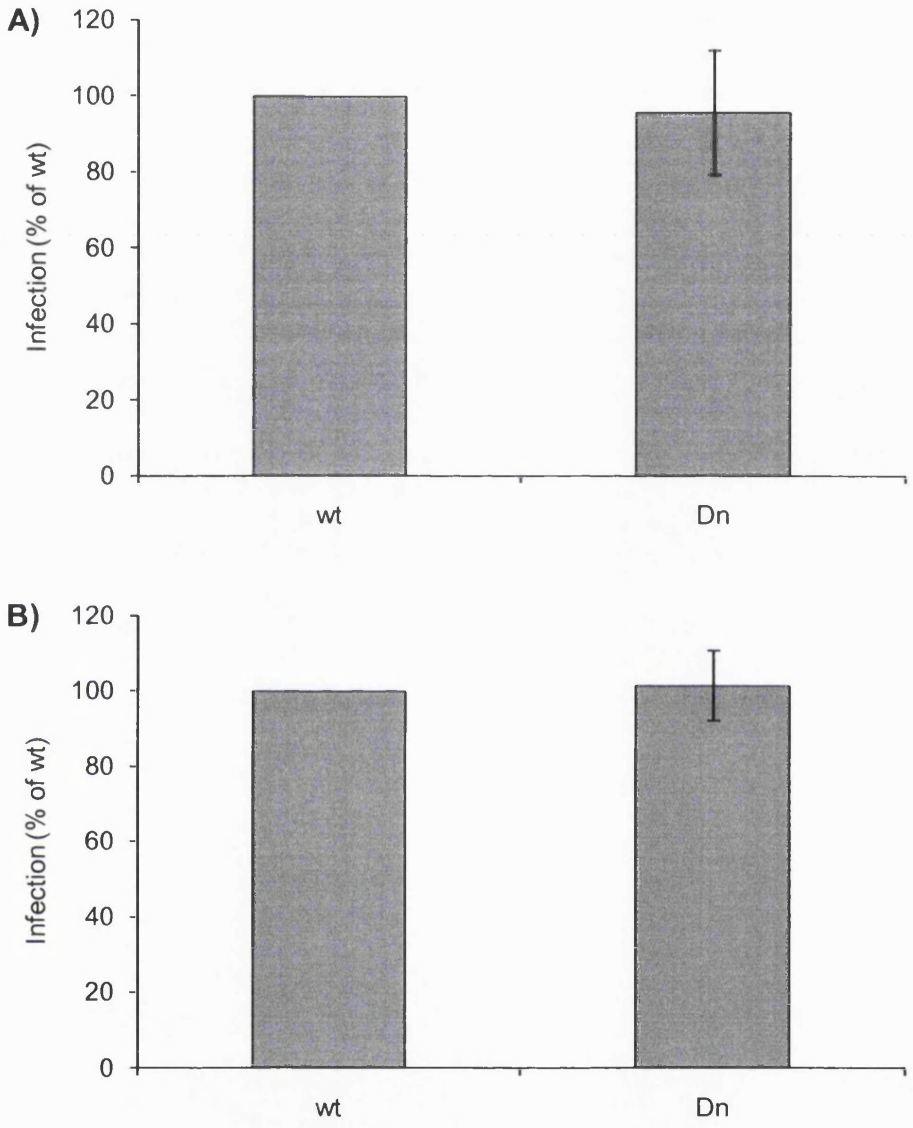

Figure 6.7: Expression of Dn Caveolin-1 does not inhibit BTV-1 infection of BHK cells (II)
BHK cells were transfected to express wt or Dn Caveolin-1 for 12 h and infected with BTV-1 (m.o.i. = 0.5) (see Figure 6.6). The cells expressing wt or Dn Caveolin-1 were scored (n ≥150 cells) for the presence of NS2 by confocal microscopy. The frequency of NS2 labelling for cells expressing Dn Caveolin-1 was normalised to NS2 labelling for the cells expressing the wt protein. Graphs (A) and (B) show the mean and standard deviation of triplicate transfections for two independent experiments.

cholesterol-dependent endocytosis, did not inhibit infection of BHK cells. Together, these observations indicate that cholesterol-dependent endocytosis pathways are unlikely to be used for entry. These observations are in agreement with previously published work using nystatin which was shown not to inhibit infection of Vero cells by BTV-10 (Forzan et al., 2007).

As caveolae-mediated endocytosis originates at lipid rafts the results presented in this chapter support the conclusion that caveolae are not needed for BTV-1 infection of BHK cells. This conclusion is in agreement with the failure of Dn Dynamin-2 to inhibit BTV-1 entry and infection of BHK cells (see Chapter 5). Similarly, the failure of Dn Caveolin-1 to inhibit BTV-1 infection of BHK cells also supports a lack of a role for caveolae in entry. In conclusion, the results shown in Chapters 5 and 6 strongly suggest that BTV-1 entry and infection of BHK cells does not require caveolae or other cholesterol sensitive endocytic pathways.

7 The Role of Macropinocytosis in BTV-1 Entry and Infection

7.1 Introduction

The data presented in earlier Chapters has shown that BTV-1 infection is clathrin-, dynamin-2-, cholesterol- and caveolin-1-independent but requires a low pH step. Therefore, it appears that BTV-1 does not require the most commonly used endocytic mechanisms utilised by viruses for entry and infection. Next macropinocytosis and macropinocytosis-like endocytosis entry mechanisms were investigated (see Section 1.5.2.3). Macropinocytosis is characterised by actin-dependent reorganisations of the plasma membrane to form macropinosomes, morphologically heterogenic vesicles that lack coat structures and is responsible for the majority of fluid-phase uptake in a number of cell-types. Macropinocytosis is also exploited by a number of important animal pathogens for cell invasion and possibly the avoidance of immune surveillance (Mercer and Helenius, 2008). The ability of BTV-1 to utilise macropinocytosis for entry and infection was investigated using a number of pharmacological and dominant-negative inhibitors that are known to inhibit macropinocytosis (see Section 1.5.2.3.1).

The role of dynamin in macropinocytosis is not clear. Some studies have reported a role for dynamin while others have concluded that macropinocytosis is dynamin-independent (Schafer, 2004). These discrepancies may be, in part explained by the different methods used to inhibit dynamin function. The experiments described in Chapter 5 used a dominant-negative mutant of the *'aa'* splice variant of dynamin-2. These experiments showed that BTV-1 entry and infection were not inhibited by Dn Dynamin-2 '*aa*'. However, it has recently been shown that dominant-negative mutants of the different splice variants of dynamin-2 differentially inhibit endocytic pathways (Cao et al., 2007). Therefore, to further understand the role of dynamin in BTV-1 entry into BHK cells the effect of dynasore, a rapid-acting reversible dynamin inhibitor was investigated (Macia et al., 2006; Thompson and McNiven, 2006).

7.2 The Effect of EIPA Treatment on Endocytosis

Macropinocytosis is dependent on the amiloride-sensitive Na+/H+ exchanger (Moriyama et al., 2007) and is inhibited by amiloride or its more potent analogue 5-(N-ethyl-N-isopropyl)-amiloride (EIPA) (Fretz et al., 2006). EIPA has previously been shown to inhibit entry of macropinocytosis markers (such as dextran and albumin) without affecting other endocytic pathways, such as clathrin-mediated endocytosis (Mercer and Helenius, 2009). BHK cells were incubated in serum-free medium (GMEM) for 30 minutes at 37°C. Cells were then mock-treated (Figure 7.1) or treated with 100 µM EIPA (Figure 7.2) for 30 minutes at 37°C (also in serum-free medium). The cells were then washed and allowed to internalise 568-Alexa labelled dextran (5 mg/ml) for 30 minutes or transferrin (25 µg/ml) for 15 minutes at 37°C. Entry was stopped and the cells fixed by the addition of 4% paraformaldehyde (or 4% paraformaldehyde including 0.25% glutaraldehyde for experiments involving transferrin). Cells were then processed for confocal microscopy without permabilisation. Figure 7.1, panels (A) and (B) show entry of dextran (shown as red) for mock-treated cells and confirms that macropinocytosis/fluid-phase uptake is active in BHK cells; whereas figure 7.2, panels (A) and (B) show that entry of dextran is inhibited by EIPA. Transferrin entry is a commonly used marker of clathrin-mediated endocytosis and its entry was examined to determine if EIPA inhibited clathrin-mediated endocytosis. Figure 7.1, panels (C) and (D) show entry of transferrin in mock-treated cells. Figure 7.2, panels (C) and (D) show that entry of transferrin also appeared normal in EIPA treated cells demonstrating that 100 µM EIPA did not inhibit the clathrin-mediated pathway.

7.3 The Effect of EIPA on BTV-1 Uptake

The effect of EIPA on virus entry was also investigated. Cells were pre-treated with 100 µM EIPA (Figure 7.2) or mock-treated (Figure 7.1) as described above, and BTV-1 (13 µg/ml) bound to the cells in the presence or absence (mock) of the drug for 40 minutes on ice. Unbound virus was removed by washing and entry initiated by the

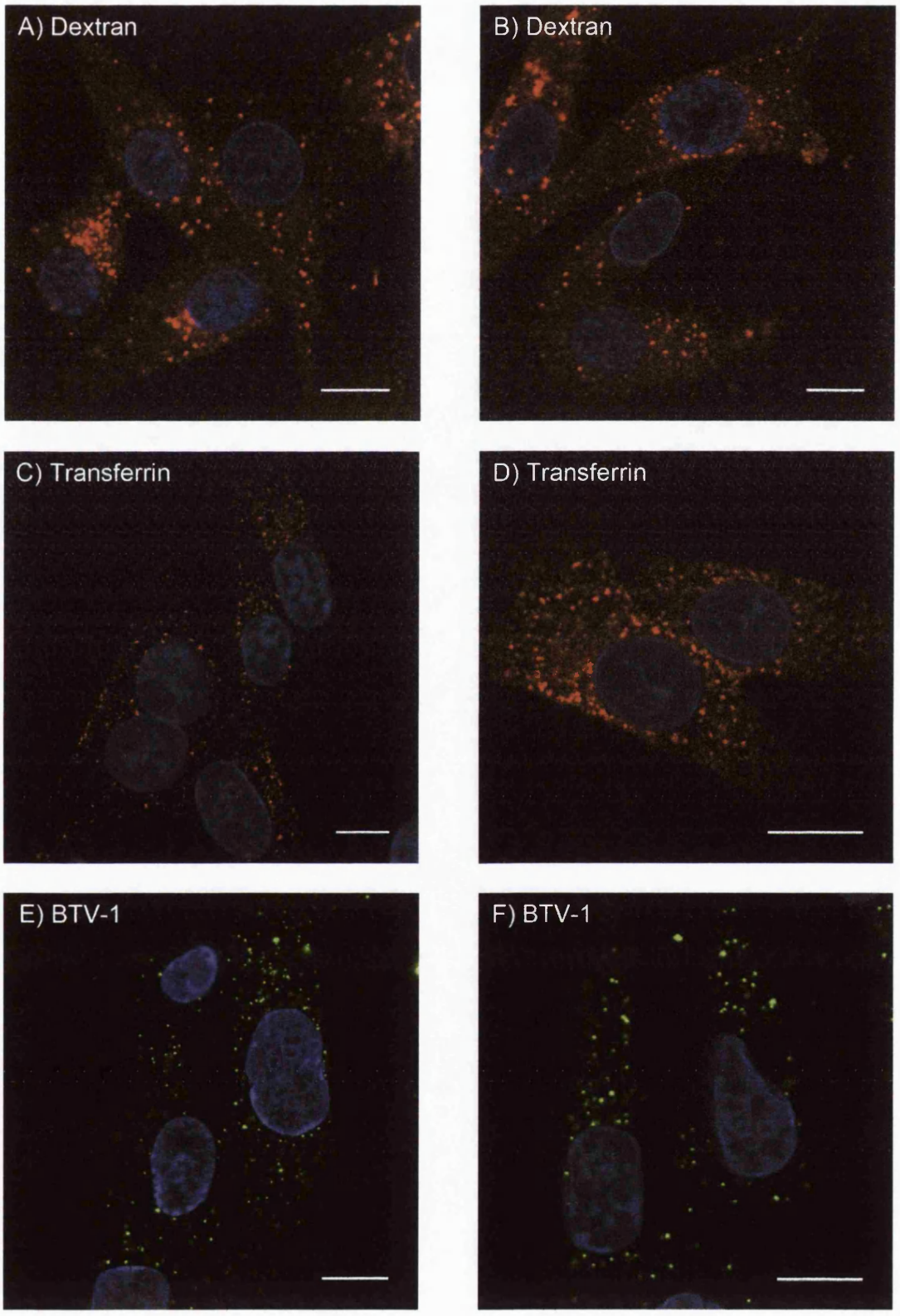

Figure 7.1: Entry of BTV-1, transferrin and dextran by mock-treated BHK cells
BHK cells were mock-treated with DMSO for 30 min and then incubated at 37°C with 568-Alexa labelled dextran (5 mg/ml) (Panels A and B) or BTV-1 (Panels E and F) for 30 min, or with 568-Alexa labelled transferrin (25 μg/ml) for 15 min (Panels C and D). Entry was stopped by the addition of 4% PFM (including 0.25% glutaraldehyde for transferrin) and the cells processed for confocal microscopy. Virus was detected using PM10 (anti-VP5) shown as green. Dextran and transferrin are shown as red. The cell nuclei are shown as blue. Scale bar = 10 μm.

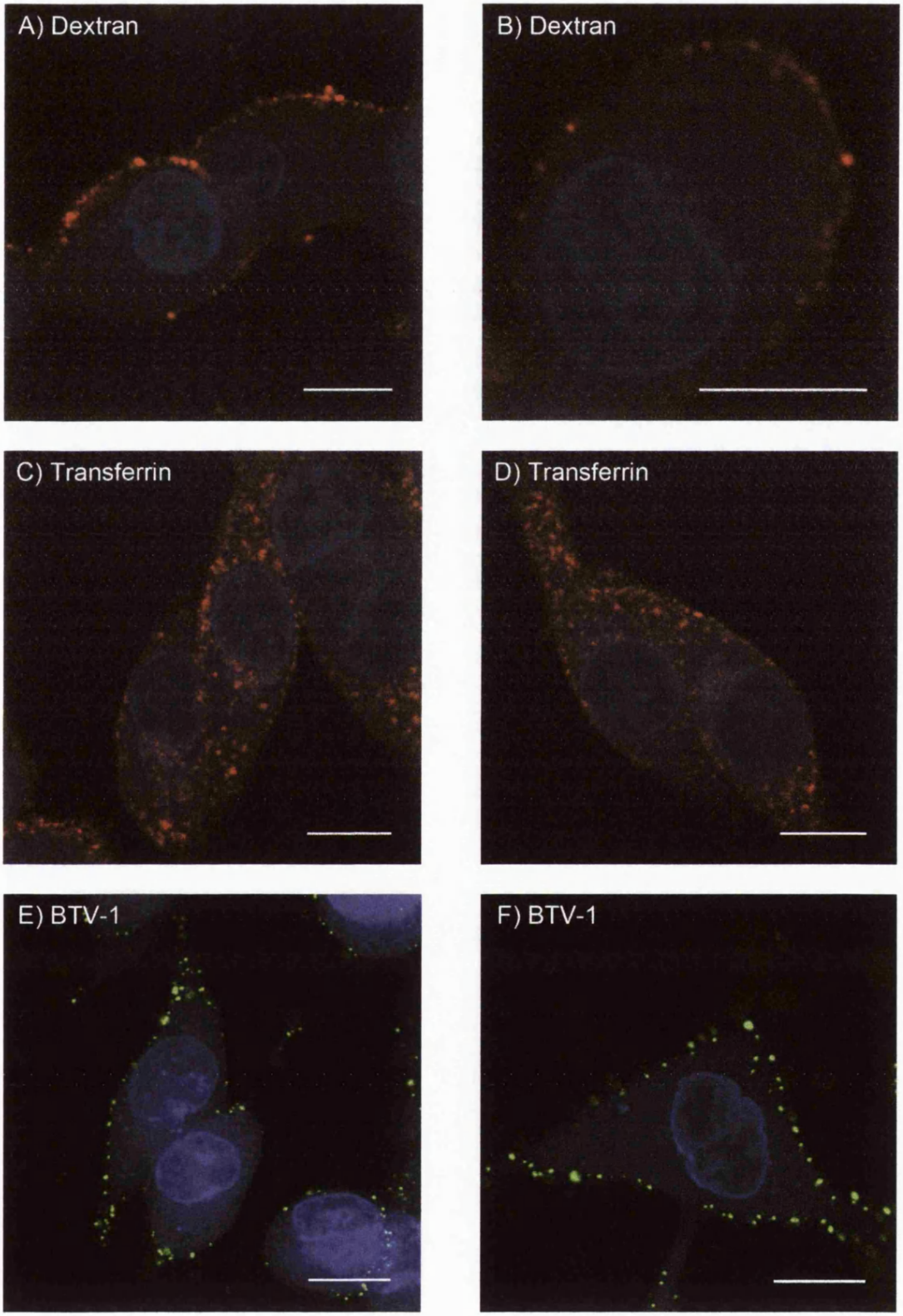

Figure 7.2: Entry of BTV-1 and dextran, but not transferrin is blocked by EIPA
BHK cells were pre-treated with 100 μM EIPA for 30 min and then incubated at 37°C with 568-Alexa labelled dextran (5 mg/ml) (Panels A and B) or BTV-1 (Panels E and F) for 30 min, or with 568-Alexa labelled transferrin (25 μg/ml) for 15 min (Panels C and D). Entry was stopped by the addition of 4% PFM (including 0.25% glutaraldehyde for transferrin) and the cells processed for confocal microscopy. Virus was detected using PM10 (anti-VP5) shown as green. Dextran and transferrin are shown as red. The cell nuclei are shown as blue. Scale bar = 10 μm.

addition of pre-warmed medium (37°C). After 30 minutes, entry was stopped and the cells fixed by the addition of 4% paraformaldehyde. The cells were then permeabilised with 0.1% Triton X-100 and labelled for BTV using PM10 (anti-VP5) and a goat, anti-Mouse Alexa-fluor 488-conjugated secondary antibody as described in Chapter 3. Figure 7.1, panels (E) and (F) shows that virus (shown as green) appeared to enter the cells normally following mock-treatment. In contrast, treatment with 100 µM EIPA inhibited entry of BTV-1 almost completely (Figure 7.2, Panels E and F). The above experiments show that 100 µM EIPA inhibits entry of dextran (a marker of macropinocytosis) and BTV-1 but not transferrin (a marker of clathrin-mediated endocytosis). This suggests that BTV-1 entry may be dependent on a form of fluid-phase uptake such as macropinocytosis.

7.4 The Effect of Actin Disruption on BTV-1 Infection of BHK Cells

Macropinocytosis is also dependent on actin-driven reorganisation of the plasma membrane and as a result can be inhibited by altering the state of actin polymerisation using cytochalasin D or latrunculin A (see Section 1.5.2.3.1). Cytochalasin D acts by binding to the apical tip of F actin whilst latrunculin A sequesters actin monomers (Coue et al., 1987; Sampath and Pollard, 1991). The effect of cytochalasin D and latrunculin A on BTV-1 infection were investigated.

To confirm disruption of the actin cytoskeleton, cells were pre-treated with 2 µM or 1 µM cytochalasin D or 1.5 µM latrunculin A for 30 minutes at 37°C. The drug was washed away with cold medium and the cells fixed by the addition of 4% paraformaldehyde for 40 minutes at room temperature. Cells were then permeabilised with 0.1% Triton X-100, blocked in block buffer and actin filaments labelled by incubation with 488-Alexa labelled phalloidin for 10 minutes at room temperature (see Method 2.6.3).

Figure 7.3, panels (A) and (B) shows the intact actin cytoskeleton in mock-treated cells. Figure 7.3, panel (C) shows cells treated with 2 µM cytochalasin D, and

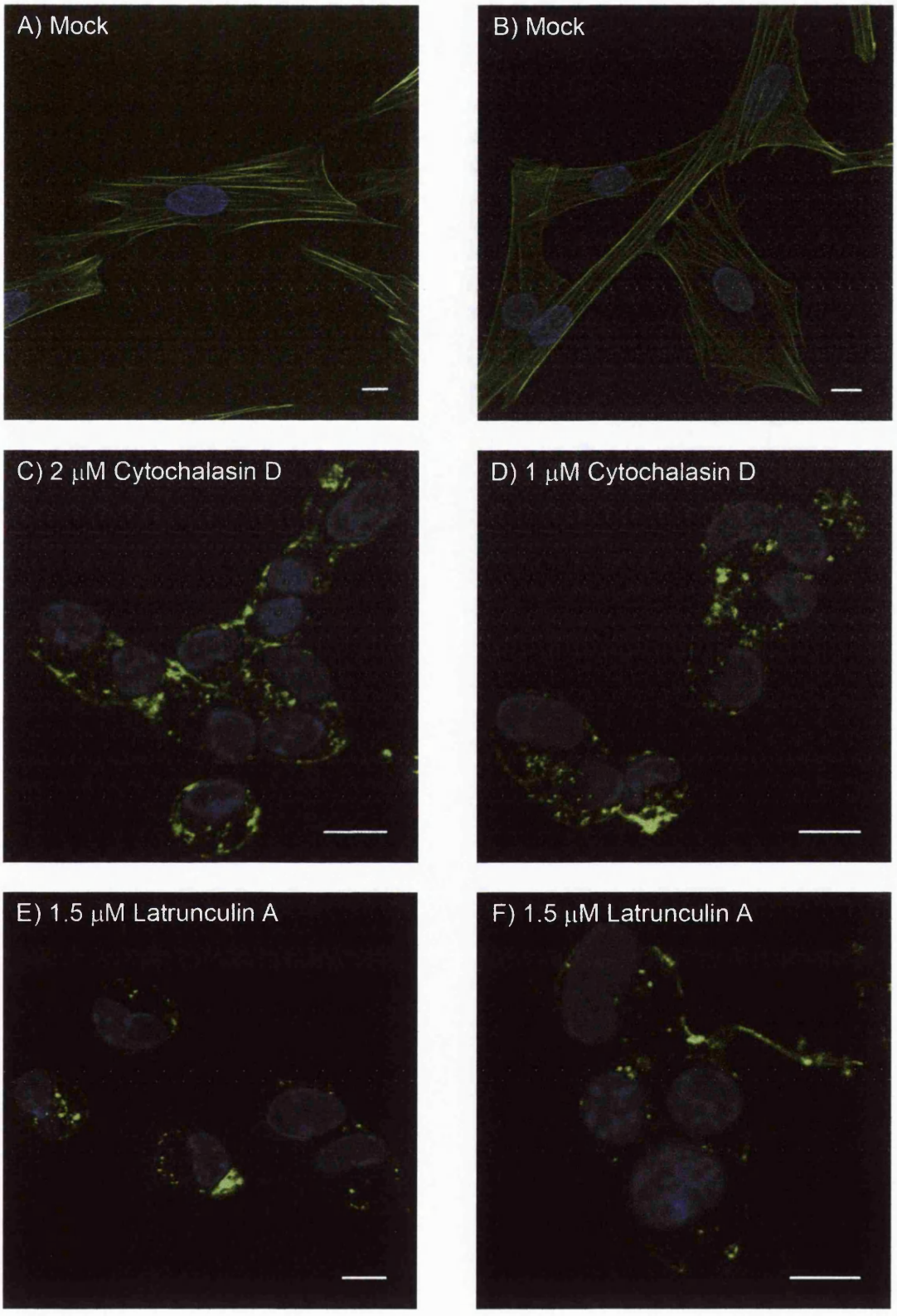

Figure 7.3: Disruption of the celluar actin cytoskeleton
BHK cells were mock-treated (Panels A and B) or treated with 2 μM (Panel C) or 1 μM (Panel D) cytochalasin D or 1.5 μM latrunculin A (Panels E and F) at 37°C for 30 min. The cells were then fixed with 4% PFM and processed for confocal microscopy. The actin cytoskelton was visualised by labelling with phalloidin and is shown as green. The cell nuclei are shown as blue. Scale bar = 10 μm.

panel (D) 1 µM cytochalasin and that the actin cytoskeleton had been disrupted. Similarly, figure 7.3, panels (E) and (F) show that treatment of cells with 1.5 µM latrunculin A also disrupts the actin cytoskeleton.

Next the effect of cytochalasin D and latrunculin A on BTV-1 infection of BHK cells was investigated (Figure 7.4 and 7.5). Cells were mock-treated (Mock) or pre-treated with 2 µM or 1 µM cytochalasin D, or 1.5 µM latrunculin A for 30 minutes at 37°C and then infected with BTV-1 (m.o.i. = 0.5) for 1 hour at 37°C in the presence or absence (Mock) of the drug. Excess virus and drug were removed by washing with medium, and infection continued for a further 11 hours. When added as a post-treatment cytochalasin D or latrunculin A was present for 1.5 hours immediately after the 1 hour incubation with virus. The effects of cytochalasin D and latrunculin A are likely to be reversed after drug washout. This could result in virus that has bound to the cells in the presence of the drug being internalised in an actin dependent way after the disruptive effects of the drugs on actin filaments have reversed. However, in this experiment 25 mM ammonium chloride was added to all of the cells immediately after the 1 hour incubation with virus (see Method 2.6.7). Addition of ammonium chloride would be expected to rapidly increase endosomal pH and prevent further acid-induced infection events (see Chapter 4, Figure 4.8). This allowed the entry phase of infection (i.e. before the addition of ammonium chloride) to be separated from post-entry virus replication (i.e. after the addition of ammonium chloride). This allowed the effects of cytochalasin D or latrunculin A on entry and post-entry replication to be clearly separated as when cytochalasin D or latrunculin A was added after the addition of ammonium chloride, any inhibitory effects could only result from a block to post-entry virus replication.

Infection was stopped and the cells fixed by the addition of 4% paraformaldehyde. Infected cells were detected by labelling with Orab 1 (anti-NS2) followed by goat, anti-Rabbit Alexa-fluor 568-conjugated secondary antibody. Cells were scored for infection by confocal microscopy (n ≥300 cells). The percentage of

drug-treated cells that were positive for infection was normalised to the level of infection of the mock-treated cells. Figure 7.4, panel (A) shows quantification of the data in graph format for duplicate coverslips that were pre-treated with 2 µM or 1 µM cytochalasin D. The data shows that cytochalasin D results in a large inhibition of infection (~90%). Figure 7.4, panel (B) shows a second experiment where the drug was added to the cells before and after the incubation with virus. The mean and standard deviation for triplicate samples is shown. Again pre-treatment (Pre) of the cells with either concentration of cytochalasin D caused a large inhibitory effect on infection (by >70% compared to mock-treated cells). In contrast, when added as a post-treatment (Post) no inhibitory effect was seen demonstrating that actin disruption with cytochalasin D had no effect on post-entry virus replication.

The experiment shown in figure 7.4, panel (B) was repeated using 1.5 µM latrunculin A in place of cytochalasin D. Figure 7.5 shows quantification of the data from this experiment in graph format. The mean and standard deviation for triplicate samples is shown. As for cytochalasin D, a large inhibition of infection was seen when latrunculin A was added as a pre-treatment, whereas when added as a post-treatment no inhibition of infection was seen.

The experiments described above show that under conditions where treatment with actin inhibitors depolymerises the actin cytoskeleton, BTV-1 infection of BHK cells is inhibited. These results also show that infection is inhibited at the entry stage and not after the virus has entered the cell.

7.5 Co-localisation of Dextran and BTV-1

To further investigate the entry mechanism used by BTV-1 to infect BHK cells, BTV-1 was co-internalised with 568-Alexa labelled dextran, a commonly used marker for macropinocytosis and fluid phase uptake.

BTV-1 (13 µg/ml) in serum-free medium was bound to BHK cells for 40 minutes on ice. Unbound virus was removed by washing and entry initiated by warming the

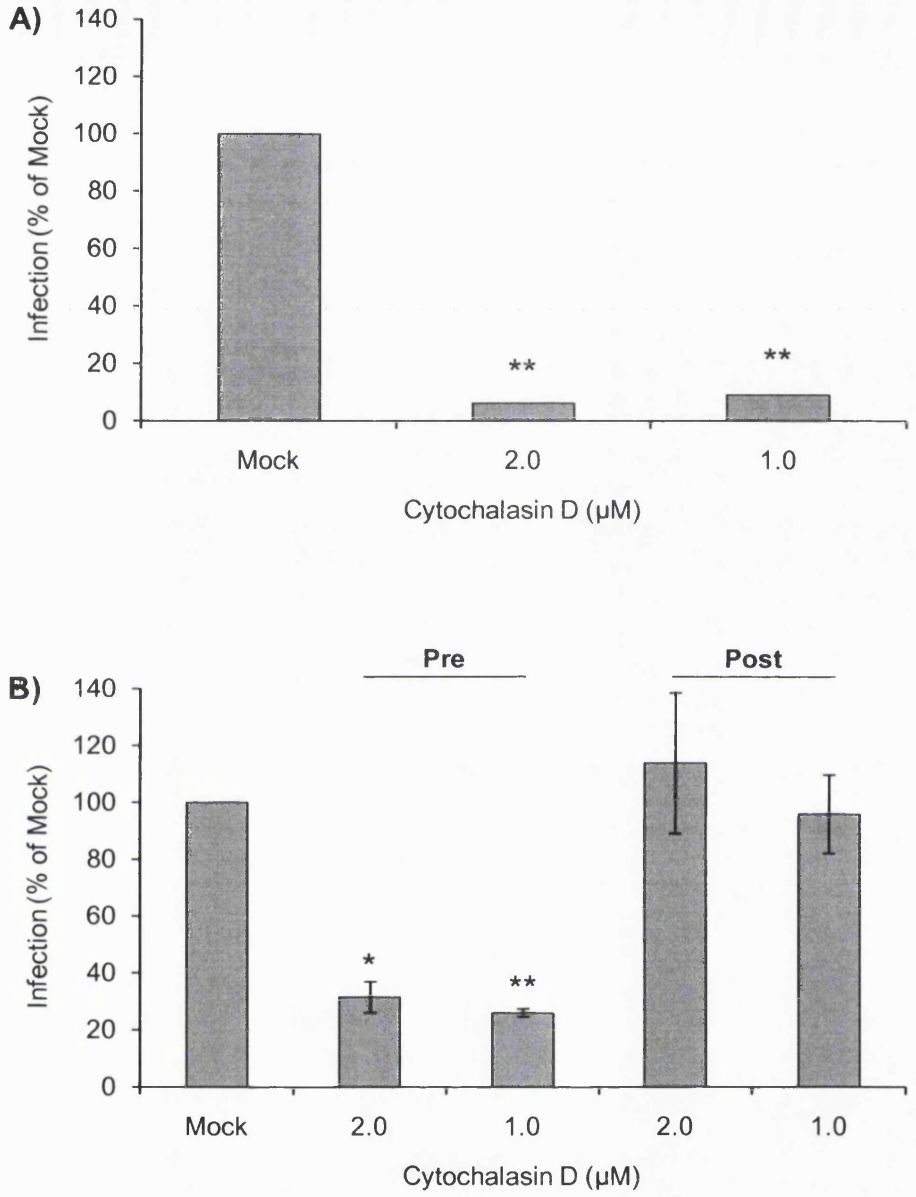

Figure 7.4: Cytochalasin D inhibits BTV-1 infection of BHK cells
Panel (A). BHK cells were mock-treated (Mock) or pre-treated with cytochalasin D (2 μM or 1 μM) for 30 min at 37°C. The cells were then incubated with BTV-1 (m.o.i. = 0.5) for 1 h at 37°C in the presence (Pre) or absence (Mock) of the drug. The cells were then washed and incubated in the presence of 25 mM ammonium chloride (see text). Panel (B). BHK cells were mock-treated (Mock) or pre-treated with cytochalasin D as for Panel (A). Additional cultures were treated with the drug for 90 min immediately after the 1 h incubation with virus (Post). After 11 h, infection was stopped and the cells fixed by the addition of 4% PFM. The cells were then processed for confocal microscopy using Orab 1 (anti-NS2) to identify infected cells. Each bar represents the number of infected cells expressed as the percentage infection of the mock-treated cells. Panel (A) shows the mean for duplicate samples. Panel (B) shows the mean and standard deviation of triplicate samples.
(*P* values: * <0.05, ** <0.01)

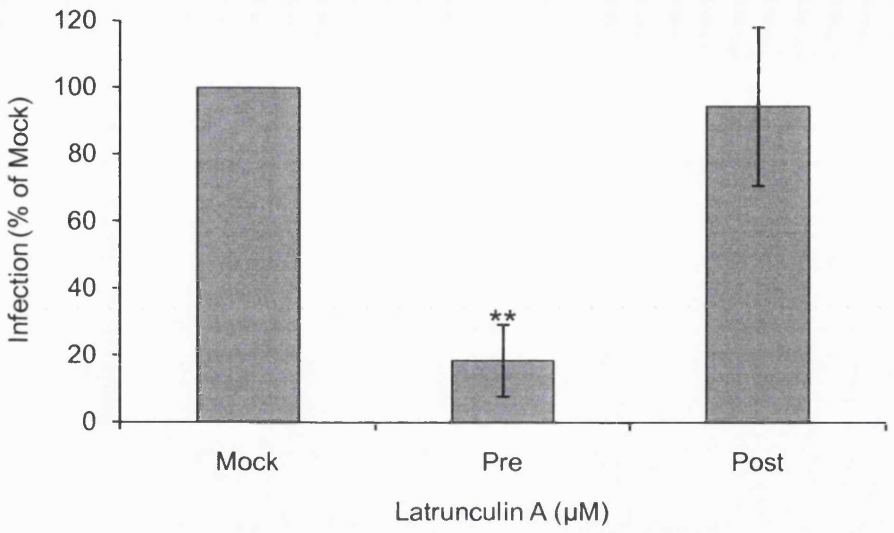

Figure 7.5: Latrunculin A inhibits BTV-1 infection of BHK cells. BHK cells were mock-treated (Mock) or pre-treated (Pre) with latrunculin A (1.5 μM) for 30 min at 37°C. The cells were then incubated with BTV-1 (m.o.i. = 0.5) for 1 h at 37°C in the presence or absence (Mock) of the drug. The cells were then washed and incubated in the presence of 25 mM ammonium chloride (see text). Additional cultures were treated with the drug for 90 min immediately after the 1 h incubation with virus (Post). After 11 h, infection was stopped and the cells fixed by the addition of 4% PFM. The cells were then processed for confocal microscopy using Orab 1 (anti-NS2) to identify infected cells. Each bar represents the number of infected cells expressed as the percentage infection of the mock-treated cells. The data is shown as the mean and standard deviation of triplicate samples (*P* values: ** <0.01).

cells to 37°C (see Method 2.6.8 and 2.6.2) in serum-free medium containing 568-Alexa labelled dextran (5 mg/ml). Virus (and dextran) was internalised for 15, 30, 60, 90 and 120 minutes. Internalisation was stopped by the addition of cold 4% paraformaldehyde. The cells were then permeablised with 0.1% Triton X-100 and processed for confocal microscopy using PM10 and a goat, anti-Guinea pig Alexa-flour 488-conjugated secondary antibody to detect input virus.

Figures 7.6 to 7.10 show representative images for each time point. Each figure shows two representative images for the specified time point; panels (A) and (B) show internalisation of dextran (shown as red); panels (C) and (D) show virus entry (shown as green) for the same cells as in panels (A) and (B) respectively. Panels (E) and (F) show merged images for red and green fluorescence. Figure 7.6 shows cells fixed after 15 minutes internalisation of virus and dextran. Dextran and virus are both observed at the cell periphery indicating similar entry kinetics. Most of the virus that had been taken up by the cells was co-localised with dextran (as shown by the presence of yellow labelling in the merged images) (Figure 7.6, Panels E and F). After 30 minutes of uptake approximately 40% of the internalised virus (BTV-1 particles, n = 100) was co-localised with dextran (Figure 7.7, Panels E and F). Figures 7.8, 7.9 and 7.10 show that a similar level of virus/dextran co-localisation was also observed after 60, 90 and 120 minutes post-entry respectively. These data suggest that BTV-1 is using an entry mechanism that shares characteristics with macropinocytosis.

7.6 Expression of Dn Rab 34 Inhibits BTV-1 infection of BHK Cells

Rab 34 has been implicated as a regulator of macropinocytosis in some cell types (Sun et al., 2003). Therefore the role of Rab 34 in BTV-1 infection of BHK cells was investigated using a dominant-negative Rab 34 mutant which has been shown to inhibit macropinocytosis in mouse fibroblast cells (Sun et al., 2003).

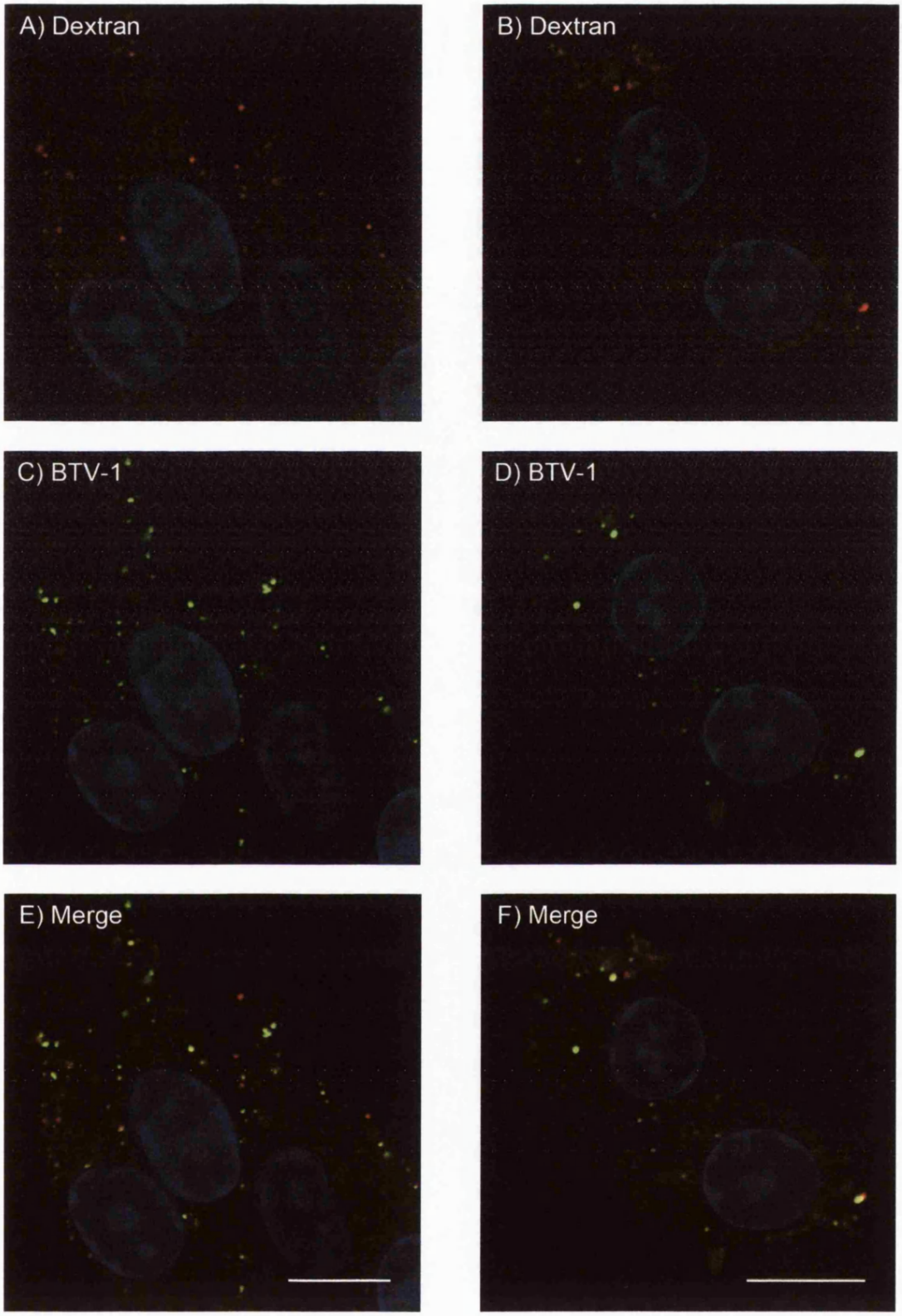

Figure 7.6: BTV-1 co-localises with dextran after 15 minutes of co-internalisation
BTV-1 (13 μg/ml) was pre-bound to BHK cells for 40 min on ice. Unbound virus was removed by washing and entry initiated by warming the cells to 37°C. Virus was co-internalised in the presence of 568-Alexa labelled dextran (5 mg/ml) for 15 min (shown as red). The cells were fixed with cold 4% PFM and processed for confocal microscopy. Virus was detected using PM10 (anti-VP5) and is shown as green. Panels (A) and (B) show entry of dextran. Panels (C) and (D) show entry of virus for the same cells as in panels (A) and (B) respectively. Panels (E) and (F) show merged images for red and green fluoresence. The cell nuclei are shown as blue. Scale bar = 10 μm.

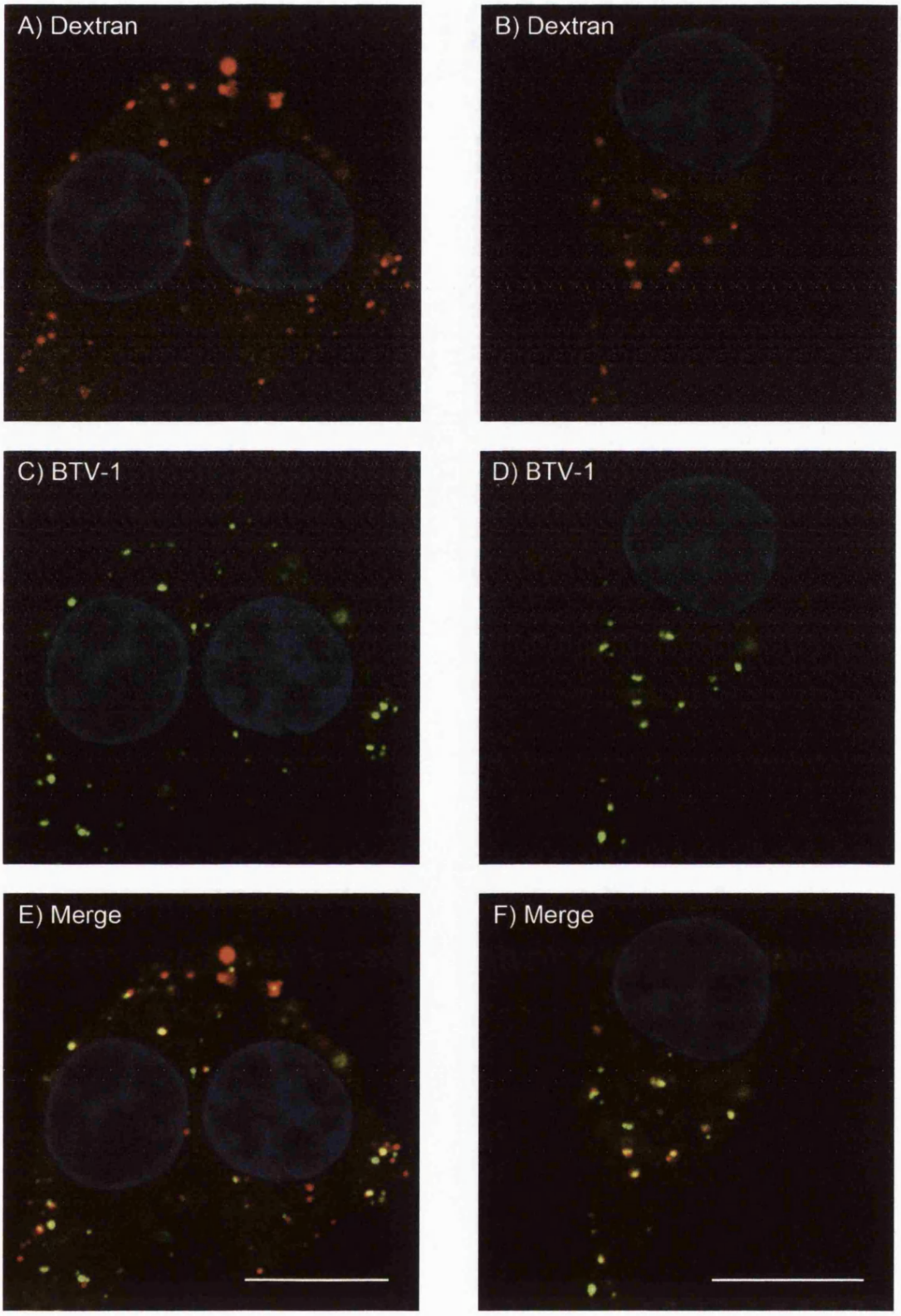

Figure 7.7: BTV-1 co-localises with dextran after 30 minutes of co-internalisation
BTV-1 (13 μg/ml) was pre-bound to BHK cells for 40 min on ice. Unbound virus was removed by washing and entry initiated by warming the cells to 37°C. Virus was co-internalised in the presence of 568-Alexa labelled dextran (5 mg/ml) for 30 min (shown as red). The cells were fixed with cold 4% PFM and processed for confocal microscopy. Virus was detected using PM10 (anti-VP5) and is shown as green. Panels (A) and (B) show entry of dextran. Panels (C) and (D) show entry of virus for the same cells as in panels (A) and (B) respectively. Panels (E) and (F) show merged images for red and green fluoresence. The cell nuclei are shown as blue. Scale bar = 10 μm.

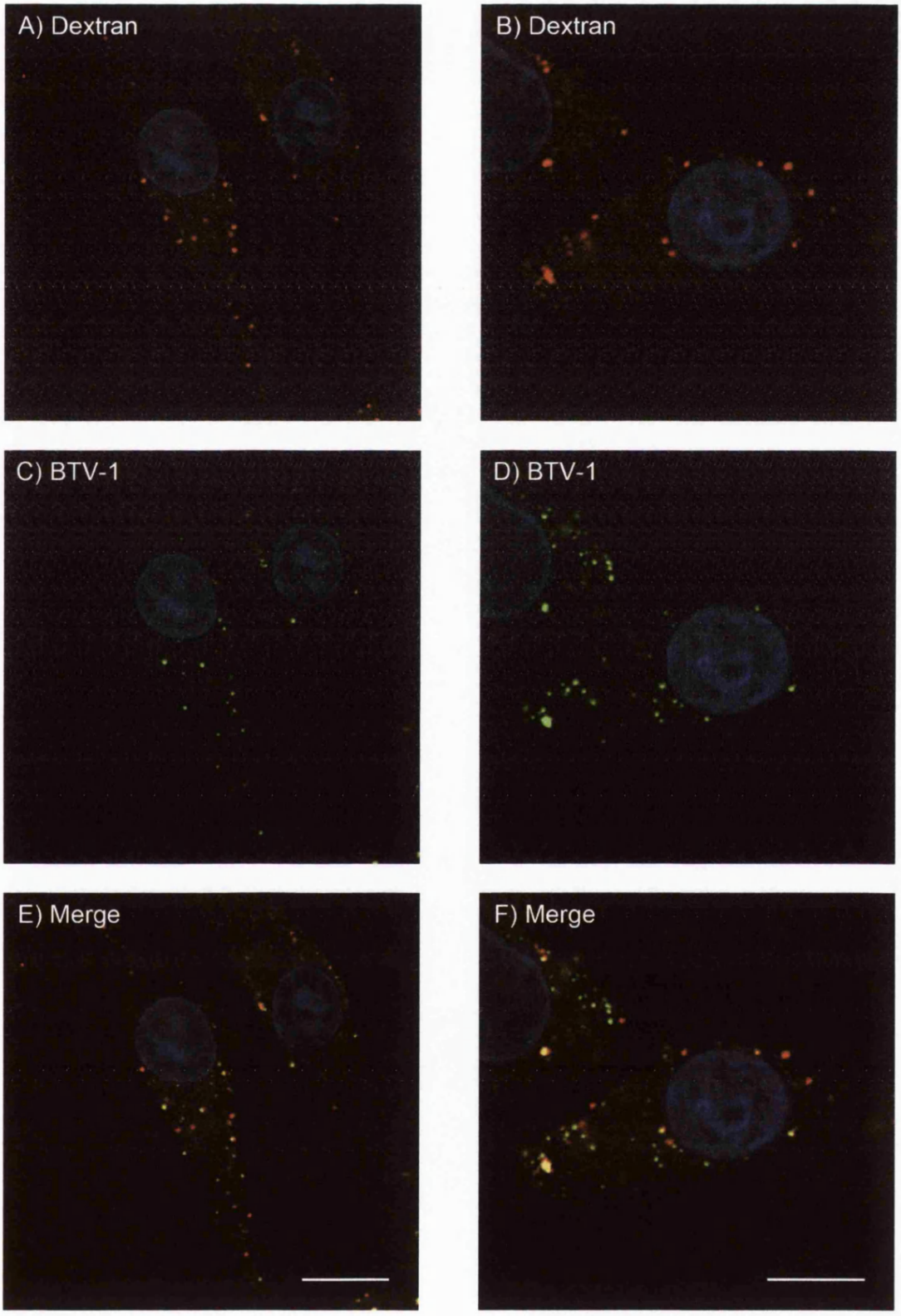

Figure 7.8: BTV-1 co-localises with dextran after 60 minutes of co-internalisation
BTV-1 (13 μg/ml) was pre-bound to BHK cells for 40 min on ice. Unbound virus was removed by washing and entry initiated by warming the cells to 37°C. Virus was co-internalised in the presence of 568-Alexa labelled dextran (5 mg/ml) for 60 min (shown as red). The cells were fixed with cold 4% PFM and processed for confocal microscopy. Virus was detected using PM10 (anti-VP5) and is shown as green. Panels (A) and (B) show entry of dextran. Panels (C) and (D) show entry of virus for the same cells as in panels (A) and (B) respectively. Panels (E) and (F) show merged images for red and green fluoresence. The cell nuclei are shown as blue. Scale bar = 10 μm.

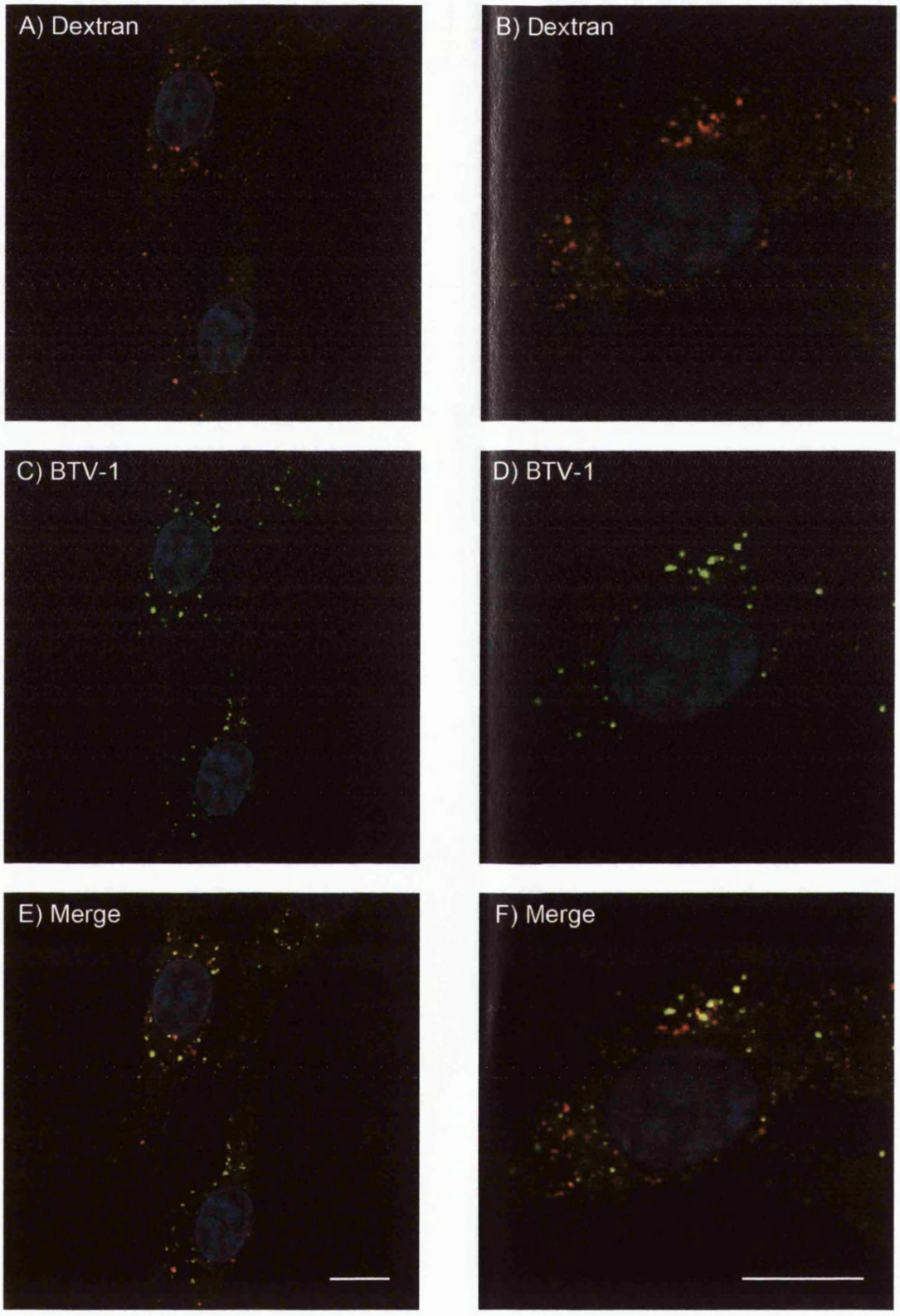

Figure 7.9: BTV-1 co-localises with dextran after 90 minutes of co-internalisation
BTV-1 (13 μg/ml) was pre-bound to BHK cells for 40 min on ice. Unbound virus was removed by washing and entry initiated by warming the cells to 37°C. Virus was co-internalised in the presence of 568-Alexa labelled dextran (5 mg/ml) for 90 min (shown as red). The cells were fixed with cold 4% PFM and processed for confocal microscopy. Virus was detected using PM10 (anti-VP5) and is shown as green. Panels (A) and (B) show entry of dextran. Panels (C) and (D) show entry of virus for the same cells as in panels (A) and (B) respectively. Panels (E) and (F) show merged images for red and green fluoresence. The cell nuclei are shown as blue. Scale bar = 10 μm.

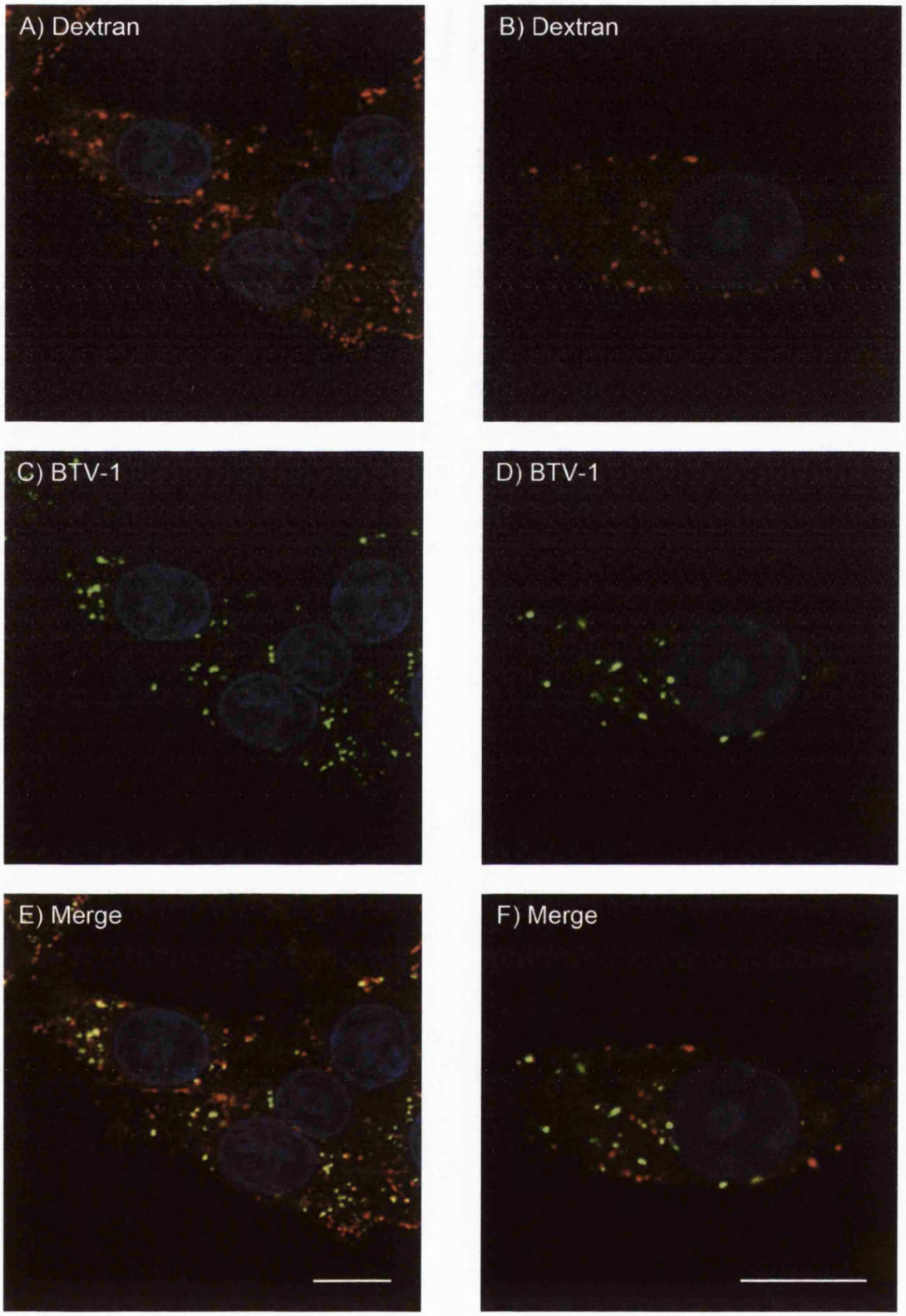

Figure 7.10: BTV-1 co-localises with dextran after 120 minutes of co-internalisation
BTV-1 (13 μg/ml) was pre-bound to BHK cells for 40 min on ice. Unbound virus was removed by washing and entry initiated by warming the cells to 37°C. Virus was co-internalised in the presence of 568-Alexa labelled dextran (5 mg/ml) for 120 min (shown as red). The cells were fixed with cold 4% PFM and processed for confocal microscopy. Virus was detected using PM10 (anti-VP5) and is shown as green. Panels (A) and (B) show entry of dextran. Panels (C) and (D) show entry of virus for the same cells as in panels (A) and (B) respectively. Panels (E) and (F) show merged images for red and green fluoresence. The cell nuclei are shown as blue. Scale bar = 10 μm.

BHK cells were transfected to express wt or Dn Rab 34 as described above. At 12 hours post-transfection, the cells were infected with BTV-1 (m.o.i. = 0.5) for 1 hour at 37°C. Excess virus was removed by washing and infection continued for a further 11 hours. At this point, infection was stopped by the addition of 4% paraformaldehyde and the cells processed for confocal microscopy. Wild type and Dn Rab 34 expressing cells were identified by eGFP fusion tags (shown as green). Infected cells were identified by labelling with Orab 1 (anti-NS2) and a goat, anti-Rabbit Alexa-fluor 568-conjugated secondary antibody, as described in Chapter 3 (shown as red). Figure 7.11, panel (A) shows BTV-1 infection (shown as Red) whilst panel (B) shows an overlay of cells expressing wt Rab 34 (shown as green). Figure 7.11, panels (C) and (E) show BTV-1 infection (shown as red), with panels (D) and (F) showing an overlay with cells expressing Dn Rab 34 (shown as green).

Cells expressing wt and Dn Rab 34 (n ≥150 expressing cells) were scored for infection by confocal microscopy. The percentage of cells expressing the dominant-negative protein that were positive for infection was normalised to the results obtained for cells expressing the wt protein. Figure 7.12, panels (A) and (B) show quantification of this data in graph format. The mean and standard deviation is shown for two independent experiments each using triplicate samples. This data shows that expression of Dn Rab 34 inhibited BTV-1 infection of BHK cells by 40-43%. However, as I was unable to find a suitable control ligand to demonstrate that Rab 34 had been inhibited, the results obtained and shown here using Dn Rab 34 must be considered as preliminary.

7.7 Further studies to investigate the role of dynamin in BTV-1 infection of BHK cells

The data presented in Chapter 5 showed that BTV-1 entry and infection of BHK cells was not inhibited by a dominant-negative mutant of the *'aa'* splice variant of dynamin-2 which is known to inhibit both clathrin- and caveolae-mediated endocytosis. Dominant-negative mutants of all the dynamin-2 splice variants (*'aa', 'ab', 'ba' and 'bb'*)

are known to inhibit clathrin-mediated endocytosis whereas only dominant-negative mutants of the *'ba'* and *'bb'* splice variants significantly inhibit macropinocytosis/fluid-phase uptake (Cao et al., 2007). To further investigate the role of dynamin in BTV-1 entry, the effect of dynasore was investigated. Dynasore is a recently discovered, rapid-acting and reversible dynamin inhibitor that is believed to inhibit all forms of dynamin (Kirchhausen et al., 2008; Macia et al., 2006). As the effects of dynasore are rapidly reversed on drug washout, the inhibitor remained present throughout the assays.

Initially entry of dextran (a commonly used marker of fluid-phase entry) was examined in dynasore treated cells. BHK cells were incubated in serum-free medium (GMEM) for 1 hour at 37°C. The cells were then mock-treated or treated with 100 µM dynasore (see Figure 7.13) for 30 minutes at 37°C (also in serum-free medium). The cells were then allowed to internalise 568-Alexa labelled dextran (5 mg/ml) for 30 minutes at 37°C in the presence or absence (mock) of the drug. Entry of dextran was stopped and the cells fixed by the addition of 4% paraformaldehyde. Cells were then processed for confocal microscopy. Figure 7.13, panels (A) and (B) shows that dextran internalisation (shown as red) was inhibited in dynasore treated cells compared to mock-treated cells (See Figure 7.1, Panels A and B). These data show that 100 µM dynasore inhibits macropinocytosis/fluid-phase entry in BHK cells, and suggests that dynamin had been successfully inhibited by the dynasore treatment.

To further verify that dynasore was inhibiting endogenous dynamin, entry of transferrin (a commonly used marker of clathrin-mediated endocytosis) was examined in dynasore treated cells. BHK cells were treated with 100 µM dynasore or mock-treated and allowed to internalise 568-Alexa labelled transferrin (25 µg/ml) for 15 minutes at 37°C as described above. Entry of transferrin was stopped and the cells fixed by the addition of 4% paraformaldehyde including 0.25% glutaraldehyde. Cells were then processed for confocal microscopy. Figure 7.13, panels (C) and (D) show that entry of transferrin (shown as red) was effectively inhibited in dynasore treated

cells when compared to mock-treated cells (See Figure 7.1). This data shows that dynasore is inhibiting clathrin-mediated endocytosis as well as fluid-phase entry in BHK cells and confirms inhibition of endogenous dynamin.

Next the effect of dynasore on BTV-1 entry was investigated. Cells were pre-treated with 100 µM dynasore or mock-treated as above and BTV-1 (13 µg/ml) bound to the cells in the presence or absence (mock) of the drug for 40 minutes on ice. Unbound virus was removed by washing and entry initiated by the addition of pre-warmed medium (37°C) also in the presence or absence (mock) of the drug. After 30 minutes entry was stopped and the cells fixed by the addition of 4% paraformaldehyde. The cells were then permeabilised with 0.1% Triton X-100 and labelled for BTV-1 using PM10 (anti-VP5) and a goat, anti-Guinea pig Alexa-fluor 488-conjugated secondary antibody, as described in Chapter 3. Figure 7.13, panels (E) and (F) shows that virus entry into BHK cells was strongly inhibited by treatment with 100 µM dynasore.

The data presented in Chapter 5 showed that expression of a dominant-negative mutant of the *'aa'* splice variant of dynamin-2 did not inhibit BTV-1 entry or infection in BHK cells, suggesting that entry and infection is dynamin-independent. However, the data presented above shows that treatment of BHK cells with dynasore inhibits entry of BTV-1, suggesting that the entry mechanism is dependent on a form of dynamin that is not inhibited by the dominant-negative mutant of the '*aa*' splice variant of dynamin-2. This differential sensitivity of BTV-1 entry by BHK cells to inhibition by dynasore and a dominant-negative mutant of the *'aa'* splice variant of dynamin-2 are shared by macropinocytosis/fluid-phase entry.

The above studies suggest that the dominant-negative mutant of the *'aa'* splice variant of dynamin-2 would not inhibit entry of dextran. Therefore, to determine if expression of Dn Dynamin-2 inhibited macropinocytosis/fluid-phase entry mechanisms in BHK cells, the effect of expression of this mutant on dextran entry was studied.

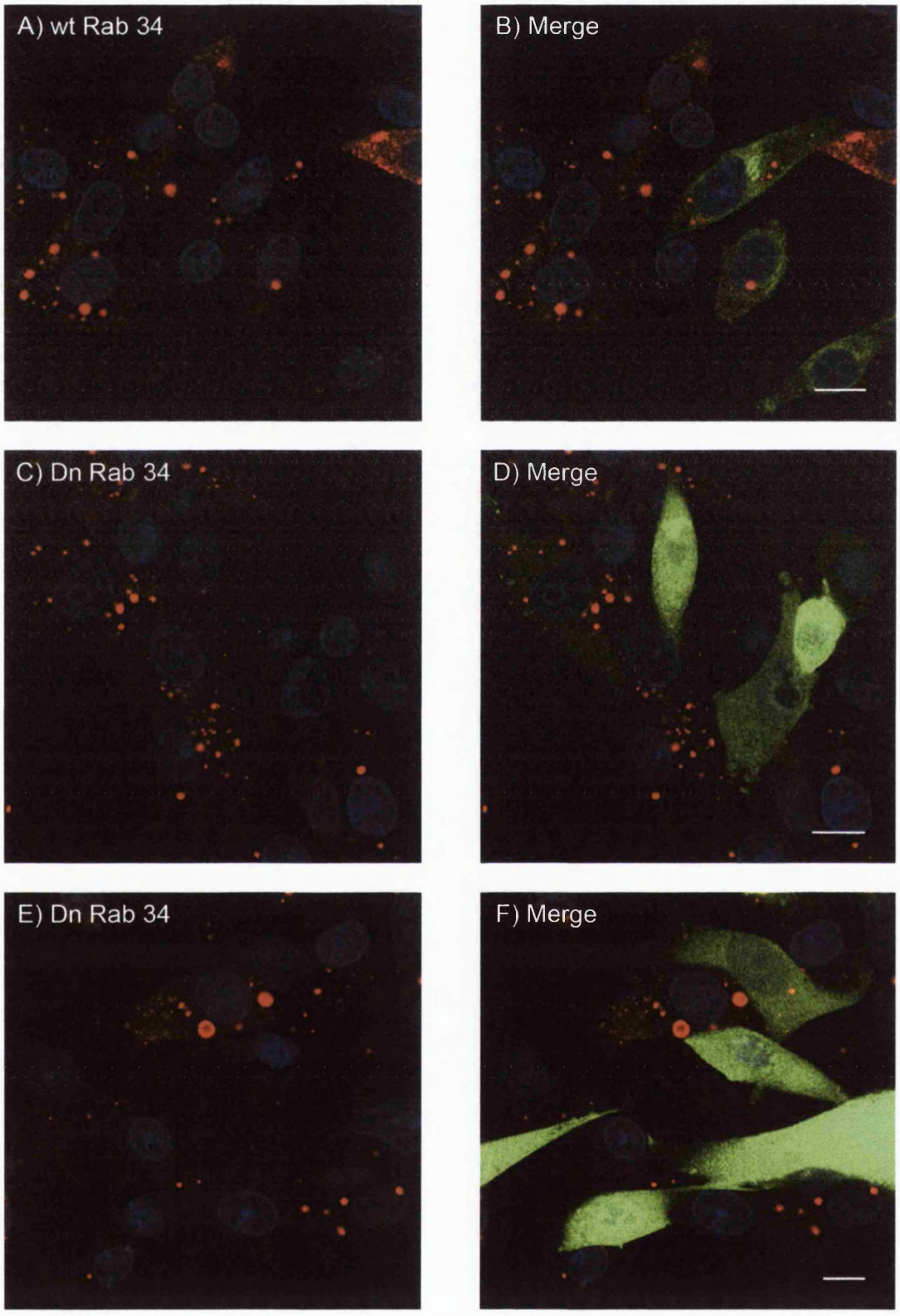

Figure 7.11: Expression of Dn Rab 34 inhibits BTV-1 infection of BHK cells (I)
BHK cells were transfected to express wt (A) and (B) or Dn Rab 34 (C-F) for 12 h and then infected with BTV-1 (m.o.i. = 0.5). Wt and Dn Rab 34 expressing cells are shown as green. Infected cells were identified by labelling with Orab 1 (anti-NS2) and are shown as red. Panels (B), (D) and (F) show merged images for red and green fluorescence. The cell nuclei are shown as blue. Scale bar = 10 μm.

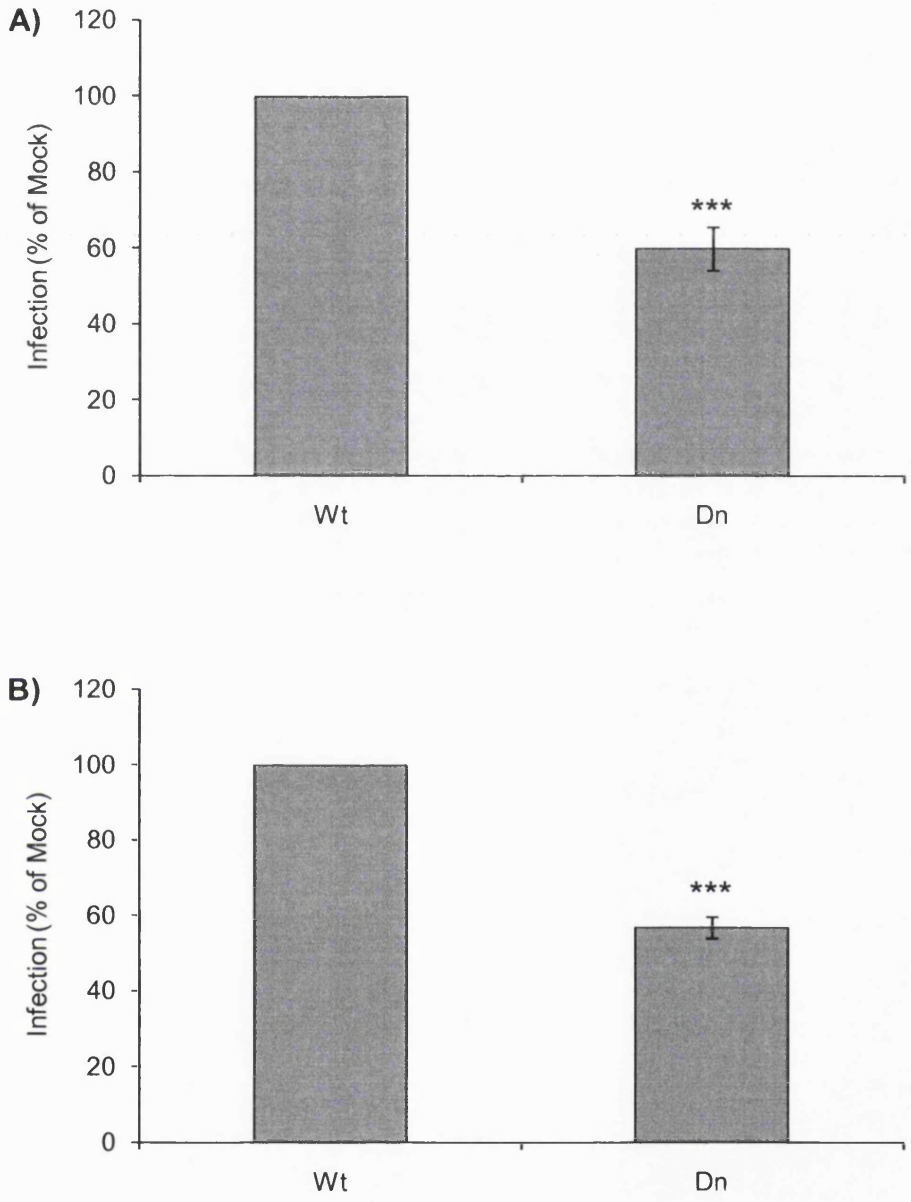

Figure 7.12: Expression of Dn Rab 34 inhibits BTV-1 infection of BHK cells (II)
BHK cells were transfected to express wt or Dn Rab 34 and infected with BTV-1 (see Figure 7.11). The cells expressing wt or Dn Rab 34 cells were scored for the presence of NS2 by confocal microscopy (n ≥150 cells). The frequency of NS2 labelling for cells expressing Dn Rab 34 was normalised to NS2 labelling for the cells expressing the wt protein. The mean and standard deviation of triplicate samples is shown for two independent experiments (A) and (B) (*P* values: *** <0.001).

BHK cells were transfected to express wt or Dn Dynamin-2 (see Chapter 5). At 12 hours post-transfection, the cells were allowed to internalise 568-Alexa labelled dextran (shown as red on Figure 7.14) for 30 minutes at 37°C. Transfected cells expressing wt or Dn Dynamin-2 were identified by the eGFP tag (shown as green). Figure 7.14, panels (B), (D) and (F) show merged images for red and green fluorescence for the same cells shown in panels (A), (C) and (E) respectively. Cells expressing wt Dynamin-2 (Figure 7.14, Panels A and B) showed normal entry of dextran that was indistinguishable from that seen in cells of the non-expressing population. Cells expressing Dn Dynamin-2 (Figure 7.14, Panels C-F) also showed normal entry of dextran as compared to cells expressing the wild type protein and cells of the non-expressing population. These observations confirm that expression of Dn Dynamin-2 does not inhibit fluid-phase entry mechanisms, and that BTV-1 entry is dependent on a form of dynamin, other than the *'aa'* splice variant of dynamin-2.

7.8 Conclusions

The results of this Chapter show that treatment of BHK cells with EIPA (an inhibitor of the N+/H+ exchanger) blocks entry of dextran and BTV-1, but not transferrin. These results add further support to the conclusion that BTV-1 infection of BHK cells is not dependent on clathrin-mediated endocytosis as virus (and not transferrin) enters BHK cells via an EIPA sensitive mechanism. EIPA is known to inhibit macropinocytosis/fluid-phase entry which suggests that BTV-1 could be using macropinocytosis or a similar entry mechanism for infection. This conclusion was supported by the data showing that BTV-1 infection of BHK cells is inhibited by disruption of the actin cytoskeleton and the observation that virus is co-localised with dextran (a marker for macropinocytosis) during entry, both characteristics of macropinocytosis. Expression of Dn Rab 34 was also shown to inhibit BTV-1 infection of BHK cells. As Rab 34 has been reported as a regulator of macropinocytosis in some

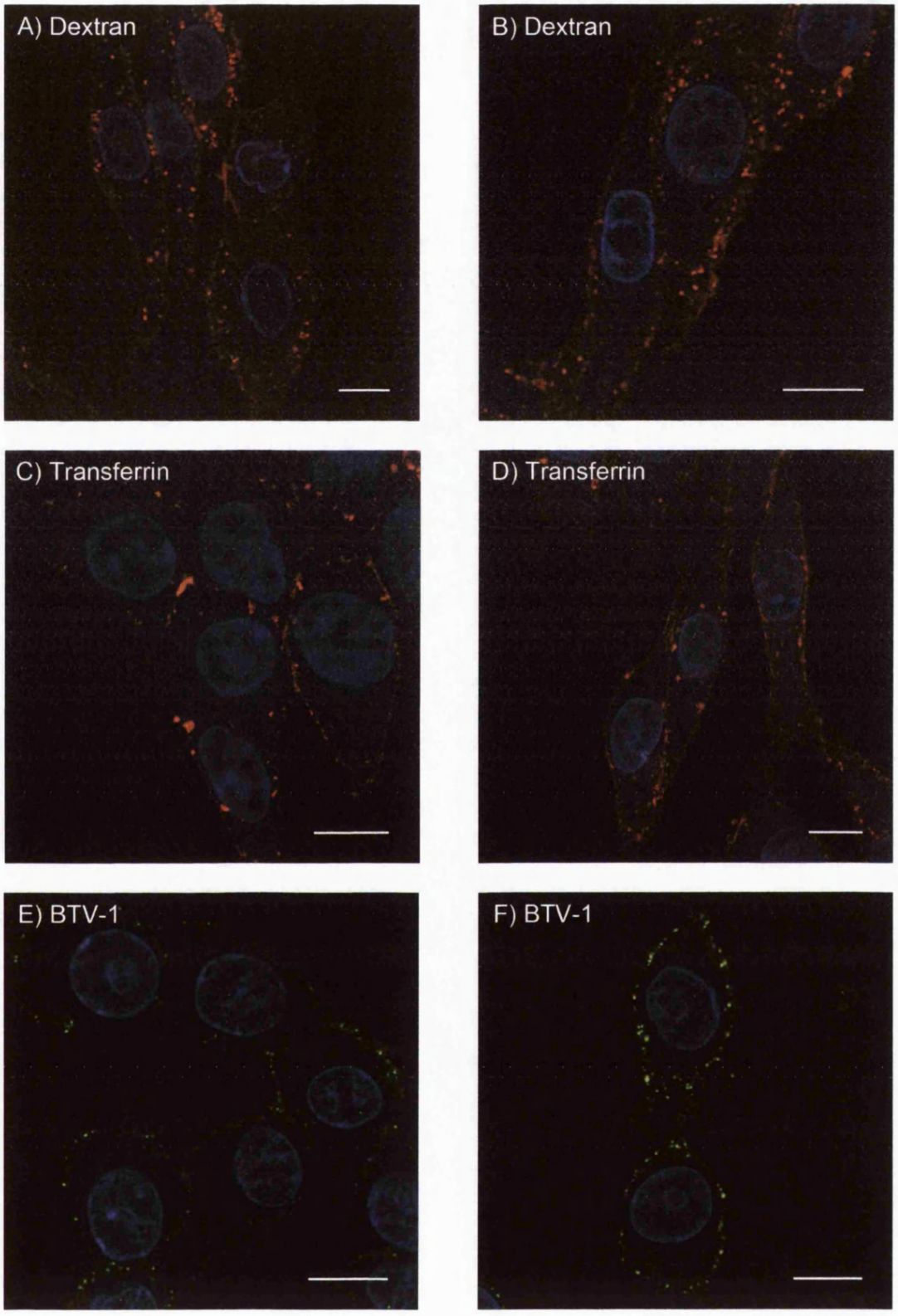

Figure 7.13: BTV-1, transferrin and dextran entry is blocked by dynasore
BHK cells were pre-treated with 100 μM dynasore for 30 min and then incubated at 37°C with 568-Alexa labelled dextran (5 mg/ml) (Panels A and B) or BTV-1 (Panels E and F) for 30 min, or with 568-Alexa labelled transferrin (25 μg/ml) (Panels C and D) for 15 min. Entry was stopped by the additon of 4% PFM (including 0.25% glutaraldehyde for transferrin) and the cells processed for confocal microscopy. Virus was detected using PM10 (anti-VP5) shown as green. Dextran and transferrin are shown as red. The cell nuclei are shown as blue. Scale bar = 10 μm.

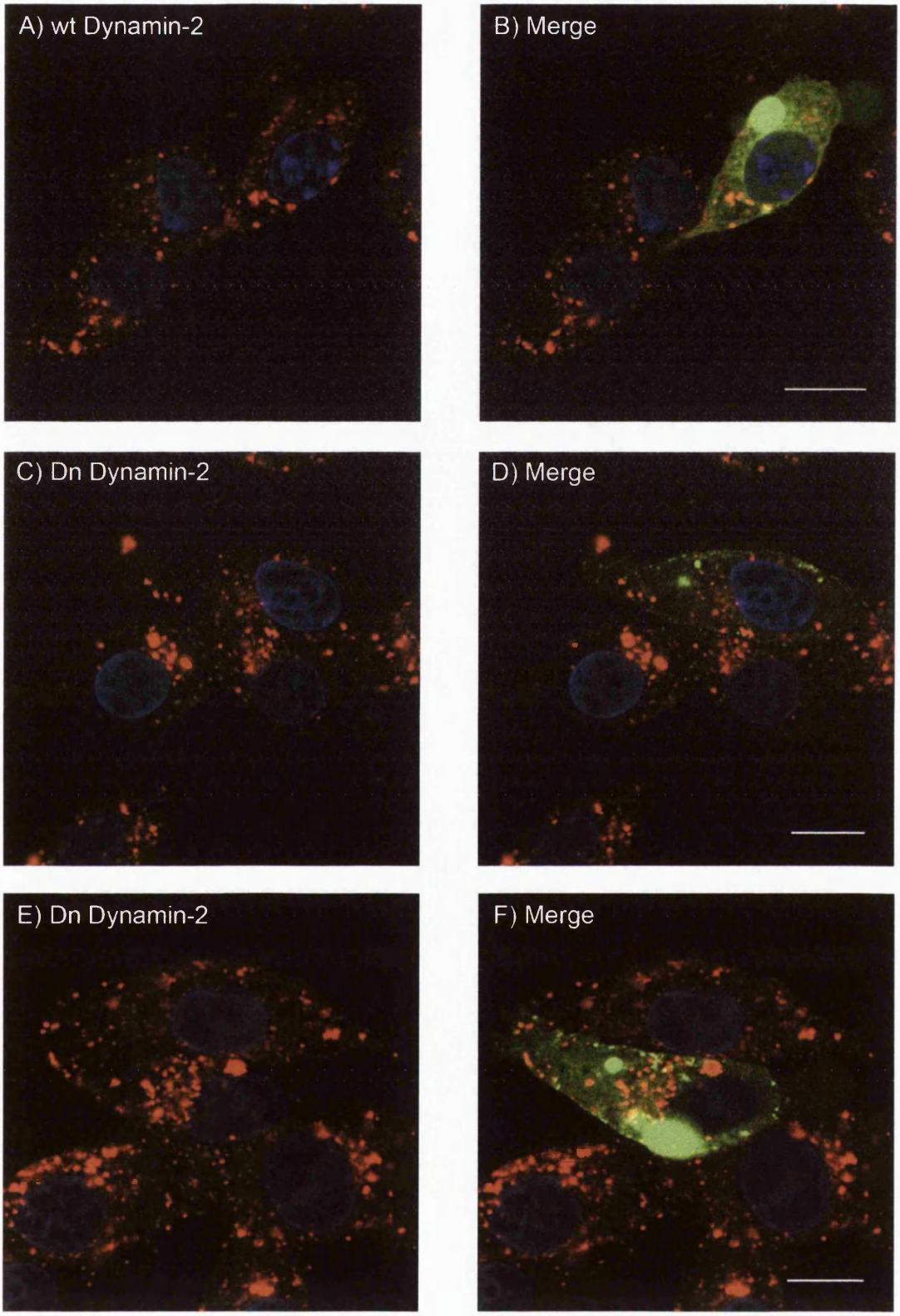

Figure 7.14: Expression of Dn Dynamin-2 does not inhibit entry of dextran
BHK cells were transfected to express either wt (A) and (B) or Dn Dynamin-2 (C-F) for 12 h and then incubated at 37°C with 568-Alexa labelled dextran (5 mg/ml) for 30 min. Entry was stopped by the addition of 4% PFM and the cells processed for confocal microscopy. Cells expressing wt or Dn Dynamin-2 are shown as green. Dextran is shown as red. The cell nuclei are shown as blue. Scale bar = 10 μm.

cell types, this observation also supports a macropinocytosis or macropinocytosis-like entry mechanism for BTV-1 entry.

The role of dynamin in macropinocytosis has not been clearly established. The results presented in this Chapter show that dynasore, an inhibitor of dynamin, blocked entry of BTV-1. These observations appear to contradict those made in Chapter 5 which show that a dominant-negative mutant of the *'aa'* splice variant of dynamin-2 did not inhibit BTV-1 entry or infection of BHK cells. This apparent discrepancy was explained by showing that dynasore also inhibited entry of dextran and transferrin whereas the above dominant-negative mutant only inhibited entry of transferrin (and not dextran). These observations are consistent with a recent study which showed that only dominant-negative mutants of the *'ba'* and *'bb'* splice variants of dynamin-2 inhibit macropinocytosis/fluid-phase entry, hence uptake of dextran (Cao et al., 2007). These results suggest that the BTV-1 BHK cell entry mechanism is dependent on a form of dynamin that is not inhibited by expression of the *'aa'* splice variant of dynamin-2, a characteristic also shared by macropinocytosis.

In summary, the co-localisation of virus with dextran during entry, the sensitivity of virus entry and infection to EIPA, actin disruption, expression of Dn-Rab34 and dynasore show that the BTV-1 BHK-cell entry mechanism shares many characteristics in common with macropinocytosis.

8 Analysis of BTV post-entry trafficking

8.1 Introduction

The results presented in the previous Chapters show that; (i) BTV-1 infection of BHK cells is clathrin-independent and occurs via an entry pathway that shares characteristics with macropinocytosis, and (ii) infection is dependent on the prevailing low pH within acidic endosomes. Macropinosomes can deliver cargo to acidic endosomes (Hamasaki et al., 2004). In some cell types, they fuse with lysosomes while in others they recycle their contents back to the extracellular space, most likely via early- and recycling-endosomes (Jones, 2007; Racoosin and Swanson, 1993).

The experiments undertaken in this Chapter investigated the BTV-1 post-entry intracellular virus trafficking itinerary, using co-localisation of virus with 568-Alexa labelled transferrin to label early- and recycling-endosomes, and with a monoclonal antibody (Mab 4A1) to LAMP-1, to label LAMP-positive late-endosomes and lysosomes.

8.2 BTV-1 does not Co-localise with Early- or Recycling-Endosomes

Initially BTV-1 trafficking to early- and recycling-endosomes was investigated. BTV-1 (13 µg/ml) was bound to BHK cells for 40 minutes on ice, unbound virus removed by washing and entry initiated by the addition of warm medium (37°C) (see Method 2.6.8). Virus was internalised for 15, 30, 60, 90 and 120 minutes. Fifteen minutes before the cells were fixed; 568-Alexa labelled transferrin (25 µg/ml) was added to the culture medium to label early- and recycling-endosomes. Virus and transferrin internalisation was stopped by the addition of cold 4% paraformaldehyde including 0.25% glutaraldehdye. The cells were then permeablised with 0.1% Triton X-100 and processed for confocal microscopy using PM10 and a goat, anti-Guinea pig Alexa-fluor 488-conjugated secondary antibody to detect input virus.

Figures 8.1 to 8.5 show representative images for each time point. Each figure shows two representative images; panels (A) and (B) show transferrin (shown as red); panels (C) and (D) show virus (shown as green) for the same cells whereas panels (E) and (F) show merged images for red and green fluorescence. Figure 8.1 shows images representative of 15 minutes virus and transferrin co-entry; no co-localisation was seen and the majority of the virus was located at the cell surface (as seen in Chapter 3, Figure 3.2). In contrast, transferrin had entered the cells suggesting that transferrin and BTV-1 are taken up with different kinetics. Similarly, virtually no co-localisation of virus with transferrin was seen at any of the other time points investigated (30 minutes: Figure 8.2, 60 minutes: Figure 8.3, 90 minutes: Figure 8.4 and 120 minutes: Figure 8.5). These results show that during the first 120 minutes of entry, virus is not delivered to transferrin positive endosomes (i.e. early- and recycling-endosomes) further supporting the conclusion that BTV-1 entry is clathrin-independent.

8.3 BTV-1 Co-localises with Late-Endosomes or Lysosomes

BTV-1 trafficking to late-endosomes and lysosomes was also investigated. BTV-1 was bound to BHK cells and internalised for 15, 30, 60, 90 and 120 minutes as described above but without the addition of transferrin. Virus internalisation was stopped and the cells fixed by the addition of ice cold 4% paraformaldehyde. The cells were dual labelled for input virus with PM10 and a goat, anti-Guinea pig Alexa-fluor 488-conjugated secondary antibody, and late-endosomes or lysosomes using an antibody for LAMP-1, (Mab 4A1) and a goat, anti-Mouse IgG Alexa-fluor 488-conjugated secondary antibody. For this experiment the cells were permeablised with 0.5% Saponin (in place of 0.1% Triton X-100) for 15 minutes and 0.1% Saponin was included in all subsequent steps. The specificity of the secondary antibodies for their target species of primary antibody was confirmed by showing a lack of cross-reactivity to non-target species of primary antibodies (see Method 2.6.4).

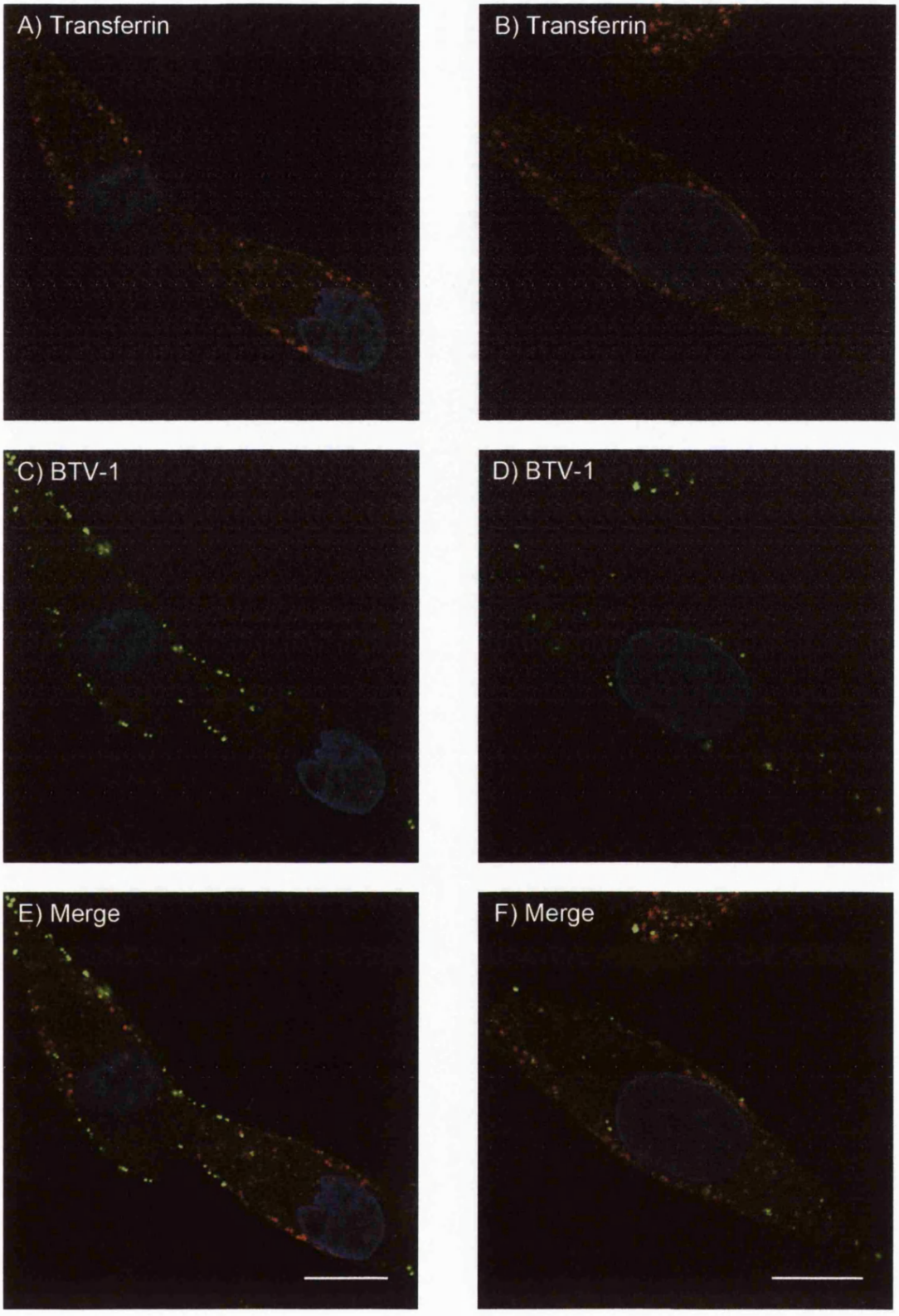

Figure 8.1: BTV-1 is not delivered to early-endosomes (15 minutes)
BTV-1 was pre-bound to BHK cells for 40 min on ice. Entry was initiated by warming to 37°C in the presence of 568-Alexa labelled transferrin (25 μg/ml). After 15 min, entry was stopped and the cells fixed by the addition of 4% PFM including 0.25% glutaraldehyde. Input virus was detected using PM10 (anti-VP5) and is shown as green (Panels C and D). Transferrin (Panels A and B) is shown as red. Panels (E) and (F) show merged images for red and green fluoresence. The cell nuclei are shown as blue. Scale bar = 10 μm.

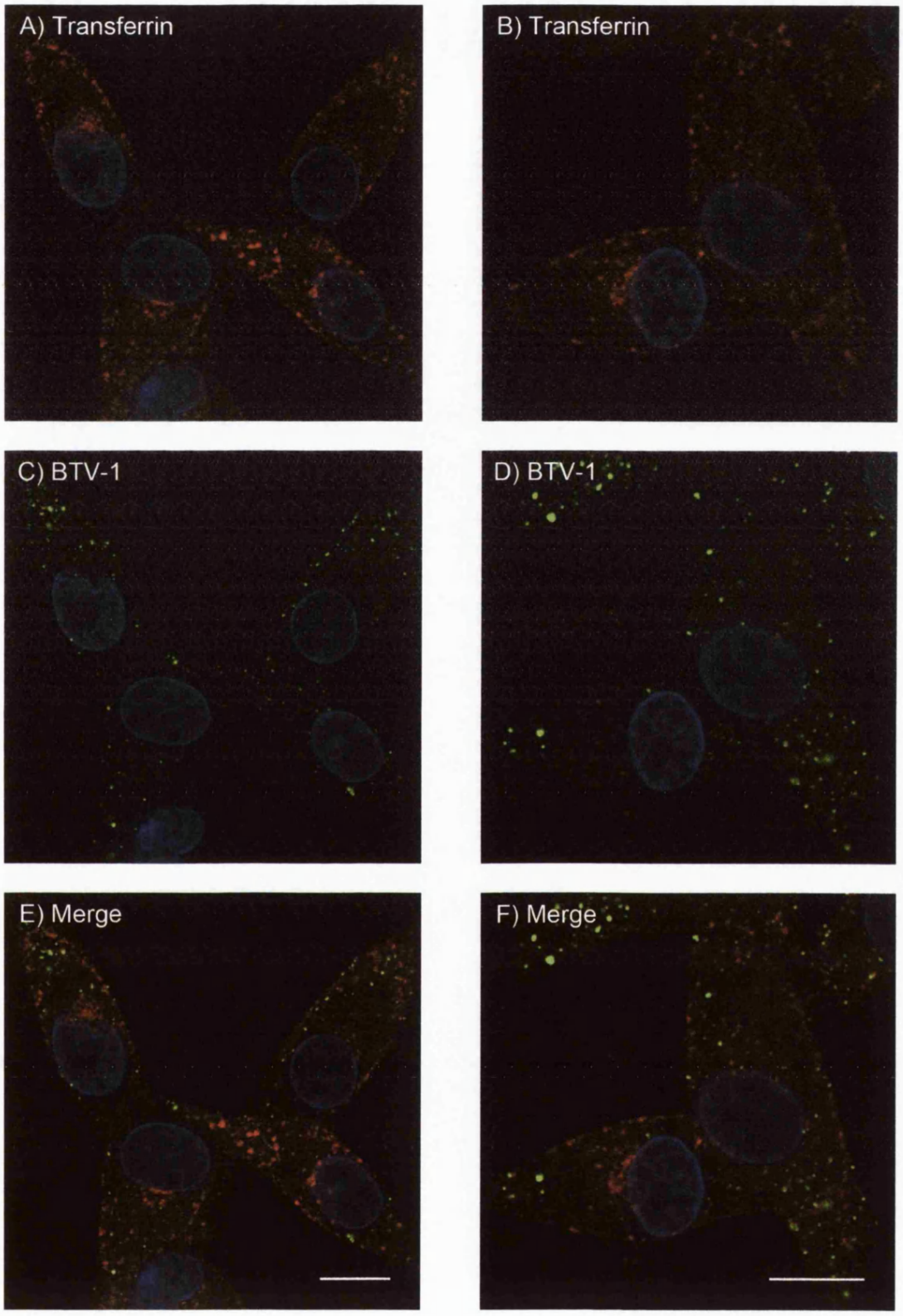

Figure 8.2: BTV-1 is not delivered to early-endosomes (30 minutes)
BTV-1 was pre-bound to BHK cells for 40 min on ice. Entry was initiated by warming to 37°C. After 30 min, entry was stopped and the cells fixed by the addition of 4% PFM including 0.25% glutaraldehyde. Input virus was detected using PM10 (anti-VP5) and is shown as green (Panels C and D). 15 min before the cells were fixed 568-Alexa labelled transferrin (25 μg/ml) (shown as red) was added to the cells to label early- and re-cycling endosomes (Panels A and B). Panels (E) and (F) show merged images for red and green fluoresence. The cell nuclei are shown as blue. Scale bar = 10 μm.

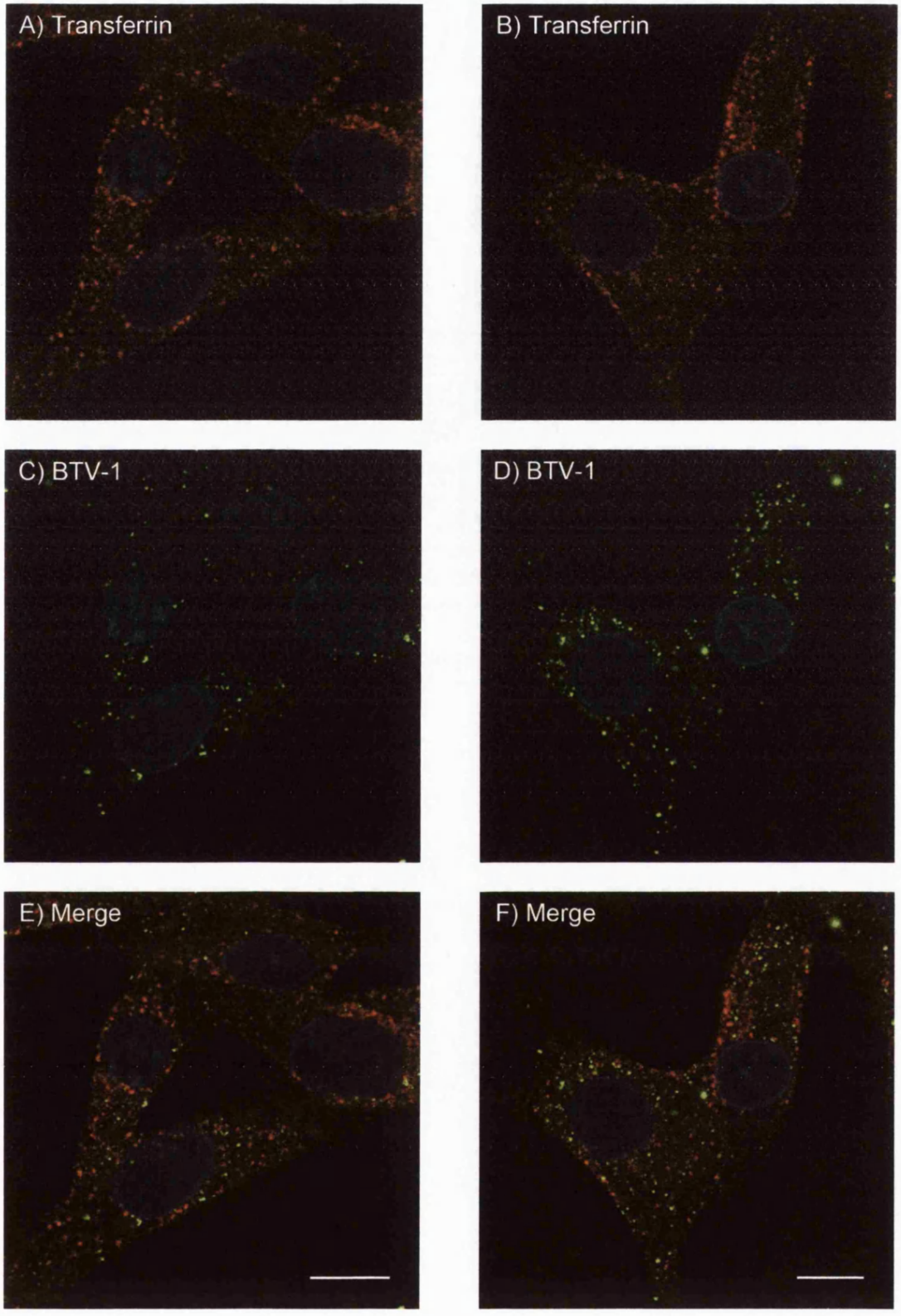

Figure 8.3: BTV-1 is not delivered to early-endosomes (60 minutes)
BTV-1 was pre-bound to BHK cells for 40 min on ice. Entry was initiated by warming to 37°C. After 60 min, entry was stopped and the cells fixed by the addition of 4% PFM including 0.25% glutaraldehyde. Input virus was detected using PM10 (anti-VP5) and is shown as green (Panels C and D). 15 min before the cells were fixed 568-Alexa labelled transferrin (25 μg/ml) (shown as red) was added to the cells to label early- and re-cycling endosomes (Panels A and B). Panels (E) and (F) show merged images for red and green fluoresence. The cell nuclei are shown as blue. Scale bar = 10 μm.

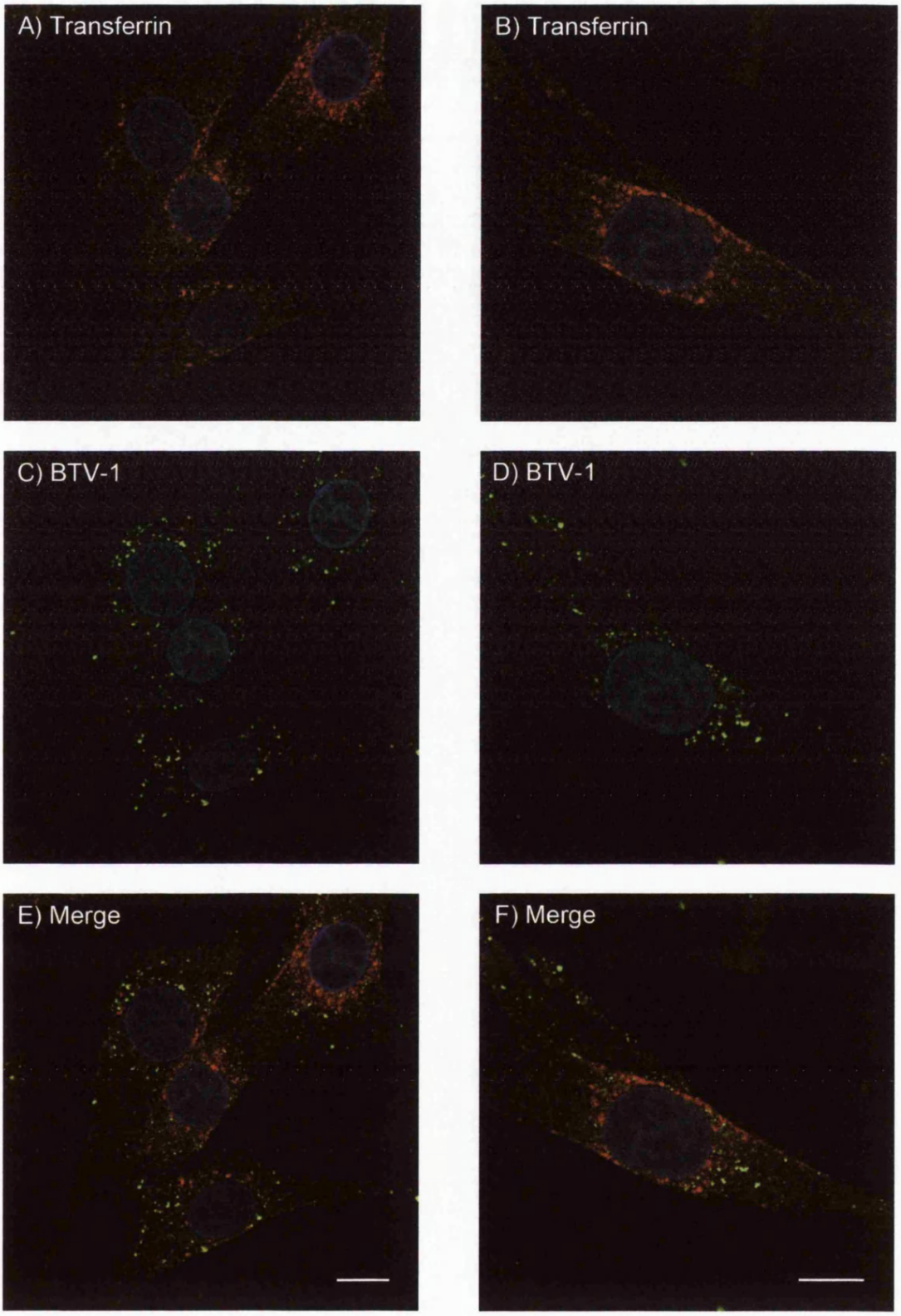

Figure 8.4: BTV-1 is not delivered to early-endosomes (90 minutes)
BTV-1 was pre-bound to BHK cells for 40 min on ice. Entry was initiated by warming to 37°C. After 90 min, entry was stopped and the cells fixed by the addition of 4% PFM including 0.25% glutaraldehyde. Input virus was detected using PM10 (anti-VP5) and is shown as green (Panels C and D). 15 min before the cells were fixed 568-Alexa labelled transferrin (25 μg/ml) (shown as red) was added to the cells to label early- and re-cycling endosomes (Panels A and B). Panels (E) and (F) show merged images for red and green fluoresence. The cell nuclei are shown as blue. Scale bar = 10 μm.

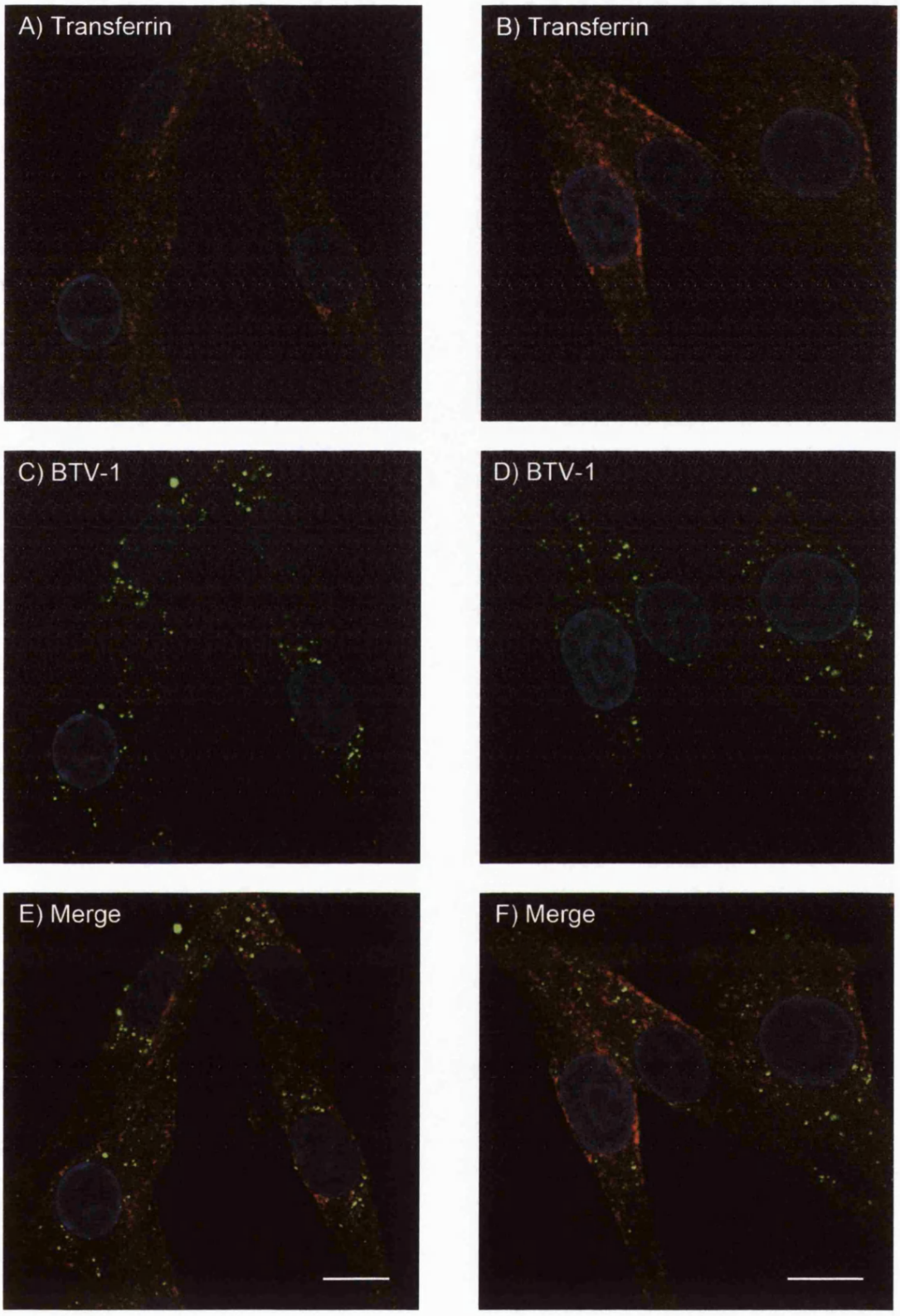

Figure 8.5: BTV-1 is not delivered to early-endosomes (120 minutes)
BTV-1 was pre-bound to BHK cells for 40 min on ice. Entry was initiated by warming to 37°C. After 120 min, entry was stopped and the cells fixed by the addition of 4% PFM including 0.25% glutaraldehyde. Input virus was detected using PM10 (anti-VP5) and is shown as green (Panels C and D). 15 min before the cells were fixed 568-Alexa labelled transferrin (25 μg/ml) (shown as red) was added to the cells to label early- and re-cycling endosomes (Panels A and B). Panels (E) and (F) show merged images for red and green fluoresence. The cell nuclei are shown as blue. Scale bar = 10 μm.

Figures 8.6 to 8.10 show representative images for each time point. On each figure panels (A) and (B) show labelling for LAMP-1 (shown as red); panels (C) and (D) show labelling for BTV-1 (shown as green) for the same cells, whereas panels (E) and (F) show merged images for red and green fluorescence.

Figure 8.6 shows images representative of 15 minutes post-entry. At this time point virtually no co-localisation was seen between virus and LAMP-1. At 30 minutes post-entry approximately 34% of the internalised virus (Virus particles [BTV-positive fluorescent green spots], n = 191) was co localised with LAMP-1 (as indicated by yellow fluorescence in the merged images; Figure 8.7, Panels E and F). A similar amount of co-localisation was seen between virus and LAMP-1 at 60 minutes (Figure 8.8) and at 90 minutes post-entry (Figure 8.9). By 120 minutes post-entry, approximately 54% of the internalised virus (Virus particles, n = 175) was co-localised with LAMP-1. This corresponds with the data showing that BTV-1 is delivered to acidic compartments with a $t_{1/2}$ of approximately 120 minutes (see Chapter 4, Figures 4.7 and 4.8)

8.4 Conclusion

The results presented in this Chapter show that BTV-1 does not co-localise with transferrin during the first 120 minutes of entry, indicating that the virus does not enter early- or recycling-endosomes. These observations add further support to a clathrin-independent entry mechanism. However, BTV-1 was seen to co-localise with LAMP-1 positive compartments from ~30 minutes post-entry. The extent of virus co-localisation with LAMP-1 appeared to increase during entry and by 2 hours approximately half of the virus was co-localised with LAMP-1. Thus the kinetics of virus delivery to LAMP-1 positive compartments appears to agree with the rate of virus transport to acidic endosomes (see Chapter 4).

Taken together, the above results show that the entry route used by BTV-1 to infect BHK cells appears to by-pass early-endosomes and delivers virus directly to

LAMP-1 positive compartments (late endosomes and/or lysosomes). This is consistent with acid-induced virus uncoating and core-particle membrane-penetration (i.e. infection) taking place from within late-endosomes or lysosomes. However, it is possible that virus is exposed to a low pH before it is delivered to LAMP-1 positive compartments and it cannot yet be stated with certainty that late-endosomes and/or lysosomes are directly involved in infection. The identification of the precise site of and mechanisms of infection requires further study (see Chapter 10).

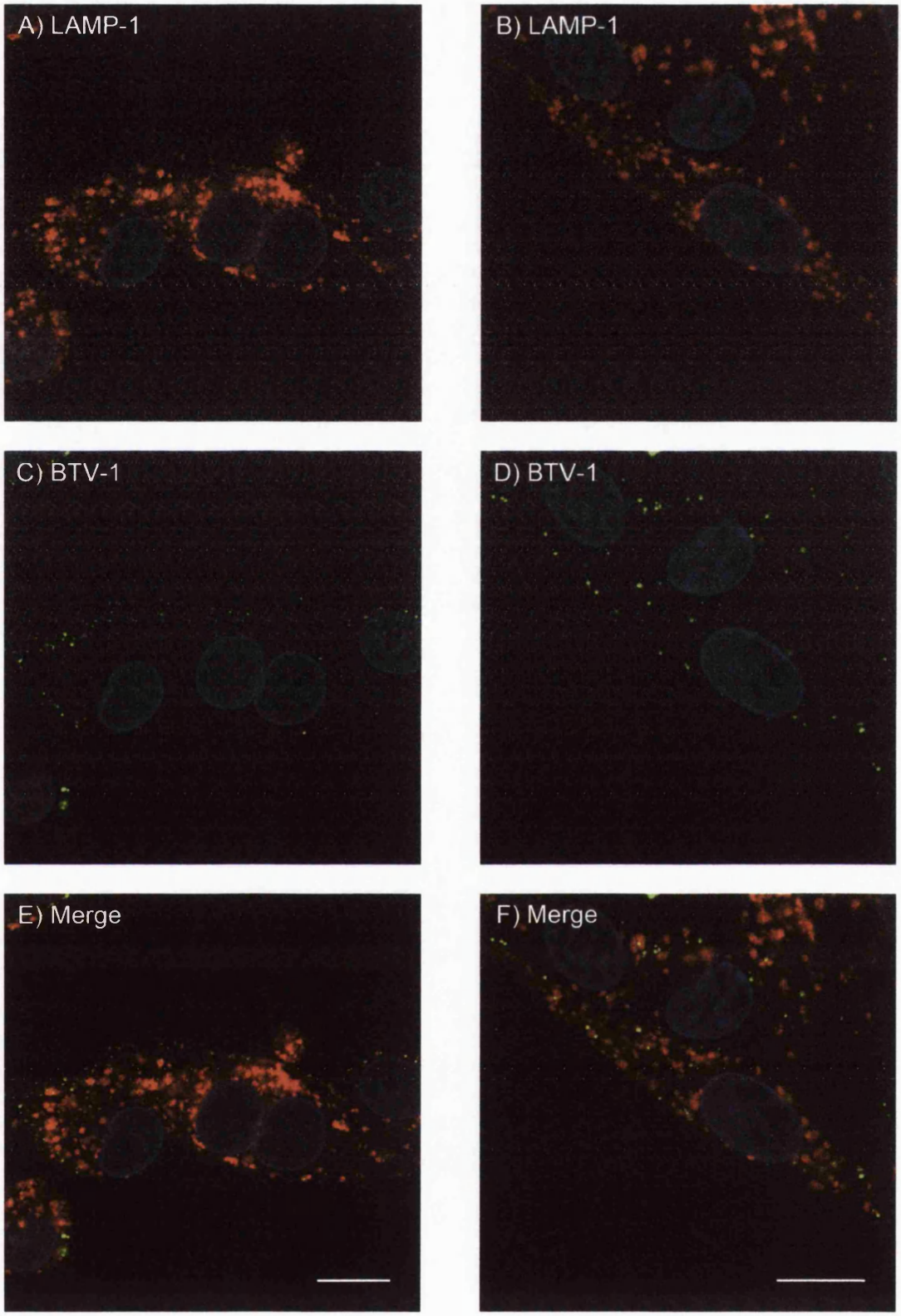

Figure 8.6: BTV-1 is delivered to late-endosomes (15 minutes)
BTV-1 was pre-bound to BHK cells for 40 min on ice. Entry was initiated by warming to 37°C. After 15 min, entry was stopped and the cells fixed by the addition of 4% PFM. Input virus was detected using PM10 (anti-VP5) and is shown as green (Panels C and D). The fixed cells were also labelled for LAMP-1 using Mab 4A1 (shown as red in panels A and B). Panels (E) and (F) show merged images for red and green fluoresence. The cell nuclei are shown as blue. Scale bar = 10 μm.

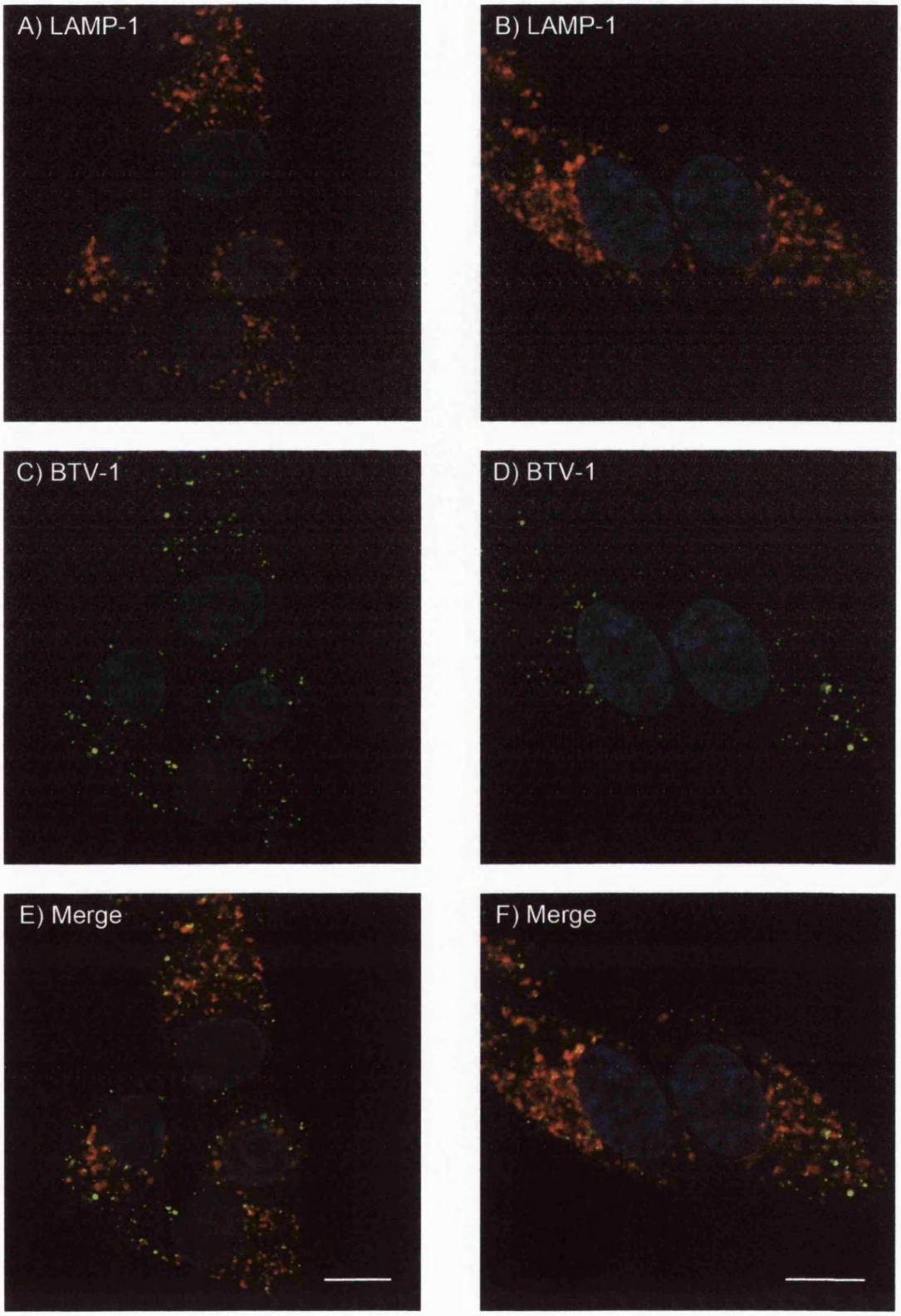

Figure 8.7: BTV-1 is delivered to late-endosomes (30 minutes)
BTV-1 was pre-bound to BHK cells for 40 min on ice. Entry was initiated by warming to 37°C. After 30 min, entry was stopped and the cells fixed by the addition of 4% PFM. Input virus was detected using PM10 (anti-VP5) and is shown as green (Panels C and D). The fixed cells were also labelled for LAMP-1 using Mab 4A1 (shown as red in panels A and B). Panels (E) and (F) show merged images for red and green fluoresence. The cell nuclei are shown as blue. Scale bar = 10 μm.

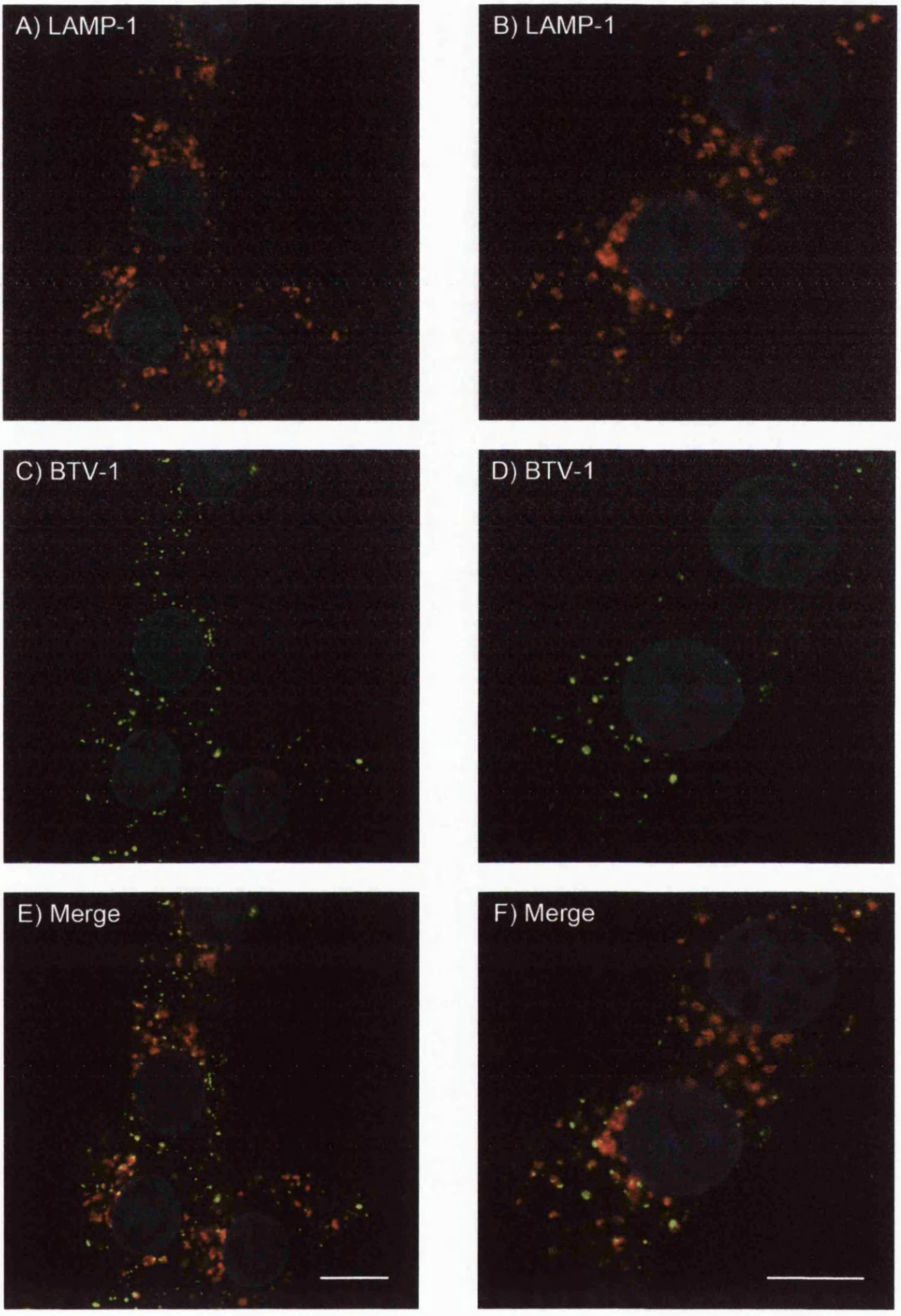

Figure 8.8: BTV-1 is delivered to late-endosomes (60 minutes)
BTV-1 was pre-bound to BHK cells for 40 min on ice. Entry was initiated by warming to 37°C. After 60 min, entry was stopped and the cells fixed by the addition of 4% PFM. Input virus was detected using PM10 (anti-VP5) and is shown as green (Panels C and D). The fixed cells were also labelled for LAMP-1 using Mab 4A1 (shown as red in panels A and B). Panels (E) and (F) show merged images for red and green fluoresence. The cell nuclei are shown as blue. Scale bar = 10 μm.

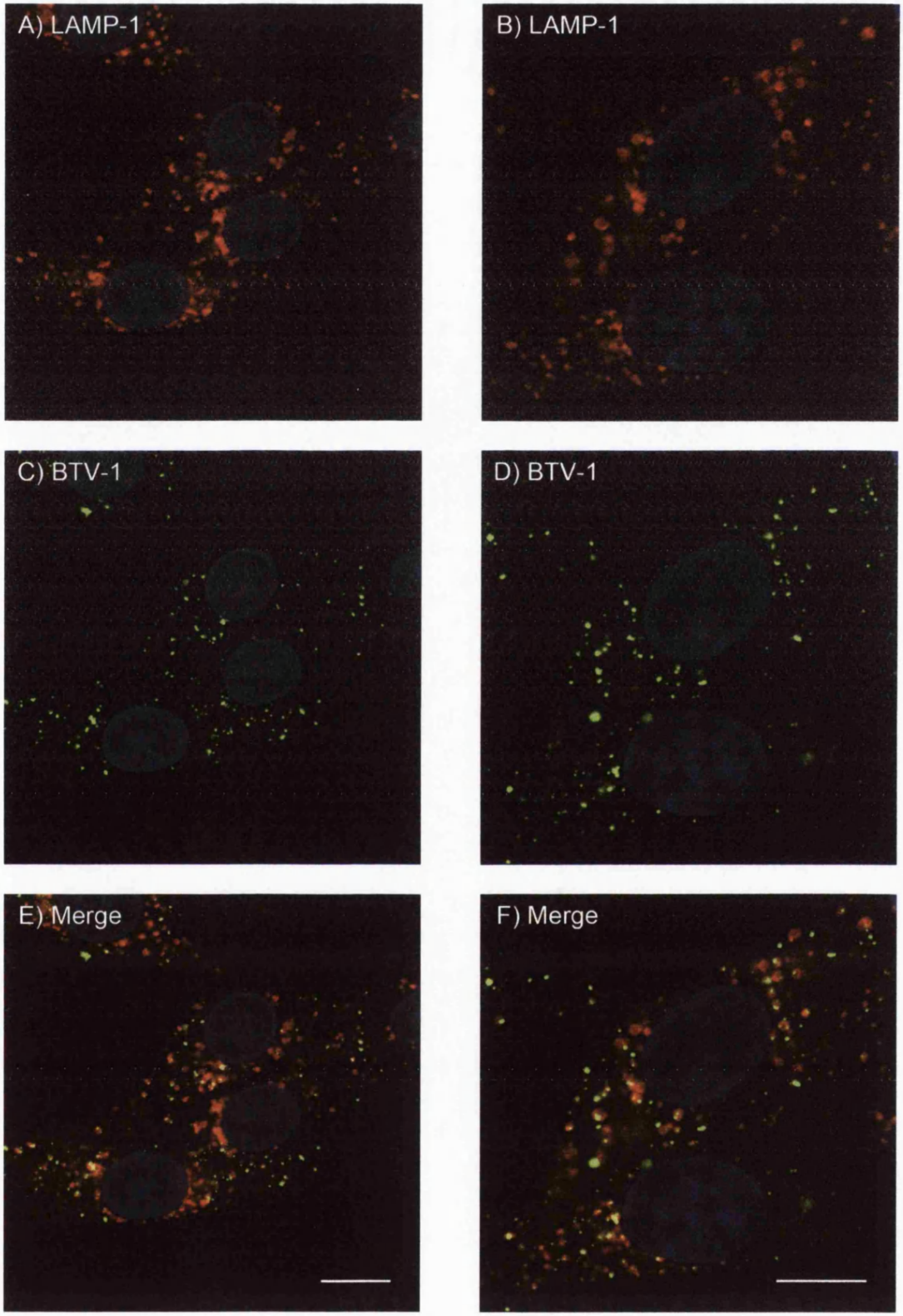

Figure 8.9: BTV-1 is delivered to late-endosomes (90 minutes)
BTV-1 was pre-bound to BHK cells for 40 min on ice. Entry was initiated by warming to 37°C. After 90 min, entry was stopped and the cells fixed by the addition of 4% PFM. Input virus was detected using PM10 (anti-VP5) and is shown as green (Panels C and D). The fixed cells were also labelled for LAMP-1 using Mab 4A1 (shown as red in panels A and B). Panels (E) and (F) show merged images for red and green fluoresence. The cell nuclei are shown as blue. Scale bar = 10 μm.

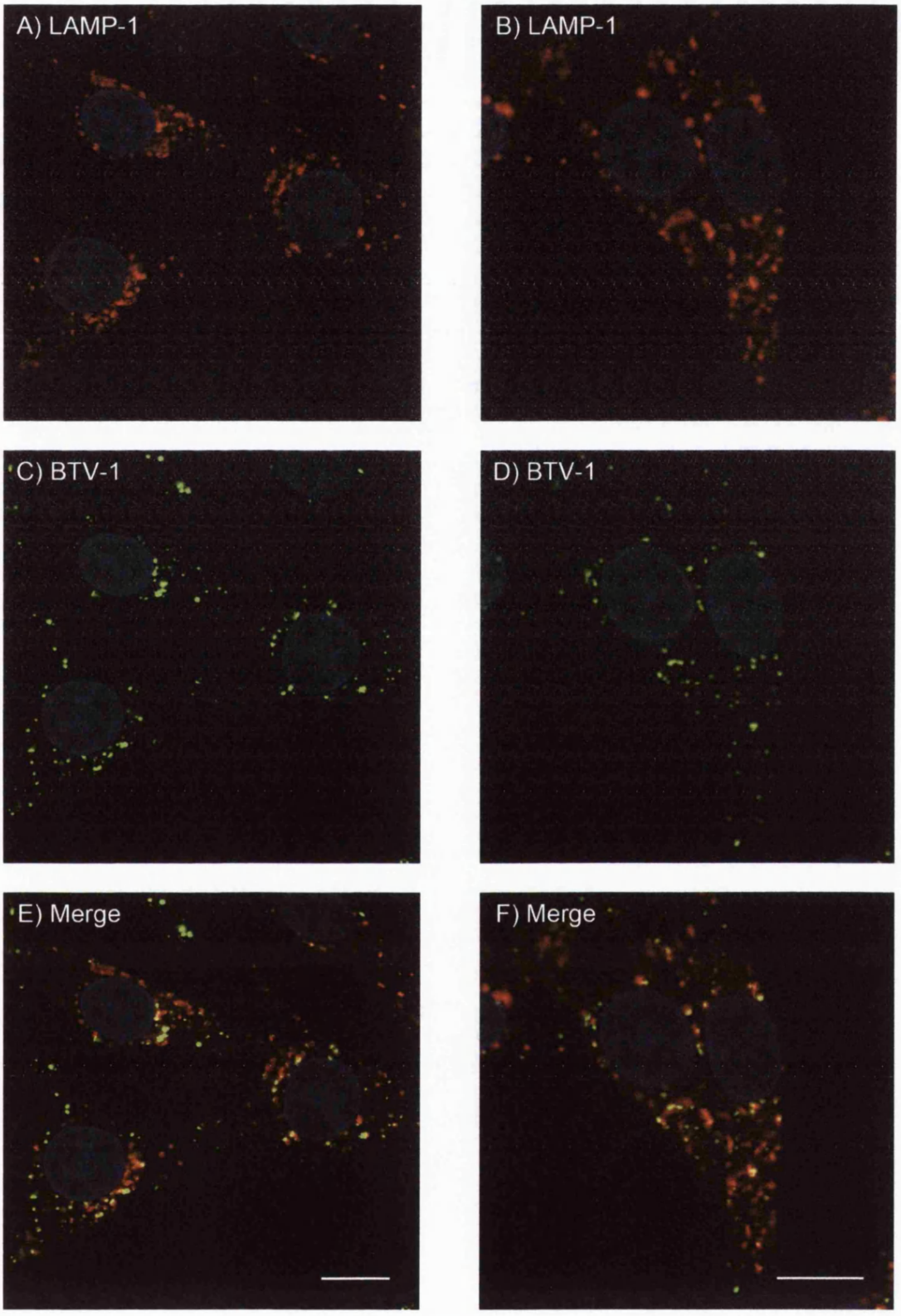

Figure 8.10: BTV-1 is delivered to late-endosomes (120 minutes)
BTV-1 was pre-bound to BHK cells for 40 min on ice. Entry was initiated by warming to 37°C. After 120 min, entry was stopped and the cells fixed by the addition of 4% PFM. Input virus was detected using PM10 (anti-VP5) and is shown as green (Panels C and D). The fixed cells were also labelled for LAMP-1 using Mab 4A1 (shown as red in panels A and B). Panels (E) and (F) show merged images for red and green fluoresence. The cell nuclei are shown as blue. Scale bar = 10 μm.

9 Discussion

The aims of this Thesis were to gain a better understanding of the mechanism of endocytosis used by BTV to enter and infect mammalian cells; and to map the intracellular trafficking pathway of the viral particle through the cell. To achieve this objective the effects of pharmacological and dominant-negative inhibitors of specific endocytic pathways on BTV-1 entry and infection of a number of mammalian cell lines have been investigated.

Two methods to quantify BTV-1 infection at a low m.o.i. were successfully developed; an enzyme-linked immunospot assay and a confocal microscopy assay. These techniques have been useful tools in quantifying infection in the presence of pharmacological or dominant-negative inhibitors as they identify individual infected cells (see Chapter 3).

Bluetongue virus infection is acid activated and can be inhibited by raising endosomal pH using reagents such as concanamycin-A or ammonium chloride. Consistent with this, in a recent study Forzan *et al.* concluded that BTV-10 infection of Vero and Hela cells occurs via clathrin-mediated endocytosis, with capsid disassembly and membrane-penetration by the core-particle occurring from within early-endosomes (Forzan et al., 2007). In this thesis it was confirmed that active endosomal acidification is required for BTV-1 infection of BHK, Vero and BPAEC cells (see Figures 4.1 to 4.6). Using BHK cells it was shown that raising endosomal pH did not appear to inhibit expression of virus attachment receptors or subsequent virus entry (see Figures 4.9 to 4.11). Similarly post-entry virus replication was not influenced by raising endosomal pH (see Figures 4.7 and 4.8). These results are consistent with acid-induced membrane-penetration from within an acidic compartment.

The studies presented in this thesis identified a macropinocytosis-like entry pathway that is used by BTV-1 to infect mammalian cells. Previous studies have concluded that BTV-10 infects mammalian cells by clathrin-mediated endocytosis

(Forzan et al., 2007). Hence, BTV appears to be able to use more than one endocytosis pathway for infection. The pathways used for infection may be determined by virus serotype (My study used BTV-1 and Forzan *et al.* used BTV-10), or may vary with cell type. The studies described in this thesis were for the first part carried out in BHK, BPAEC and Vero cells, whilst the studies by Forzan *et al.* were carried out using two cell lines; HeLa for studies with siRNA and Vero for studies with pharmacological inhibitors.

In both studies, the requirement for low pH was investigated and the results confirmed the requirement for acid induced infection. In this thesis concanamycin-A and ammonium chloride were used, whilst Forzan *et al.* used bafilomycin, all of which are commonly used reagents for raising endosomal pH. The two studies also agree that lipid rafts are not required for BTV entry and infection by the use of nystatin and methyl-β-cyclodextrin.

The conclusion that BTV-10 uses the clathrin-mediated pathway for entry and infection were based on experiments showing that chlorpromazine (a pharmacological inhibitor of clathrin-mediated endocytosis that has been used extensively by others to demonstrate clathrin-mediated endocytosis of several viruses) inhibited BTV-10 infection of Vero cells. However, evidence to show chlorpromazine inhibited entry of transferrin (a marker of clathrin-mediated endocytosis) or virus was not shown. Similarly, the possible effect of chlorpromazine on post-entry virus replication was not investigated as the drug was left in contact throughout the entire experiment. I also used 25 µM chlorpromazine to inhibit BTV-1 infection of Vero and BHK cells. However, although chlorpromazine was found to inhibit BTV-1 infection, entry of transferrin into both cell lines was not inhibited at drug concentrations up to 100 µM, despite extended pre-treatment of the cells with the inhibitor for 1 hour at 37°C. The above observation made direct comparison between the chlorpromazine experiments difficult.

Forzan *et al.*, (Forzan et al., 2007), also showed that HeLa cells transfected with siRNAs targeted to the μ2 subunit of the clathrin-adaptor complex failed to internalise transferrin or support BTV-10 infection. However, virus binding to the transfected cells was not observed leading the authors to suggest that the failure to see infection could have resulted from a depletion of virus receptors from the cell membranes. Nevertheless it is highly likely that BTV can use clathrin-mediated endocytosis and a macropinocytosis-like entry mechanism and the factors that determine pathway selection have yet to be determined.

In contrast to the previous study by Forzan *et al.*, (Forzan et al., 2007) the data presented in this thesis strongly suggests that the clathrin-mediated pathway is not the major entry route used by BTV-1 for infection of BHK cells. This conclusion is based on a number of key observations. Firstly, BTV-1 entry into BHK cells was not inhibited by expression of three different dominant-negative inhibitors of clathrin-mediated endocytosis; Dn Eps15 (see Figures 4.12 to 4.14), AP180C (see Figures 4.15 and 4.16), and Dn Dynamin-2 (see Figures 5.2 and 5.3). Similarly infection of BHK cells was not inhibited by expression of AP180C (see Figures 4.17 and 4.18), or Dn Dynamin-2 (see Figures 5.4 and 5.5). Secondly, during the first 2 hours of entry into BHK cells, BTV-1 co-localisation with transferrin (a commonly used marker for clathrin-mediated endocytosis) was not seen at any time point investigated (see Figures 8.1 to 8.5). This data again strongly suggests that for entry of BTV-1 into BHK cells, clathrin-mediated endocytosis is not the major entry pathway and that early-endosomes are not the compartment from which membrane-penetration occurs. Finally, although a low endosomal pH was found to be essential for infection, the kinetics of BTV-1 entry to acidic compartments showed a $t_{1/2}$ of ~2 hours (see Figures 4.7 and 4.8), which is considerably slower than expected for entry by the clathrin pathway (Ehrlich et al., 2004).

BTV-1 infection of BHK cells is not inhibited by Dn Dynamin-2 suggesting that other endocytosis pathways dependent on dynamin such as the caveolae pathway are

not used. Expression of Dn Caveolin-1 (see Figures 6.6 and 6.7) also did not inhibit BTV-1 infection, thus supporting the conclusion that caveolae-mediated endocytosis is not required for infection. However, due to the lack of a control ligand to show that caveolae-mediated endocytosis had been inhibited in BHK cells, the results obtained using Dn Caveolin-1 must be regarded as preliminary.

As well as caveolin-1, the caveolae-mediated pathway is dependent on lipid rafts and cholesterol. A number of non-caveolae entry pathways also originate from lipid rafts. BHK cells treated with Methyl-β-Cyclodextrin and labelled with filipin III were shown to have greatly reduced plasma membrane fluorescence indicating that cholesterol had been efficiently and selectively extracted from the plasma membrane (see Figure 6.1). Under the same conditions Methyl-β-Cyclodextrin treatment did not block BTV-1 infection of BHK or Vero cells (see Figures 6.2 to 6.4). Similarly, treatment of cells with nystatin and progesterone, which is known to inhibit cholesterol dependent endocytosis, did not inhibit infection of BHK cells (see Figure 6.5). Together, these observations indicate that cholesterol-dependent endocytosis pathways are unlikely to be used for BTV-1 entry and also support the conclusion that the caveolae-mediated pathway is not used. These observations are in agreement with previously published work using nystatin which was shown not to inhibit infection of Vero cells by BTV-10 (Forzan et al., 2007).

The majority of acid-activated viruses are taken up by 'classical' clathrin-mediated endocytosis and delivered to early-endosomes and/or late-endosomes where membrane-penetration occurs (see Section 1.5.1) (Marsh and Helenius, 2006). The observation that BTV-1 infection requires active endosomal acidification but not clathrin-mediated endocytosis suggests that virus particles are delivered to acidic compartments via an alternative 'non-clathrin' route. One possible alternative entry pathway is the CLIC/GEEC (CLathrin Independent Carriers/GPI-AP Enriched Endocytic Compartments) pathway (see Section 1.5.2.2.1). This pathway can deliver cargo to acidic vesicles (GEECs) which can then fuse with early- and recycling-endosomes

thereby further exposing their contents to a low pH environment (Chadda et al., 2007; Chatterjee and Mayor, 2001; Kalia et al., 2006; Sabharanjak et al., 2002). However the CLIC/GEEC pathway is highly sensitive to cholesterol depletion (Sabharanjak et al., 2002). Here I have shown that treatment with Methyl-β-Cyclodextrin did not inhibit BTV-1 infection of BHK cells (see Figures 6.2 and 6.3). Therefore it is highly unlikely that the CLIC/GEEC pathway mediates BTV-1 infection of BHK cells. Although cholesterol depletion did not inhibit BTV-1 infection of BHK cells, in some experiments the frequency of infection appeared to increase suggesting that when cholesterol dependent endocytosis is inhibited, BTV-1 infection may be more efficient (See Figures 6.2 and 6.4). One possible explanation for this phenomenon could be that the cell may compensate for the block to cholesterol sensitive pathways by up-regulating other endocytosis pathways, one of which may be used by BTV-1 for productive infection. Two pathways operate in mammalian cells for fluid-phase entry, namely macropinocytosis and the CLIC/GEEC pathway. It is unclear if macropinocytosis is sensitive to cholesterol depletion as results obtained for different cell types appear contradictory (see Section 1.5.2.3). If the CLIC/GEEC pathway is inhibited by cholesterol depletion this raises the possibility that macropinocytosis may be up-regulated to compensate for the reduction in fluid-phase entry and that macropinocytosis, or a macropinocytosis-like pathway may be used by BTV-1 to enter and infect BHK cells.

Recent studies have shown that vesicles that are derived from clathrin-independent pathways can fuse with early- or late-endosomes (Delaney et al., 2002; Naslavsky et al., 2003; Neumann-Giesen et al., 2007; Nishi and Saigo, 2007; Payne et al., 2007; Pelkmans et al., 2004; Sharma et al., 2003), and a number of viruses such as herpes simplex virus (Nishi and Saigo, 2007); human papillomavirus type 31 (Smith et al., 2008); SV40 (Pelkmans et al., 2004) and HIV (Vidricaire and Tremblay, 2007) have been shown to use such mechanisms for infection. This data presented in this thesis shows that BTV-1 does not appear to co-localise with early-endosomes during entry

into BHK cells as demonstrated by a lack of co-localisation with transferrin (see Figures 8.1 to 8.5). Transferrin and BTV-1 also appeared to have different entry kinetics; with BTV-1 being slower to enter BHK cells (see Figure 8.1). This data suggests that the entry mechanism used by BTV-1 is unlikely to involve a 'non-clathrin' entry pathway that merges with early-endosomes. Viruses can also use clathrin-independent entry pathways for delivery of cargo to late-endosomes. For example, lymphocytic choriomeningitis virus (LCMV) and kaposi's sarcoma associated herpesvirus (KSHV) are internalised by clathrin-independent mechanisms that result in virus delivery to late-endosomes without the involvement of early-endosomal compartments (Quirin et al., 2008; Raghu et al., 2009; Rojek et al., 2008a). The pathway described for LCMV entry appears distinct from that described here for BTV-1 in several ways including that LCMV entry and infection are not blocked by inhibitors of macropinocytosis. The entry route used by KSHV appears more similar to that described here for BTV-1 since it also shares characteristics of macropinocytosis; however, unlike BTV-1, entry of KSHV was shown not to be inhibited by dynasore and is dynamin-independent.

The data described in this Thesis strongly suggests that BTV-1 enters BHK cells via macropinocytosis or a macropinocytosis-like pathway. This conclusion is based on the data described above and also a number of other observations with pharmacological and dominant-negative inhibitors of macropinocytosis. EIPA, an inhibitor of the N^+/H^+ ion exchanger (see Section 1.5.2.3.1), inhibited entry of dextran, a marker for fluid phase uptake, and BTV-1 but not transferrin (see Figure 7.2). Two inhibitors of the actin cytoskeleton, cytochalasin D and latrunculin A, inhibited BTV-1 infection of BHK cells by 70 to 90% (see Figures 7.4 and 7.5). Dominant-negative Rab 34, which has been shown to inhibit macropinocytosis in 10T1/2 cells (Sun et al., 2003), inhibited BTV-1 infection of BHK cells by 40% as compared to the levels of infection seen in wt Rab 34 expressing cells (see Figures 7.11 and 7.12). BTV-1 was found to co-localise with dextran when they were co-internalised (see Figures 7.6 to 7.10). Dextran and virus were both observed at the cell periphery after 15 minutes of

entry, indicating similar entry kinetics. After 30 minutes of entry, approximately 40% of the internalised virus (BTV-1 particles, n = 100) were co-localised with dextran (see Figure 7.7).

On the basis of virus co-localisation with dextran, sensitivity to EIPA or actin disruption and inhibition of infection caused by expression of dominant-negative Rab 34, the BTV-1/BHK entry pathway appears to be most closely related to macropinocytosis (Mercer and Helenius, 2009). A number of other viruses have been shown to exploit macropinocytosis, or macropinocytosis-like endocytic pathways, for cell entry and infection including vaccinia virus (Huang et al., 2008; Locker et al., 2000; Mercer and Helenius, 2008), coxsackievirus B3 (Coyne et al., 2007), HIV (Marechal et al., 2001), KSHV (Raghu et al., 2009), echovirus 11 (Karjalainen et al., 2008; Liberali et al., 2008) and adenovirus type 3 (Amstutz et al., 2008). Adenoviruses type 2 also requires macropinocytosis for entry; however macropinocytosis is not used directly for virus entry but appears to enhance virus escape from early-endosomes (Meier et al., 2002).

The life of macropinosomes as separate organelles is believed to be relatively short and they can fuse with early-endosomes or with lysosomes (Hamasaki et al., 2004; Hewlett et al., 1994; Jones, 2007; Racoosin and Swanson, 1993). Macropinosomes have been shown to shrink after internalization and as a result they become acidified (Racoosin and Swanson, 1993; Swanson and Watts, 1995). This could provide the low pH environment required to trigger BTV-1 infection. However, acidification by this mechanism is unlikely to be required for BTV infection as it would not be inhibited by concanamycin-A.

The entry route used by BTV-1 to infect BHK cells appears to by-pass early-endosomes. However, despite not trafficking to early-endosomes, BTV-1 appeared to accumulate in late-endosomes or lysosomes during the first 2 hours of entry as shown by co-localisation with LAMP-1 (see Figures 8.6 to 8.10). The time dependent

appearance of virus in LAMP-1 compartments was similar to the kinetics of virus delivery to acidic compartments, as determined using concanamycin-A. These observations suggest that infection (i.e. acid induced membrane-penetration) occurs from within LAMP-1 positive late-endosomes or lysosomes. However, one cannot yet be certain that these compartments are directly involved in infection, as the intermediate steps in virus trafficking from the plasma membrane to LAMP-1 positive compartments are currently unknown, and it is possible that virus could be exposed to acid on transit to these LAMP-1 positive vesicles. The identification of the precise site of and mechanisms of infection requires further study.

The role of dynamin in clathrin- and caveolae-mediated endocytosis is clear and well established (see Section 1.5.1.1). In contrast the role of dynamin in macropinocytosis is unclear and studies investigating its role have given conflicting results (Cao et al., 2007; Huang et al., 2008; Meier et al., 2002; Mercer and Helenius, 2008; Schlunck et al., 2004). It has been suggested that these discrepancies could result, in part from the use of different methods to trigger macropinocytosis (Liu et al., 2008) and by the use of different approaches to inhibit dynamin (Cao et al., 2007; Ferguson et al., 2007; Liu et al., 2008; McNiven et al., 2000). Similarly, viruses that use macropinocytosis for infection display different sensitivities to dynamin inhibition (Huang et al., 2008; Mercer and Helenius, 2008). Dynamin is expressed in mammalian cells as three distinct isoforms, dynamin-1 to -3 (Cao et al., 2007), with each isoform existing as a number of alternative splice variants. The splice variants of dynamin-2 appear to differentially regulate endocytic processes (Cao et al., 2007). Dominant-negative mutants of each splice variant of dynamin-2 ('*aa*', '*ab*', '*ba*', and '*bb*') inhibit clathrin-mediated endocytosis whereas only two ('*ba*' and '*bb*') significantly inhibit entry of dextran, suggesting a role for the '*ba*' and '*bb*' splice variants in regulating fluid-phase entry or macropinocytosis. The data obtained showing that Dn Dynamin-2 does not inhibit BTV-1 entry or infection of BHK cells used the '*aa*' splice variant, known to inhibit clathrin-mediated endocytosis. This dominant-negative protein inhibited entry of

transferrin (see Figure 5.1) but did not inhibit entry of dextran (see Figure 7.14); indicating that macropinocytosis and fluid-phase entry is likely to remain active in BHK cells expressing this dominant-negative mutant. In contrast, entry of BTV-1, transferrin and dextran were inhibited by dynasore (see Figure 7.13). Since it is likely that dynasore inhibits all forms of dynamin, this observation suggests that the BHK/BTV-1 entry mechanism is dependent on a form of dynamin that is not inhibited by expression of the dominant-negative mutant of the '*aa*' splice variant of dynamin-2, further likening BTV-1 entry to macropinocytosis.

In conclusion, a pathway for BTV-1 entry and infection of BHK cells that is independent of clathrin, caveolae and cholesterol, but is dependent on a form of dynamin, delivers virus to LAMP-1 positive compartments (late-endosomes or lysosomes) directly without first passing through early-endosomes, and shares characteristics with macropinocytosis has been described in this Thesis.

The entry mechanism described for BTV-1 into BHK cells differs from the recent report investigating the BTV-10 entry pathway in Vero and HeLa cells (Forzan et al., 2007). Hence, BTV joins the increasing number of viruses that appear to be able to utilise more than one endocytic pathway for initiation of infection (Damm et al., 2005; Raghu et al., 2009; Rojek et al., 2008b; Sieczkarski and Whittaker, 2002; Suksanpaisan et al., 2009). BTV has a wide tropism *in vivo* and infects a variety of different cell types in its mammalian and insect hosts (see Section 1.2) (Maclachlan et al., 2009; Schwartz-Cornil et al., 2008). It is possible that this broad tropism and the requirement to replicate in evolutionary distant hosts results, in part from an ability to use multiple entry routes to initiate infection. Moreover, BTV can exist in at least three different forms that are all considered to be infectious (see Section 1.3.1). These include intact virus particles, infectious sub-viral particles, and core-particles (Mertens et al., 1996). These different particle types have different surface proteins, and may therefore also use different receptors and different entry mechanisms for infection (Mertens and Diprose, 2004).

The data obtained for this Thesis has provided some interesting insights into the BTV-1 cell entry pathway, however, the entry route(s) used by BTV to infect its natural target cells and the relevance of these pathways in the animal and insect hosts requires further study.

10 Future Work

10.1 Comparing the entry mechanisms of BTV-10 and BTV-1

The results presented in this Thesis have provided new insights into the entry mechanisms used by BTV for infection. The data indicates that BTV-1 entry into BHK cells is by macropinocytosis or a macropinocytosis-like pathway. These results differ from the previously published work using BTV-10 which concluded that entry into Vero and HeLa cells occurs via clathrin-mediated endocytosis (Forzan et al., 2007). Future studies to determine if these differences are the result of using different cell types or different virus serotypes would help clarify the infectious entry mechanisms of BTV.

10.2 Investigating Macropinocytosis

Sensitivity to Na+/H+ exchangers (such as EIPA) and actin disruption are not the only criteria to classify macropinocytosis (Mercer and Helenius, 2009). It would therefore be interesting to extend the research presented here to include other inhibitors of macropinocytosis.

BTV-1 cell entry could be further characterised in future experiments by studying the activity of kinases required by macropinocytosis. One such kinase is the p21-activated kinase (PAK1) (Dharmawardhane et al., 2000); which has been observed in membrane ruffles and is required for actin remodelling and macropinosome formation. PAK1 phosphorylates CtBP1/BARS (C-terminal-binding protein-1/Brefeldin A-ADP-ribosylated substrate) which is strongly implicated in the closure of macropinosomes (Mercer and Helenius, 2009). Transfection experiments using the PAK1 auto-inhibitory domain (AID), which functions as a dominant-negative inhibitor, and a dominant-negative mutant (D355A) of CtBP-1 could be performed to further determine the role of macropinocytosis in BTV entry and infection.

Macropinocytosis involves actin-dependent reorganisation of the plasma membrane (as blebbing, lamellipodial or circular ruffles) which subsequently close-up to form macropinosomes (Mercer and Helenius, 2009). Transmission electron

microscopy experiments on cells undertaking virus entry could be performed, to visualise the size, shape and coat structures of the virus containing vesicles.

10.3 Further Studies on the Role of Dynamin

The role of dynamin in macropinocytosis and BTV-1 entry remains to be fully understood. The Dn Dynamin-2 '*aa*' splice variant was shown to inhibit transferrin uptake but not entry of dextran or entry and infection of BHK cells by BTV-1 (see Chapter 5). However the dynamin inhibitor dynasore blocked entry of transferrin, dextran and BTV-1, suggesting that a form of dynamin is required (see Chapter 7). In mammalian cells, dynamin is expressed as 3 distinct isoforms: dynamin1-3, and each as a number of splice variants (Cao et al., 2007). To further define the role of dynamin in BTV-1 entry and infection, the experiments carried out for Dn Dynamin-2 '*aa*' could be repeated using dominant-negative versions of the '*ab*', *'ba'* and *'bb*' splice variants and with Dn Dynamin-3.

10.4 Intracellular Trafficking of BTV

BTV-1 was shown to co-localise with LAMP-1 positive compartments but not transferrin, suggesting that the cellular site of virus uncoating and membrane-penetration by the viral core-particle was from late-endosomes or lysosomes and not from early- or recycling-endosomes. Virus was also shown to co-localise with dextran, which is taken up by macropinocytosis and fluid-phase mechanisms, suggesting virus enters by a similar route.

The data presented however, does not definitively determine the site of capsid uncoating and membrane-penetration by the core-particle. To further investigate uncoating, mono-specific antibodies could be used to visualise the separation of the outer-capsid (VP5) and the core-particle (VP7) by confocal microscopy. To further improve the study of BTV endocytosis, the virus particle could also be directly labelled by direct conjugation to alexa dyes. This fluorescent virus-particle could be used in cell

entry experiments; to identify the site of virus disassembly and host-cell membrane-penetration, and to follow virus entry in real-time, in live-cells.

Cargo delivered to early-endosomes by clathrin-mediated endocytosis, may traffic to either recycling-endosomes or to late-endosomes (and lysosomes) whilst macropinosomes can also recycle their contents or deliver cargo directly to late-endosomes or lysosomes, by-passing early-endosomes on route (Hamasaki et al., 2004; Racoosin and Swanson, 1993). The involvement of early-, late- and recycling-endosomes in virus uncoating and infection could be further investigated using expression of Dn Rab 5 (to inhibit early-endosome fusions), Dn Rab 7 (to inhibit late-endosome fusions) or Dn Rab 4 and Dn Rab 11 (to inhibit recycling pathways) (Johns et al., 2009).

10.5 Expansion of the Studies using More Relevant Cell Types

The data presented in this Thesis and the previous study by Forzan *et al.* (Forzan et al., 2007) provide interesting and novel insights into BTV entry and infection but have limitations as the cell lines used are not the natural target cells infected in ruminants or insects (see Section 1.2). To reveal the entry pathway or pathways, utilised by BTV to enter more relevant cell types other mammalian cell lines could be studied such as the bovine aorta endothelial cells (BPAEC) used in Chapter 4. Similarly, the entry mechanisms into immune cells such as dendritic cells, or for the infection of insect cells could be studied.

10.6 Investigating BTV Virus Types

As BTV has been shown to have several different infectious particle types each with the potential for different entry mechanisms (see Sections 1.3.1.6 and 1.6); it would be interesting to investigate the entry mechanisms of ISVP and core-particles. These pathways could be determined using the same techniques and experiments outlined in this Thesis.

Publications

Gold, S., Monaghan, P., Mertens, P. and Jackson, T. (2010). A clathrin independent macropinocytosis-like entry mechanism used by bluetongue virus-1 during infection of BHK cells. PLoS One, Volume 5, Issue (6), e11360.

Bibliography

Abban, C.Y., Bradbury, N.A., and Meneses, P.I. (2008). HPV16 and BPV1 infection can be blocked by the dynamin inhibitor dynasore. Am J Ther *15*, 304-311.

Acosta, E.G., Castilla, V., and Damonte, E.B. (2009). Alternative infectious entry pathways for dengue virus serotypes into mammalian cells. Cell Microbiol *11*, 1533-1549.

Agosto, M.A., Ivanovic, T., and Nibert, M.L. (2006). Mammalian reovirus, a nonfusogenic nonenveloped virus, forms size-selective pores in a model membrane. Proc Natl Acad Sci U S A *103*, 16496-16501.

Allen, W.E., Jones, G.E., Pollard, J.W., and Ridley, A.J. (1997). Rho, Rac and Cdc42 regulate actin organization and cell adhesion in macrophages. J Cell Sci *110 (Pt 6)*, 707-720.

Allison, A.B., Goekjian, V.H., Potgieter, A.C., Wilson, W.C., Johnson, D.J., Mertens, P.P., and Stallknecht, D.E. (2010). Detection of a novel reassortant epizootic hemorrhagic disease virus (EHDV) in the USA containing RNA segments derived from both exotic (EHDV-6) and endemic (EHDV-2) serotypes. J Gen Virol *91*, 430-439.

Amstutz, B., Gastaldelli, M., Kalin, S., Imelli, N., Boucke, K., Wandeler, E., Mercer, J., Hemmi, S., and Greber, U.F. (2008). Subversion of CtBP1-controlled macropinocytosis by human adenovirus serotype 3. EMBO J *27*, 956-969.

Amyere, M., Mettlen, M., Van Der Smissen, P., Platek, A., Payrastre, B., Veithen, A., and Courtoy, P.J. (2002). Origin, originality, functions, subversions and molecular signalling of macropinocytosis. Int J Med Microbiol *291*, 487-494.

Amyere, M., Payrastre, B., Krause, U., Van Der Smissen, P., Veithen, A., and Courtoy, P.J. (2000). Constitutive macropinocytosis in oncogene-transformed fibroblasts depends on sequential permanent activation of phosphoinositide 3-kinase and phospholipase C. Mol Biol Cell *11*, 3453-3467.

Anderson, J., Mertens, P.P., and Hemiman, K.A. (1993). A competitive ELISA for the detection of anti-tubule antibodies using a monoclonal antibody against bluetongue virus non-structural protein NS1. J Virol Methods *43*, 167-175.

Araki, N., Hatae, T., Furukawa, A., and Swanson, J.A. (2003). Phosphoinositide-3-kinase-independent contractile activities associated with Fcgamma-receptor-mediated phagocytosis and macropinocytosis in macrophages. J Cell Sci *116*, 247-257.

Arias, C.F., Isa, P., Guerrero, C.A., Mendez, E., Zarate, S., Lopez, T., Espinosa, R., Romero, P., and Lopez, S. (2002). Molecular biology of rotavirus cell entry. Arch Med Res *33*, 356-361.

Arnaout, M.A., Goodman, S.L., and Xiong, J.P. (2002). Coming to grips with integrin binding to ligands. Curr Opin Cell Biol *14*, 641-651.

Baldet, T., Delecolle, J.C., Cetre-Sossah, C., Mathieu, B., Meiswinkel, R., and Gerbier, G. (2008). Indoor activity of Culicoides associated with livestock in the bluetongue virus (BTV) affected region of northern France during autumn 2006. Prev Vet Med *87*, 84-97.

Barratt-Boyes, S.M., Rossitto, P.V., Stott, J.L., and MacLachlan, N.J. (1992). Flow cytometric analysis of in vitro bluetongue virus infection of bovine blood mononuclear cells. J Gen Virol *73 (Pt 8)*, 1953-1960.

Barton, E.S., Forrest, J.C., Connolly, J.L., Chappell, J.D., Liu, Y., Schnell, F.J., Nusrat, A., Parkos, C.A., and Dermody, T.S. (2001). Junction adhesion molecule is a receptor for reovirus. Cell *104*, 441-451.

Bayer, N., Prchla, E., Schwab, M., Blaas, D., and Fuchs, R. (1999). Human rhinovirus HRV14 uncoats from early endosomes in the presence of bafilomycin. FEBS Lett *463*, 175-178.

Beer, C., Andersen, D.S., Rojek, A., and Pedersen, L. (2005). Caveola-dependent endocytic entry of amphotropic murine leukemia virus. J Virol *79*, 10776-10787.

Bellve, K.D., Leonard, D., Standley, C., Lifshitz, L.M., Tuft, R.A., Hayakawa, A., Corvera, S., and Fogarty, K.E. (2006). Plasma membrane domains specialized for clathrin-mediated endocytosis in primary cells. J Biol Chem *281*, 16139-16146.

Benmerah, A., Bayrou, M., Cerf-Bensussan, N., and Dautry-Varsat, A. (1999). Inhibition of clathrin-coated pit assembly by an Eps15 mutant. J Cell Sci *112 (Pt 9)*, 1303-1311.

Berryman, S., Clark, S., Monaghan, P., and Jackson, T. (2005). Early events in integrin alphavbeta6-mediated cell entry of foot-and-mouth disease virus. J Virol *79*, 8519-8534.

Bhattacharya, B., Noad, R.J., and Roy, P. (2007). Interaction between Bluetongue virus outer capsid protein VP2 and vimentin is necessary for virus egress. Virol J *4*, 7.

Bittman, R., and Fischkoff, S.A. (1972). Fluorescence studies of the binding of the polyene antibiotics filipin 3, amphotericin B, nystatin, and lagosin to cholesterol. Proc Natl Acad Sci U S A *69*, 3795-3799.

Borsa, J., Sargent, M.D., Lievaart, P.A., and Copps, T.P. (1981). Reovirus: evidence for a second step in the intracellular uncoating and transcriptase activation process. Virology *111*, 191-200.

Brower, D.L. (2003). Platelets with wings: the maturation of Drosophila integrin biology. Curr Opin Cell Biol *15*, 607-613.

Bunch, T.A., Helsten, T.L., Kendall, T.L., Shirahatti, N., Mahadevan, D., Shattil, S.J., and Brower, D.L. (2005). Amino acid changes in drosophila alpha PS2beta PS integrins that affect ligand affinity. J Biol Chem.

Burman, A., Clark, S., Abrescia, N.G., Fry, E.E., Stuart, D.I., and Jackson, T. (2006). Specificity of the VP1 GH loop of Foot-and-Mouth Disease virus for alphav integrins. J Virol *80*, 9798-9810.

Burroughs, J.N., O'Hara, R.S., Smale, C.J., Hamblin, C., Walton, A., Armstrong, R., and Mertens, P.P. (1994). Purification and properties of virus particles, infectious subviral particles, cores and VP7 crystals of African horsesickness virus serotype 9. J Gen Virol *75 (Pt 8)*, 1849-1857.

Campbell, J.A., Schelling, P., Wetzel, J.D., Johnson, E.M., Forrest, J.C., Wilson, G.A., Aurrand-Lions, M., Imhof, B.A., Stehle, T., and Dermody, T.S. (2005). Junctional adhesion molecule a serves as a receptor for prototype and field-isolate strains of mammalian reovirus. J Virol *79*, 7967-7978.

Cao, H., Chen, J., Awoniyi, M., Henley, J.R., and McNiven, M.A. (2007). Dynamin 2 mediates fluid-phase micropinocytosis in epithelial cells. J Cell Sci *120*, 4167-4177.

Cao, H., Garcia, F., and McNiven, M.A. (1998). Differential distribution of dynamin isoforms in mammalian cells. Mol Biol Cell *9*, 2595-2609.

Cao, H., Thompson, H.M., Krueger, E.W., and McNiven, M.A. (2000). Disruption of Golgi structure and function in mammalian cells expressing a mutant dynamin. J Cell Sci *113 (Pt 11)*, 1993-2002.

Carpenter, S., Wilson, A. and Mellor, P.S. (In press). Culicoides and the emergence of bluetongue virus in northern Europe. Cell.

Chadda, R., Howes, M.T., Plowman, S.J., Hancock, J.F., Parton, R.G., and Mayor, S. (2007). Cholesterol-sensitive Cdc42 activation regulates actin polymerization for endocytosis via the GEEC pathway. Traffic *8*, 702-717.

Chandran, K., and Nibert, M.L. (2003). Animal cell invasion by a large nonenveloped virus: reovirus delivers the goods. Trends Microbiol *11*, 374-382.

Chatterjee, S., and Mayor, S. (2001). The GPI-anchor and protein sorting. Cell Mol Life Sci *58*, 1969-1987.

Chemello, M.E., Aristimuno, O.C., Michelangeli, F., and Ruiz, M.C. (2002). Requirement for vacuolar H+ -ATPase activity and Ca2+ gradient during entry of rotavirus into MA104 cells. J Virol *76*, 13083-13087.

Chen, C., and Zhuang, X. (2008). Epsin 1 is a cargo-specific adaptor for the clathrin-mediated endocytosis of the influenza virus. Proc Natl Acad Sci U S A *105*, 11790-11795.

Ciarlet, M., Crawford, S.E., and Estes, M.K. (2001). Differential infection of polarized epithelial cell lines by sialic acid-dependent and sialic acid-independent rotavirus strains. J Virol *75*, 11834-11850.

Clark, S.M., Roth, J.R., Clark, M.L., Barnett, B.B., and Spendlove, R.S. (1981). Trypsin enhancement of rotavirus infectivity: mechanism of enhancement. J Virol *39*, 816-822.

Clemente, R., and de la Torre, J.C. (2009). Cell entry of Borna disease virus follows a clathrin-mediated endocytosis pathway that requires Rab5 and microtubules. J Virol *83*, 10406-10416.

Coue, M., Brenner, S.L., Spector, I., and Korn, E.D. (1987). Inhibition of actin polymerization by latrunculin A. FEBS Lett *213*, 316-318.

Coulson, B.S., Londrigan, S.L., and Lee, D.J. (1997). Rotavirus contains integrin ligand sequences and a disintegrin-like domain that are implicated in virus entry into cells. Proc Natl Acad Sci U S A *94*, 5389-5394.

Cox, D., Chang, P., Zhang, Q., Reddy, P.G., Bokoch, G.M., and Greenberg, S. (1997). Requirements for both Rac1 and Cdc42 in membrane ruffling and phagocytosis in leukocytes. J Exp Med *186*, 1487-1494.

Coyne, C.B., Shen, L., Turner, J.R., and Bergelson, J.M. (2007). Coxsackievirus entry across epithelial tight junctions requires occludin and the small GTPases Rab34 and Rab5. Cell Host Microbe *2*, 181-192.

Daecke, J., Fackler, O.T., Dittmar, M.T., and Krausslich, H.G. (2005). Involvement of clathrin-mediated endocytosis in human immunodeficiency virus type 1 entry. J Virol *79*, 1581-1594.

Damm, E.M., Pelkmans, L., Kartenbeck, J., Mezzacasa, A., Kurzchalia, T., and Helenius, A. (2005). Clathrin- and caveolin-1-independent endocytosis: entry of simian virus 40 into cells devoid of caveolae. J Cell Biol *168*, 477-488.

Darpel, K.E. (2007). The Bluetongue Virus 'Ruminant Host-Insect Vector' Transmission cycle, The Role of *Culicoides* saliva proteins in infection (University of London).

Darpel, K.E., Batten, C.A., Veronesi, E., Shaw, A.E., Anthony, S., Bachanek-Bankowska, K., Kgosana, L., bin-Tarif, A., Carpenter, S., Muller-Doblies, U.U., *et al.* (2007). Clinical signs and pathology shown by British sheep and cattle infected with bluetongue virus serotype 8 derived from the 2006 outbreak in northern Europe. Vet Rec *161*, 253-261.

Darpel, K.E., Batten, C.A., Veronesi, E., Williamson, S., Anderson, P., Dennison, M., Clifford, S., Smith, C., Philips, L., Bidewell, C., *et al.* (2009). Transplacental transmission of bluetongue virus 8 in cattle, UK. Emerg Infect Dis *15*, 2025-2028.

De Clercq, K., Mertens, P., De Leeuw, I., Oura, C., Houdart, P., Potgieter, A.C., Maan, S., Hooyberghs, J., Batten, C., Vandemeulebroucke, E., *et al.* (2009). Emergence of bluetongue serotypes in Europe, part 2: the occurrence of a BTV-11 strain in Belgium. Transbound Emerg Dis *56*, 355-361.

Delaney, K.A., Murph, M.M., Brown, L.M., and Radhakrishna, H. (2002). Transfer of M2 muscarinic acetylcholine receptors to clathrin-derived early endosomes following clathrin-independent endocytosis. J Biol Chem *277*, 33439-33446.

DeTulleo, L., and Kirchhausen, T. (1998). The clathrin endocytic pathway in viral infection. EMBO J *17*, 4585-4593.

Dharmawardhane, S., Schurmann, A., Sells, M.A., Chernoff, J., Schmid, S.L., and Bokoch, G.M. (2000). Regulation of macropinocytosis by p21-activated kinase-1. Mol Biol Cell *11*, 3341-3352.

Dicara, D., Burman, A., Clark, S., Berryman, S., Howard, M.J., Hart, I.R., Marshall, J.F., and Jackson, T. (2008). Foot-and-mouth disease virus forms a highly stable, EDTA-resistant complex with its principal receptor, integrin alphavbeta6: implications for infectiousness. J Virol *82*, 1537-1546.

Diprose, J.M., Burroughs, J.N., Sutton, G.C., Goldsmith, A., Gouet, P., Malby, R., Overton, I., Zientara, S., Mertens, P.P., Stuart, D.I., *et al.* (2001). Translocation portals for the substrates and products of a viral transcription complex: the bluetongue virus core. Embo J *20*, 7229-7239.

Diseases, I.S.f.I. (2006). Bluetongue, ovine - Netherlands: confirmed. ProMED-mail, 200608182311.

Doherty, G.J., and McMahon, H.T. (2009a). Mechanisms of Endocytosis. Annu Rev Biochem.

Doherty, G.J., and McMahon, H.T. (2009b). Mechanisms of endocytosis. Annu Rev Biochem *78*, 857-902.

Dowrick, P., Kenworthy, P., McCann, B., and Warn, R. (1993). Circular ruffle formation and closure lead to macropinocytosis in hepatocyte growth factor/scatter factor-treated cells. Eur J Cell Biol *61*, 44-53.

Eaton, B.T., and Hyatt, A.D. (1989). Association of bluetongue virus with the cytoskeleton. Subcell Biochem *15*, 233-273.

Eaton, B.T., Hyatt, A.D., and White, J.R. (1988). Localization of the nonstructural protein NS1 in bluetongue virus-infected cells and its presence in virus particles. Virology *163*, 527-537.

Edeling, M.A., Smith, C., and Owen, D. (2006). Life of a clathrin coat: insights from clathrin and AP structures. Nat Rev Mol Cell Biol *7*, 32-44.

Ehrlich, M., Boll, W., Van Oijen, A., Hariharan, R., Chandran, K., Nibert, M.L., and Kirchhausen, T. (2004). Endocytosis by random initiation and stabilization of clathrin-coated pits. Cell *118*, 591-605.

Eskelinen, E.L. (2006). Roles of LAMP-1 and LAMP-2 in lysosome biogenesis and autophagy. Mol Aspects Med *27*, 495-502.

Estes, M.K., Graham, D.Y., and Mason, B.B. (1981). Proteolytic enhancement of rotavirus infectivity: molecular mechanisms. J Virol *39*, 879-888.

Falcone, S., Cocucci, E., Podini, P., Kirchhausen, T., Clementi, E., and Meldolesi, J. (2006). Macropinocytosis: regulated coordination of endocytic and exocytic membrane traffic events. J Cell Sci *119*, 4758-4769.

Ferguson, S.M., Brasnjo, G., Hayashi, M., Wolfel, M., Collesi, C., Giovedi, S., Raimondi, A., Gong, L.W., Ariel, P., Paradise, S., *et al.* (2007). A selective activity-dependent requirement for dynamin 1 in synaptic vesicle endocytosis. Science *316*, 570-574.

Fivaz, M., Vilbois, F., Thurnheer, S., Pasquali, C., Abrami, L., Bickel, P.E., Parton, R.G., and van der Goot, F.G. (2002). Differential sorting and fate of endocytosed GPI-anchored proteins. EMBO J *21*, 3989-4000.

Fletcher, R.D., Hirschfield, J.E., and Forbes, M. (1965). A common mode of antiviral action for ammonium ions and various amines. Nature *207*, 664-665.

Ford, M.G., Mills, I.G., Peter, B.J., Vallis, Y., Praefcke, G.J., Evans, P.R., and McMahon, H.T. (2002). Curvature of clathrin-coated pits driven by epsin. Nature *419*, 361-366.

Ford, M.G., Pearse, B.M., Higgins, M.K., Vallis, Y., Owen, D.J., Gibson, A., Hopkins, C.R., Evans, P.R., and McMahon, H.T. (2001). Simultaneous binding of PtdIns(4,5)P2 and clathrin by AP180 in the nucleation of clathrin lattices on membranes. Science *291*, 1051-1055.

Forrest, J.C., and Dermody, T.S. (2003). Reovirus receptors and pathogenesis. J Virol *77*, 9109-9115.

Forzan, M., Marsh, M., and Roy, P. (2007). Bluetongue virus entry into cells. J Virol *81*, 4819-4827.

Forzan, M., Wirblich, C., and Roy, P. (2004). A capsid protein of nonenveloped Bluetongue virus exhibits membrane fusion activity. Proc Natl Acad Sci U S A *101*, 2100-2105.

Fraile-Ramos, A., Kohout, T.A., Waldhoer, M., and Marsh, M. (2003). Endocytosis of the viral chemokine receptor US28 does not require beta-arrestins but is dependent on the clathrin-mediated pathway. Traffic *4*, 243-253.

Fretz, M., Jin, J., Conibere, R., Penning, N.A., Al-Taei, S., Storm, G., Futaki, S., Takeuchi, T., Nakase, I., and Jones, A.T. (2006). Effects of Na+/H+ exchanger inhibitors on subcellular localisation of endocytic organelles and intracellular dynamics of protein transduction domains HIV-TAT peptide and octaarginine. J Control Release *116*, 247-254.

Fu, H., Leake, C.J., Mertens, P.P., and Mellor, P.S. (1999). The barriers to bluetongue virus infection, dissemination and transmission in the vector, Culicoides variipennis (Diptera: Ceratopogonidae). Arch Virol *144*, 747-761.

Gastaldelli, M., Imelli, N., Boucke, K., Amstutz, B., Meier, O., and Greber, U.F. (2008). Infectious adenovirus type 2 transport through early but not late endosomes. Traffic *9*, 2265-2278.

Gerondopoulos, A., Jackson, T., Monaghan, P., Doyle, N., and Roberts, L.O. (2010). Murine norovirus-1 cell entry is mediated through a non-clathrin, non-caveolae, dynamin and cholesterol dependent pathway. J Gen Virol.

Ghiasi, H., Purdy, M.A., and Roy, P. (1985). The complete sequence of bluetongue virus serotype 10 segment 3 and its predicted VP3 polypeptide compared with those of BTV serotype 17. Virus Res *3*, 181-190.

Gibbs, E.P., Lawman, M.J., and Herniman, K.A. (1979). Preliminary observations on transplacental infection of bluetongue virus in sheep-a possible overwintering mechanism. Res Vet Sci *27*, 118-120.

Glebov, O.O., Bright, N.A., and Nichols, B.J. (2006). Flotillin-1 defines a clathrin-independent endocytic pathway in mammalian cells. Nat Cell Biol *8*, 46-54.

Gold, E.S., Underhill, D.M., Morrissette, N.S., Guo, J., McNiven, M.A., and Aderem, A. (1999). Dynamin 2 is required for phagocytosis in macrophages. J Exp Med *190*, 1849-1856.

Goldenberg, N.M., Grinstein, S., and Silverman, M. (2007). Golgi-bound Rab34 is a novel member of the secretory pathway. Mol Biol Cell *18*, 4762-4771.

Gouet, P., Diprose, J.M., Grimes, J.M., Malby, R., Burroughs, J.N., Zientara, S., Stuart, D.I., and Mertens, P.P. (1999). The highly ordered double-stranded RNA genome of bluetongue virus revealed by crystallography. Cell *97*, 481-490.

Graham, K.L., Fleming, F.E., Halasz, P., Hewish, M.J., Nagesha, H.S., Holmes, I.H., Takada, Y., and Coulson, B.S. (2005). Rotaviruses interact with alpha4beta7 and

alpha4beta1 integrins by binding the same integrin domains as natural ligands. J Gen Virol *86*, 3397-3408.

Graham, K.L., Takada, Y., and Coulson, B.S. (2006). Rotavirus spike protein VP5* binds alpha2beta1 integrin on the cell surface and competes with virus for cell binding and infectivity. J Gen Virol *87*, 1275-1283.

Grimes, J.M., Burroughs, J.N., Gouet, P., Diprose, J.M., Malby, R., Zientara, S., Mertens, P.P., and Stuart, D.I. (1998). The atomic structure of the bluetongue virus core. Nature *395*, 470-478.

Grimes, J.M., Jakana, J., Ghosh, M., Basak, A.K., Roy, P., Chiu, W., Stuart, D.I., and Prasad, B.V. (1997). An atomic model of the outer layer of the bluetongue virus core derived from X-ray crystallography and electron cryomicroscopy. Structure *5*, 885-893.

Grimmer, S., van Deurs, B., and Sandvig, K. (2002). Membrane ruffling and macropinocytosis in A431 cells require cholesterol. J Cell Sci *115*, 2953-2962.

Guglielmi, K.M., Johnson, E.M., Stehle, T., and Dermody, T.S. (2006). Attachment and cell entry of mammalian orthoreovirus. Curr Top Microbiol Immunol *309*, 1-38.

Guirakhoo, F., Catalan, J.A., and Monath, T.P. (1995). Adaptation of bluetongue virus in mosquito cells results in overexpression of NS3 proteins and release of virus particles. Archives of Virology *140*, 967-974.

Hamasaki, M., Araki, N., and Hatae, T. (2004). Association of early endosomal autoantigen 1 with macropinocytosis in EGF-stimulated A431 cells. Anat Rec A Discov Mol Cell Evol Biol *277*, 298-306.

Hao, W., Luo, Z., Zheng, L., Prasad, K., and Lafer, E.M. (1999). AP180 and AP-2 interact directly in a complex that cooperatively assembles clathrin. J Biol Chem *274*, 22785-22794.

Hassan, S.H., Wirblich, C., Forzan, M., and Roy, P. (2001). Expression and functional characterization of bluetongue virus VP5 protein: role in cellular permeabilization. J Virol *75*, 8356-8367.

Hassan, S.S., and Roy, P. (1999). Expression and functional characterization of bluetongue virus VP2 protein: role in cell entry. J Virol *73*, 9832-9842.

Helenius, A., Kartenbeck, J., Simons, K., and Fries, E. (1980). On the entry of Semliki forest virus into BHK-21 cells. J Cell Biol *84*, 404-420.

Hemati, B., Contreras, V., Urien, C., Bonneau, M., Takamatsu, H.H., Mertens, P.P., Breard, E., Sailleau, C., Zientara, S., and Schwartz-Cornil, I. (2009). Bluetongue virus targets conventional dendritic cells in skin lymph. J Virol *83*, 8789-8799.

Henley, J.R., Krueger, E.W., Oswald, B.J., and McNiven, M.A. (1998). Dynamin-mediated internalization of caveolae. J Cell Biol *141*, 85-99.

Hernaez, B., and Alonso, C. (2010). Dynamin- and clathrin-dependent endocytosis in African swine fever virus entry. J Virol *84*, 2100-2109.

Heuser, J. (1980). Three-dimensional visualization of coated vesicle formation in fibroblasts. J Cell Biol *84*, 560-583.

Hewlett, L.J., Prescott, A.R., and Watts, C. (1994). The coated pit and macropinocytic pathways serve distinct endosome populations. J Cell Biol *124*, 689-703.

Hinshaw, J.E., and Schmid, S.L. (1995). Dynamin self-assembles into rings suggesting a mechanism for coated vesicle budding. Nature *374*, 190-192.

Hofmann, M.A., Renzullo, S., Mader, M., Chaignat, V., Worwa, G., and Thuer, B. (2008). Genetic characterization of toggenburg orbivirus, a new bluetongue virus, from goats, Switzerland. Emerg Infect Dis *14*, 1855-1861.

Holzinger, A. (2009). Jasplakinolide: an actin-specific reagent that promotes actin polymerization. Methods Mol Biol *586*, 71-87.

Holzinger, A., and Meindl, U. (1997). Jasplakinolide, a novel actin targeting peptide, inhibits cell growth and induces actin filament polymerization in the green alga Micrasterias. Cell Motil Cytoskeleton *38*, 365-372.

Hourrigan, J.L., and Klingsporn, A.L. (1975). Bluetongue: the disease in cattle. Aust Vet J *51*, 170-174.

Huang, C.Y., Lu, T.Y., Bair, C.H., Chang, Y.S., Jwo, J.K., and Chang, W. (2008). A novel cellular protein, VPEF, facilitates vaccinia virus penetration into HeLa cells through fluid phase endocytosis. J Virol *82*, 7988-7999.

Huismans, H., and Erasmus, B.J. (1981). Identification of the serotype-specific and group-specific antigens of bluetongue virus. Onderstepoort J Vet Res *48*, 51-58.

Huismans, H., van Dijk, A.A., and Els, H.J. (1987). Uncoating of parental bluetongue virus to core and subcore particles in infected L cells. Virology *157*, 180-188.

Huss, M., and Wieczorek, H. (2009). Inhibitors of V-ATPases: old and new players. J Exp Biol *212*, 341-346.

Hyatt, A.D., Eaton, B.T., and Brookes, S.M. (1989). The release of bluetongue virus from infected cells and their superinfection by progeny virus. Virology *173*, 21-34.

Hyatt, A.D., Gould, A.R., Coupar, B., and Eaton, B.T. (1991). Localization of the non-structural protein NS3 in bluetongue virus-infected cells. J Gen Virol *72 (Pt 9)*, 2263-2267.

Hyatt, A.D., Zhao, Y., and Roy, P. (1993). Release of bluetongue virus-like particles from insect cells is mediated by BTV nonstructural protein NS3/NS3A. Virology *193*, 592-603.

I.R.Hutchinson (1999). The Role of VP7 (T13) in Initiation of Infection by Bluetongue Virus. In Division of Molecular Biology (University of Hertfordshire), pp. 195.

ICTV (2008). (International Committee on Taxonomy of Viruses).

Ilangumaran, S., and Hoessli, D.C. (1998). Effects of cholesterol depletion by cyclodextrin on the sphingolipid microdomains of the plasma membrane. Biochem J *335 (Pt 2)*, 433-440.

Izmailyan, R.A., Huang, C.Y., Mohammad, S., Isaacs, S.N., and Chang, W. (2006). The envelope G3L protein is essential for entry of vaccinia virus into host cells. J Virol *80*, 8402-8410.

Jackson, R.L., Busch, S.J., and Cardin, A.D. (1991). Glycosaminoglycans: molecular properties, protein interactions, and role in physiological processes. Physiol Rev *71*, 481-539.

Jackson, T., Clark, S., Berryman, S., Burman, A., Cambier, S., Mu, D., Nishimura, S., and King, A.M. (2004). Integrin alphavbeta8 functions as a receptor for foot-and-mouth disease virus: role of the beta-chain cytodomain in integrin-mediated infection. J Virol *78*, 4533-4540.

Jackson, T., Sharma, A., Ghazaleh, R.A., Blakemore, W.E., Ellard, F.M., Simmons, D.L., Newman, J.W., Stuart, D.I., and King, A.M. (1997). Arginine-glycine-aspartic acid-specific binding by foot-and-mouth disease viruses to the purified integrin alpha(v)beta3 in vitro. J Virol *71*, 8357-8361.

Jennings, D.M., and Mellor, P.S. (1987). Variation in the responses of Culicoides variipennis (Diptera, Ceratopogonidae) to oral infection with bluetongue virus. Arch Virol *95*, 177-182.

Jiang, J., and Coombs, K.M. (2005). Infectious entry of reovirus cores into mammalian cells enhanced by transfection. J Virol Methods *128*, 88-92.

Johns, H.L., Berryman, S., Monaghan, P., Belsham, G.J., and Jackson, T. (2009). A dominant-negative mutant of rab5 inhibits infection of cells by foot-and-mouth disease virus: implications for virus entry. J Virol *83*, 6247-6256.

Jones, A.T. (2007). Macropinocytosis: searching for an endocytic identity and role in the uptake of cell penetrating peptides. J Cell Mol Med *11*, 670-684.

Jovic, M., Sharma, M., Rahajeng, J., and Caplan, S. (2010). The early endosome: a busy sorting station for proteins at the crossroads. Histol Histopathol *25*, 99-112.

Kalia, M., Kumari, S., Chadda, R., Hill, M.M., Parton, R.G., and Mayor, S. (2006). Arf6-independent GPI-anchored protein-enriched early endosomal compartments fuse with sorting endosomes via a Rab5/phosphatidylinositol-3'-kinase-dependent machinery. Mol Biol Cell *17*, 3689-3704.

Kaljot, K.T., Shaw, R.D., Rubin, D.H., and Greenberg, H.B. (1988). Infectious rotavirus enters cells by direct cell membrane penetration, not by endocytosis. J Virol *62*, 1136-1144.

Karjalainen, M., Kakkonen, E., Upla, P., Paloranta, H., Kankaanpaa, P., Liberali, P., Renkema, G.H., Hyypia, T., Heino, J., and Marjomaki, V. (2008). A Raft-derived, Pak1-regulated entry participates in alpha2beta1 integrin-dependent sorting to caveosomes. Mol Biol Cell *19*, 2857-2869.

Kee, S.H., Cho, E.J., Song, J.W., Park, K.S., Baek, L.J., and Song, K.J. (2004). Effects of endocytosis inhibitory drugs on rubella virus entry into VeroE6 cells. Microbiol Immunol *48*, 823-829.

Keljo, D.J., Kuhn, M., and Smith, A. (1988). Acidification of endosomes is not important for the entry of rotavirus into the cell. J Pediatr Gastroenterol Nutr *7*, 257-263.

Keller, P., and Simons, K. (1998). Cholesterol is required for surface transport of influenza virus hemagglutinin. J Cell Biol *140*, 1357-1367.

Kerr, M.C., and Teasdale, R.D. (2009). Defining macropinocytosis. Traffic *10*, 364-371.

Kirchhausen, T., and Harrison, S.C. (1981). Protein organization in clathrin trimers. Cell *23*, 755-761.

Kirchhausen, T., Macia, E., and Pelish, H.E. (2008). Use of dynasore, the small molecule inhibitor of dynamin, in the regulation of endocytosis. Methods Enzymol *438*, 77-93.

Kirchner, E., Guglielmi, K.M., Strauss, H.M., Dermody, T.S., and Stehle, T. (2008). Structure of reovirus sigma1 in complex with its receptor junctional adhesion molecule-A. PLoS Pathog *4*, e1000235.

Kirkham, M., Fujita, A., Chadda, R., Nixon, S.J., Kurzchalia, T.V., Sharma, D.K., Pagano, R.E., Hancock, J.F., Mayor, S., and Parton, R.G. (2005). Ultrastructural identification of uncoated caveolin-independent early endocytic vehicles. J Cell Biol *168*, 465-476.

Knaus, U.G., Wang, Y., Reilly, A.M., Warnock, D., and Jackson, J.H. (1998). Structural requirements for PAK activation by Rac GTPases. J Biol Chem *273*, 21512-21518.

Koivusalo, M., Welch, C., Hayashi, H., Scott, C.C., Kim, M., Alexander, T., Touret, N., Hahn, K.M., and Grinstein, S. (2010). Amiloride inhibits macropinocytosis by lowering submembranous pH and preventing Rac1 and Cdc42 signaling. J Cell Biol *188*, 547-563.

Koumbati, M., Mangana, O., Nomikou, K., Mellor, P.S., and Papadopoulos, O. (1999). Duration of bluetongue viraemia and serological responses in experimentally infected European breeds of sheep and goats. Vet Microbiol *64*, 277-285.

Krishan, A. (1972). Cytochalasin-B: time-lapse cinematographic studies on its effects on cytokinesis. J Cell Biol *54*, 657-664.

Kumari, S., and Mayor, S. (2008). ARF1 is directly involved in dynamin-independent endocytosis. Nat Cell Biol *10*, 30-41.

Lajoie, P., and Nabi, I.R. (2007). Regulation of raft-dependent endocytosis. J Cell Mol Med *11*, 644-653.

Lakadamyali, M., Rust, M.J., and Zhuang, X. (2004). Endocytosis of influenza viruses. Microbes Infect *6*, 929-936.

Lamaze, C., Dujeancourt, A., Baba, T., Lo, C.G., Benmerah, A., and Dautry-Varsat, A. (2001). Interleukin 2 receptors and detergent-resistant membrane domains define a clathrin-independent endocytic pathway. Mol Cell *7*, 661-671.

Lanzetti, L., Palamidessi, A., Areces, L., Scita, G., and Di Fiore, P.P. (2004). Rab5 is a signalling GTPase involved in actin remodelling by receptor tyrosine kinases. Nature *429*, 309-314.

Le Blois, H., French, T., Mertens, P.P., Burroughs, J.N., and Roy, P. (1992). The expressed VP4 protein of bluetongue virus binds GTP and is the candidate guanylyl transferase of the virus. Virology *189*, 757-761.

Li, Z., Baker, M.L., Jiang, W., Estes, M.K., and Prasad, B.V. (2009). Rotavirus architecture at subnanometer resolution. J Virol *83*, 1754-1766.

Liberali, P., Kakkonen, E., Turacchio, G., Valente, C., Spaar, A., Perinetti, G., Bockmann, R.A., Corda, D., Colanzi, A., Marjomaki, V., *et al.* (2008). The closure of Pak1-dependent macropinosomes requires the phosphorylation of CtBP1/BARS. EMBO J *27*, 970-981.

Liebl, D., Difato, F., Hornikova, L., Mannova, P., Stokrova, J., and Forstova, J. (2006). Mouse polyomavirus enters early endosomes, requires their acidic pH for productive infection, and meets transferrin cargo in Rab11-positive endosomes. J Virol *80*, 4610-4622.

Liu, Y.W., Surka, M.C., Schroeter, T., Lukiyanchuk, V., and Schmid, S.L. (2008). Isoform and splice-variant specific functions of dynamin-2 revealed by analysis of conditional knock-out cells. Mol Biol Cell *19*, 5347-5359.

Locker, J.K., Kuehn, A., Schleich, S., Rutter, G., Hohenberg, H., Wepf, R., and Griffiths, G. (2000). Entry of the two infectious forms of vaccinia virus at the plasma membane is signaling-dependent for the IMV but not the EEV. Mol Biol Cell *11*, 2497-2511.

Lopez, S., and Arias, C.F. (2004). Multistep entry of rotavirus into cells: a Versaillesque dance. Trends Microbiol *12*, 271-278.

Losson, B., Mignon, B., Paternostre, J., Madder, M., De Deken, R., De Deken, G., Deblauwe, I., Fassotte, C., Cors, R., Defrance, T., *et al.* (2007). Biting midges overwintering in Belgium. Vet Rec *160*, 451-452.

Lundmark, R., Doherty, G.J., Howes, M.T., Cortese, K., Vallis, Y., Parton, R.G., and McMahon, H.T. (2008). The GTPase-activating protein GRAF1 regulates the CLIC/GEEC endocytic pathway. Curr Biol *18*, 1802-1808.

Lunt, R.A., Melville, L., Hunt, N., Davis, S., Rootes, C.L., Newberry, K.M., Pritchard, L.I., Middleton, D., Bingham, J., Daniels, P.W., *et al.* (2006). Cultured skin fibroblast cells derived from bluetongue virus-inoculated sheep and field-infected cattle are not a source of late and protracted recoverable virus. J Gen Virol *87*, 3661-3666.

Maan, S., Maan, N.S., Ross-smith, N., Batten, C.A., Shaw, A.E., Anthony, S.J., Samuel, A.R., Darpel, K.E., Veronesi, E., Oura, C.A., *et al.* (2008). Sequence analysis of bluetongue virus serotype 8 from the Netherlands 2006 and comparison to other European strains. Virology *377*, 308-318.

Maan, S., Maan, N.S., Samuel, A.R., Rao, S., Attoui, H., and Mertens, P.P. (2007a). Analysis and phylogenetic comparisons of full-length VP2 genes of the 24 bluetongue virus serotypes. J Gen Virol *88*, 621-630.

Maan, S., Rao, S., Maan, N.S., Anthony, S.J., Attoui, H., Samuel, A.R., and Mertens, P.P. (2007b). Rapid cDNA synthesis and sequencing techniques for the genetic study of bluetongue and other dsRNA viruses. J Virol Methods *143*, 132-139.

Macia, E., Ehrlich, M., Massol, R., Boucrot, E., Brunner, C., and Kirchhausen, T. (2006). Dynasore, a cell-permeable inhibitor of dynamin. Dev Cell *10*, 839-850.

Maclachlan, N.J., Drew, C.P., Darpel, K.E., and Worwa, G. (2009). The pathology and pathogenesis of bluetongue. J Comp Pathol *141*, 1-16.

Maginnis, M.S., Forrest, J.C., Kopecky-Bromberg, S.A., Dickeson, S.K., Santoro, S.A., Zutter, M.M., Nemerow, G.R., Bergelson, J.M., and Dermody, T.S. (2006). Beta1 integrin mediates internalization of mammalian reovirus. J Virol *80*, 2760-2770.

Mannova, P., and Forstova, J. (2003). Mouse polyomavirus utilizes recycling endosomes for a traffic pathway independent of COPI vesicle transport. J Virol *77*, 1672-1681.

Marechal, V., Prevost, M.C., Petit, C., Perret, E., Heard, J.M., and Schwartz, O. (2001). Human immunodeficiency virus type 1 entry into macrophages mediated by macropinocytosis. J Virol *75*, 11166-11177.

Marsh, M., ed. (2001). Endocytosis, First edn (Oxford, Oxford University Press).

Marsh, M., and Helenius, A. (2006). Virus entry: open sesame. Cell *124*, 729-740.

Marth, T., and Kelsall, B.L. (1997). Regulation of interleukin-12 by complement receptor 3 signaling. J Exp Med *185*, 1987-1995.

Martin-Acebes, M.A., Gonzalez-Magaldi, M., Sandvig, K., Sobrino, F., and Armas-Portela, R. (2007). Productive entry of type C foot-and-mouth disease virus into susceptible cultured cells requires clathrin and is dependent on the presence of plasma membrane cholesterol. Virology *369*, 105-118.

Martinez, C.G., Guinea, R., Benavente, J., and Carrasco, L. (1996). The entry of reovirus into L cells is dependent on vacuolar proton-ATPase activity. J Virol *70*, 576-579.

Matlin, K.S., Reggio, H., Helenius, A., and Simons, K. (1981). Infectious entry pathway of influenza virus in a canine kidney cell line. J Cell Biol *91*, 601-613.

Mayor, S., and Pagano, R.E. (2007). Pathways of clathrin-independent endocytosis. Nat Rev Mol Cell Biol *8*, 603-612.

McNiven, M.A., Cao, H., Pitts, K.R., and Yoon, Y. (2000). The dynamin family of mechanoenzymes: pinching in new places. Trends Biochem Sci *25*, 115-120.

Meier, O., Boucke, K., Hammer, S.V., Keller, S., Stidwill, R.P., Hemmi, S., and Greber, U.F. (2002). Adenovirus triggers macropinocytosis and endosomal leakage together with its clathrin-mediated uptake. J Cell Biol *158*, 1119-1131.

Meiswinkel, R., Baldet, T., de Deken, R., Takken, W., Delecolle, J.C., and Mellor, P.S. (2008). The 2006 outbreak of bluetongue in northern Europe--the entomological perspective. Prev Vet Med *87*, 55-63.

Mellor, P.P.C.M.P.S. (2003). Bluetongue. State Veterinary Journal, DEFRA *13*, 18-25.

Mellor, P.S. (1990). The replication of bluetongue virus in Culicoides vectors. Curr Top Microbiol Immunol *162*, 143-161.

Mellor, P.S. (2000). Replication of arboviruses in insect vectors. J Comp Pathol *123*, 231-247.

Menzies, F.D., McCullough, S.J., McKeown, I.M., Forster, J.L., Jess, S., Batten, C., Murchie, A.K., Gloster, J., Fallows, J.G., Pelgrim, W., *et al.* (2008). Evidence for transplacental and contact transmission of bluetongue virus in cattle. Vet Rec *163*, 203-209.

Mercer, J., and Helenius, A. (2008). Vaccinia virus uses macropinocytosis and apoptotic mimicry to enter host cells. Science *320*, 531-535.

Mercer, J., and Helenius, A. (2009). Virus entry by macropinocytosis. Nat Cell Biol *11*, 510-520.

Merrifield, C.J., Perrais, D., and Zenisek, D. (2005). Coupling between clathrin-coated-pit invagination, cortactin recruitment, and membrane scission observed in live cells. Cell *121*, 593-606.

Mertens, P.P., Brown, F., and Sangar, D.V. (1984). Assignment of the genome segments of bluetongue virus type 1 to the proteins which they encode. Virology *135*, 207-217.

Mertens, P.P., Burroughs, J.N., and Anderson, J. (1987). Purification and properties of virus particles, infectious subviral particles, and cores of bluetongue virus serotypes 1 and 4. Virology *157*, 375-386.

Mertens, P.P., Burroughs, J.N., Walton, A., Wellby, M.P., Fu, H., O'Hara, R.S., Brookes, S.M., and Mellor, P.S. (1996). Enhanced infectivity of modified bluetongue virus particles for two insect cell lines and for two Culicoides vector species. Virology *217*, 582-593.

Mertens, P.P., and Diprose, J. (2004). The bluetongue virus core: a nano-scale transcription machine. Virus Res *101*, 29-43.

Mertens, P.P., Pedley, S., Cowley, J., Burroughs, J.N., Corteyn, A.H., Jeggo, M.H., Jennings, D.M., and Gorman, B.M. (1989). Analysis of the roles of bluetongue virus outer capsid proteins VP2 and VP5 in determination of virus serotype. Virology *170*, 561-565.

Mertens, P.P.C., Maan, S., Samuel, A. & Attoui, H. (2005). Orbivirus. In Virus Taxonomy, VIIIth Report of the ICTV, M.A.M. C. M. Fauquet, J. Maniloff, U. Desselberger & L. A. Ball, ed. (London, Elsevier/Academic Press), pp. 466-483.

Miele, A.E., Watson, P.J., Evans, P.R., Traub, L.M., and Owen, D.J. (2004). Two distinct interaction motifs in amphiphysin bind two independent sites on the clathrin terminal domain beta-propeller. Nat Struct Mol Biol *11*, 242-248.

Miranda, A.F., Godman, G.C., Deitch, A.D., and Tanenbaum, S.W. (1974a). Action of cytochalasin D on cells of established lines. I. Early events. J Cell Biol *61*, 481-500.

Miranda, A.F., Godman, G.C., and Tanenbaum, S.W. (1974b). Action of cytochalasin D on cells of established lines. II. Cortex and microfilaments. J Cell Biol *62*, 406-423.

Mishra, S.K., Agostinelli, N.R., Brett, T.J., Mizukami, I., Ross, T.S., and Traub, L.M. (2001). Clathrin- and AP-2-binding sites in HIP1 uncover a general assembly role for endocytic accessory proteins. J Biol Chem *276*, 46230-46236.

Misinzo, G., Delputte, P.L., Lefebvre, D.J., and Nauwynck, H.J. (2009). Porcine circovirus 2 infection of epithelial cells is clathrin-, caveolae- and dynamin-independent, actin and Rho-GTPase-mediated, and enhanced by cholesterol depletion. Virus Res *139*, 1-9.

Miyauchi, K., Kim, Y., Latinovic, O., Morozov, V., and Melikyan, G.B. (2009). HIV enters cells via endocytosis and dynamin-dependent fusion with endosomes. Cell *137*, 433-444.

Moriyama, T., Marquez, J.P., Wakatsuki, T., and Sorokin, A. (2007). Caveolar endocytosis is critical for BK virus infection of human renal proximal tubular epithelial cells. J Virol *81*, 8552-8562.

Mu, F.T., Callaghan, J.M., Steele-Mortimer, O., Stenmark, H., Parton, R.G., Campbell, P.L., McCluskey, J., Yeo, J.P., Tock, E.P., and Toh, B.H. (1995). EEA1, an early endosome-associated protein. EEA1 is a conserved alpha-helical peripheral membrane protein flanked by cysteine "fingers" and contains a calmodulin-binding IQ motif. J Biol Chem *270*, 13503-13511.

Murphy, F.A., Borden, E.C., Shope, R.E., and Harrison, A. (1971). Physicochemical and morphological relationships of some arthropod-borne viruses to bluetongue virus--a new taxonomic group. Electron microscopic studies. J Gen Virol *13*, 273-288.

Nankoe, S.R., and Sever, S. (2006). Dynasore puts a new spin on dynamin: a surprising dual role during vesicle formation. Trends Cell Biol *16*, 607-609.

Naslavsky, N., Weigert, R., and Donaldson, J.G. (2003). Convergence of non-clathrin- and clathrin-derived endosomes involves Arf6 inactivation and changes in phosphoinositides. Mol Biol Cell *14*, 417-431.

Neumann-Giesen, C., Fernow, I., Amaddii, M., and Tikkanen, R. (2007). Role of EGF-induced tyrosine phosphorylation of reggie-1/flotillin-2 in cell spreading and signaling to the actin cytoskeleton. J Cell Sci *120*, 395-406.

Nicoziani, P., Vilhardt, F., Llorente, A., Hilout, L., Courtoy, P.J., Sandvig, K., and van Deurs, B. (2000). Role for dynamin in late endosome dynamics and trafficking of the cation-independent mannose 6-phosphate receptor. Mol Biol Cell *11*, 481-495.

Nishi, K., and Saigo, K. (2007). Cellular internalization of green fluorescent protein fused with herpes simplex virus protein VP22 via a lipid raft-mediated endocytic pathway independent of caveolae and Rho family GTPases but dependent on dynamin and Arf6. J Biol Chem *282*, 27503-27517.

Nobes, C., and Marsh, M. (2000). Dendritic cells: new roles for Cdc42 and Rac in antigen uptake? Curr Biol *10*, R739-741.

Norkin, L.C., and Kuksin, D. (2005). The caveolae-mediated sv40 entry pathway bypasses the golgi complex en route to the endoplasmic reticulum. Virol J *2*, 38.

Norman, A.W., Demel, R.A., de Kruyff, B., and van Deenen, L.L. (1972). Studies on the biological properties of polyene antibiotics. Evidence for the direct interaction of filipin with cholesterol. J Biol Chem *247*, 1918-1929.

Nunez, J.I., Molina, N., Baranowski, E., Domingo, E., Clark, S., Burman, A., Berryman, S., Jackson, T., and Sobrino, F. (2007). Guinea pig-adapted foot-and-mouth

disease virus with altered receptor recognition can productively infect a natural host. J Virol *81*, 8497-8506.

O'Donnell, V., Larocco, M., and Baxt, B. (2008). Heparan sulfate-binding foot-and-mouth disease virus enters cells via caveola-mediated endocytosis. J Virol *82*, 9075-9085.

O'Donnell, V., LaRocco, M., Duque, H., and Baxt, B. (2005). Analysis of foot-and-mouth disease virus internalization events in cultured cells. J Virol *79*, 8506-8518.

Ohkuma, S., and Poole, B. (1978). Fluorescence probe measurement of the intralysosomal pH in living cells and the perturbation of pH by various agents. Proc Natl Acad Sci U S A *75*, 3327-3331.

OIE (2006). Bluetongue in the Netherlands. Disease Information 19, 34.

Owen, D.J., Collins, B.M., and Evans, P.R. (2004). Adaptors for clathrin coats: structure and function. Annu Rev Cell Dev Biol *20*, 153-191.

Pannocchia, A., Revelli, S., Tamponi, G., Giorgianni, A., Todde, R., Bosia, A., and Ghigo, D. (1996). Reversal of doxorubicin resistance by the amiloride analogue EIPA in multidrug resistant human colon carcinoma cells. Cell Biochem Funct *14*, 11-18.

Parsonson, I.M., Luedke, A.J., Barber, T.L., and Walton, T.E. (1994a). Bluetongue virus infection in pregnant ewes. Am J Vet Res *55*, 666-669.

Parsonson, I.M., Thompson, L.H., and Walton, T.E. (1994b). Experimentally induced infection with bluetongue virus serotype 11 in cows. Am J Vet Res *55*, 1529-1534.

Parton, R.G., and Simons, K. (2007). The multiple faces of caveolae. Nat Rev Mol Cell Biol *8*, 185-194.

Payne, C.K., Jones, S.A., Chen, C., and Zhuang, X. (2007). Internalization and trafficking of cell surface proteoglycans and proteoglycan-binding ligands. Traffic *8*, 389-401.

Pelchen-Matthews, A., Kramer, B., and Marsh, M. (2003). Infectious HIV-1 assembles in late endosomes in primary macrophages. J Cell Biol *162*, 443-455.

Pelkmans, L. (2005). Secrets of caveolae- and lipid raft-mediated endocytosis revealed by mammalian viruses. Biochim Biophys Acta *1746*, 295-304.

Pelkmans, L., Burli, T., Zerial, M., and Helenius, A. (2004). Caveolin-stabilized membrane domains as multifunctional transport and sorting devices in endocytic membrane traffic. Cell *118*, 767-780.

Pelkmans, L., and Helenius, A. (2002). Endocytosis via caveolae. Traffic *3*, 311-320.

Pelkmans, L., and Helenius, A. (2003). Insider information: what viruses tell us about endocytosis. Curr Opin Cell Biol *15*, 414-422.

Pelkmans, L., Kartenbeck, J., and Helenius, A. (2001). Caveolar endocytosis of simian virus 40 reveals a new two-step vesicular-transport pathway to the ER. Nat Cell Biol *3*, 473-483.

Pelkmans, L., Puntener, D., and Helenius, A. (2002). Local actin polymerization and dynamin recruitment in SV40-induced internalization of caveolae. Science *296*, 535-539.

Pesavento, J.B., Crawford, S.E., Estes, M.K., and Prasad, B.V. (2006). Rotavirus proteins: structure and assembly. Curr Top Microbiol Immunol *309*, 189-219.

Peter, B.J., Kent, H.M., Mills, I.G., Vallis, Y., Butler, P.J., Evans, P.R., and McMahon, H.T. (2004). BAR domains as sensors of membrane curvature: the amphiphysin BAR structure. Science *303*, 495-499.

Pietiainen, V., Marjomaki, V., Upla, P., Pelkmans, L., Helenius, A., and Hyypia, T. (2004). Echovirus 1 endocytosis into caveosomes requires lipid rafts, dynamin II, and signaling events. Mol Biol Cell *15*, 4911-4925.

Pietiainen, V.M., Marjomaki, V., Heino, J., and Hyypia, T. (2005). Viral entry, lipid rafts and caveosomes. Ann Med *37*, 394-403.

Praefcke, G.J., and McMahon, H.T. (2004). The dynamin superfamily: universal membrane tubulation and fission molecules? Nat Rev Mol Cell Biol *5*, 133-147.

Prchla, E., Kuechler, E., Blaas, D., and Fuchs, R. (1994). Uncoating of human rhinovirus serotype 2 from late endosomes. J Virol *68*, 3713-3723.

Pu, Y., and Zhang, X. (2008). Mouse hepatitis virus type 2 enters cells through a clathrin-mediated endocytic pathway independent of Eps15. J Virol *82*, 8112-8123.

Purse, B.V., Mellor, P.S., Rogers, D.J., Samuel, A.R., Mertens, P.P., and Baylis, M. (2005). Climate change and the recent emergence of bluetongue in Europe. Nat Rev Microbiol *3*, 171-181.

Quan, C.M., and Doane, F.W. (1983). Ultrastructural evidence for the cellular uptake of rotavirus by endocytosis. Intervirology *20*, 223-231.

Quirin, K., Eschli, B., Scheu, I., Poort, L., Kartenbeck, J., and Helenius, A. (2008). Lymphocytic choriomeningitis virus uses a novel endocytic pathway for infectious entry via late endosomes. Virology *378*, 21-33.

Racoosin, E.L., and Swanson, J.A. (1993). Macropinosome maturation and fusion with tubular lysosomes in macrophages. J Cell Biol *121*, 1011-1020.

Raghu, H., Sharma-Walia, N., Veettil, M.V., Sadagopan, S., and Chandran, B. (2009). Kaposi's sarcoma-associated herpesvirus utilizes an actin polymerization-dependent macropinocytic pathway to enter human dermal microvascular endothelial and human umbilical vein endothelial cells. J Virol *83*, 4895-4911.

Ramadevi, N., Burroughs, N.J., Mertens, P.P., Jones, I.M., and Roy, P. (1998). Capping and methylation of mRNA by purified recombinant VP4 protein of bluetongue virus. Proc Natl Acad Sci U S A *95*, 13537-13542.

Rojek, J.M., Perez, M., and Kunz, S. (2008a). Cellular entry of lymphocytic choriomeningitis virus. J Virol *82*, 1505-1517.

Rojek, J.M., Sanchez, A.B., Nguyen, N.T., de la Torre, J.C., and Kunz, S. (2008b). Different mechanisms of cell entry by human-pathogenic Old World and New World arenaviruses. J Virol *82*, 7677-7687.

Rothberg, K.G., Heuser, J.E., Donzell, W.C., Ying, Y.S., Glenney, J.R., and Anderson, R.G. (1992). Caveolin, a protein component of caveolae membrane coats. Cell *68*, 673-682.

Roy, P. (1989). Bluetongue virus genetics and genome structure. Virus Res *13*, 179-206.

Roy, P. (2005). Bluetongue virus proteins and particles and their role in virus entry, assembly, and release. Adv Virus Res *64*, 69-123.

Roy, P., Fukusho, A., Ritter, G.D., and Lyon, D. (1988). Evidence for genetic relationship between RNA and DNA viruses from the sequence homology of a putative polymerase gene of bluetongue virus with that of vaccinia virus: conservation of RNA polymerase genes from diverse species. Nucleic Acids Res *16*, 11759-11767.

Ruiz, M.C., Leon, T., Diaz, Y., and Michelangeli, F. (2009). Molecular biology of rotavirus entry and replication. ScientificWorldJournal *9*, 1476-1497.

Rust, M.J., Lakadamyali, M., Zhang, F., and Zhuang, X. (2004). Assembly of endocytic machinery around individual influenza viruses during viral entry. Nat Struct Mol Biol *11*, 567-573.

Sabharanjak, S., Sharma, P., Parton, R.G., and Mayor, S. (2002). GPI-anchored proteins are delivered to recycling endosomes via a distinct cdc42-regulated, clathrin-independent pinocytic pathway. Dev Cell *2*, 411-423.

Sampath, P., and Pollard, T.D. (1991). Effects of cytochalasin, phalloidin, and pH on the elongation of actin filaments. Biochemistry *30*, 1973-1980.

Sanchez-San Martin, C., Lopez, T., Arias, C.F., and Lopez, S. (2004). Characterization of rotavirus cell entry. J Virol *78*, 2310-2318.

Sandvig, K., and Olsnes, S. (1980). Diphtheria toxin entry into cells is facilitated by low pH. J Cell Biol *87*, 828-832.

Sandvig, K., Torgersen, M.L., Raa, H.A., and van Deurs, B. (2008). Clathrin-independent endocytosis: from nonexisting to an extreme degree of complexity. Histochem Cell Biol *129*, 267-276.

Santman-Berends, I.M., van Wuijckhuise, L., Vellema, P., and van Rijn, P.A. (2009). Vertical transmission of bluetongue virus serotype 8 virus in Dutch dairy herds in 2007. Vet Microbiol.

Santy, L.C., and Casanova, J.E. (2001). Activation of ARF6 by ARNO stimulates epithelial cell migration through downstream activation of both Rac1 and phospholipase D. J Cell Biol *154*, 599-610.

Schafer, D.A. (2004). Regulating actin dynamics at membranes: a focus on dynamin. Traffic *5*, 463-469.

Schlunck, G., Damke, H., Kiosses, W.B., Rusk, N., Symons, M.H., Waterman-Storer, C.M., Schmid, S.L., and Schwartz, M.A. (2004). Modulation of Rac localization and function by dynamin. Mol Biol Cell *15*, 256-267.

Schnatwinkel, C., Christoforidis, S., Lindsay, M.R., Uttenweiler-Joseph, S., Wilm, M., Parton, R.G., and Zerial, M. (2004). The Rab5 effector Rabankyrin-5 regulates and coordinates different endocytic mechanisms. PLoS Biol *2*, E261.

Schwartz-Cornil, I., Mertens, P.P., Contreras, V., Hemati, B., Pascale, F., Breard, E., Mellor, P.S., MacLachlan, N.J., and Zientara, S. (2008). Bluetongue virus: virology, pathogenesis and immunity. Vet Res *39*, 46.

Sharma, D.K., Choudhury, A., Singh, R.D., Wheatley, C.L., Marks, D.L., and Pagano, R.E. (2003). Glycosphingolipids internalized via caveolar-related endocytosis rapidly merge with the clathrin pathway in early endosomes and form microdomains for recycling. J Biol Chem *278*, 7564-7572.

Sieczkarski, S.B., Brown, H.A., and Whittaker, G.R. (2003). Role of protein kinase C betaII in influenza virus entry via late endosomes. J Virol *77*, 460-469.

Sieczkarski, S.B., and Whittaker, G.R. (2002). Influenza virus can enter and infect cells in the absence of clathrin-mediated endocytosis. J Virol *76*, 10455-10464.

Smith, J.L., Campos, S.K., Wandinger-Ness, A., and Ozbun, M.A. (2008). Caveolin-1-dependent infectious entry of human papillomavirus type 31 in human keratinocytes proceeds to the endosomal pathway for pH-dependent uncoating. J Virol *82*, 9505-9512.

Song, J., Khachikian, Z., Radhakrishna, H., and Donaldson, J.G. (1998). Localization of endogenous ARF6 to sites of cortical actin rearrangement and involvement of ARF6 in cell spreading. J Cell Sci *111 (Pt 15)*, 2257-2267.

Sonnichsen, B., De Renzis, S., Nielsen, E., Rietdorf, J., and Zerial, M. (2000). Distinct membrane domains on endosomes in the recycling pathway visualized by multicolor imaging of Rab4, Rab5, and Rab11. J Cell Biol *149*, 901-914.

Spoden, G., Freitag, K., Husmann, M., Boller, K., Sapp, M., Lambert, C., and Florin, L. (2008). Clathrin- and caveolin-independent entry of human papillomavirus type 16--involvement of tetraspanin-enriched microdomains (TEMs). PLoS One *3*, e3313.

Stan, R.V. (2005). Structure of caveolae. Biochim Biophys Acta *1746*, 334-348.

Stauber, N., Martinez-Costas, J., Sutton, G., Monastyrskaya, K., and Roy, P. (1997). Bluetongue virus VP6 protein binds ATP and exhibits an RNA-dependent ATPase function and a helicase activity that catalyze the unwinding of double-stranded RNA substrates. J Virol *71*, 7220-7226.

Stuart, D.I., Gouet, P., Grimes, J., Malby, R., Diprose, J., Zientara, S., Burroughs, J.N., and Mertens, P.P. (1998). Structural studies of orbivirus particles. Arch Virol Suppl *14*, 235-250.

Suksanpaisan, L., Susantad, T., and Smith, D.R. (2009). Characterization of dengue virus entry into HepG2 cells. J Biomed Sci *16*, 17.

Sun, P., Yamamoto, H., Suetsugu, S., Miki, H., Takenawa, T., and Endo, T. (2003). Small GTPase Rah/Rab34 is associated with membrane ruffles and macropinosomes and promotes macropinosome formation. J Biol Chem *278*, 4063-4071.

Sun, X., Yau, V.K., Briggs, B.J., and Whittaker, G.R. (2005). Role of clathrin-mediated endocytosis during vesicular stomatitis virus entry into host cells. Virology *338*, 53-60.

Swanson, J.A., and Watts, C. (1995). Macropinocytosis. Trends Cell Biol *5*, 424-428.

Szmaragd, C., Wilson, A., Carpenter, S., Mertens, P.P., Mellor, P.S., and Gubbins, S. (2007). Mortality and case fatality during the recurrence of BTV-8 in northern Europe in 2007. Vet Rec *161*, 571-572.

Tabachnick, W.J., Robertson, M.A., and Murphy, K.E. (1996). Culicoides variipennis and bluetongue disease. Research on arthropod-borne animal diseases for control and prevention in the year 2000. Ann N Y Acad Sci *791*, 219-226.

Takamatsu, H., Mellor, P.S., Mertens, P.P., Kirkham, P.A., Burroughs, J.N., and Parkhouse, R.M. (2003). A possible overwintering mechanism for bluetongue virus in the absence of the insect vector. J Gen Virol *84*, 227-235.

Tan, B.H., Nason, E., Staeuber, N., Jiang, W., Monastryrskaya, K., and Roy, P. (2001). RGD tripeptide of bluetongue virus VP7 protein is responsible for core attachment to Culicoides cells. J Virol *75*, 3937-3947.

Temizel, E.M., Yesilbag, K., Batten, C., Senturk, S., Maan, N.S., Clement-Mertens, P.P., and Batmaz, H. (2009). Epizootic hemorrhagic disease in cattle, Western Turkey. Emerg Infect Dis *15*, 317-319.

Thompson, H.M., and McNiven, M.A. (2006). Discovery of a new 'dynasore'. Nat Chem Biol *2*, 355-356.

Tyler, K.L., Clarke, P., DeBiasi, R.L., Kominsky, D., and Poggioli, G.J. (2001). Reoviruses and the host cell. Trends Microbiol *9*, 560-564.

Ungewickell, E., and Branton, D. (1981). Assembly units of clathrin coats. Nature *289*, 420-422.

Urakawa, T., Ritter, D.G., and Roy, P. (1989). Expression of largest RNA segment and synthesis of VP1 protein of bluetongue virus in insect cells by recombinant baculovirus: association of VP1 protein with RNA polymerase activity. Nucleic Acids Res *17*, 7395-7401.

Urbe, S., Huber, L.A., Zerial, M., Tooze, S.A., and Parton, R.G. (1993). Rab11, a small GTPase associated with both constitutive and regulated secretory pathways in PC12 cells. FEBS Lett *334*, 175-182.

Urrutia, R., Henley, J.R., Cook, T., and McNiven, M.A. (1997). The dynamins: redundant or distinct functions for an expanding family of related GTPases? Proc Natl Acad Sci U S A *94*, 377-384.

van der Sluijs, P., Hull, M., Webster, P., Male, P., Goud, B., and Mellman, I. (1992). The small GTP-binding protein rab4 controls an early sorting event on the endocytic pathway. Cell *70*, 729-740.

Van Dijk, A.A., and Huismans, H. (1980). The in vitro activation and further characterization of the bluetongue virus-associated transcriptase. Virology *104*, 347-356.

Van Dijk, A.A., and Huismans, H. (1988). In vitro transcription and translation of bluetongue virus mRNA. J Gen Virol *69 (Pt 3)*, 573-581.

Van Hamme, E., Dewerchin, H.L., Cornelissen, E., Verhasselt, B., and Nauwynck, H.J. (2008). Clathrin- and caveolae-independent entry of feline infectious peritonitis virus in monocytes depends on dynamin. J Gen Virol *89*, 2147-2156.

Vasquez, R.J., Howell, B., Yvon, A.M., Wadsworth, P., and Cassimeris, L. (1997). Nanomolar concentrations of nocodazole alter microtubule dynamic instability in vivo and in vitro. Mol Biol Cell *8*, 973-985.

Verwoerd, D.W., Els, H.J., De Villiers, E.M., and Huismans, H. (1972). Structure of the bluetongue virus capsid. J Virol *10*, 783-794.

Vidricaire, G., and Tremblay, M.J. (2007). A clathrin, caveolae, and dynamin-independent endocytic pathway requiring free membrane cholesterol drives HIV-1 internalization and infection in polarized trophoblastic cells. J Mol Biol *368*, 1267-1283.

Wang, G., Hernandez, R., Weninger, K., and Brown, D.T. (2007). Infection of cells by Sindbis virus at low temperature. Virology *362*, 461-467.

Wang, H., and Jiang, C. (2009). Influenza A virus H5N1 entry into host cells is through clathrin-dependent endocytosis. Sci China C Life Sci *52*, 464-469.

Wang, H., Yang, P., Liu, K., Guo, F., Zhang, Y., Zhang, G., and Jiang, C. (2008). SARS coronavirus entry into host cells through a novel clathrin- and caveolae-independent endocytic pathway. Cell Res *18*, 290-301.

Wang, L.H., Rothberg, K.G., and Anderson, R.G. (1993). Mis-assembly of clathrin lattices on endosomes reveals a regulatory switch for coated pit formation. J Cell Biol *123*, 1107-1117.

Weissmann, G., and Sessa, G. (1967). The action of polyene antibiotics on phospholipid-cholesterol structures. J Biol Chem *242*, 616-625.

West, M.A., Bretscher, M.S., and Watts, C. (1989). Distinct endocytotic pathways in epidermal growth factor-stimulated human carcinoma A431 cells. J Cell Biol *109*, 2731-2739.

West, M.A., Prescott, A.R., Eskelinen, E.L., Ridley, A.J., and Watts, C. (2000). Rac is required for constitutive macropinocytosis by dendritic cells but does not control its downregulation. Curr Biol *10*, 839-848.

White, D.M., Wilson, W.C., Blair, C.D., and Beaty, B.J. (2005). Studies on overwintering of bluetongue viruses in insects. J Gen Virol *86*, 453-462.

Wilson, A., Mellor, P.S., Szmaragd, C., and Mertens, P.P. (2009). Adaptive strategies of African horse sickness virus to facilitate vector transmission. Vet Res *40*, 16.

Wilson, A.J., and Mellor, P.S. (2009). Bluetongue in Europe: past, present and future. Philos Trans R Soc Lond B Biol Sci *364*, 2669-2681.

Wu, X., Chen, S.Y., Iwata, H., Compans, R.W., and Roy, P. (1992). Multiple glycoproteins synthesized by the smallest RNA segment (S10) of bluetongue virus. J Virol *66*, 7104-7112.

Xu, G., Wilson, W., Mecham, J., Murphy, K., Zhou, E.M., and Tabachnick, W. (1997). VP7: an attachment protein of bluetongue virus for cellular receptors in Culicoides variipennis. J Gen Virol *78 (Pt 7)*, 1617-1623.

Yoshimura, A., and Ohnishi, S. (1984). Uncoating of influenza virus in endosomes. J Virol *51*, 497-504.

Zarate, S., Espinosa, R., Romero, P., Mendez, E., Arias, C.F., and Lopez, S. (2000). The VP5 domain of VP4 can mediate attachment of rotaviruses to cells. J Virol *74*, 593-599.

Zarate, S., Romero, P., Espinosa, R., Arias, C.F., and Lopez, S. (2004). VP7 mediates the interaction of rotaviruses with integrin alphavbeta3 through a novel integrin-binding site. J Virol *78*, 10839-10847.

Zerial, M., and McBride, H. (2001). Rab proteins as membrane organizers. Nat Rev Mol Cell Biol *2*, 107-117.

Appendix I

PAGE showing a typical preparation of purified BTV-1

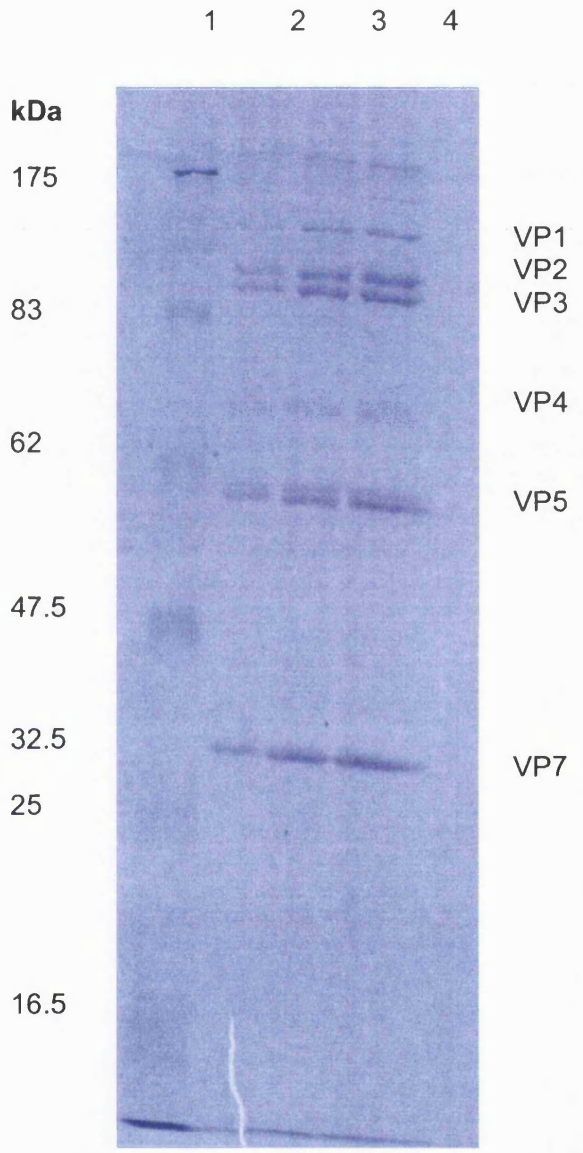

Lane 1: Size markers (kDa)
Lane 2: 1.25 µg/ml purified BTV-1
Lane 3: 2.5 µg/ml purified BTV-1
Lane 4: 5 µg/ml purified BTV-1

The SDS-PAGE Gel was run as described in method 2.3.1, using an 8% resolving gel with a 4% stacking gel.

Appendix II

Validation by western blot of antibodies used to detect BTV-1

Each SDS-PAGE was run as described in method 2.3.1, using an 8% resolving gel with a 4% stacking gel.

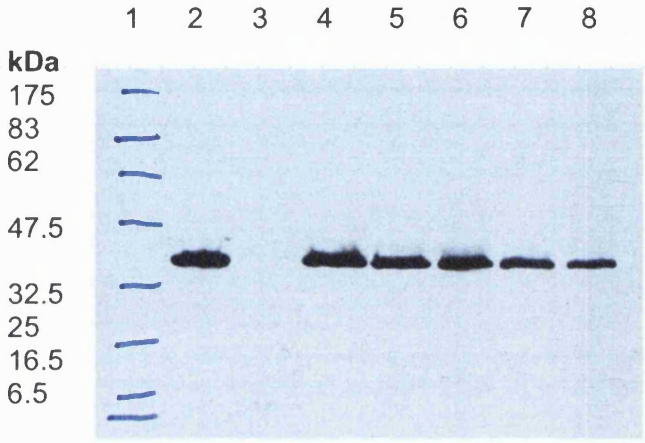

Actin: 42 kDa

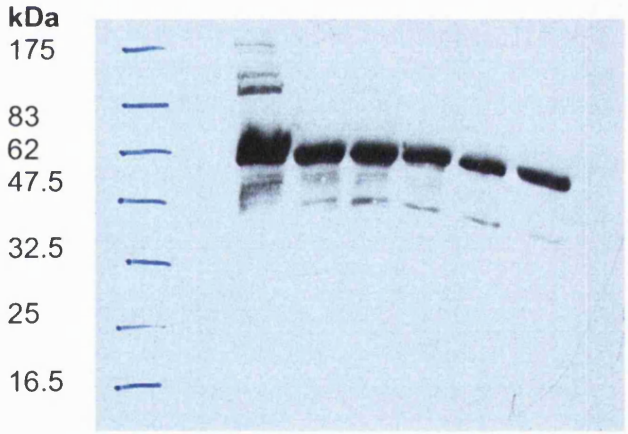

PM10, anti-VP5: 59 kDa

Lane 1: Size markers (kDa)
Lane 2: 20 µl Uninfected BHK cell lysate
Lane 3: 1.5 µg/ml Purified BTV-1
Lane 4: 20 µl BTV-1 Infected BHK cell lysate (24 hour)
Lane 5: 15 µl BTV-1 Infected BHK cell lysate (24 hour)
Lane 6: 10 µl BTV-1 Infected BHK cell lysate (24 hour)
Lane 7: 5 µl BTV-1 Infected BHK cell lysate (24 hour)
Lane 8: 2.5 µl BTV-1 Infected BHK cell lysate (24 hour)

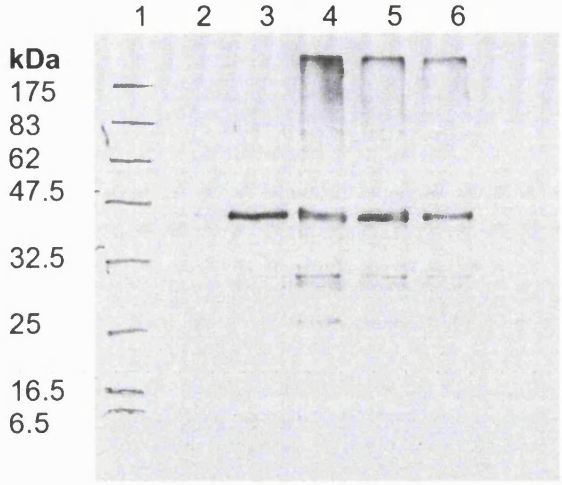

Orab 1, anti-NS2: 40 kDa

Lane 1: Size markers (kDa)
Lane 2: 10 µl Uninfected BHK cell lysate
Lane 3: 1.5 µg/ml Purified BTV-1
Lane 4: 10 µl BTV-1 Infected BHK cell lysate (24 hour)
Lane 5: 5 µl BTV-1 Infected BHK cell lysate (24 hour)
Lane 6: 2.5 µl BTV-1 Infected BHK cell lysate (24 hour)